

NASA CR-

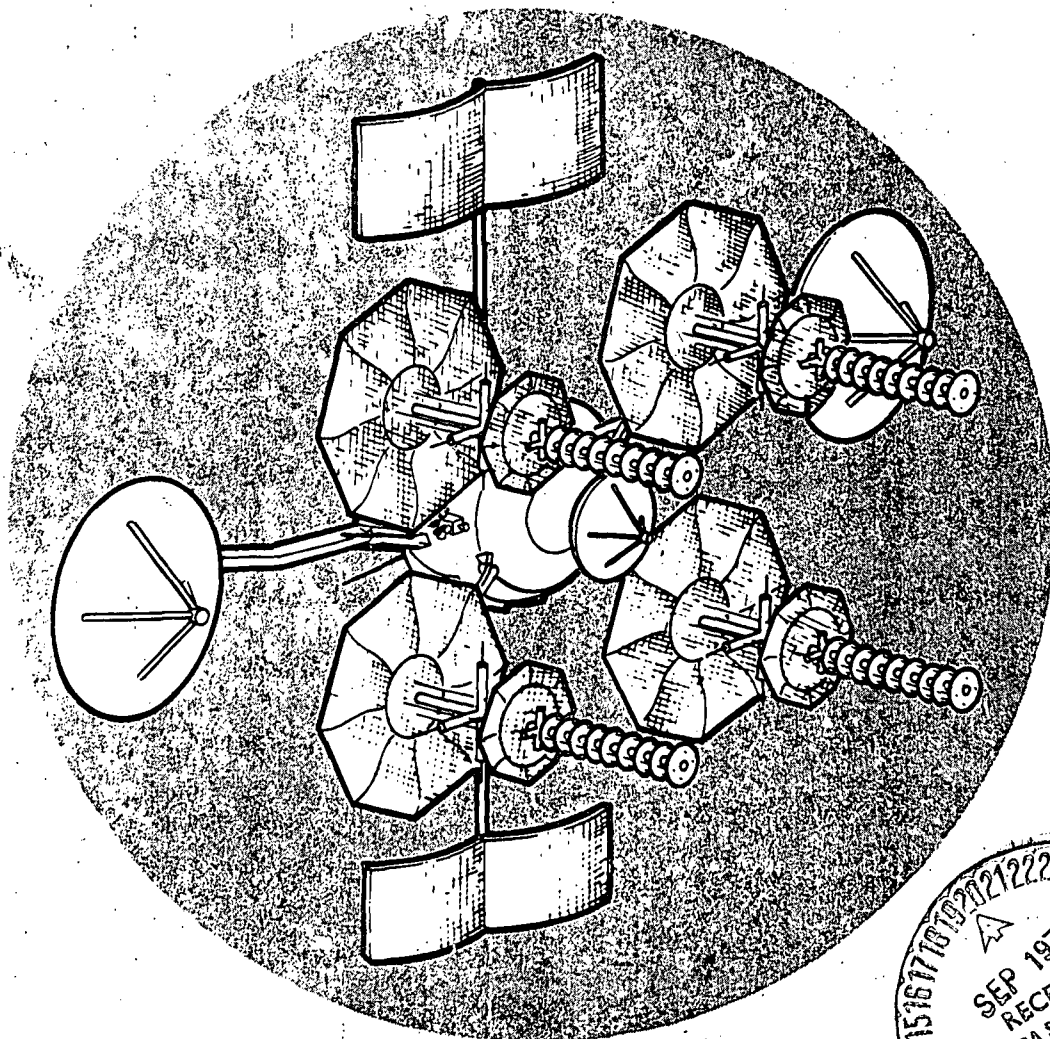
139/66
144665

SD 72-SA-0133-3

PART I FINAL REPORT

TRACKING & DATA RELAY SATELLITE SYSTEM CONFIGURATION & TRADEOFF STUDY

VOLUME III TELECOMMUNICATIONS SERVICE SYSTEM



OCTOBER 1972

SUBMITTED TO
GODDARD SPACE FLIGHT CENTER
NATIONAL AERONAUTICS & SPACE ADMINISTRATION



Space Division
North American Rockwell

IN ACCORDANCE WITH
CONTRACT NAS5-21705

PART I FINAL REPORT

**TRACKING & DATA RELAY SATELLITE SYSTEM
CONFIGURATION & TRADEOFF STUDY**

**VOLUME III
TELECOMMUNICATIONS SERVICE SYSTEM**

T. E. Hill

T. E. Hill
TDRS STUDY MANAGER

OCTOBER 1972

SUBMITTED TO
GODDARD SPACE FLIGHT CENTER
NATIONAL AERONAUTICS & SPACE ADMINISTRATION



Space Division
North American Rockwell

IN ACCORDANCE WITH
CONTRACT NAS5-21705

Page intentionally left blank



FOREWORD

This report summarizes the results of Part I of the study conducted under Contract NAS5-2107, Tracking and Data Relay Satellite Configuration and Systems Trade-off Study - 3-Axis Stabilized Configuration. The study was conducted by the Space Division of North American Rockwell Corporation for the Goddard Space Flight Center of the National Aeronautics and Space Administration.

The study is in two parts. Part I of the study considered all elements of the TDRS system but emphasized the design of a 3-axis stabilized satellite and a telecommunications system optimized for support of low and medium data rate user spacecraft constrained to be launched on a Delta 2914. Part II will emphasize upgrading the spacecraft design to provide telecommunications support to low and high, or low, medium and high data rate users, considering launches with the Atlas/Centaur and the Space Shuttle.

The report consists of the following seven volumes.

- | | |
|--|-----------------|
| 1. Summary | SD 72-SA-0133-1 |
| 2. System Engineering | SD 72-SA-0133-2 |
| 3. Telecommunications Service System | SD 72-SA-0133-3 |
| 4. Spacecraft and Subsystem Design | SD 72-SA-0133-4 |
| 5. User Impact and Ground Station Design | SD 72-SA-0133-5 |
| 6. Cost Estimates | SD 72-SA-0133-6 |
| 7. Telecommunications System Summary | SD 72-SA-0133-7 |

Acknowledgment is given to the following individuals for their participation in and contributions to the conduct of this study:

M.A. Cantor	North American Rockwell	System Engineering and Spacecraft Design
A.A. Nussberger	"	Electrical Power
W.C. Shmill	"	"
R.E. Oglevie	"	Stabilization and Control
A.F. Boyd	"	"
R.N. Yee	"	Propulsion
A.D. Musenow	"	Thermal Control
T.F. Rudiger	"	Flight Mechanics
J.W. Collins	"	Satellite Design
P.H. Dirnbach	"	Reliability
W.F. Deutsch	"	Telecommunications Design
S.H. Turkel	"	Operations Analysis
A. Forster	"	Cost
A.F. Anderson	"	Integration
T.T. Noji	AIL-Division of Cutler-Hammer	Telecommunications Design
L. Swartz	"	"
D.M. DeVito	The Magnavox Company	Telecommunication System Analysis
D. Cartier	"	Ground Station Design
R.H. French	"	Operations Analysis
G. Shaushanian	"	User Transponder Design

Page intentionally left blank



TABLE OF CONTENTS

VOLUME I

Section	Page
1.0 SUMMARY	1-1
1.1 SYSTEM CONCEPT	1-3
1.2 SATELLITE LAUNCH AND DEPLOYMENT	1-7
1.2.1 Deployment Analysis	1-7
1.2.2 Launch Analysis	1-8
1.2.3 Launch and Deployment Profile	1-11
1.3 TELECOMMUNICATIONS DESIGN	1-13
1.3.1 Telecommunications System Analysis	1-13
1.3.2 Telecommunications Subsystem Design	1-25
1.3.3 Telecommunications Relay Performance	1-29
1.4 SPACECRAFT MECHANICAL AND STRUCTURAL DESIGN	1-35
1.5 ELECTRICAL POWER SUBSYSTEM	1-51
1.6 ATTITUDE STABILIZATION AND CONTROL SUBSYSTEM	1-54
1.7 AUXILIARY PROPULSION SUBSYSTEM	1-57
1.7.1 Reaction Control Subsystem	1-57
1.7.2 Apogee Motor	1-60
1.8 THERMAL CONTROL	1-60
1.9 RELIABILITY	1-64
1.10 USER TRANSPONDER DESIGN	1-66
1.10.1 LDR Transponder	1-66
1.10.2 MDR Transponder	1-66
1.11 NETWORK OPERATIONS AND CONTROL	1-68
1.12 TDRS GROUND STATION	1-77
1.13 RECOMMENDATIONS	1-82

VOLUME II

2.0 SYSTEM ENGINEERING	2-1
2.1 MISSION ANALYSIS	2-1
2.1.1 Network Configuration	2-1
2.1.2 TDRS Operational Plan	2-6
2.1.3 Performance Sensitivity	2-19
2.1.4 TDRS On-Orbit Payload Capability	2-21
2.1.5 Launch and Deployment Profile	2-22
2.1.6 Launch and Deployment Timeline	2-27
2.2 NETWORK OPERATIONS AND CONTROL	2-33
2.2.1 TDRS System Concept	2-33
2.2.2 Primary System Elements and Their Operational and Functional Interfaces	2-37
2.2.3 TDRSS Functional Analysis	2-48
2.2.4 TDRS Operational Phase Sequence of Events	2-113
2.3 SYSTEM RELIABILITY ANALYSIS	2-139



VOLUME III

Section	Page
3.0 TELECOMMUNICATIONS SYSTEM ANALYSIS	3-1
3.1 RELAY SYSTEM REQUIREMENTS AND CONSTRAINTS	3-1
3.1.1 Design Goals	3-1
3.1.2 System Design Criteria	3-1
3.1.3 Telecommunication System Description	3-3
3.2 THE INTERFERENCE PROBLEM	3-4
3.2.1 Radio Frequency Interference	3-6
3.2.2 "Trash Noise" and Its Effect on the TDRS Channels	3-11
3.2.3 The TDRS User Propagation Path	3-16
3.3 FREQUENCY SELECTION	3-21
3.3.1 Frequency Trades	3-21
3.3.2 Frequency Plan	3-25
3.4 MODULATION AND CODING	3-25
3.4.1 Impact of Forward Error Control on the Medium and Low Data Rate Users	3-25
3.4.2 Voice Coding for Manned Users of the Tracking and Data Relay Satellite System	3-32
3.5 RELAY SYSTEM PERFORMANCE ANALYSIS	3-37
3.5.1 Forward (Command) Link Communications Performance	3-39
3.5.2 Return (Telemetry) Link Communications Performance	3-44
3.5.3 TDRS Tracking Performance	3-51
3.5.4 Pseudo-Random Code Acquisition and Tracking	3-67
3.5.5 Manned User Performance	3-76
3.6 REFERENCES	
4.0 TDRS TELECOMMUNICATION SUBSYSTEM	4-1
4.1 TELECOMMUNICATION SYSTEM REQUIREMENTS	4-7
4.1.1 Design Goals and Criteria	4-7
4.1.2 Requirements and Constraints	4-10
4.2 TELECOMMUNICATION SYSTEM DESIGN DESCRIPTION	4-12
4.2.1 Frequency Plan	4-12
4.2.2 Functional Description	4-22
4.2.3 Telecommunications Subsystem Size, Weight, and Power Summary	4-30
4.3 LOW DATA RATE LINK	4-32
4.3.1 Return Link	4-32
4.3.2 LDR Antenna	4-61
4.3.3 LDR Transponder	4-68



Section	Page
4.3.4	Performance Specification for LDR Transponder 4-81
4.3.5	Size, Weight, and Power Summary for LDR Transponder 4-86
4.4	MEDIUM DATA RATE LINK 4-87
4.4.1	MDR System Analysis and Trades 4-87
4.4.2	MDR Antennas 4-95
4.4.3	MDR Transceiver 4-100
4.4.4	Performance Specification for MDR Transponder 4-110
4.5	TDRS/GS LINK 4-119
4.5.1	System Analysis and Trades 4-119
4.5.2	TDRS/GS Link Antenna 4-124
4.5.3	TDRS/GS Transceiver 4-128
4.5.4	Performance Specification for the TDRS/GS Link Transponder 4-146
4.5.5	Size, Weight, and Power Summary of TDRS/GS Link Transponder 4-150
4.6	FREQUENCY SOURCE 4-151
4.6.1	System Analysis and Tradeoffs 4-151
4.6.2	Detailed Description of the Frequency Source 4-153
4.6.3	Performance Specification for the TDRS Frequency Source 4-157
4.6.4	Size, Weight, and Power Summary for TDRS Frequency Source 4-161
4.7	TRACKING, TELEMETRY, AND COMMAND SYSTEM 4-162
4.7.1	Mechanization Trades 4-163
4.7.2	Detailed Description of TT&C Transponder 4-163
4.7.3	Performance Specification for the TDRS Tracking, Telemetry and Command Subsystem 4-170
4.7.4	Size, Weight, and Power Summary for TT&C 4-172
4.8	TDRS TRACKING/ORDER WIRE TRANSPONDER 4-173
4.8.1	System Analysis and Trades 4-173
4.8.2	Detailed Description of TDRS Tracking Order Wire 4-175
4.8.3	Performance Specification for TDRS Tracking/Order Wire Transponder 4-177
4.8.4	Size, Weight, and Power Summary for the TDRS Tracking/Order Wire Transponder 4-179
4.9	Ku-BAND BEACON 4-179
4.9.1	System Description 4-179
4.9.2	Performance Specification of the Ku-Band Beacon 4-181
4.9.3	Size, Weight, and Power Summary of the Ku-Band Beacon 4-181



VOLUME IV

Section		Page
5.0	SPACECRAFT MECHANICAL AND STRUCTURAL DESIGN	5-1
5.1	TDRS BASELINE CONFIGURATION	5-2
	5.1.1 Deployed Configuration	5-2
	5.1.2 Launch Configuration	5-2
5.2	SPACECRAFT BODY STRUCTURE	5-6
5.3	ANTENNA MECHANICAL DESIGN	5-9
	5.3.1 MDR Antennas	5-9
	5.3.2 LDR UHF-VHF Array Structural Construction	5-9
	5.3.3 TDRS/GS Antenna	5-10
	5.3.4 TT&C Antennas	5-10
	5.3.5 Ku- and S-Band Tracking/ Order Wire Antennas	5-13
5.4	SOLAR ARRAY PANELS AND DRIVE MECHANISM	5-13
	5.4.1 Solar Panels	5-13
	5.4.2 Drive Mechanism	5-14
5.5	SUBSYSTEMS INSTALLATION	5-14
5.6	ACCESSIBILITY AND SERVICING PROVISIONS	5-21
5.7	MASS PROPERTIES	5-21
5.8	SUBSYSTEM INTEGRATION	5-21
6.0	ATTITUDE STABILIZATION AND CONTROL SUBSYSTEM (ASCS)	6-1
6.1	PERFORMANCE REQUIREMENTS	6-1
6.2	DISTURBANCE TORQUES AND MOMENTUM STORAGE REQUIREMENTS	6-3
	6.2.1 Solar Pressure Torques	6-3
	6.2.2 Antenna Gimbaling Disturbances	6-8
	6.2.3 Momentum Storage Requirements	6-8
6.3	SYSTEM MECHANIZATION TRADE STUDIES	6-13
	6.3.1 Transfer Orbit and Deployment Phase	6-13
	6.3.2 On-Orbit Phase Torquer and Momentum Storage Subsystem Trades	6-15
	6.3.3 Attitude Determination Sensor Trades	6-22
6.4	BASELINE SYSTEM DESCRIPTION	6-25
	6.4.1 Spin Stabilized Control Mode	6-25
	6.4.2 Three-Axis Stabilized Control System	6-30
6.5	APS Performance Requirements	6-33
	6.5.1 Propellant Requirements	6-33
	6.5.2 Thruster Performance Requirements	6-36
	6.5.3 Reaction Jet Configuration	6-39



Section		Page
7.0	PROPULSION SYSTEM	7-1
	7-1 APS REQUIREMENTS AND CRITERIA	7-1
	7-2 ANALYSIS AND TRADE STUDIES	7-2
	7-3 SUBSYSTEM DESIGN	7-7
	7.3.1 Description	7-7
	7.3.2 Performance	7-8
	7-4 DESIGN CONSIDERATIONS	7-16
	7.4.1 Operating Life	7-16
	7.4.2 Thrust Vector Alignment	7-17
	7.4.3 Performance Verification	7-17
	7-5 APOGEE MOTOR	7-17
8.0	ELECTRICAL POWER SUBSYSTEM (EPS)	8-1
	8.1 EPS SUMMARY	8-1
	8.1.1 Alternative Concepts	8-3
	8.1.2 Requirements	8-5
	8.1.3 EPS Description	8-13
	8.2 PRIMARY POWER GENERATION ASSEMBLY	8-15
	8.2.1 Solar Array Function and Description	8-15
	8.2.2 Solar Array Assembly Characteristics.	8-18
	8.2.3 Operational Constraints and Growth Considerations	8-20
	8.3 ENERGY STORAGE ASSEMBLY	8-22
	8.3.1 Function and Description	8-22
	8.3.2 Assembly Characteristics	8-24
	8.3.3 Growth Considerations	8-26
	8.4 POWER CONDITIONING ASSEMBLY	8-26
	8.4.1 Function and Description	8-26
	8.4.2 Power Conditioning Assembly Characteristics	8-28
	8.4.3 Operational Constraints and Growth Considerations	8-30
	8.5 DISTRIBUTION, CONTROL AND WIRING ASSEMBLY.	8-31
	8.5.1 Function and Description	8-31
	8.5.2 Assembly Characteristics	8-31
	8.6 EFFECT OF BATTERY CAPABILITY OF TDRS VOICE TRANSMISSION	8-33
9.0	THERMAL CONTROL	9-1
	9.1 REQUIREMENTS	9-1
	9.1.1 Mission Requirements	9-1
	9.1.2 Heat Rejection Loads	9-1
	9.1.3 Temperature Limits	9-4
	9.1.4 Design Constraints and Problem Areas.	9-4



Section	Page
9.2 SYSTEM DESCRIPTION	9-7
9.2.1 Louver Radiator	9-7
9.2.2 Multilayer Insulation	9-10
9.2.3 Thermal Control Coatings	9-13
9.2.4 Equipment Component Placement	9-13
9.3 ALTERNATE CONCEPTS	9-15
9.3.1 Passive Design	9-15
9.3.2 Variable Conductance Heat Pipe Radiator	9-15
9.4 SUBSYSTEM THERMAL CONTROL	9-16
9.4.1 APS	9-16
9.4.2 Solar Array Panel	9-18
9.4.3 Antennas	9-22
9.4.4 Apogee Motor	9-22
9.4.5 Excess Power Dissipation	9-23
9.5 SYSTEM DEFINITION	9-23

10.0 RELIABILITY	10-1
10.1 DEFINITIONS	10-1
10.2 RELIABILITY GOALS AND CRITERIA	10-2
10.3 SUBSYSTEM ANALYSIS	10-5
10.3.1 Telecommunications	10-5
10.3.2 Structure and Mechanics	10-13
10.3.3 Attitude Control	10-13
10.3.4 Auxiliary Propulsion Subsystem (APS).	10-13
10.3.5 Electrical Power	10-15
10.3.6 Thermal Control	10-15
10.4 SINGLE FAILURE POINT SUMMARY	10-18
10.5 RELIABILITY PROGRAM FOR IMPLEMENTATION PHASE	10-24

VOLUME V

11.0 USER SPACECRAFT IMPACT	11-1
11.1 USER SPACECRAFT TRANSPONDER CONCEPTS AND TRADES	11-1
11.1.1 LDR Transponder	11-1
11.1.2 MDR Transponder	11-5
11.2 USER SPACECRAFT TRANSPONDER MECHANIZATION	11-7
11.2.1 LDR Transponder	11-7
11.2.2 MDR Transponder	11-15
11.3 CONCLUSIONS	11-19
12.0 TDRS GROUND STATION DESIGN	12-1
12.1 REQUIREMENTS AND CONSTRAINTS	12-1
12.1.1 Uplink Requirements and Constraints	12-1
12.1.2 Downlink Requirements and Constraints	12-3



Section	Page
12.2 TDRS GROUND STATION	12-4
12.2.1 TDRS GS Antenna Subsystem	12-4
12.2.2 Antenna Site Analysis	12-5
12.3 ANTENNA SITE ISOLATION ANALYSIS	12-6
12.4 Ku-BAND GROUND STATION ANTENNA	12-6
12.4.1 TDRS Ground Station Receiver Front End	12-8
12.4.2 TDRS Ground Station FM Demodulator and Demultiplexer.	12-8
12.4.3 TDRS Ground Station LDR Processing	12-9
12.4.4 TDRS Ground RF Transmitter	12-9
12.4.5 TDRS Ground Station FDM Multiplexing	12-9
12.4.6 TDRS Ground Station Frequency Source	12-10
12.4.7 TDRS Ground Link Backup Mode	12-10
12.5 DESIGN CONSIDERATIONS	12-11
12.5.1 Signal Categories	12-11
12.5.2 LDR Command/Tracking (Uplink).	12-11
12.5.3 LDR Telemetry	12-13
12.5.4 LDR/MDR Tracking (Downlink)	12-13
12.5.5 MDR Command (P/BU)/Uplink Voice (P/BU)/Tracking	12-13
12.5.6 MDR Telemetry (P/BU)	12-14
12.5.7 TDRS Order Wire	12-14
12.5.8 MDR Downlink Voice (P/BU) (Manned User)	12-17
12.5.9 TDRS Command/Tracking (P/BU)	12-17
12.5.10 TDRS Telemetry (P/BU)	12-17
12.5.11 TDRS Tracking (Downlink) (P/BU)	12-17
12.5.12 Ground Station/Network Communications	12-19
12.6 CONCEPT DESCRIPTION	12-19
12.6.1 LDR Command/Tracking (Uplink).	12-20
12.6.2 LDR Telemetry	12-20
12.6.3 LDR/MDR Tracking (Downlink)	12-21
12.6.4 MDR Command (P/BU)/Uplink Voice (P/BU) Tracking	12-21
12.6.5 MDR Telemetry (P/BU)	12-21
12.6.6 TDRS Order Wire	12-22
12.6.7 MDR Downlink Voice (P/BU) (Manned User)	12-22
12.6.8 TDRS Command/Tracking (P/BU)	12-22
12.6.9 TDRS Telemetry (P/BU)	12-23
12.6.10 TDRS Tracking (Downlink) (P/BU)	12-23
12.6.11 Ground Station/Network Communications	12-23
12.6.12 Demodulation Tracking Unit	12-23
12.6.13 Modulation Unit	12-25
12.6.14 Control and Monitor Subsystem.	12-26
12.7 CONCLUSIONS AND RECOMMENDATIONS	12-31



VOLUME VI

Section	Page
13.0 COSTING	13-1
13.1 INTRODUCTION	13-1
13.1.1 Cost Analysis	13-1
13.1.2 TDRSS Program Cost Estimates	13-1
13.2 TDRSS BASELINE DESCRIPTION	13-3
13.2.1 TDRSS Operational Concept	13-3
13.2.2 TDRS Design Concept	13-5
13.2.3 TDRS Technical Characteristics	13-5
13.3 TDRSS COSTING REQUIREMENTS	13-5
13.3.1 Costing Ground Rules	13-5
13.3.2 Costing Work Breakdown Structure	13-9
13.3.3 Schedules	13-10
13.4 SPACECRAFT COST ANALYSIS	13-14
13.4.1 Cost Methodology	13-14
13.4.2 Alternate Cost Models Description	13-15
13.4.3 TDRS Cost Estimates Based on Alternate Cost Models	13-17
13.4.4 Selected TDRS Cost Models	13-19
GLOSSARY	13-25
APPENDIX 13A. SAMSO/NR NORMALIZED COST MODEL	13A-1

VOLUME VII

14.0 TELECOMMUNICATIONS SYSTEM SUMMARY	14-1
14.1 INTRODUCTION	14-1
14.2 SYSTEM SERVICE AND PERFORMANCE SUMMARY	14-4
14.2.1 LDR Return Link	14-4
14.2.2 LDR Forward Link	14-6
14.2.3 MDR Link Performance	14-8



Section	Page
14.3 LINK BUDGET	14-12
14.3.1 LDR Return Link Budget	14-12
14.3.2 LDR Forward Link Budget.	14-14
14.3.3 MDR Return Link Budget	14-14
14.3.4 MDR Forward Link Budget.	14-17
14.3.5 TDRS/GS Return Link Budget	14-17
14.3.6 TDRS/GS Forward Link Budget	14-20
14.3.7 Tracking/Order Wire	14-24
14.3.8 Ku-Band Beacon	14-24
14.4 SUBSYSTEM TERMINAL CHARACTERISTICS	14-24
14.4.1 TDRS Telecommunication Subsystem	14-24
14.4.2 User Transponder Design.	14-26
14.4.3 Ground Station Terminal Characteristics	14-33

Page intentionally left blank



ILLUSTRATIONS

Figure		Page
3-1	Forward Link Interference Diagram	3-5
3-2	Return Link Interference Diagram	3-5
3-3	RFI Power Density for TDRS Located at 11°W	3-7
3-4	RFI Power Density for TDRS Located at 143°W	3-7
3-5	RFI Power Density for TDRS Located at 112°E	3-8
3-6	RFI Power Density at User Spacecraft (1000-km Altitude and Omnidirectional Antenna)-Satellite Location 50°N/30°E	3-8
3-7	RFI Power Density at User Spacecraft (1000-km Altitude and Omnidirectional Antenna)-Satellite Location 38°N/85°W	3-8
3-8	Galactic Temperature Over a Hemisphere	3-12
3-9A	Antenna Coordinate System	3-14
3-9B	Geometry When Distributed Source Is Small Compared to Range	3-14
3-10	Geometry for θ_1 Calculations	3-14
3-11A	Power Density Profile of Miami at 305.5 MHz	3-15
3-11B	Temperature Profile of Miami at 305.5 MHz, Measured Traveling North at 18,000 Feet (5490 M)	3-15
3-12	Trash Noise at User Spacecraft	3-16
3-13	Relative Specular and Diffuse Reflected Power Versus Grazing Angle	3-18
3-14	Multipath/Direct Signal Ratio as a Function of Orbital Altitude	3-18
3-15	TDRS Multipath Geometry	3-18
3-16	Projected Multipath Level	3-20
3-17	Comparison of Sequential and Rate 1/3 Maximum Likelihood Decoder Performance	3-28
3-18	Rate 1/2 Maximum Likelihood Decoder Performance	3-28
3-19	Optimum Binary PSK and Δ PSK Versus E/N_0	3-29
3-20	General Encoder for Convolutional Code	3-29
3-21	Sequential Decoder (R=1/2 Systematic Code)	3-31
3-22	Maximum-Likelihood (Viterbi) Decoder	3-31
3-23	Bell Aero's Adp-NBFM	3-33
3-24	PDM Modulation and Modulator Waveforms	3-34
3-25	PDM Demodulator and Demodulator Waveforms	3-35
3-26	Companded Delta Coder (IBM)	3-36
3-27	Sentence Intelligibility Versus PB Intelligibility	3-36
3-28	Comparison of PDM and Adaptive Δ - Modulation Voice	3-38
3-29	Performance of Typical Adaptive Delta Modulator	3-38
3-30	Forward Link Performance at VHF - Chip Rate = 32 Kilo-chips per Second	3-41
3-31	Forward Link Performance at VHF - Chip Rate = 64 Kilo-chips per Second	3-41



Figure		Page
3-32	Forward Link Performance at UHF - Chip Rate = 32 Kilo-chips per Second	3-42
3-33	Forward Link Performance at UHF - Chip Rate = 100 Kilo-chips per Second	3-42
3-34	Forward Link Performance at UHF - Chip Rate = 320 Kilo-chips per Second	3-42
3-35	Forward Link Bit Rate as a Function of One RFI Source (in Band)	3-43
3-36	Return Link Performance at 136 MHz (User Altitude = 300 km; Reflection Coefficient = 1.0)	3-46
3-37	Return Link Performance at 136 MHz (User Altitude = 300 km; Reflection Coefficient = 0.05)	3-46
3-38	Return Link Performance at 136 MHz (User Altitude = 4800 km; Reflection Coefficient = 1.0)	3-47
3-39	Return Link Performance at 136 MHz (User Altitude = 4800 km; Reflection Coefficient = 0.05)	3-47
3-40	Impact of Forward Error Control on the Return Link Performance at 136 MHz	3-49
3-41	Return Link Performance at 136 MHz as a Function of User Transmit Power	3-49
3-42	Assumed Locations for the TDRS Ranging Stations	3-52
3-43	Functional Design of the TDRS Ranging Concept	3-52
3-44	TDRS Position Location as a Function of Inclination Angle	3-55
3-45	One-Way Ranging System	3-57
3-46	Doppler Signal Extraction	3-59
3-47	Forward Link RMS Range Error Versus RFI Power Density at VHF	3-68
3-48	Forward Link RMS Range Error Versus RFI Power Density at UHF	3-68
3-49	Forward Link Range Error Versus RFI Power Density - Chip Rate = 320 Kilochips per Second	3-69
3-50	Return Link RMS Range Error Versus RFI Power Density at 136 MHz	3-69
3-51	Forward Link Range Rate Error at VHF - Chip Rate = 32 Kilochips per Second	3-69
3-52	Forward Link Range Rate Error at UHF - Chip Rate = 32 Kilochips per Second	3-70
3-53	Forward Link Range Rate Error at UHF - Chip Rate = 320 Kilochips per Second	3-71
3-54	Return Link Range Error at 136 MHz - Chip Rate = 1000 Kilochips per Second	3-71
3-55	LDR Receiver	3-74
3-56	PN Synchronization Time	3-75



Figure		Page
4-1	Space Geometry for Two Satellite TDRSS Network	4-2
4-2	Ku-Band Transmission from TDRS to Ground Station	4-15
4-3	Ground Return Link Operating at Common Frequency	4-17
4-4	MDR-Ground Link Interference at Ku-Band	4-18
4-5	MDR Return Link Frequency Plan	4-19
4-6	TDRS Forward Link Spectrum for Ku-Band Operation	4-20
4-7	TDRS Forward Link S-Band Backup Mode	4-21
4-8	TDRS/GS Return Link Backup Mode Spectrum	4-23
4-9	TDRS Telecommunications Subsystem	4-23
4-10	Telecommunications Subsystem Block Diagram	4-25
4-11	AGIPA Approach for LDR Return Link	4-33
4-12	HPBW Characteristics of LDR Ring Array	4-34
4-13	LDR Return Link F-FOV vs. AGIPA	4-34
4-14	Adaptive Antenna for 8-Channel PN Receiver	4-36
4-15	RFI Model for Atlantic Scenario	4-37
4-16	RFI Model for Pacific Scenario	4-37
4-17	VHF Quad Array of Backfire Elements for F-FOV and AGIPA Approaches	4-38
4-18	Atlantic View	4-39
4-19	Atlantic View - Signal No. 1	4-41
4-20	Atlantic View - Signal No. 2	4-42
4-21	Atlantic View - Signal No. 3	4-43
4-22	Atlantic View - Signal No. 4	4-44
4-23	Atlantic View - Signal No. 5	4-45
4-24	Atlantic View - Signal No. 6	4-46
4-25	Atlantic View - Signal No. 7	4-47
4-26	SIR Improvement: F-FOV vs. AGIPA	4-48
4-27	VHF Quad Array of Backfire Elements for F-FOV and AGIPA Approaches	4-50
4-28	Scan Loss: F-FOV vs. AGIPA	4-50
4-29	LDR Return Link Performance: F-FOV vs. AGIPA	4-51
4-30	LDR Forward Link Transmitter Tradeoff	4-52
4-31	Block Diagram for UHF Satellite Steering - Separate Output Amplifiers	4-57
4-32	LDR Forward Link Performance Achievable Data Rate; Range Error and Range Rate Error	4-59
4-33	Recommended Dual Frequency LDR Transponder	4-60
4-34	Dual Frequency (VHF-UHF) LDR Antenna	4-63
4-35	VHF/UHF Backfire Antenna Dimensions	4-65
4-36	VHF Backfire Antenna Patterns	4-66



Figure		Page
4-37	Backfire Antenna Gain Curves as a Function of Large Reflector Diameter	4-67
4-38	Functional Block Diagram of LDR Transceiver	4-70
4-39	LDR Receiver Block Diagram	4-72
4-40	LDR Summing Network	4-73
4-41	LDR Receiver	4-75
4-42	IF Summing Network	4-76
4-43	LDR Transmitter Divider Network	4-77
4-44	LDR Transmitter Divider	4-79
4-45	LDR Transmitter Block Diagram	4-80
4-46	Driver Output Amplifier Assembly	4-82
4-47	Transmitter Assembly	4-82
4-48	MDR Link Requirements and Constraints	4-88
4-49	MDR Return Link: Space Geometry for Ts Calculation	4-88
4-50	MDR Return Link: Space Loss Ts vs. Aspect Angle	4-89
4-51	MDR Link Antenna Requirements: S-Band	4-90
4-52	MDR Link Antenna Requirements: Ku-Band	4-91
4-53	MDR Link Frequency Selection	4-93
4-54	MDR Link Support of Space Shuttle	4-93
4-55	Comparison of PDM and Adaptive Δ -Modulation Voice	4-94
4-56	Comparison of Antenna Gain vs. Weight - Planar Array Versus Parabolic Dish	4-97
4-57	Weight vs. Aperture Size for Planar Arrays and Radiation, Inc. Parabolic Dish Designs	4-98
4-58	MDR Link Dual Frequency Parabolic Dish Design	4-98
4-59	RF Block Diagram MDR Antenna Cassegrain Ku-Band/Apex S-Band	4-99
4-60	Summary of MDR Transceiver Mechanization Tradeoffs	4-102
4-61	MDR Transmitter - Solid-State Versus TWTA	4-103
4-62	Dual Frequency MDR Transmitter	4-105
4-63	MDR Transceiver Block Diagram	4-105
4-64	MDR No. 1 Baseline Receiver	4-106
4-65	MDR No. 2 Baseline Receiver	4-107
4-66	MDR Receiver Layout	4-109
4-67	MDR No. 1 Transmitter Block Diagram	4-111
4-68	MDR No. 2 Transmitter Block Diagram	4-113
4-69	Typical MDR Transmitter Assembly	4-114
4-70	MDR No. 1 Module A	4-115
4-71	Probability Distribution of Rainfall Rates, Washington, D.C.	4-121
4-72	Link Reliability Versus Rain Margin for Cooled and Un-cooled Receivers	4-121
4-73	Ground Link Transceiver Tradeoff Considerations	4-123



Figure		Page
4-74	Comparison of Antenna Gain vs. Weight	4-125
4-75	Tandem Link Calculation	4-131
4-76	CNR Requirement in Tandem Link as a Function of CNR Degradation Through TDRS	4-132
4-77	Candidate TDRS/GS Multiplexing Configurations	4-135
4-78	Second IF Frequency Spectrum SG/TDRS Receiver	4-138
4-79	GS/TDRS Baseline Receiver	4-139
4-80	TDRS/GS Receiver	4-140
4-81	TDRS/GS Transmitter	4-142
4-82	TDRS/GS Transmitter Baseband Frequency Assignment	4-143
4-83	TDRS/GS Transmitter Primary and Redundant Units	4-147
4-84	LO Power Distribution Network	4-152
4-85	Frequency Source Design Approach	4-154
4-86	Typical Reference Loop	4-155
4-87	Typical Cleanup Loop	4-156
4-88	Frequency Source Block Diagram	4-158
4-89	Frequency Source Redundancy Model	4-159
4-90	Frequency Source Layout	4-160
4-91	TT&C Block Diagram	4-162
4-92	Element Patterns	4-165
4-93	TT&C Transponder Block Diagram	4-167
4-94	TT&C Modem	4-169
4-95	TT&C Processor Block Diagram	4-170
4-96	Location System Block Diagram	4-174
4-97	Axial Mode Helical Antenna Beamwidth vs. Length	4-176
4-98	Proposed Construction of S-Band Beacon Antenna	4-176
4-99	Ku-Band Beacon	4-180



TABLES

Table		Page
3-1	Telecommunications Service Requirements	3-2
3-2	Key Design Features of Low Data Rate Service	3-3
3-3	Key Design Features of the Medium Data Rate Service	3-4
3-4	RFI Sources at User S/C in the 127.7 - 127.85 MHz Band	3-9
3-5	Estimated RFI Sources at the TDRS	3-10
3-6	Estimated RFI Sources at the User	3-10
3-7	RFI Sources in the Band 400.5 - 401.5 MHz	3-11
3-8	Low Altitude Spacecraft Population Projections: 1976-1980	3-19
3-9	TDRSS Ground/Space Link Frequency Band Selection	3-22
3-10	TDRSS Space /Space Link Frequency Band Selection	3-22
3-11	Bandwidth Spreading Required to Meet IRAC Specifications	3-24
3-12	System Frequency Plan	3-25
3-13	Viterbi Decoding Output Error Rate Performance	3-27
3-14	Cost and Performance Data for R = 1/2 Maximum Likelihood Decoder	3-30
3-15	Forward Link Power Requirements for MDR Service	3-44
3-16	Return Link Power Requirements for MDR Service	3-50
3-17	TDRS Location Accuracy (TDRS at 11° W)	3-53
3-18	TDRS Location Accuracy (TDRS at 143° W)	3-53
3-19	TDRS Location Accuracy (TDRS at 143° W)	3-54
3-20	TDRS Location Accuracy (TDRS at 143° W) (After 24 Hours of Tracking)	3-54
3-21	S-Band Ranging Power Budgets	3-56
3-22	User Spacecraft Tracking Requirements	3-56
3-23	Space Shuttle Requirements and Constraints	3-76
3-24	Forward Link Power Budget for Shuttle	3-77
3-25	Carrier-to-Noise Density Required for Support in Forward Link	3-78
3-26	Estimates of Additional Gain Required to Support Space Shuttle in Forward Link	3-78
3-27	Carrier-to-Noise Density Required for Shuttle Support in Return Link	3-79
3-28	Return Link Power Budget for Shuttle	3-80
4-1	Summary of TDRS Telecommunication Implementation Requirements and Constraints	4-11
4-2	TDRS Frequency Plan	4-13
4-3	Telecommunications Subsystem Size, Weight, and Power Summary	4-31
4-4	Low Data Rate Forward Link Requirements, Constraints	4-52
4-5	LDR Forward Link TDRS Implementation Tradeoff Matrix	4-53



Table		Page
4-6	LDR Forward Link ERP for Several Implementation Approaches	4-54
4-7	LDR Forward Link Capabilities	4-58
4-8	Comparison of Candidate LDR Transceiver Approaches	4-60
4-9	Summary of Candidate LDR Antenna Configurations	4-62
4-10	Dual Frequency LDR Antenna Considerations	4-63
4-11	Summary of LDR Receiver Tradeoffs	4-69
4-12	Summary of LDR Transmitter Tradeoffs	4-70
4-13	MDR Link Approaches	4-87
4-14	Summary of Candidate MDR Antennas	4-96
4-15	RF Efficiency Budget	4-101
4-16	Feed/Microwave System Weight Budget	4-101
4-17	Weight Budget and Power Summary for S- and Ku- Band MDR Antenna	4-101
4-18	MDR Receiver Tradeoff Summary	4-103
4-19	Transmitter Power in dBw Versus Ground Antenna Diameter and Type of Receiver	4-122
4-20	TDRS/GS Link Characteristics	4-123
4-21	Comments on Candidate Ground Link Antenna Designs	4-126
4-22	Weight Budget and Power Summary for Ku-Band System	4-128
4-23	TDRS/GS Receiver Mechanization Trades Summary	4-129
4-24	Ground Return Link Requirements	4-130
4-25	Transmitter System Summary	4-136
4-26	FDM/FM Characteristics	4-145
4-27	Frequency Source Tradeoffs	4-153
4-28	Summary of TT&C Tradeoffs and Recommendations	4-164
4-29	Location Receiver Parameters	4-173
4-30	Ku-Band Beacon Power Budget	4-179



3.0 TELECOMMUNICATIONS SYSTEM ANALYSIS

In this section the results of the telecommunications subsystem analysis are presented. Included are the relay system requirements and constraints, interference analysis, frequency selection, modulation and coding analysis, and the performance analysis of the relay system.

3.1 RELAY SYSTEM REQUIREMENTS AND CONSTRAINTS

Among the constraints that impact the TDRSS are the capabilities of the Thor/Delta, the radio frequency interference (RFI) and multipath environment, and inclement weather at the ground station. The booster payload capability implies a limit on the weight, power, and volume of the spacecraft which correspondingly limit antenna size, system redundancy, etc. From the outset the RFI and multipath phenomena has presented itself as the single most important technical problem area. Years of study by Marnavox and AIL in the areas of pseudonoise (PN) modulation concepts and the Adaptive Ground Implemented Phased Array (AGIPA), respectively, offers a viable solution to the problem.

In the sections that follow the system design goals will be established along with the design criteria and a description of the recommended system will be presented.

3.1.1 Design Goals

The basic design goal of this study is to provide a viable, cost-effective telecommunication service to a variety of user spacecraft while minimizing the effects of RFI in the LDR user links, multipath propagation, and power/gain constraints.

Telecommunication support provided to the LDR, MDR and manned users is presented in Table 3-1. The manned user is the Space Shuttle. In addition to those presented in the table, the ground station/TDRS link is required to operate at Ku-band, with a rain margin of +17.5 dB. Exact frequencies for the specified links are provided in Sections 3.2 and 3.3, which are concerned with the interference problem and frequency selection, respectively.

3.1.2 System Design Criteria

As stated, the main objectives of this program are to maximize the efficiency of an earth-orbiting spacecraft to provide a tracking and data relay function and to configure the system such that it is compatible with the post-1977 support needs of the tracking and data acquisition network.

Table 3.1. Telecommunications Service Requirements
(as per SOW)

Description	LDR User	MDR User	Manned User (Shuttle)
Number of users	Forward: Minimum of 1 Return: 20	Minimum of 1	Minimum of 1
Frequency	Forward: VHF, UHF, S-band Return: VHF	S- or X- or Ku-band	S-band, VHF-band
Communications requirement	Forward: 100 to 1000 bps Return: 1 to 10 kbps	Forward: 100 to 1000 bps Return: 10 to 1000 kbps	Forward: 2 kbps 1 or 2 voice at 19.2 kbps Return: 76.8 kbps 1 or 2 voice at 19.2 kbps
Constraints	<ul style="list-style-type: none"> *Linear transponder in return link *High RFI *Flux density (IRAC): VHF < -144 dBw/m²/4 khz UHF < -150 dBw/m²/4 khz S-band < -154 dBw/m²/ 4 khz *EIRP = +30 dBw/channel (VHF, UHF) = +41 dBw/channel(S) *BER = 10⁻⁵ 	<ul style="list-style-type: none"> *Linear TDRS transponder return link *Variable frequency *Flux density (IRAC): S-band < -154 dBw/m²/4 khz X-band < -150 dBw/m²/4 khz Ku-band < -152 dBw/m²/ 4 khz *BER = 10⁻⁵ 	<ul style="list-style-type: none"> *User antenna gain = +3 dB *BER Voice: 10⁻³ Data: 10⁻⁴ *User transmit power = 16 dBw

3-2

SD 72-SA-0133



Space Division
North American Rockwell

The basic guidelines followed in the design of the telecommunications system are fourfold; namely, minimize support costs, minimize impact on user spacecraft communications terminal, and maximize system flexibility while minimizing risk. Moreover, during the course of the study an attempt has been made to maximize link performance, to minimize weight and power, and to provide a system with high reliability and graceful degradation.

3.1.3 Telecommunication System Description

The basic recommended telecommunications system to provide service for LDR and MDR users is contained herein.

3.1.3.1 Low Data Rate Service

The low data rate service is a UHF command link with two TDRS steered beams and a high gain antenna. System EIRP at UHF is +30 dBw/beam minimum. The telemetry link employs AGIPA concept which provides twenty independent beams (one for each user). The user spacecraft are discriminated by use of unique PN codes in the return link. The AGIPA concept provides an adaptive spatial and polarization filtering of RFI, and an optimization of the signal-to-interference ratio. The system (AGIPA) includes the option of a fixed-field-of-view backup. The key design features of the low data rate services are shown in Table 3-2.

Table 3-2. Key Design Features of the Low Data Rate Service

Forward Link	Frequency band Polarization EIRP (at 31° (0.54 rad) FOV)	400.5 to 401.5 MHz Circular Steered beam 30 dBw data/36 dBw voice @ 25% duty cycle F-FOV 24 dBw
Return Link	Frequency band Polarization G/T _s AGIPA FFOV	136 to 138 MHz Linear 2 planes -14.4 dB/°K* -18.8 dB/°K*
Antenna Configuration		Backfire antenna 4-element array
Transceiver configuration		Frequency translating

*Assumes nominal antenna temperature of 800°K; however, T in this frequency is variable.

3.1.3.2 Medium Data Rate Service

The MDR user telecommunications service comprise a dual frequency feature; namely, an S-band link to support current MDR users and a Ku-band link to support future MDR users (i.e., high performance users). Two MDR users can obtain simultaneous support via two 6.5 ft (2.0 M) dishes on board the



TDRS. In addition, the MDR service capability can provide support to manned users such as space shuttle. The system antenna tracking consists of open-loop tracking at S-band and an autotrack at Ku-band. Furthermore, the MDR antenna system can serve as a backup for the GS/TDRS link. The MDR service design features are shown in Table 3-3.

Table 3-3. Key Design Features of the Medium Data Rate Service

Forward Link	Frequency EIRP	S-/Ku-band S-band data - 41 dBw; voice = 47 dBw at 25% duty cycle Ku-band 45.6 dBw
	Polarization	Circular
Return Link	Frequency G/T _s	S-/Ku-band 3.9/20.4 dB
	Polarization	Circular
Antenna Configuration		2 S- and Ku-band Parabolic reflectors
Transceiver configuration		Frequency translating

The MDR service as configured is essentially a "bent pipe" on the return link, thereby providing support for a variety of MDR users regardless of the signal formats employed.

3.2 THE INTERFERENCE PROBLEM

A functional description of the interference problems in the forward and return link is shown in Figures 3-1 and 3-2, respectively. The TDRS and User Spacecraft will be confronted with four basic types of interference, namely:

1. Unintentional, upward directed, radio frequency interference (RFI) originating from communications equipment located on earth.
2. Background interference (i.e., "trash noise") originating primarily in urban areas and is the composite of such things as ignition noise, switching transients, corona, and other forms of man-made noise.
3. Multipath interference between the direct path signal in the USER/TDRS link and a replica of that signal which has been reflected off the earth.

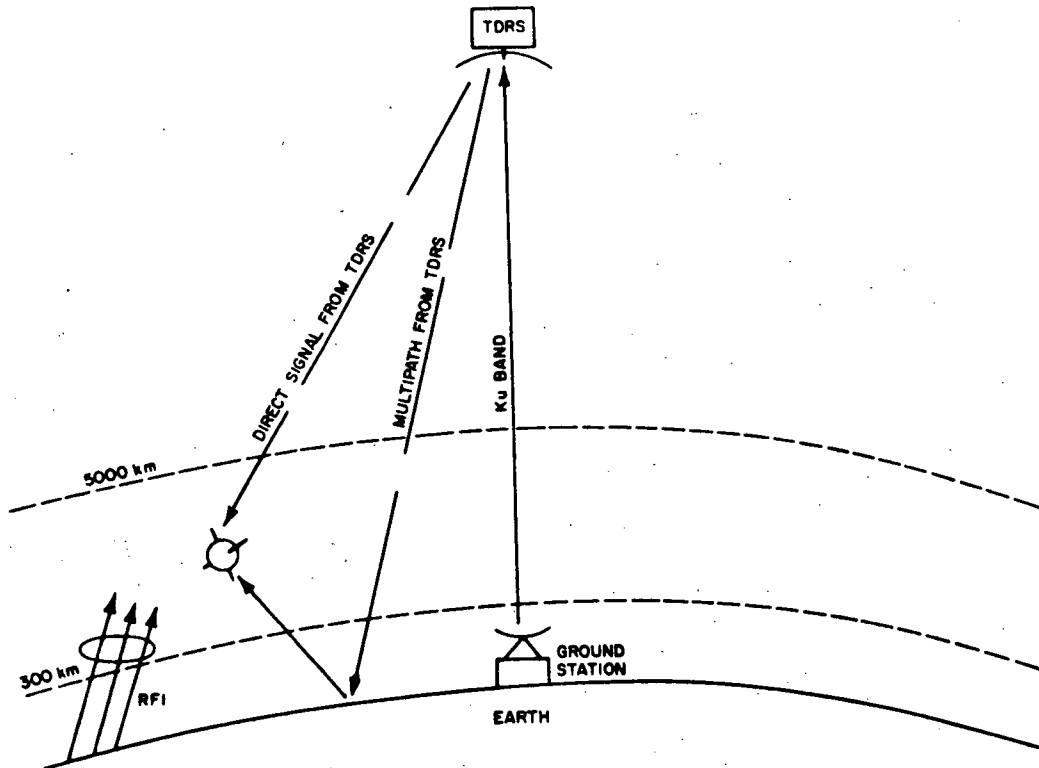


Figure 3-1. Forward Link Interference Diagram

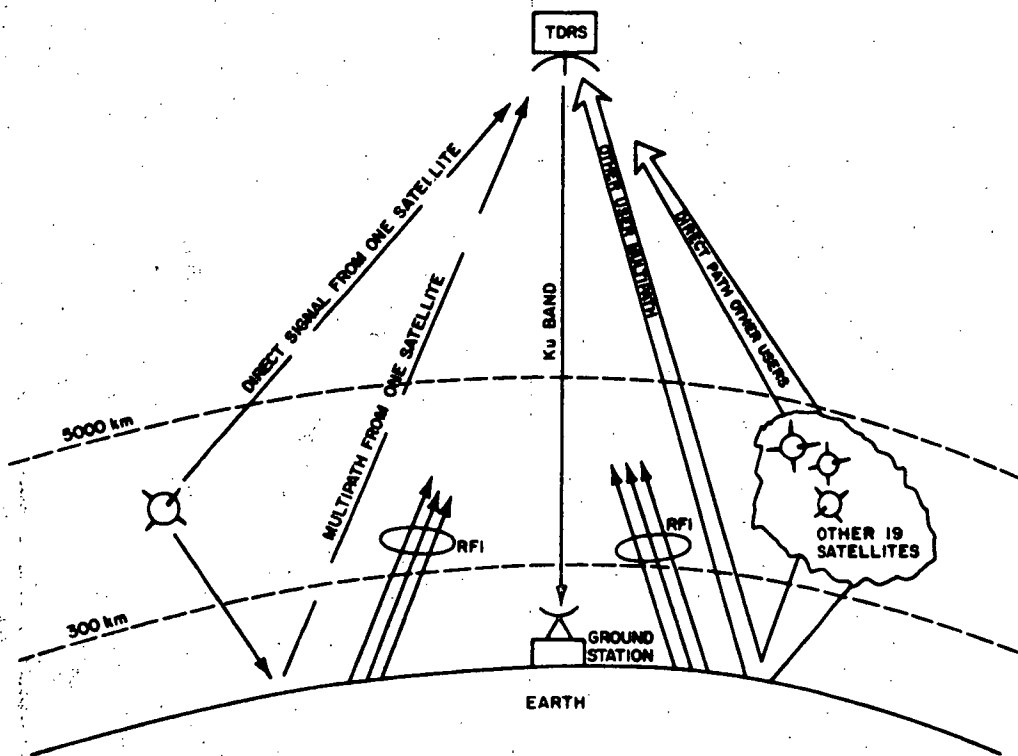


Figure 3-2. Return Link Interference Diagram

4. Co-channel interference between one user and all the other users in the same band. This is peculiar to the return link where all users are simultaneously accessing TDRS through the same channel.

In the sections that follow each of the aforementioned sources of interference will be discussed and their impact on the channel performance evaluated.

3.2.1 Radio Frequency Interference (RFI)

Unintentional, upward directed RFI from emitters located on the earth and in view of both the TDRS and user spacecraft can be a source of interference which will be deleterious. In this section is presented RFI data for the following TDRS/USER links:

<u>Forward Link</u>	<u>Return Link</u>
117.5 MHz (+25 kHz)	137-138 MHz
127.7-127.85 MHz	
148-155 MHz	
400.5-401.5 MHz	

Some of these bands contain relatively high powered constant envelope narrow-band RFI. To evaluate the impact of RFI on the performance of the forward and return links, Magnavox, with the assistance of Mr. John W. Bryan of NASA/Goddard Space Flight Center, has evaluated information relative to RFI in the bands of interest. From computer tabulations provided by Bryan, an estimate of the worst case RFI distribution at the TDRS and user has been derived.

Moreover, ESL, Incorporated recently concluded two related studies for NASA/GSFC (References 3-1 and 3-2) which explain the radio frequency interference problems relating to the TDRSS and the user spacecraft. The RFI modeling by ESL consists of examination of data contained in the International Frequency List compiled by the International Frequency Registration Board of the International Telecommunications Union, the Jeppesen Air Manuals, CONUS emitter tabulations from the Electromagnetic Compatibility Analysis Center and other sources. By a series of prediction programs ESL was able to provide an estimate of the power that would be received from each source of RFI at the TDRS in synchronous orbit with a 16 dB antenna gain. Figures 3-3, 3-4, and 3-5 present a graphical indication of the RFI power density at TDRSS positions of 11°W, 143°W, 112°E, respectively. These densities as presented here are distributed over the frequency band 117 to 155 MHz.

An assessment has been made of the impact of RFI on the user spacecraft. Two user locations are assumed, 50°N/30°E and 38°N/85°W, and the RFI density levels at the user spacecraft are shown in Figures 3-6 and 3-7 respectively. In each case the user spacecraft is equipped with an omnidirectional antenna

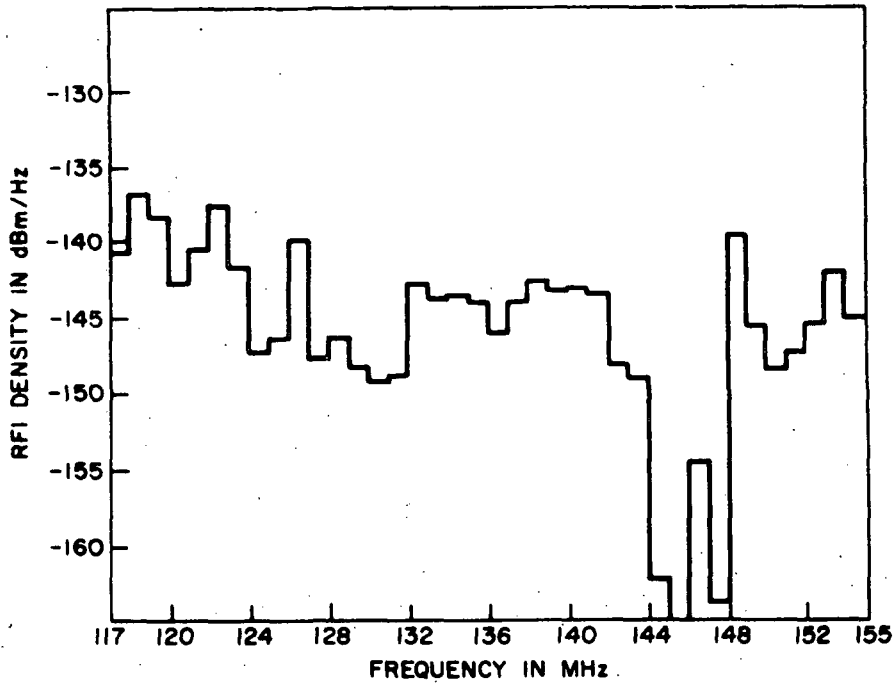


Figure 3-3. RFI Power Density for TDRS Located at 11°W

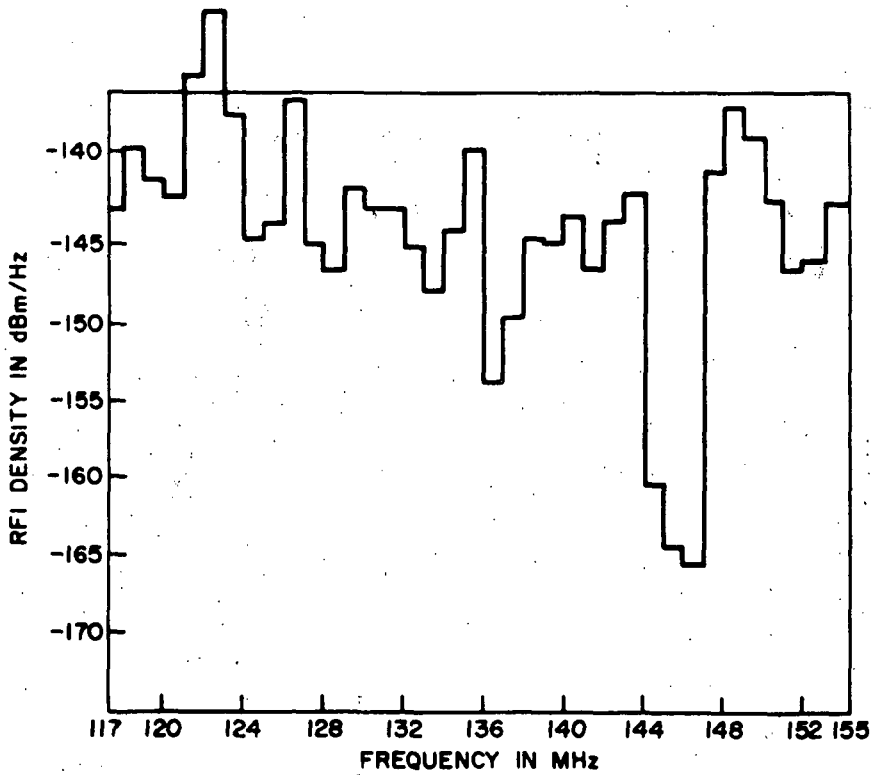


Figure 3-4. RFI Power Density for TDRS Located at 143°W

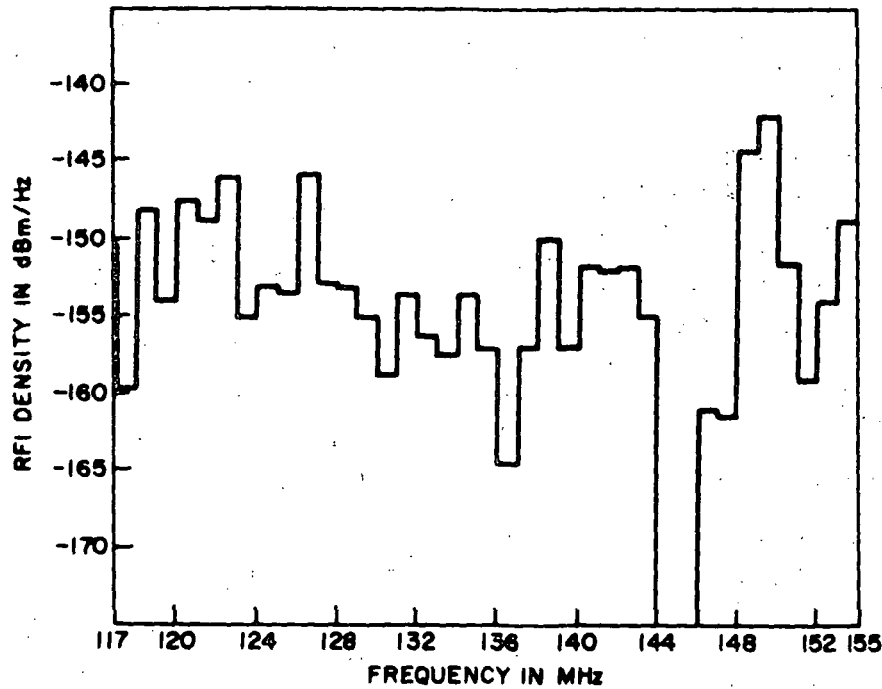


Figure 3-5. RFI Power Density for TDRS Located at 112°E

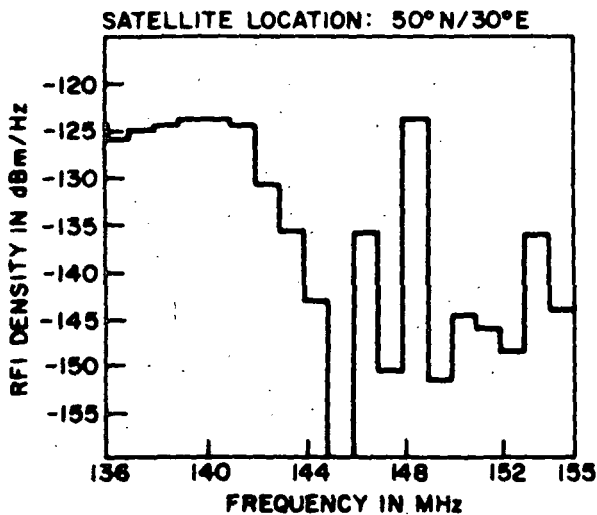


Figure 3-6. RFI Power Density at User Spacecraft (1000-km Altitude and Omnidirectional Antenna-- Satellite Location 50°N/30°E

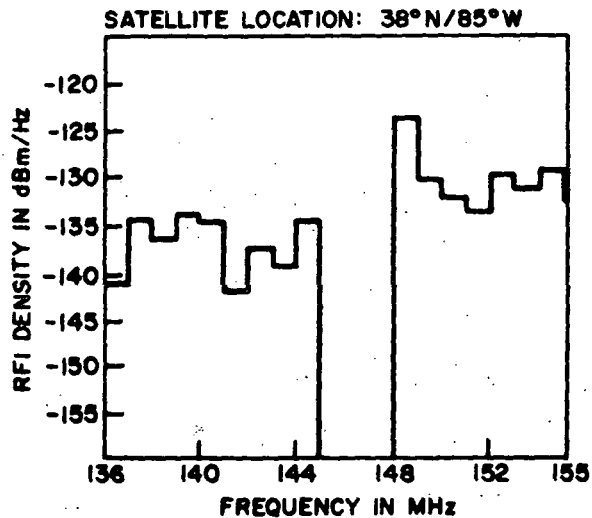


Figure 3-7. RFI Power Density at User Spacecraft (1000-km Altitude) and Omnidirectional Antenna-- Satellite Location 38°N/85° W



and is at an altitude of 1000 kilometers. As an indication of the coverage of this user spacecraft, a satellite at 1000 km centered at 38°N and 88°W will, with an omnidirectional antenna, be in view of all of CONUS, and parts of Mexico and Canada.

Research leads to the conclusion that of the bands of interest the 148-155 MHz band is the least usable as a command band. The number of emitters in the 127.70-127.85 MHz band has been estimated by Bryan as being: 28 communication emitters assigned to the band and 122 communication emitters capable of being tuned in the band. Bryan has conducted a frequency search in this band so that their effect on the user spacecraft might be assessed.

The assumptions made regarding user spacecraft for this assessment are the same as those mentioned previously, including the following:

1. All ground-based emitters are on and modulated.
2. All antenna patterns are uniform, omnidirectional, and zero dB gain.
3. Ground-based emitters are uncorrelated.

The input RFI power at the USER/SC in a 20 kHz band centered around the carrier has been computed and is shown in Table 3-4.

Table 3-4.

RFI Sources at User S/C in the 127.7-127.85 MHz Band

Frequency	Average Power in 10 kHz Band	No. of Emitters
127.70 MHz	-83.4 dBm	6
127.75 MHz	-84.5 dBm	2
127.80 MHz	-81.0 dBm	14
127.85 MHz	-85.0 dBm	1

The number of emitters in the bands 136-138 MHz and 148-155 MHz both at the TDRS and the user spacecraft has been compiled by ESL and are presented in Tables 3-5 and 3-6 respectively. Also shown in the table are the expected RFI power levels at the TDRS and the user spacecraft for various satellite locations.

Table 3-5. Estimated RFI Sources at the TDRS

TDRS Location - (Synchronous Altitude)						
Band	11°W		143 W		112°E	
	Power (dBm)	Number of Emitters	Power (dBm)	Number of Emitters	Power (dBm)	Number of Emitters
136-137	-81.3	132	-87.8	56	-99.4	5
137-138	-79.4	235	-84.3	100	-91.8	10
148-149	-75.1	114	-70.8	789	-79.3	25
149-150	-81.0	70	-72.9	852	-76.9	58
154-155	-80.6	252	-79.9	216	-89.5	46

Table 3-6. Estimated RFI Sources at the User

User Location (Altitude - 1000 km)				
Band	38°N-88°W		50°N-30°E	
	Power (dBm)	Number of Emitters	Power (dBm)	Number of Emitters
136-137	-86.7	5	-71.0	130
137-138	-79.4	25	-70.0	178
148-149	-68.7	80	-69.0	15
149-150	-75.2	53	-97.0	2
154-155	-74.0	127	-89.6	6

The remaining band of interest is that in the range 400.5 MHz to 401.5 MHz. As of this time no attempt has been made to assess the effective RFI power at the user spacecraft. We have, however, compiled through the International Frequency List an estimate of the number of potential RFI sources in this band. This compilation is presented in Table 3-7 for the various ITU regions.



Table 3-7. RFI Sources in the Band 400.5-401.5 MHz

ITU Region No.	Emitter Power on the Ground (Watts)				
	0 - .9	1 - 9	10 - 99	100 - 999	≥1000
I	59	4	1	1	1
II	61	1	-	-	-
III	62	12		10	

3.2.2 "Trash Noise" and its Effect on the TDRS Channels

There is another important source of noise which should be considered and evaluated for its impact on TDRS/User channel. Specifically, this interference is the sum total of the "trash" - a more or less continuous background noise which originates in an urban environment and is due primarily to such things as ignition noise, switching transients, corona, etc. This continuous low level interference will interfere with the desired signals in the command band, and can have a deleterious effect on the antenna temperature at the user spacecraft.

Lincoln Laboratories associated with the Massachusetts Institute of Technology over the past several years has carried out the most comprehensive measurement and evaluation of this continuous background noise. They have concluded that those cities associated with the eastern seaboard can be modeled as an interference source with power uniformly distributed over an aperture which represents the city, and that in the UHF band (216-369 MHz) the power density/square meter/Hz will be in the range of 3×10^{-18} to 1×10^{-18} watts per square meter per Hz. These numbers are representative for moderately large cities such as Miami and Philadelphia, whereas New York City and its associated metropolitan area would produce as much as a 6 dB increase.

Based on experimental data the " α " law equation has been developed (Reference 3-3) to predict galactic noise temperatures with reasonable accuracy in the VHF-UHF frequency and is as follows.

$$T_g = C_g \lambda^\alpha, \quad C_g = [30 \text{ to } 300], \quad \alpha = [2.5 \text{ to } 2.86] \quad (3-1)$$

In the equation above the constant C_g is a function of the galactic activity of the region of space at which the antenna is looking. C_g is

maximum at the galactic center and minimum at its pole. Figure 3-8 plots this function at its extremes.

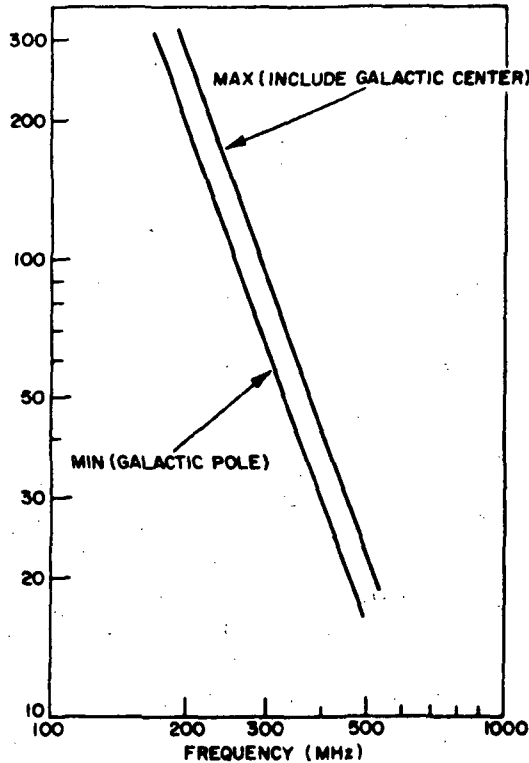


Figure 3-8. Galactic Temperature Over a Hemisphere

A receiver with gain pattern $G_r(\theta, \phi)$ relative to isotropic will receive a power dP_{tr} from a ρ distant differential source having a power density $C(\theta, \phi)$ watts/m²-Hz, area dA , a receiver bandwidth of B , and gain pattern $G_t(\theta, \phi)$ given by the following equation:

$$dP_{tr} = B \left(\frac{\lambda}{4\pi\rho} \right)^2 G_r(\theta, \phi) G_t(\theta, \phi) C(\theta, \phi) dA \quad (3-2)$$

Using the geometry of Figure 3-9 the above equation becomes

$$dP_{tr} = \frac{\lambda^2}{16\pi^2} B G_r(\theta, \phi) G_t(\theta, \phi) C(\theta, \phi) \cot \theta d\theta d\phi \quad (3-3)$$

Integrating and dividing by BK (K = Boltzman's constant) gives the general equation (3-4) for the noise temperature at a receiving antenna due to a distributed noise source, such as the "trash" noise (ignition, generating plants, etc.) radiated by an urban area.



$$T_{tr} = \frac{\lambda^2}{16\pi^2 K} \int_0^{2\pi} \int_{-\pi/2}^{\pi/2} G_r(\theta, \phi) G_t(\theta, \phi) C(\theta, \phi) \cot \theta \, d\theta \, d\phi \quad (3-4)$$

Assuming that a satellite at altitude h with an omnidirectional antenna is centered over a circular urban area of radius r , as shown in Figure 3-10, and that the effective transmitting pattern of the city is $G_t(\theta, \phi) = 1$ equation (3-4) becomes

$$T_{tr} = \frac{\lambda^2 (2\pi)}{16\pi^2 K} \int_{\theta_1}^{\pi/2} C(\theta, \phi) \cot \theta \, d\theta, \quad (3-5)$$

$$\text{where } \sin \theta_1 = \left[\frac{h}{(h^2 + r^2)^{1/2}} \right] = \left[\frac{1}{1 + (r/h)^2} \right]^{1/2}$$

Per the referenced Lincoln Laboratory report, the power density was relatively constant at 10^{-17} watts/m²-Hz over typical cities with the exception of New York which was 5-7 dB higher (see Figure 3-11). Since $C(\theta, \phi)$ is constant at C_0 equation (3-5) reduces further to

$$T_{tr} = \frac{\lambda^2}{8\pi K} C_0 \ln \left(\frac{\sin \pi/2}{\sin \theta_1} \right) = \frac{\lambda^2 C_0}{16\pi K} \ln [1 + (r/h)^2] \quad (3-6)$$

If $r \ll h$ then

$$T_{tr} = \frac{\lambda^2 C_0}{16\pi K} \left(\frac{r}{h} \right)^2 \quad (3-7)$$

Presented in Figure 3-12 is a graph depicting the "trash noise" density as a function of urban radius for various frequency bands and user spacecraft altitudes.

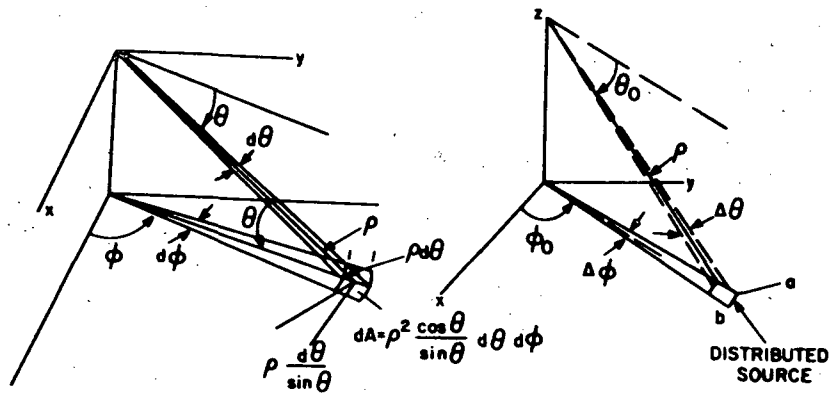


Figure 3-9A. Antenna Coordinate System

Figure 3-9B. Geometry When Distributed Source Is Small Compared to Range

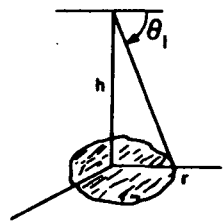


Figure 3-10. Geometry for θ_1 Calculation

3-14

SD 72-SA-0133

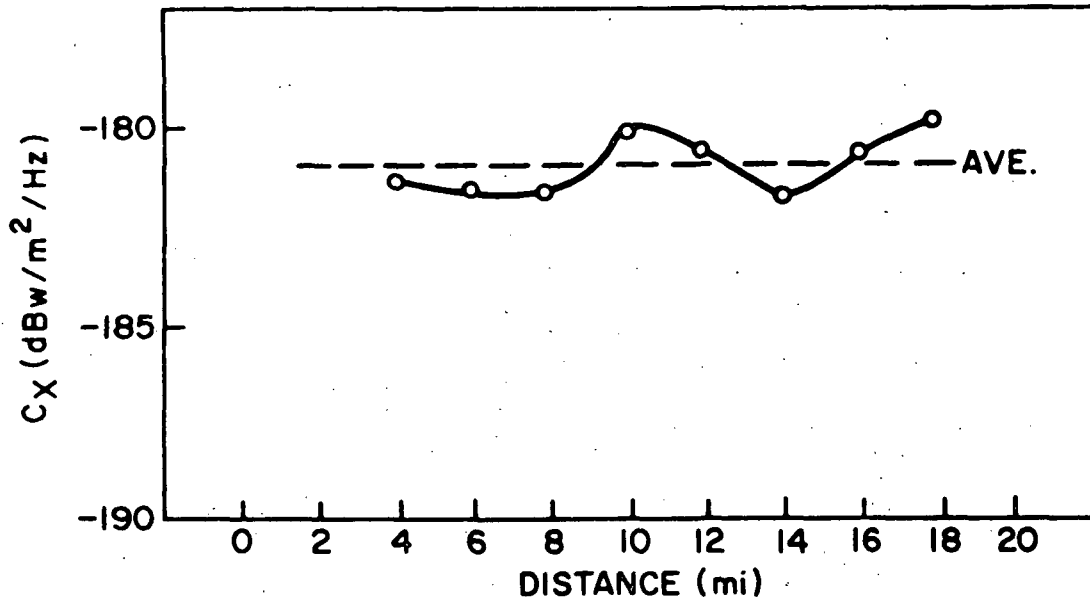


Figure 3-11A. Power Density Profile of Miami at 305.5 MHz

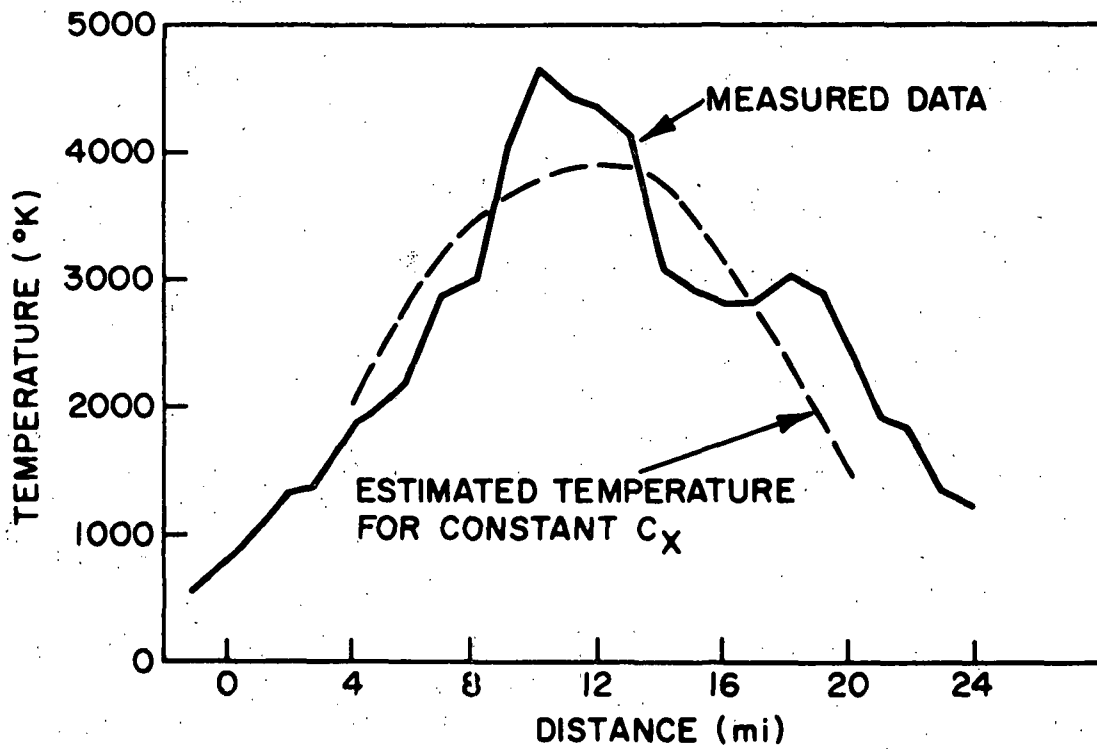


Figure 3-11B. Temperature Profile of Miami at 305.5 MHz, Measured
Traveling North at 18,000 Feet (5490 meters)

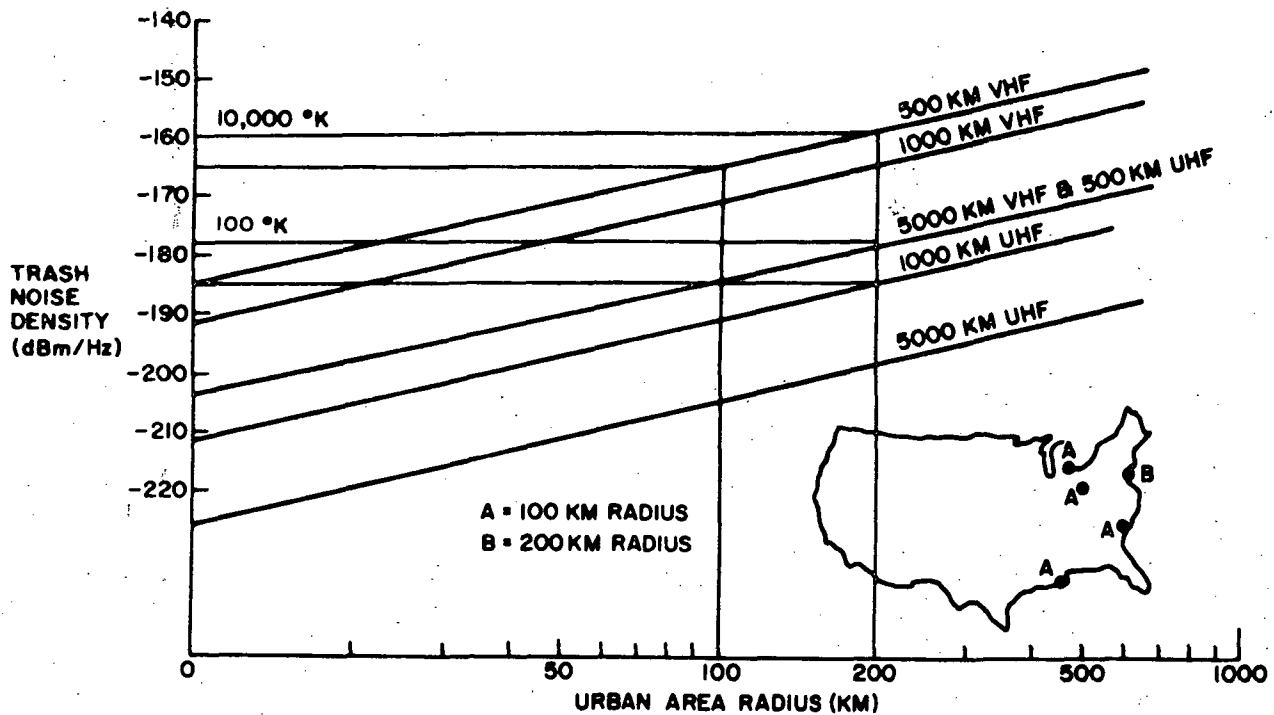


Figure 3-12. Trash Noise at User Spacecraft

It is important also to realize that due to the large field of view of even low orbiting satellites (the area of the U.S. is $9.37 \times 10^6 \text{ km}^2$ or 1.8% of the earth's surface; the field of view of a 300 km orbiting satellite is 2.2) that the radius, r , used above can be large. This is the result of the appearance of many discrete point sources acting as one large area distributed source. Radius values can range from 200-400 km for the NYC area, to 100 km for the Chicago area, to negligible for water or desert areas.

3.2.3 The TDRS User Propagation Path

As shown in Figures 3-1 and 3-2, a signal transmitted from either TDRS or user satellite will arrive at the other satellite by direct and indirect (reflection off a non-smooth earth) channels. This indirect path, commonly referred to as the multipath signal must be understood in order to predict the operation of the communication link. Therefore, it is necessary to define and analyze the parameters in both the direct and multipath channels. A brief summary is presented here and for a more detailed explanation, readers should refer to the work performed by J. N. Birch (Reference 3-4).

3.2.3.1 The Multipath Signal

A multipath signal is characterized by a time varying process which is statistically nonstationary because of the changing velocities and geometry between a user and the TDRS; however, the short-term statistics of this link can be considered stationary. This reflected signal will consist of a diffuse and specular component. The degree of diffuseness or specularity of



the reflected signal will depend upon such factors as the grazing angle ψ , the roughness σ of the earth near the point of reflection, and the correlation length L across the surface of the earth. Roughness factor σ is a measure of the RMS height variations along the surface of the earth, and the correlation length L is a measure of the degree of correlation between points along the surface of the earth. The reflected power can consist of both specular and diffuse components. The specular component is essentially a delayed replica of the transmitted signal, where as the diffuse component is noise like.

The relative expected specular and diffuse reflected power are illustrated in Figure 3-13, as a function of the grazing angle ψ for 136 MHz and an average earth roughness and correlation distance. It can be noted that the specular power decreases with frequency and the diffuse power is essentially independent of frequency. It can be seen that at low-grazing angles the divergence factor serves to diminish the multipath signal, while at high grazing angles the primary reflected energy is diffuse. Furthermore, for reasonable roughness factors and correlation lengths, the primary source of reflected power will be diffuse for grazing angles in excess of 20° at VHF or UHF. Figure 3-14 provides an indication of the multipath signal level as a function of orbital altitude of the user satellite.

Prior to defining the parameters in the channel, the dynamic geometry of the TDRS system must be analyzed to quantitatively identify each of the channel parameters. Each of the user satellites will present a unique time varying multipath geometry as illustrated in Figure 3-15. In that figure R is the direct path between the TDRS and user spacecraft, the multipath would consist of two components S_2 from TDRS to earth, and S_1 from earth to user spacecraft.

Assuming a smooth spherical earth and without considering the effects of the ionosphere and troposphere on such factors as polarization, attenuation, and path length, curves for several of the critical channel parameters have been plotted (Reference 3-5). These curves are representative of data that must be analyzed for the channel between the TDRS and user spacecraft.

3.2.3.2 The Effect of Other User's Co-channel Multipath

It is obvious from Figure 3-14 that the multipath contributed by a user depends upon its altitude and user antenna anomalies. For the moment we will defer the discussion of antenna anomalies, but system anomalies will be considered in our concluding statements.

In the forward link the plot of Figure 3-14 can be used directly; however, consider for the moment the return VHF link where 20 user signals are accessing a TDRS simultaneously. Obviously the total multipath signal consisting of the multipath from 20 users in the field of view of a TDRS will depend upon the user altitudes. These altitudes are in turn determined by the population and orbits associated with the respective users. In Table 3-8 are listed the projected satellite populations for the low altitude user spacecraft from 1976 through 1980.

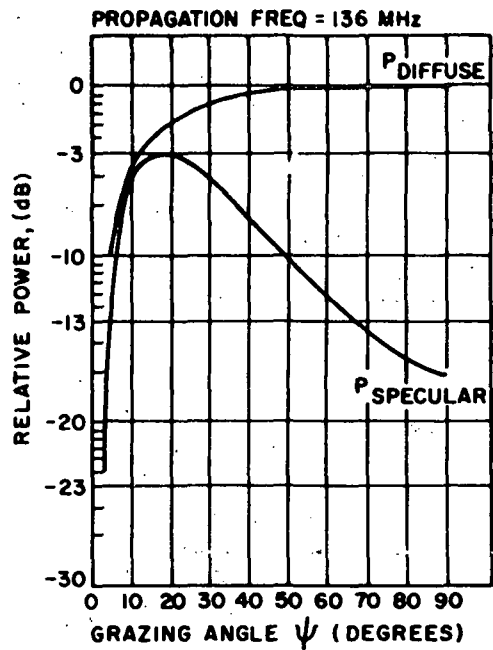


Figure 3-13. Relative Specular and Diffuse Reflected Power Versus Grazing Angle

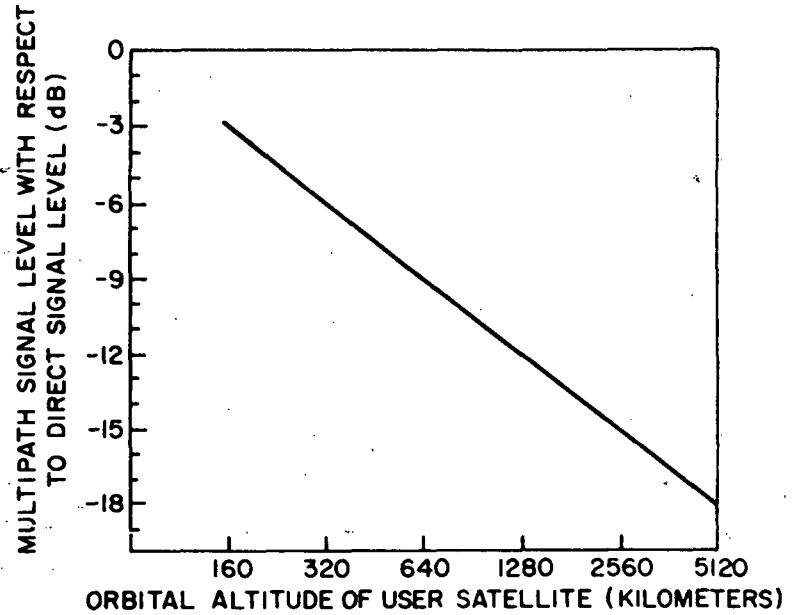


Figure 3-14. Multipath/Direct Signal Ratio as a Function of Orbital Altitude

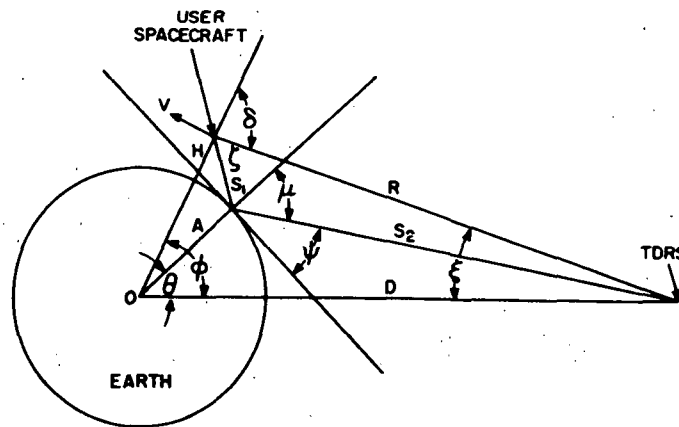


Figure 3-15. TDRS Multipath Geometry

3-18

SD 72-SA-0133



Table 3-8. Low Altitude Spacecraft
Population Projections: 1976-1980

Year	76	77	78	78	80
<u>ALTITUDES</u>					
150-276 km	1	1			
275-300	4		1	1	1
300-400	7	7	1	2	2
400-600	9	9	4	2	
700-800	10				
800-900	9	8	3		
1000-5000	10	9	2	3	3
> 5000	8		6	4	4

The table indicates that the 1976 user population is the largest. Figure 3-16 shows the total multipath contributed by the total satellite population by year.

The multipath signal contributed by 20 simultaneous users in 1976 indicates that the total multipath relative to one user is +7 dB/TDRS. (The multipath-to-one user power ratio shown in Figure 3-16 is for the entire 1976 population; Assuming one TDRS would see one-half the population at one time results in a decrease of 3 dB in that ratio.) Thus, the multipath problem in the return link is diminished from the worst case condition where all 20 users are considered to be in low orbits, e.g., 300 km.

Unless stringent and relatively expensive antenna designs are used by the low orbit user, antenna anomalies can occur in the antenna patterns. Some of the antenna patterns associated with low data rate user spacecraft have been evaluated and it was found that a nominal 0 dB antenna is impractical and one must consider at least a +3 dB variation in the low data rate user antenna. In other words, the direct path signal can be reduced by 3 dB while energy directed toward the earth can be enhanced by 3 dB, producing a 6 dB variation at times between the direct desired signal and the multipath signal.

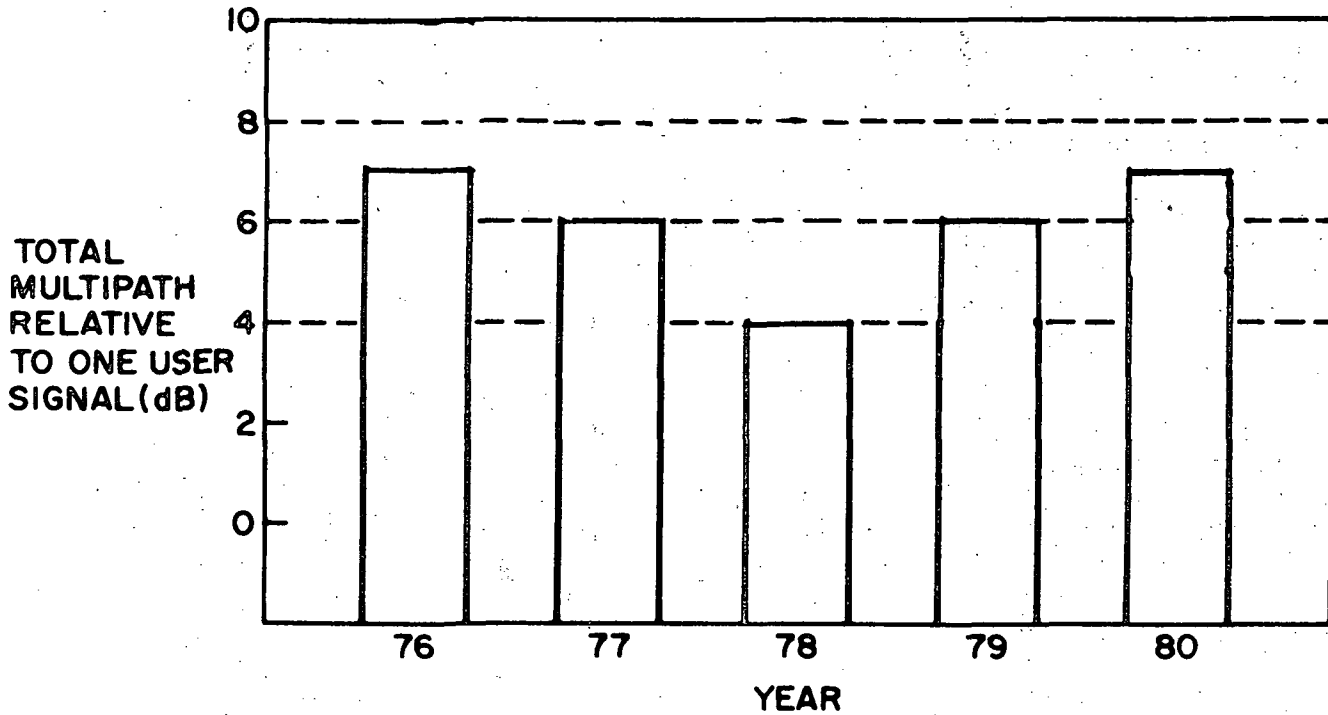


Figure 3-16. Projected Multipath Level

When a large number of user signals are accessing the TDRS, the antenna anomalies average out in the multipath signal so that for purposes of analysis the multipath signals from the various users can be considered as originating from 0 dB omnidirectional antennas.

3.2.3.3 The Direct Path Interference Due to Other Users

As shown in Figure 3-2 a return link signal will be subjected to interference not only from RFI, and user multipath signals, but from other signals originating from the 19 other user spacecraft and propagating along the direct path from user-to-TDRS. It is assumed that at the point of transmission these signals are of equal power. Their effect, therefore, will be much more pronounced than that of the return link multipath signals because while the multipath/signal ratio over the user altitudes of interest are on the order of 7 dB and the direct path interference/signal ratio is on the order of 12 dB. Moreover, as the user spacecraft of interest increases its altitude, the effect of its own multipath decreases significantly where as an increase in altitude over the range of interest (300-500 km) produces almost no change in the ratio of other users direct path power to desired signal. This effect will be shown in more detail in following sections.

3.3 FREQUENCY SELECTION

One of the objectives of this study has been to examine those portions of the electromagnetic spectrum set aside for space use, in order that a set of operationally functional operating frequencies for the TDRSS are selected. Contained herein is a description of the frequency bands of interest and a general TDRSS frequency plan.

3.3.1 Frequency Trades

A set of frequency bands, for both ground/space and space/space communications links, was provided by the TDRS Project Office at NASA/GSFC to aid in the selection of an appropriate set of frequency assignments for the various operational links. Frequency band selections, as presented by the project office, are shown in Tables 3-9 and 3-10 for the ground/space link and the space/space link, respectively.

During the course of the study four LDR forward link frequency bands were investigated, namely:

VHF { 117.50 MHz (BW = 50 kHz)
127.75 MHz (BW = 100 kHz)

UHF 401 MHz (BW = 1 MHz)

S-band 2025-2120 MHz

As will be shown in Section 3-5, an assignment at 117.5 MHz is considered to be impractical because the narrow channel bandwidth assignment (50 kHz) is not adequate to meet the range error requirements. Furthermore it does not provide enough processing gain to offset the effects of co-channel multipath. A similar objection is presented for an assignment at 127.75 MHz. In this case the 100 kHz band would appear to be adequate; however, if it is split into two 50 kHz bands (one per TDRS) it can be shown that the range accuracies specified in the work statement (namely 15 meters rms) cannot be achieved.

Table 3-9. TDRSS Ground/Space Link Frequency Band Selection

Requirement	Ground to Space Link	Space to Ground Link
Primary frequency Ku-band	13.4 to 14.0 GHz	14.6 to 15.2 GHz
Back-up frequency S-band	2200-2290 MHz	2025 to 2110 MHz
Launch Phase Station keeping VHF	148-150 MHz	136-138 MHz

Table 3-10. TDRSS Space/Space Link Frequency Band Selection

Link	LDR User Link	MDR User Link
Telemetry	VHF: 136 to 138 MHz	S-band: 2200 to 2300 MHz
Command	VHF: 108 to 132 MHz (2-100 kHz channels) UHF: 400.5 to 401.5 MHz (2-500 kHz channels)	S-band: 202- to 2120 MHz

As shown in Section 3.2, there appear to be fewer sources of RFI at UHF than at VHF, making the former a more attractive band for the LDR forward and return link. Moreover, evaluation of the "trash noise" impact indicates that this interference source is 20 dB less at UHF than at VHF (e.g., a "trash noise" temperature of 10,000°K at VHF would be on the order of 100°K at UHF), thereby reducing by two orders of magnitude the "trash noise" contribution to system noise temperatures.

On the LDR return link the 136-138 MHz band, while possessing a considerable amount of RFI (see Section 3-2), appears to be the least susceptible. Within this band indications are that the 136-137 MHz segment is the preferable one.

The MDR links, both forward and return, appear to offer no particular area of trade-off. The links are relatively RFI free; therefore, selection is merely a function of obtaining appropriate frequency assignments such that adjacent band introduce minimum interference.

The space/ground link at Ku-band has adequate bandwidth allotted to handle both forwardlink and returnlink signals in an FDM mode. One aspect of the space-ground link which has required considerable investigation has been that concerned with rainfall margin. Solutions such as increased TDRS transmit power, increase GS antenna gain, or pre- and post detection spatial diversity combining at the GS are viable solutions to this problem. AIL has investigated this problem extensively and has prescribed several alternative approaches to solve the problem.

The final item which has impacted on the frequency trades has been the recommendations by IRAC regarding the flux density observed at the earth's surface from a signal emanating from an earth orbiting satellite. For the bands of interest the more recent IRAC guidelines are as follows:

<u>Frequency Band</u>	<u>Flux Density in 4 kHz</u>
VHF	- 144 dBw/m ²
UHF	- 150 dBw/m ²
S-band	- 154 dBw/m ²
X-band	- 150 dBw/m ²
Ku-band	- 152 dBw/m ²

The carrier flux density at the earth's surface from an emitter with antenna gain G_T can be approximated by

$$\text{Flux density} = \frac{P_T \cdot G_T}{4\pi R^2} \quad (3-8)$$



where

P_T = transmit power in dBw

R = distance from the emitter to earth in meters

To conform with the IRAC measurement, which is made in a 4 kHz bandwidth, and to take into account any spectrum spreading (BW) of the signal, the following relationship is used:

$$\text{Flux density (dBw/m}^2\text{/4 kHz)} = \frac{G_T \cdot P_T \cdot 4 \times 10^3 \text{ Hz}}{(4\pi R^2) \text{ BW}} \quad (3-9)$$

With the TDRS at synchronous altitude the expression, when solved for spread bandwidth required to meet the flux density specification is,

$$\text{Spread bandwidth (BW)} = \frac{\text{EIRP} \cdot 4 \times 10^3}{4\pi R^2 \cdot [\text{Flux Density}]} \quad (3-10)$$

or in dB notation

$$\text{BW}_{\text{dB}} = \text{EIRP} + 36 - 162 - \text{Flux Density} \quad (3-11)$$

The minimum spread bandwidth required to reduce the flux density to an acceptable level is presented in Table 3-11.

Table 3-11. Bandwidth Spreading
Required to Meet IRAC Specifications

Frequency Band	EIRP	Minimum Spread Bandwidth
VHF	30 dBw	63 kHz
UHF	30 dBw	250 kHz
S-band	41 dBw	8 MHz
X-band	48 dBw	16 MHz
Ku-band	52 dBw	63 MHz



3.3.2 Frequency Plan

From the set of candidate frequencies and their associated channel bandwidths, the overall frequency plan shown in Table 3-12 has been recommended.

Table 3-12. System Frequency Plan

Links		Frequency	Channel Bandwidth
Forward Link	LDR	400.5 to 401.5 MHz	1 MHz 4-250 kHz channels
	MDR		
	S-band:	2025 to 2120 MHz	95 MHz channel
	Ku-band:	14.6 to 15.2 GHz	4-100 MHz channels
Return Link	TDRS/GS		
	Ku-band:	13.4 to 13.64 GHz	240 MHz
	VHF	148 to 150 MHz	--
	S-Band	2200 to 2290 MHz	90 MHz
Return Link	LDR	136 to 138 MHz	2 MHz (20 users multiple accessed/TDRS)
	MDR		
	S-band	2200 to 2300 MHz	20-10 MHz slots in 5 MHz steps or 100 MHz wide open (two users/TDRS)
	Ku-band	13.6 to 14.0 GHz	4-100 MHz channels
	TDRS/GS		
	Ku-band	14.6 to 15.2 GHz	200 or 600 MHz channel
VHF	136.11 MHz	--	
S-Band	2025-2110 MHz	85 MHz	

3.4 MODULATION AND CODING

3.4.1 Impact of Forward Error Control on the Medium and Low Data Rate Users

This section discusses the impact of forward error control for the medium and low data rate users of the TDRSS. Error correction coding and its benefits have been understood for many years. Recent advances in circuit technology have provided economical implementation of forward error coding techniques in digital communications systems.



Convolutional encoding with either maximum likelihood or sequential decoding are popular methods of improving link reliability, reducing EIRP, or increasing link capacity. Block codes which preceded the development of convolutional coding will not be discussed in this report, rather the benefits which can be obtained through convolutional encoding with either sequential or maximum likelihood decoding will be addressed. Shown in Figure 3-17 are the performance curves for convolutional encoding with maximum likelihood decoding for a rate 1/3 coder. The curves are shown for constraint lengths of 5 and 6 with soft decisions (3-bit quantization). Also shown in Figure 3-17 is a performance curve for a (48/24) non-systematic code with sequential decoding.

Shown in Figure 3-18 are performance curves for rate 1/2 convolutional encoding with maximum likelihood decoding with constraint lengths of 5 and 6. The results are valid for 3-bit quantization at the inputs to the decoder.

In Table 3-13 the coding gain for rate 1/2 convolutional encoding/maximum likelihood decoding is summarized.

Most modern digital communication systems, e.g., the TDRSS, are a form of PSK, delta-coded PSK (Δ PSK). For a Δ PSK signal the bit error probability (BEP) is given by $2P(1-P)$ where P is the BEP for ideal PSK. The loss in performance for Δ PSK is slight for BEP's between 10^{-3} and 10^{-5} as shown in Figure 3-19.

3.4.1.1 Convolutional Code Background

In convolutional encoding, information digits are fed to the encoder k_0 at a time; corresponding to these, n_0 digits are emitted from the encoder (where $1 \leq k_0 < n_0$). In a systematic code, the first k_0 of the n_0 are identical to the k_0 input digits, while the remaining $n_0 - k_0$ are computed check digits. If the code is non-systematic, all n_0 encoder output digits are computed in a simple but non-trivial way from the k_0 inputs. In either case, the code has rate $R = k_0/n_0$ bits/binary digit. The n_0 digits are immediately inserted into the digit stream entering the modulator. This process can be thought of as generating a code tree consisting of branches and nodes, with each branch corresponding to a particular choice of k_0 information bits and with 2 branches originating at each node. The maximum length of any path starting at the base of the tree is the code constraint length n_A channel digits.

Convolutional encoding is simple and inexpensive through use of a shift register, which consists only of delays (flip-flops) and modulo-2 adders (exclusive-OR gates). A convolutional encoder is shown in Figure 3-20. Decoding implementation varies according to the type of decoding algorithm (e.g., sequential, or Viterbi (maximum likelihood)), but in all cases the decoder must contain a replica of the encoder. Like encoding, decoding of convolutional codes takes place k_0 information digits at a time.

Table 3-13. Viterbi Decoding Output Error Rate Performance

Soft Decision Q = 8

Output Error Rate	Uncoded Δ PSK E_b / N_0	K = 7	K = 6	K = 5
		Coding Gain Over Δ PSK	Coding Gain Over Δ PSK	Coding Gain Over Δ PSK
1×10^{-6}	10.5	5.6	5.0	4.6
1×10^{-5}	9.9	5.25	4.75	4.4
1×10^{-4}	8.7	4.7	4.3	4.0
1×10^{-3}	7.4	3.8	3.5	3.3
1×10^{-2}	5.1	2.2	2.0	1.9

K = Constraint Length
 Q = Quantization Level

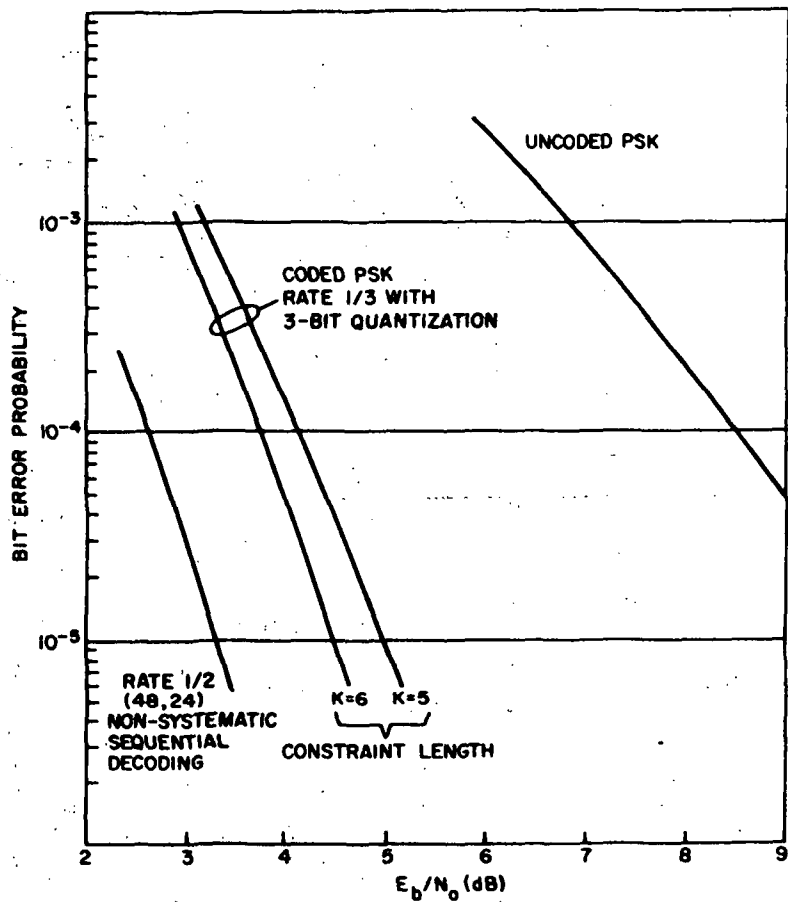


Figure 3-17. Comparison of Sequential and Rate 1/3 Maximum Likelihood Decoder Performance

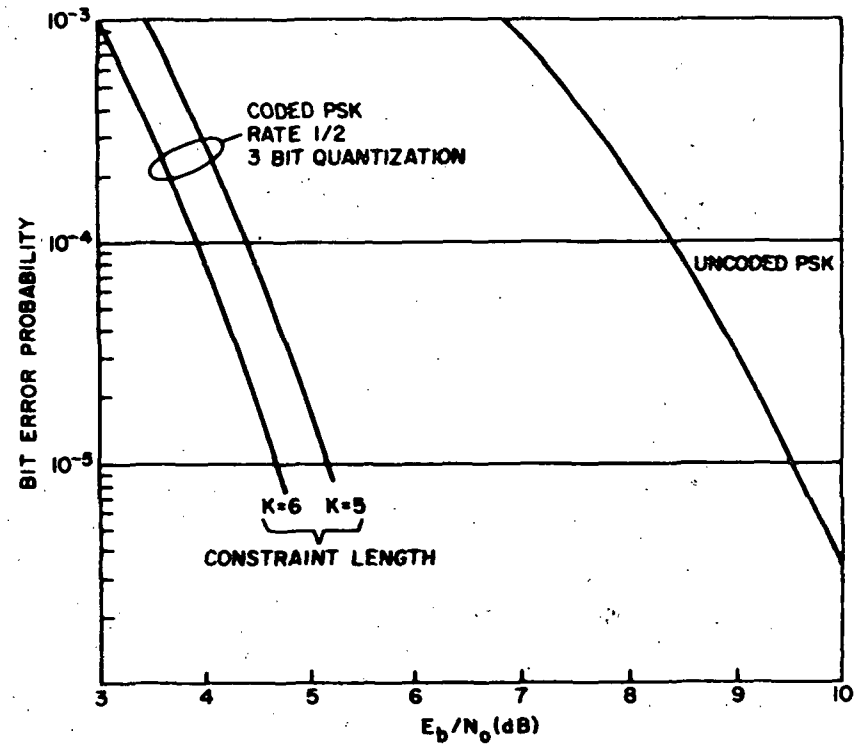


Figure 3-18. Rate 1/2 Maximum Likelihood Decoder Performance



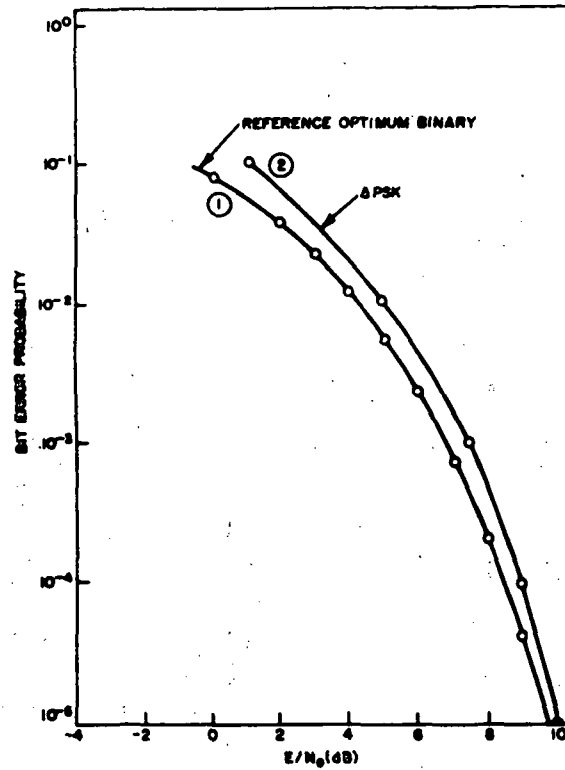


Figure 3-19. Optimum Binary PSK and Δ PSK Versus E/N_0

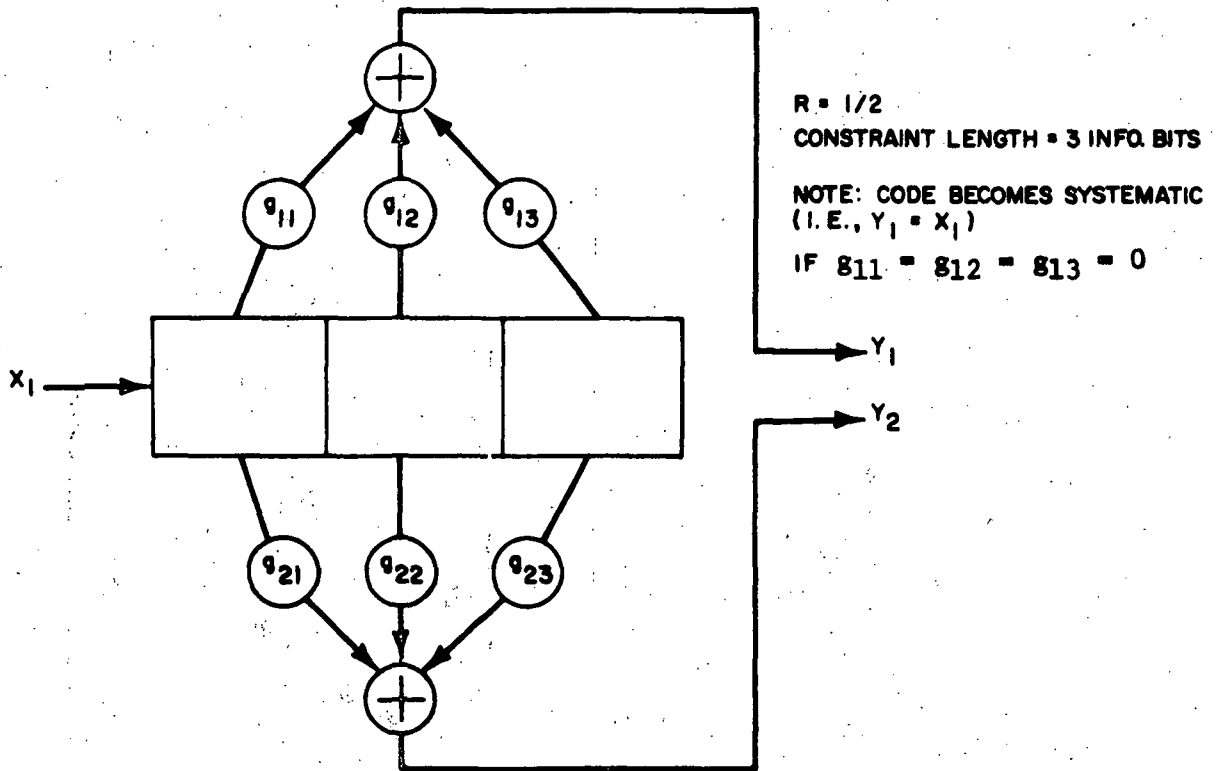


Figure 3-20. General Encoder for Convolutional Code

3.4.1.2 Sequential Decoding

Sequential decoding is relatively low in cost. An estimate of the encoder cost, based on data obtained from Magnavox Research Laboratories, is \$500 for the necessary 16 flat packs. This is for a rate 1/2 encoder operating at 100 bps to kbps with a constraint length $n_A = 128$ channel digits (i.e., 64 data bits and therefore a 64-stage LFSR). This estimate also assumes the availability of a clock external to the encoder. The decoder is more difficult to price, but based on a prototype sequential decoder, which operates at megabit rates, a \$20,000/copy cost seems accurate. Figure 3-21 shows a sequential decoder block diagram.

3.4.1.3 Maximum Likelihood (Viterbi) Decoding

The Viterbi algorithm (Reference 3-6) is a decoding algorithm which utilizes convolutional codes to generate a set of mutually orthogonal waveform sequences over the code constraint length of K information bits. The algorithm is non-sequential in the sense that it does not operate along just one code tree path at a time as sequential decoding does. Rather, it performs and keeps a record of a series of decisions numbering $2^K - 1$. In addition, the transmitted information does not constitute a continuous stream. It is instead separated at prescribed intervals by an all-zero synchronizing sequence which serves to reduce the effective transmission rate somewhat. The encoder is as shown in Figure 3-20 while Figure 3-22 shows the decoder in block diagram form.

Cost data for a rate 1/2 maximum likelihood decoder using 3-bit quantization are given in Table 3-14. These prices are for a decoder speed up to 2-megabits/sec. It can be seen that the cost (not sell price) of a maximum likelihood decoder is well below that of a sequential decoder of comparable performance. Since the encoder is identical to that for sequential decoding, encoder costs are also the same, about \$500.

Table 3-14. Cost and Performance Data
for R = 1/2 Maximum Likelihood Decoder

(Non-systematic code, 3-bit quantization, for $P_B = 10^{-5}$)

K Constraint Length	DIP's*	Parts	Wiring	Labor	Total Recurring Cost
5	240	\$2500	\$1500	\$2500	\$6500
6	500	\$4000	\$1500	\$2500	\$6500
7	1000	\$6000	\$1500	\$2500	\$6500

*MSI Dual In-Line Packages

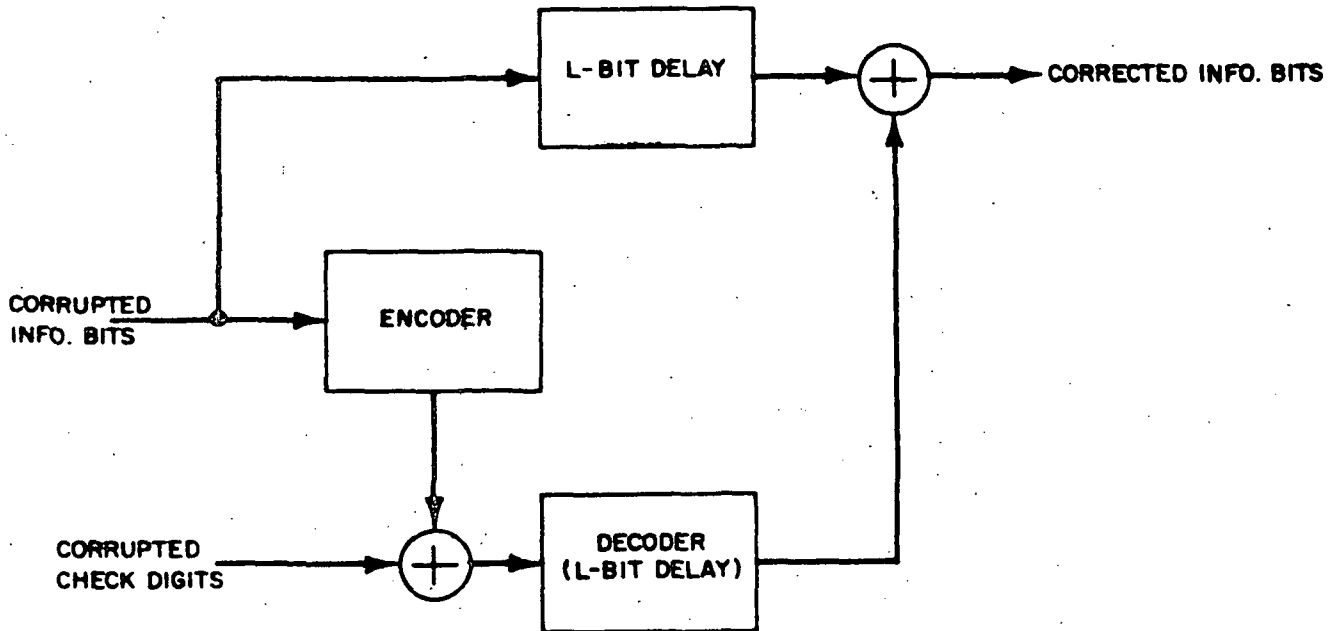


Figure 3-21. Sequential Decoder ($R = 1/2$ Systematic Code)

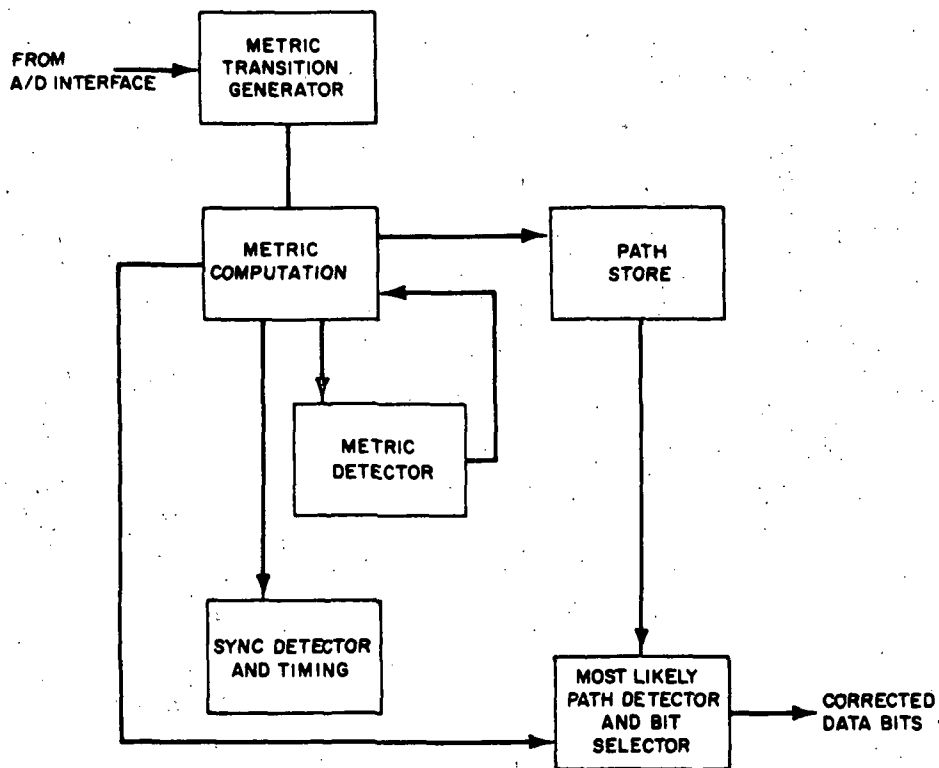


Figure 3-22. Maximum-Likelihood (Viterbi) Decoder

First decoder costs \$50K to build.

Sell price for lots of 50: \$20 K/copy for K = 5
\$30 K/copy for K = 7

In summary then, forward error correcting coding such as convolutional encoding with sequential or maximal likelihood decoding is a cost-effective way of providing, the following:

- ° additional link margins
- ° increased channel capacity
- ° reduction in EIRP
- ° completely compatible with digital and/or PN systems.

This means that a coding gain of 5 dB could provide 5 dB of additional margin, (a capacity increase by a factor of 3), or require 5 dB less EIRP from a user spacecraft.

3.4.2 Voice Coding for Manned Users of the Tracking and Data Relay Satellite System

Under NASA contract NAS5-20168 (Reference 3-7), the Magnavox Advanced Systems Analysis Office conducted a detailed analysis of advanced voice coding techniques. This study was conducted for an L-band satellite-based air traffic control system. Much of the research from that program is directly applicable to the manned users of the TDRSS.

The voice coding techniques include adaptive narrowband FM, pulse duration modulation, adaptive delta modulation, and predictive coding. Adaptive narrowband FM is an analog technique whereas pulse duration modulation is a hybrid system. Both adaptive delta mod and predictive coding are digital techniques.

The Department of Defense is supporting research in predictive coding techniques for voice signals. Predictive coders are still in the computer simulation or breadboard stage and must be considered developmental. Furthermore, the performance of the predictive coder in the presence of digital errors has not been established. The performance, cost, size, weight, power requirements, etc., for the predictive coders should be established by 1974 and high quality speech should be available with predictive coders at data rates between 3.6 to 9.6 kbps by 1975. With the advent of LSI it will be feasible to implement predictive coders in small, cost-effective packages. Predictive coding offers great promise but still is in the developmental stage. For this reason predictive coding will not be discussed further; the report will be confined to the performance of adaptive narrowband FM, pulse duration modulation, and adaptive delta modulation. Functional diagrams for the respective voice coding techniques are shown in Figures 3-23 through 3-26.

With regard to implementation, adaptive narrowband FM and adaptive delta mod require about the same order of complexity, whereas PDM is more complex on a relative basis. All three coding techniques, however, are inexpensive.

The performance of a voice coding technique is determined by two parameters: intelligibility, and quality. Of these two parameters the former is objective. It is determined by an intelligibility test measurement whereas the second is somewhat subjective, determined by the preference of the listener. The two parameters do not correlate in all cases; for example, as a function of bit error probability or as a function of carrier to noise density.

There are a number of intelligibility tests available to determine the performance of the communications system. These include: sentence tests, rhyme tests, phonetically balanced Harvard word tests, and nonsense tests. It is an accepted fact that the thousand word phonetically balanced (PB) Harvard word test is a practical test which gives maximum discrimination over all values of carrier to noise density while the sentence test is indicative of space communications messages. Shown in Figure 3-27 are curves which relate intelligibility of sentences such as space communication messages to the intelligibility scores for the 1000 word PB test. Note that a low score for the PB tests results in a high intelligibility score when space communications messages or sentences are used.

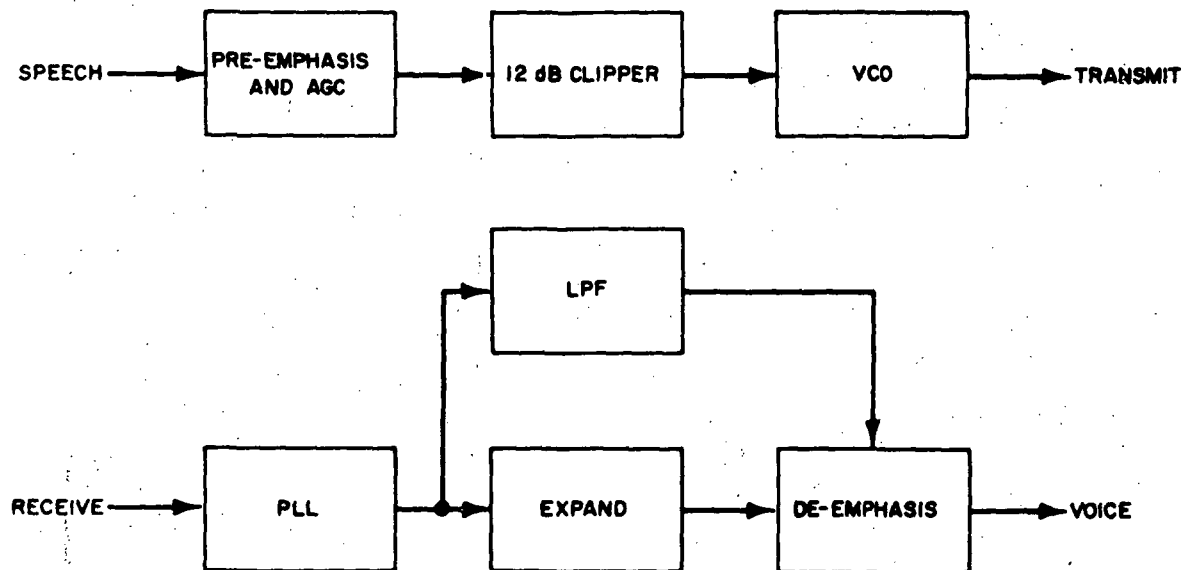


Figure 3-23. Bell Aero's Adp-NBFM

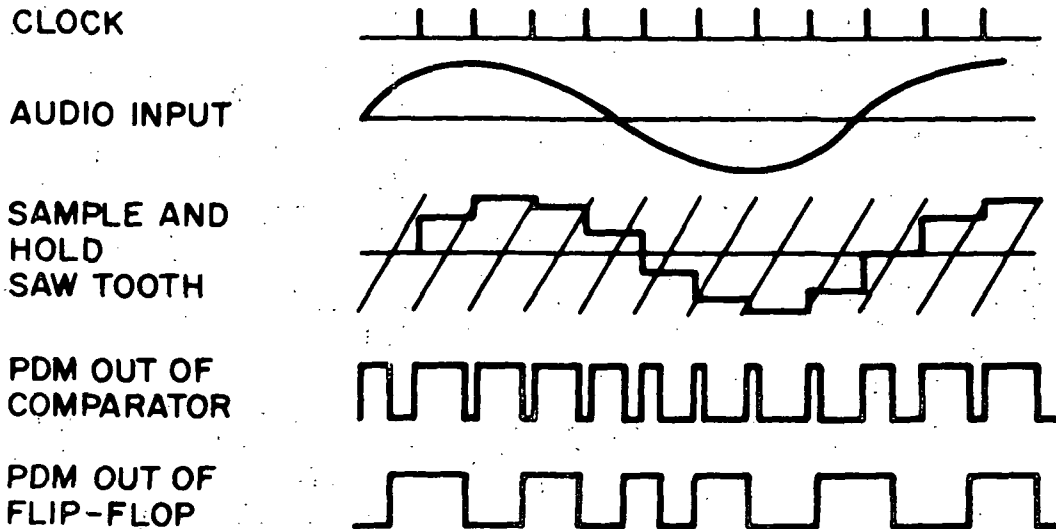
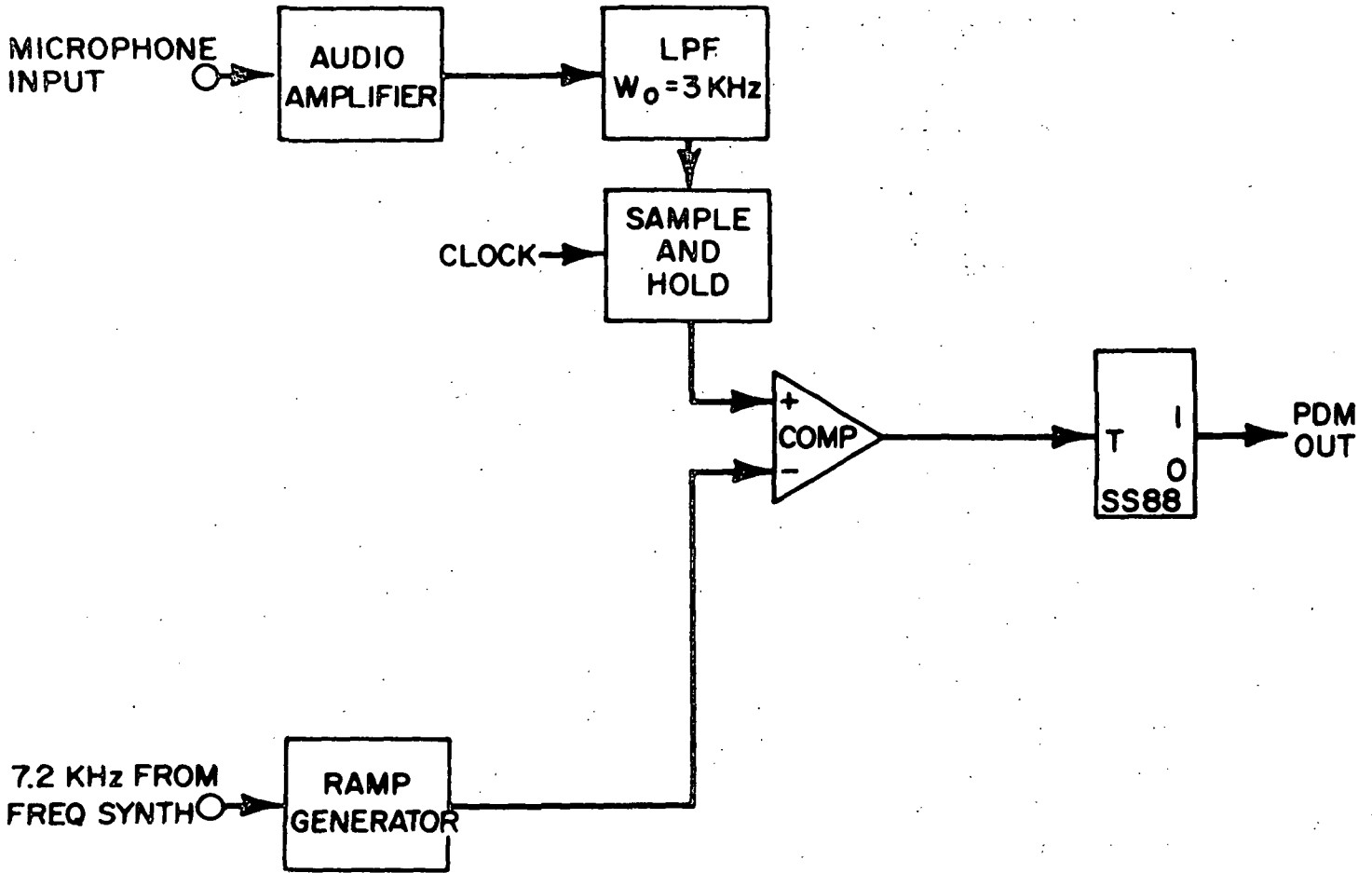


Figure 3-24. PDM Modulation and Modulator Waveforms

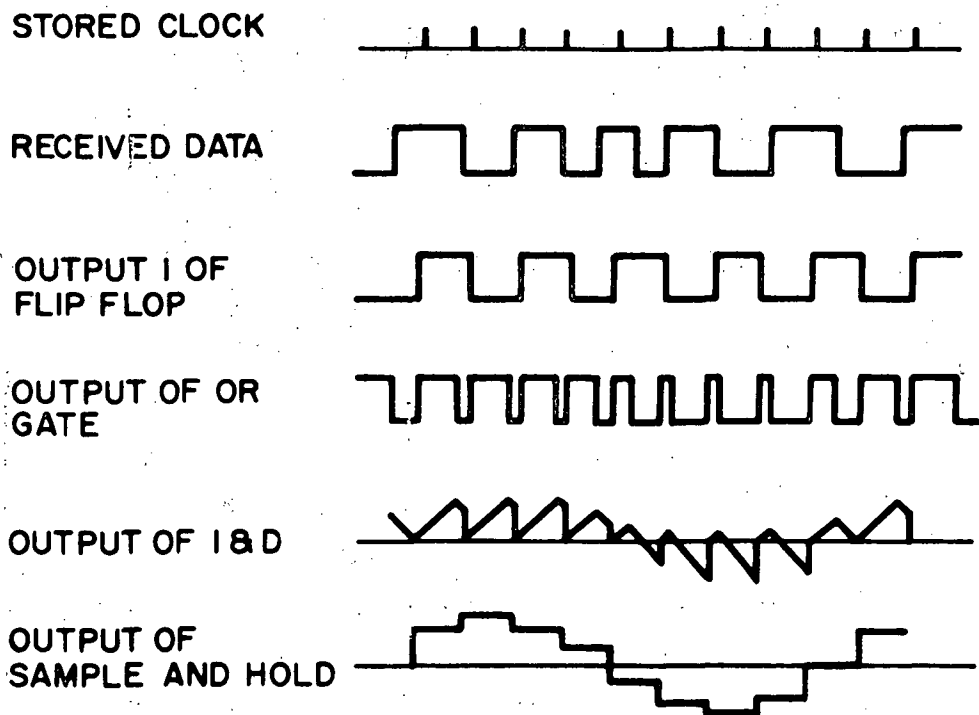
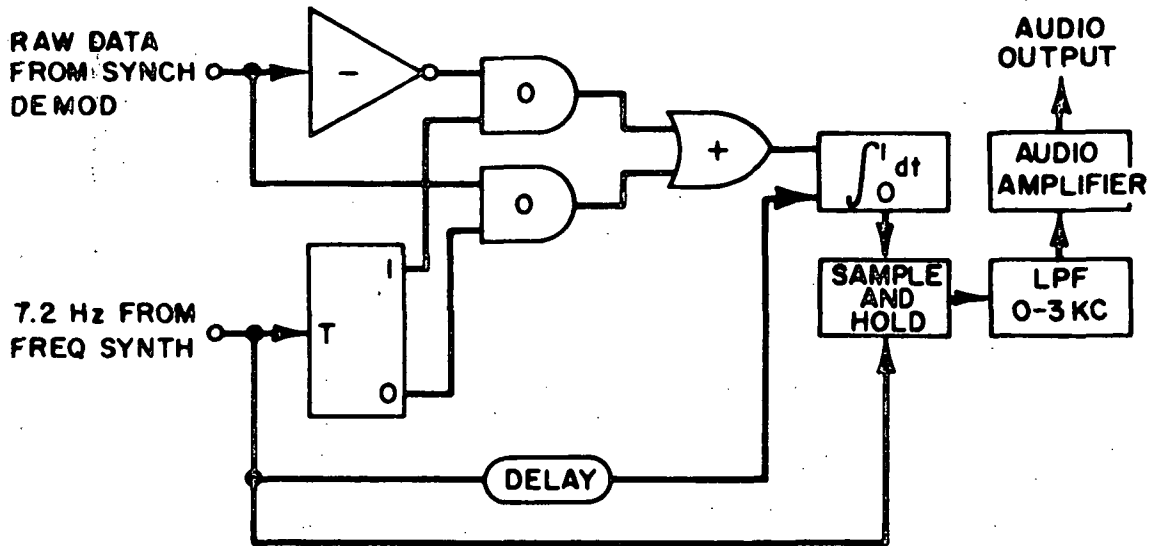


Figure 3-25. PDM Demodulator and Demodulator Waveforms

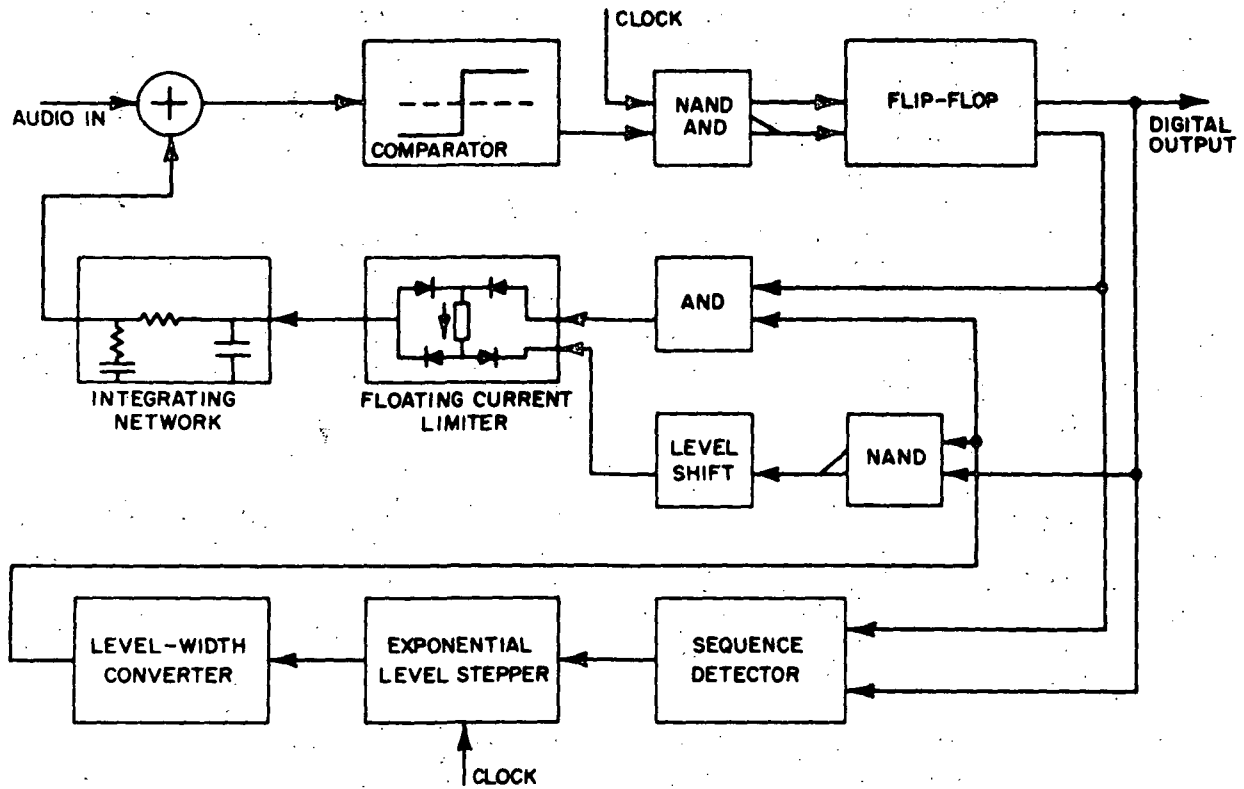


Figure 3-26. Companded Delta Coder (IBM)

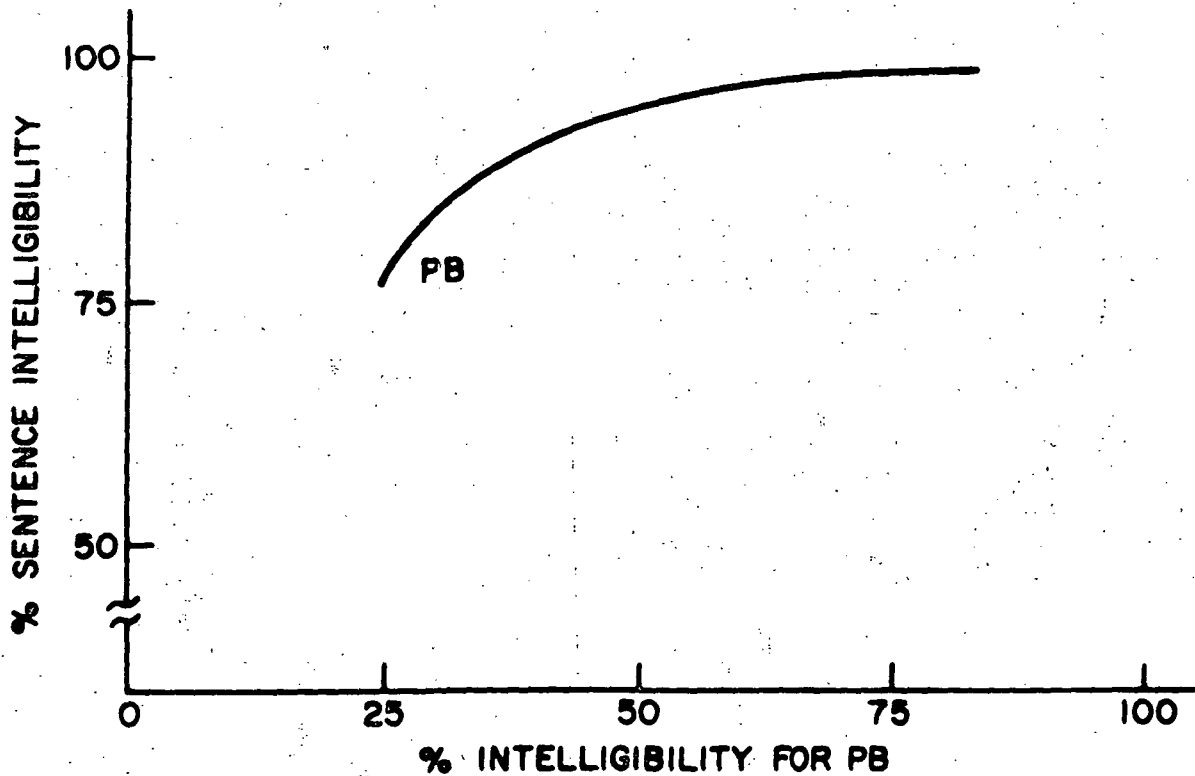


Figure 3-27. Sentence Intelligibility Versus PB Intelligibility



With regard to quality, it is often determined subjectively by allowing listeners to choose the system they prefer as opposed to rating the systems on intelligibility basis. Those systems such as adaptive narrowband FM and PDM, which exhibit little or no threshold at low values of carrier to noise density (i.e., 40 dB-Hz), usually provide higher quality than do digital systems at low values of C/N_0 . For example, adaptive delta mod, while maintaining high intelligibility at low carrier to noise densities, will, when errors become appreciable, be subjectively displeasing to a listener. Thus, at low carrier to noise densities, the adaptive delta mod renders poor quality but good intelligibility; whereas at low carrier to noise densities, both PDM and adaptive narrowband FM may have poorer intelligibility scores relative to adaptive delta mod but render higher quality. Shown in Figure 3-28 is the intelligibility score based on a PB word score of 1000 words for adaptive delta mod at 20 kbps, PDM, and ANBFM, as a function of a carrier-to-noise density. Note that there are two curves associated with adaptive delta mod. One curve indicates the performance of adaptive delta mod for perfect PSK transmission, whereas the second curve indicates the performance of adaptive delta mod when delta PSK and a Costas loop receiver is employed. The adaptive delta mod signal is impervious to reversals in the digital stream and uncoded adaptive delta mod signal should follow the performance of a perfect PSK transmission. Note that PDM and adaptive narrowband FM maintains a moderate intelligibility based on the PB word test even at low values of carrier-to-noise density, e.g., 40 dB-Hz.

Adaptive delta mod, however, has some distinct advantages. That is, an all-digital system that can be encoded with forward error control techniques, can be regenerated at various points in the system, and is simple to implement. For these reasons, and the fact that it maintains a high intelligibility at C/N_0 values between 42 and 44 dB-Hz, adaptive delta mod has been chosen by MSC for use with the Space Shuttle. Specifically, an intelligibility greater than 90% is desired and a bit error probability of no greater than 10^{-3} is required. With these two parameters, a high intelligibility and high quality are achieved. Intelligibility is achieved by requiring greater than 90% based on a PB word score of 1000 words and quality is achieved by requiring a bit error probability not to exceed 10^{-3} . Shown in Figure 3-29 is the performance of a typical adaptive delta mod as a function of the percentage of errors in the reconstructed data stream. Note that a 90% intelligibility is indicated for 10% errors with a dynamic range of approximately 30 dB.

3.5 RELAY SYSTEM PERFORMANCE ANALYSIS

Presented herein is a discussion of the TDRSS communications performance over the command and telemetry links as well as user and TDRS tracking analysis, and manned user performance. In the sections that follow particular emphasis is placed on the LDR service because of the greater constraints placed on those links.

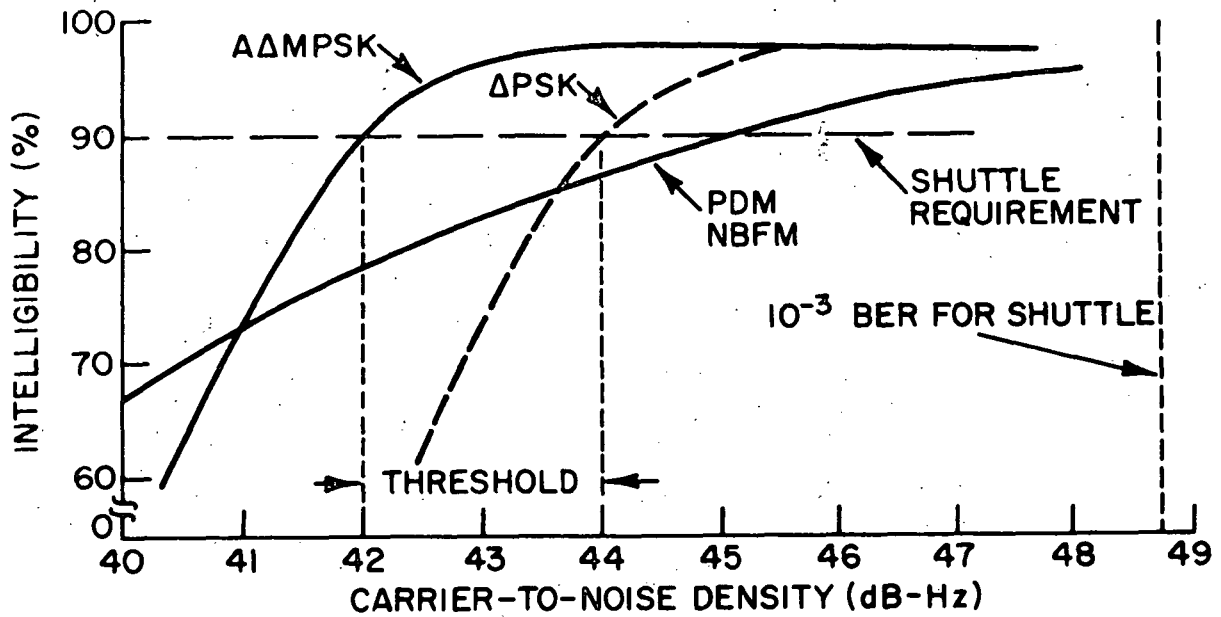


Figure 3-28. Comparison of PDM and Adaptive Δ-Modulation Voice

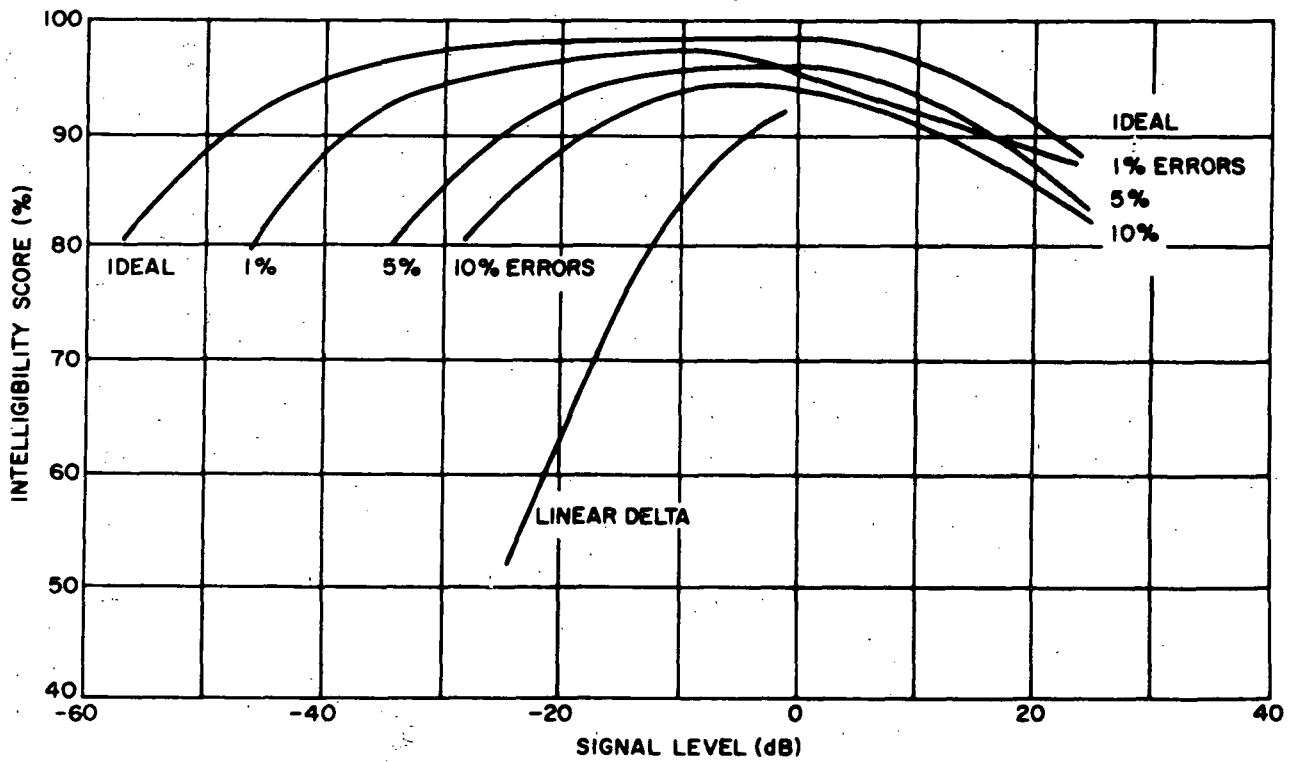


Figure 3-29. Performance of Typical Adaptive Delta Modulator



3.5.1 Forward (Command) Link Communications Performance

3.5.1.1 Low Data Rate Service

As illustrated in Figure 3-1, the forward link signal must contend with the multipath signal, and RFI in addition to ambient noise at the user spacecraft. The impact of these effects can be minimized by obtaining the maximum processing gain through a specific bandwidth allocation. It has been shown (Reference 3-8) that for a specified RF signal bandwidth, the processing gain (PG) can be maximized, but once the chip rate exceeds the RF bandwidth, increased PG by increasing the PN chip rate is offset by correlation losses due to bandwidth restriction. In practice, there are other losses not covered by theory but inherent to the system. For this reason it is advisable to maintain an RF bandwidth equal to a factor of approximately 1.5 times the chip rate, thereby insuring minimum PG losses due to bandwidth restrictions. The forward link PN chip rates, therefore, will be as follows:

Bandwidth Restriction	PN Chip Rate
50 kHz	32 kilochips/sec
100 kHz	64 kilochips/sec
150 kHz	100 kilochips/sec
250 kHz	160 kilochips/sec
500 kHz	320 kilochips/sec

The processing gain (PG) obtainable within the system RF bandwidth constraints is proportional to the ratio of PN chip rate to the bit rate. The bit rates of interest for the TDRSS are 100 to 1000 bps. The forward link communications performance in terms of output signal-to-noise ratio can be shown (Reference 3-8) to be equal to

$$\frac{S}{N} = \frac{P_u (PG)}{N' + RFI + \text{Multipath}} \quad (3-12)$$

where

P_u = signal power received at user

PG = chip rate/bit rate = processing gain

N' = input noise power

RFI = effective RFI at receiver input



$$\text{Multipath} = 4P_u/\alpha \text{ (worst case)}$$

$$\alpha = 2h/300$$

h = user altitude (300 to 5000 km)

This expression may be rewritten in terms of output carrier-to-noise density, as follows:

$$\frac{C}{N_o} = \frac{P_u}{N_I + RFI_o + 1/CR [4P_u/\alpha]} \quad (3-13)$$

└─ Chip Rate
└─ RFI Noise density
└─ Input thermal noise density

The expected output carrier-to-noise density at VHF (i.e., either 117, 127, or 148 MHz) as a function of input RFI density with system temperature and user altitude as parameters, is shown for chip rates of 32 kilochips/sec and 64 kilochips/sec in Figures 3-30 and 3-31, respectively. A similar set of curves is presented in Figures 3-32, 3-33, and 3-34 for UHF (i.e., 401 MHz), with chip rates of 32, 100, and 320 kilochips/sec respectively.

An estimate of the impact of ground based RFI sources on the forward link bit rate at VHF is shown in Figure 3-35.

From the figure it can be seen that under worst case conditions a 0 dBw (1 watt) RFI source on the ground would mean that the maximum achievable bit rate for a user at 300 km is on the order of 120 bps. For each of the aforementioned analyses, the following system budgets were assumed:

- TDRS EIRP = 30 dBw
- User Antenna Gain = -3 dBw
- Extraneous Losses = 3 dB
- BER for ΔPSK = 10⁻⁵

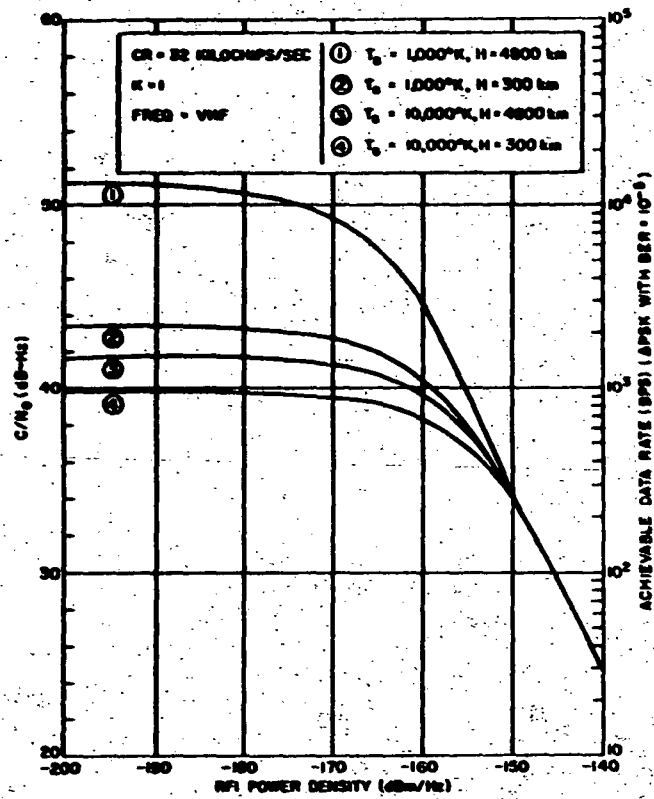


Figure 3-30. Forward Link Performance
at VHF - Chip Rate = 32 Kilochips
per Second

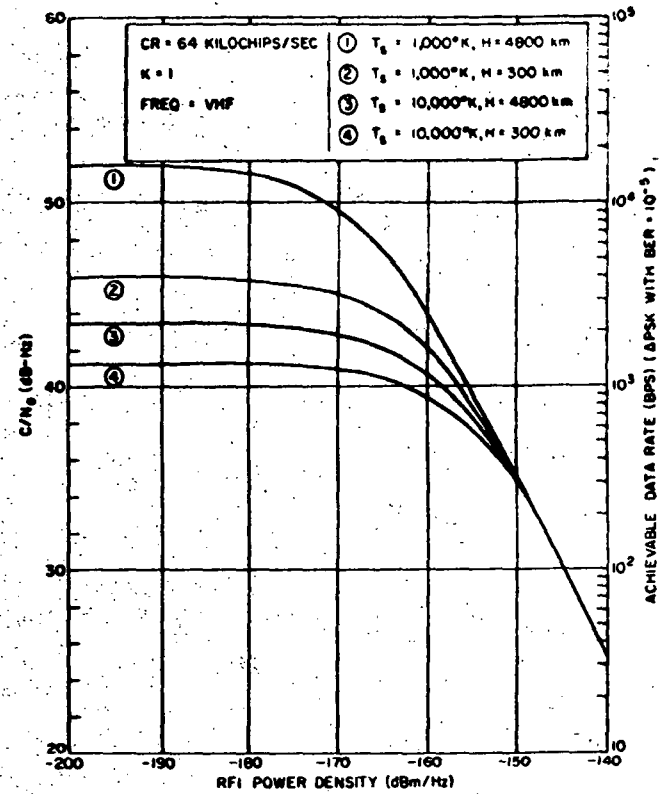


Figure 3-31. Forward Link Performance
at VHF - Chip Rate = 64 Kilochips
per Second



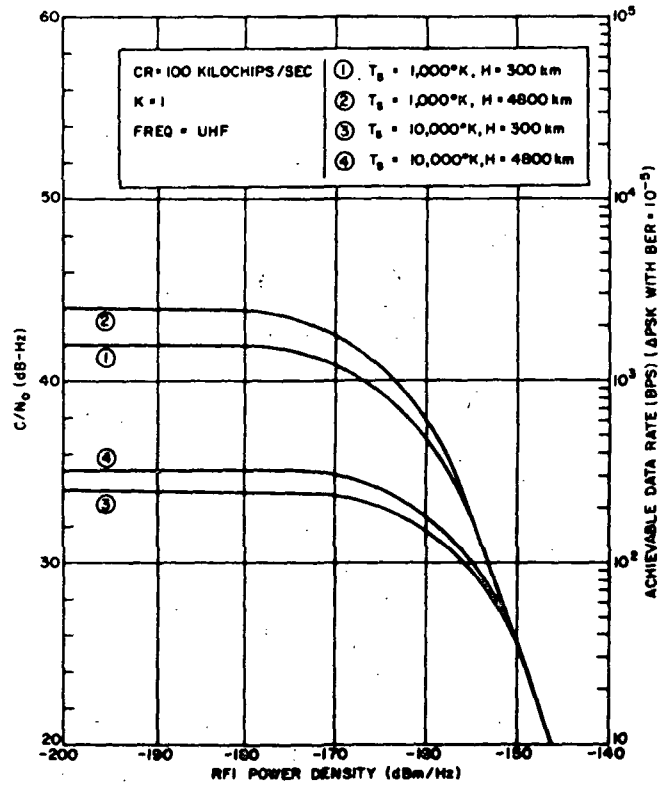
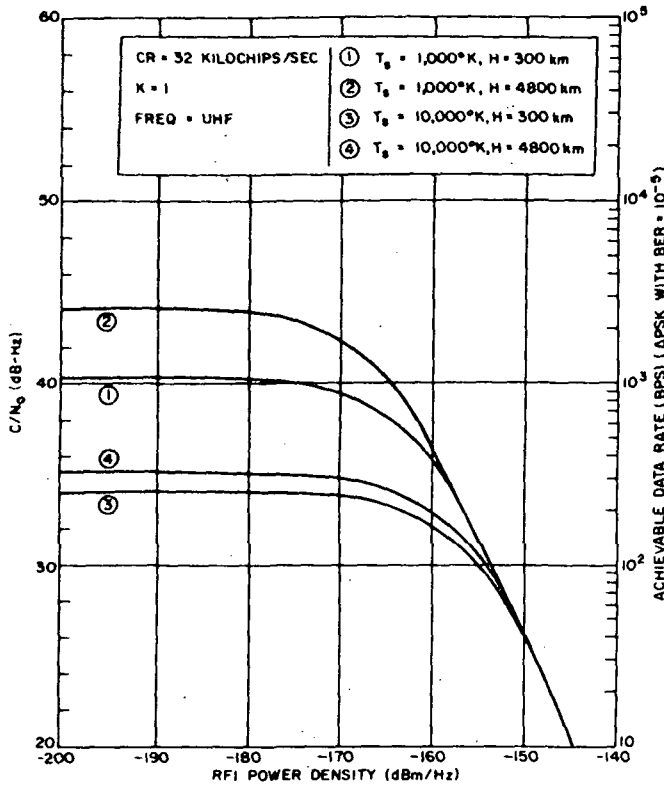


Figure 3-32. Forward Link Performance at UHF - Chip Rate = 32 Kilochips per Second

Figure 3-33. Forward Link Performance at UHF - Chip Rate = 100 Kilochips per Second

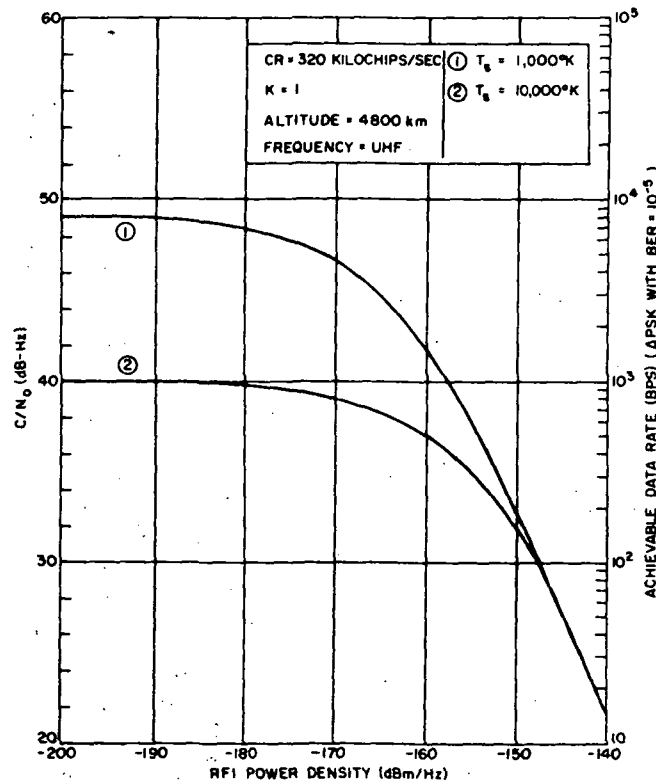


Figure 3-34. Forward Link Performance at UHF - Chip Rate = 320 Kilochips per Second

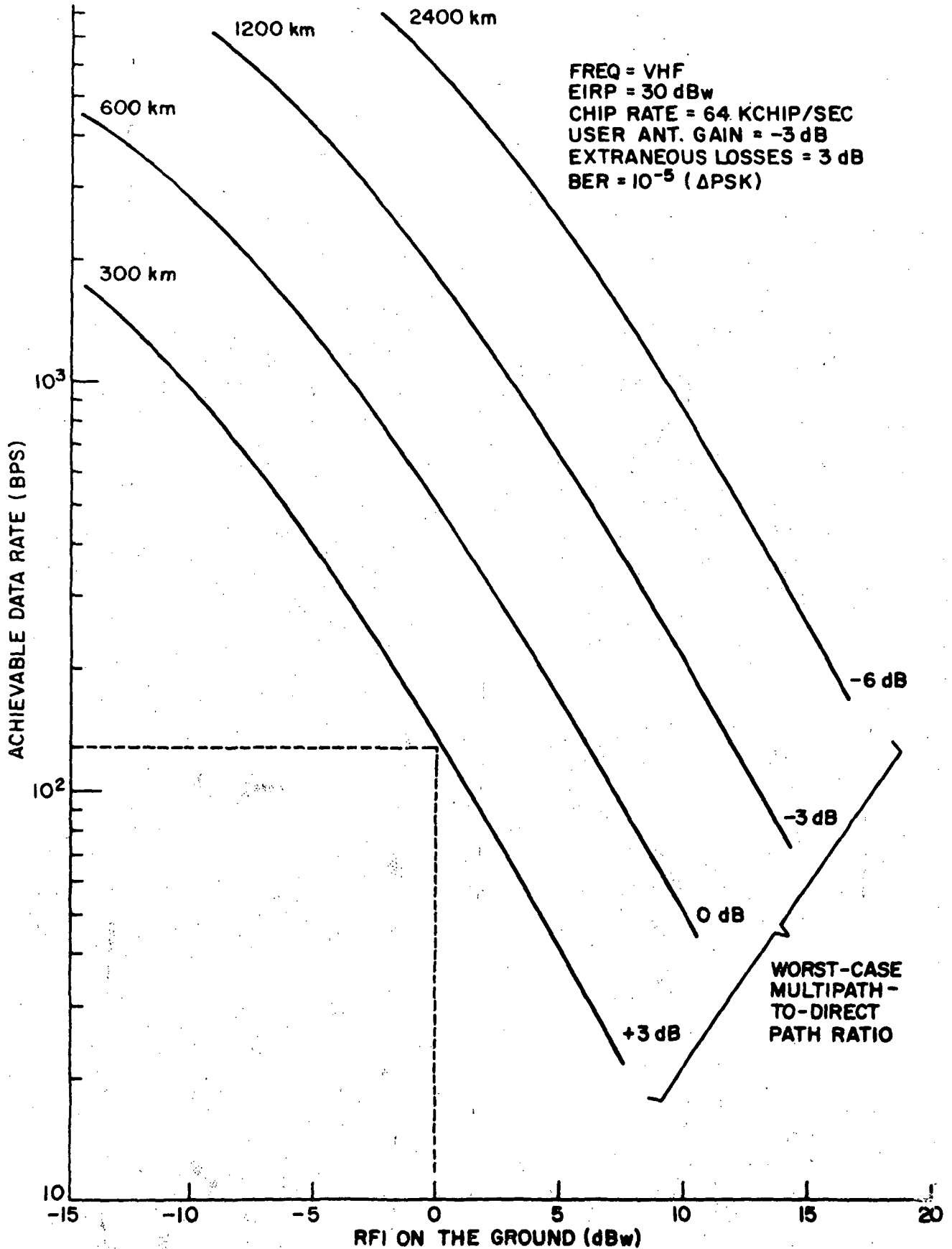


Figure 3-35. Forward Link Bit Rate as a Function of One RFI Source (in Band)



3.5.1.2 Medium Data Rate Service

The MDR forward link does not present the problems associated with LDR link, namely RFI and multipath. For a TDRS EIRP of 41 dBw, the carrier-to-noise density at the MDR user (assuming an omnidirectional antenna) is 44.6 dB-Hz. Thus, to provide support over the extremes of the data rates specified (100-1000 bps), the system using a Δ PSK carrier modulation (BER = 10^{-5}) has an estimated margin of between 4.2 and 14.2 dB. An estimate of the forward link performance is shown in Table 3-15.

Table 3-15: Forward Link Power Requirements for MDR Service

EIRP (TDRS)	41 dBw	
Δ CNR Degradation, dB	0.25 dB	
Free space loss	192 dB	
Other losses *	0.6 dB	
MDR system temperature	29.1 dB	
Noise density	-199.5 dBw/Hz	
User antenna gain	0 dB	
Carrier-to-noise density C/N_0	47.65 dB-Hz	
System performance	Support	
	100 bps	1000 bps
Bandwidth	20 dB	30 dB
E_b/N_0	27.65 dB	17.65 dB
Margin (Δ PSK; BER = 10^{-5})	16.75 dB	6.75 db

* Includes pointing and polarization losses.

3.5.2 Return (Telemetry) Link Communications Performance

3.5.2.1 Low Data Rate Service

The return link through the TDRSS must be capable of simultaneously supporting a maximum of 20 users, and the choice of PN rates, sequence lengths, and user data rates are interdependent.



The RFI data (see Section 3.2) indicates that the 136-137 MHz band appears to contain less RFI than the 137-138 MHz band. Thus, PN chip rates of 1 megachip/sec or less are attractive for the return link since higher chip rates may not improve the channel performance if the RFI increases more rapidly than the processing gain.

The return link can be implemented in either a channelized mode or a wideband co-channel mode. For example, the return link might consist of 10 channels having 2 users per channel, wherein each user employs a narrow band PN carrier with a nominal chip rate of 100 kilochips/sec. The return link also could be implemented by having 20 wideband PN signals, each user operated with a unique PN code (e.g., a Gold code) and all users are co-channel. In the wideband mode, the chip rates would be between 500-1000 kilochips/sec. Shown in Figures 3-36 through 3-39 are curves which illustrate the user bit rate which can be supported by the return link. These curves are drawn for various chip rates. The curves labeled 500 and 1000 kilochips/sec are valid for the wideband mode ($N = \text{number of users/channel} = 20$), whereas the curve labeled 100 kilochips/sec is valid for the narrow band PN mode with one ($N = 1$) or two ($N = 2$) users per channel.

The curves of Figures 3-36 through 3-39 are based on the following general equation:

$$\frac{C}{N_o} = \frac{P_{TDRS}}{N_I + RFI_o + \frac{1}{CR} \left\{ K \left[\frac{4P_{TDRS}}{\alpha} + \frac{(n-1) R P_{TDRS}}{20} \right] + (n-1) P_{TDRS} \right\}} \quad (3-14)$$

desired user multipath
other user multipath
direct other users

where

- N_I = the input noise density at TDRS
- RFI_o = the input RFI density at TDRS
- K = an attenuation factor proportional to the reflection coefficient
- n = the number of users/channel
- R = the ratio of average multipath contribution of other users (see Section 3.2.3.2, Figure 3.16) to the desired signal power (≈ 7 dB for the 1976 user s/c distribution)
- α = $2h/300$; h = user altitude
- P_{TDRS} = 37 dBm + 15 dB - Path Loss - 3 dB - 3 dB = 122.5 dBm
 - ↑ user power 5 watts typical
 - ↑ TDRS antenna
 - ↑ user antenna
 - ↑ extraneous losses

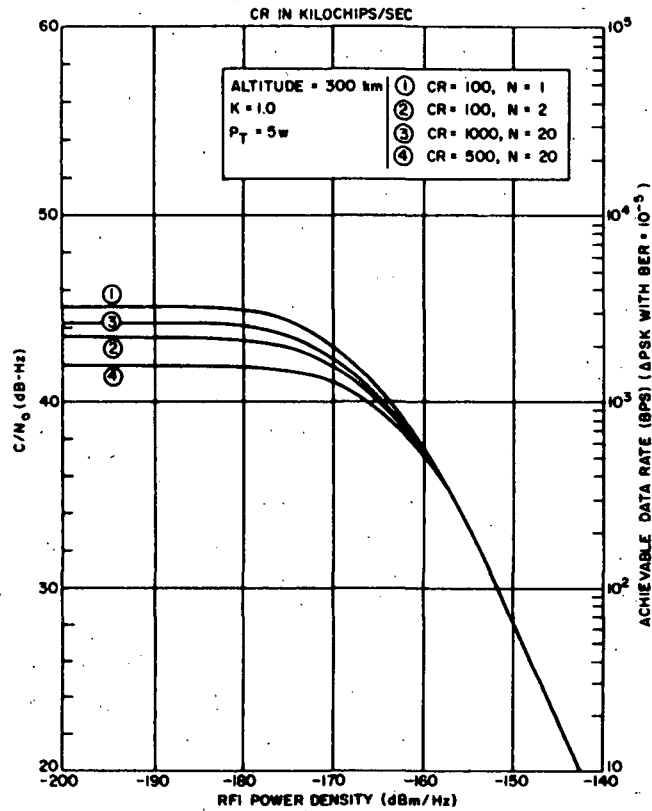


Figure 3-36. Return Link Performance at 136 MHz (User Altitude = 300 km; Reflection Coefficient = 1.0)

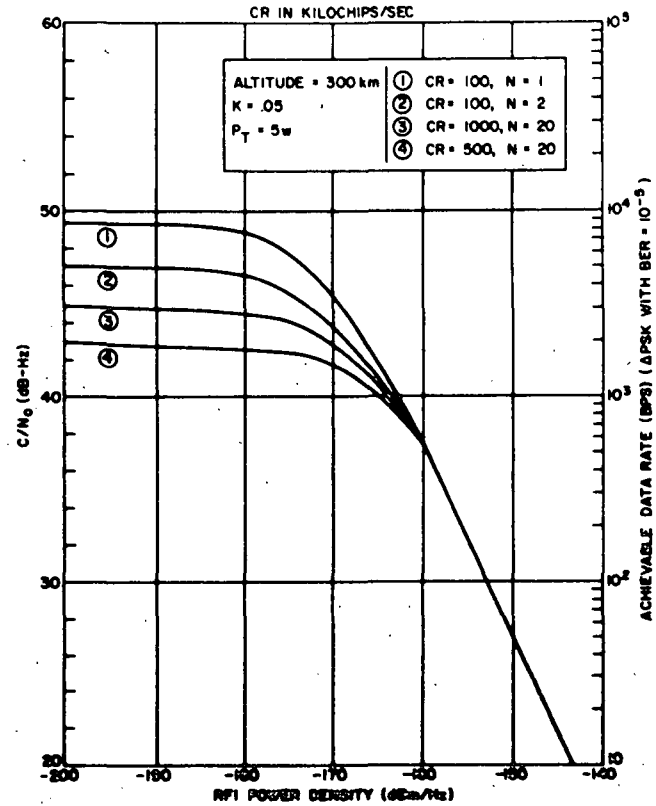


Figure 3-37. Return Link Performance at 136 MHz (User Altitude = 300 km; Reflection Coefficient = 0.05)



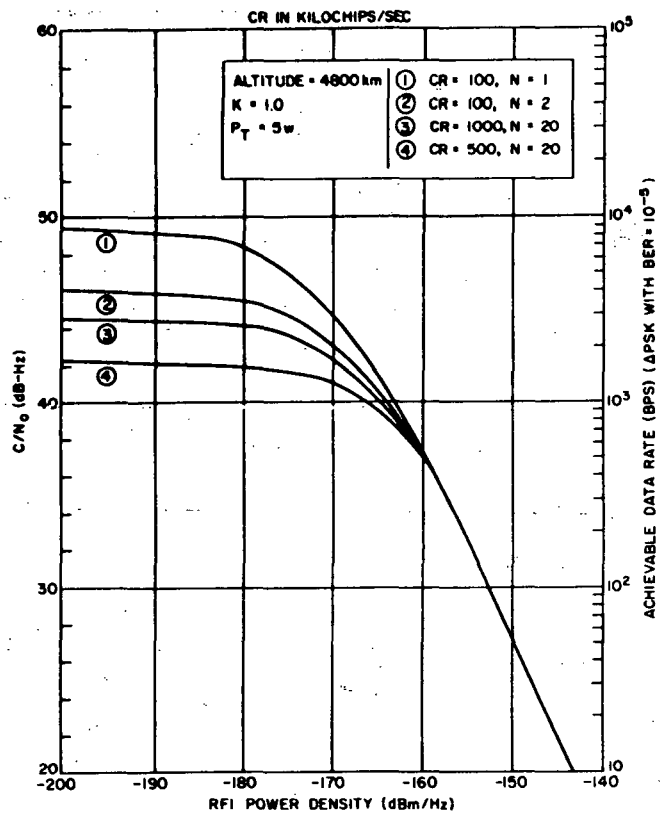


Figure 3-38. Return Link Performance at 136 MHz (User Altitude = 4800 km; Reflection Coefficient = 1.0)

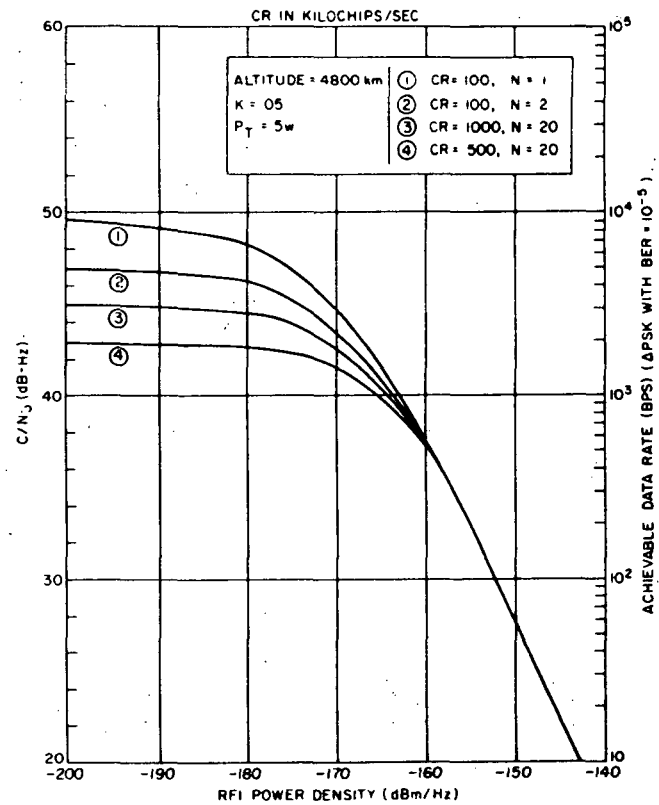


Figure 3-39. Return Link Performance at 136 MHz (User Altitude = 4800 km; Reflection Coefficient = 0.05)





Equation 3-14 relates the output carrier-to-noise density ratio for a given user power level at the TDRS, the ratio of the chip rate to data rate (processing gain), the noise density per channel, the number of users accessing each channel, the RFI per channel, and the multipath per channel. The curves in Figures 3-36 through 3-39 are conservative in that all potential losses including path loss, extraneous losses, user antenna anomalies, have been considered. The curves in Figures 3-36 through 3-39 are based on five watt user power levels. There are two distinct regions associated with the performance curves: 1) a region where all curves converge and have essentially equal performance; this region illustrates that RFI limits the performance of all the systems; 2) a second region in which the curves separate, and performance is limited by noise and multipath and other user signals.

The total multipath for the wideband curves is based on the 1976 satellite population estimates (discussed in Section 3.2). The narrowband (100 kilochips/sec) mode can outperform the 500 kilochip wideband mode under the following assumptions:

User power	5 watts
Extraneous loss	3 dB
User antenna gain	-3 dB
TDRS antenna gain	15 dB
TDRS T_s	1000° Kelvin
Assumed sys margin	0 dB

However, the final choice of return link chip rates will be greatly influenced by the return link ranging errors (see Section 3.5.3.4).

The curves show that all the systems are RFI limited and when the RFI level is -160 dBm/Hz (a realistic value), none of the techniques will support a data rate of 1000 bits/sec.

They also indicate which user bit rates can be supported by the return link with a 5-watt user power level. If forward error control is applied to the return link (e.g., rate 1/2 (48,24) nonsystematic convolutional code) the data rate can be increased by a factor of 4 (Figure 3-40). Thus, forward error control is highly recommended for the return link. With error control, the return link can support 2000 bits/sec at BEP of 10^{-5} in the presence of -160 dBm/Hz RFI. The application of an adaptive ground implemented phased array (AGIPA) can enhance system performance in the presence of RFI by another 5 to 15 dB, thereby increasing the achievable bit rates on the return link to greater than 7 kbps (worst case).

Increasing user power levels in the return link is a tempting approach to enhance the performance of the return link. However, power sources on board the low data rate user satellites limit the available EIRP. Shown in Figure 3-41 is the uncoded user bit rate which can be supported at a 10^{-5}

bit error probability as a function of the RFI level in the return link. These curves are based on equation 3-14 and are drawn for user power levels of 5, 10, 20, and 40 watts and in all cases the PN chip rate is 1000 kilochips/sec for all users. Note that an increase in user power levels of 3, 6, or 9 dB with reference to 5 watts does not result in a comparable increase in user data rate. Thus, there are diminishing returns when user power is increased beyond five to ten watts.

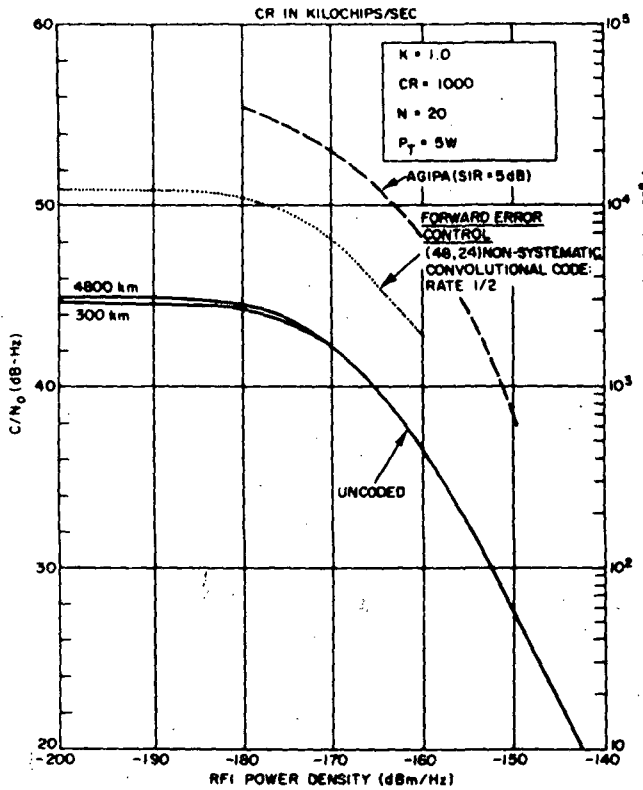


Figure 3-40. Impact of Forward Error Control on the Return Link Performance at 136 MHz

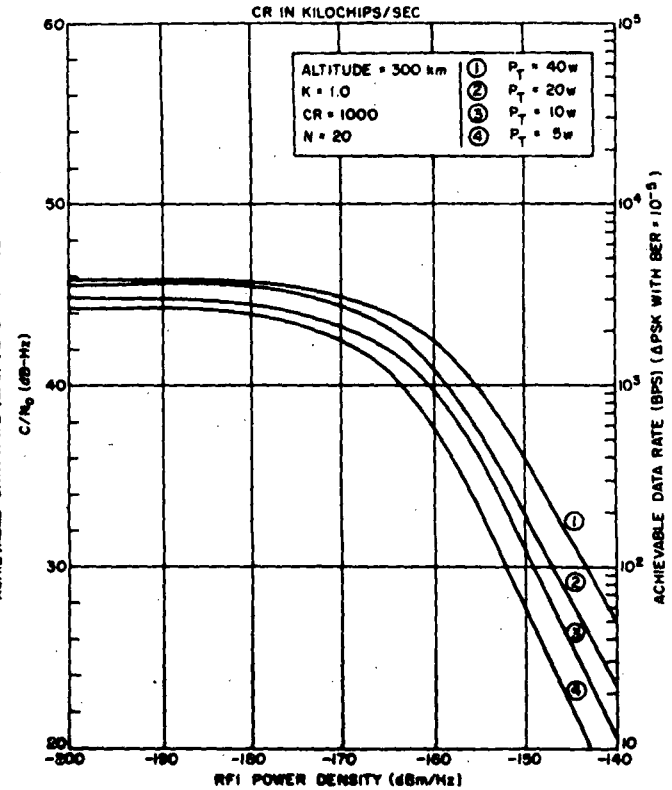


Figure 3-41. Return Link Performance at 136 MHz as a Function of User Transmit Power

3.5.2.2 Medium Data Rate Service

Similar to the forward link the MDR return link performance analysis is rather straightforward. In Table 3-16 an estimate is made regarding the EIRP which is required for the MDR user to support the specified return link



data rates (i.e., 10 to 1000 bkps). The expression used to determine the user EIRP is

$$EIRP_{user} = (C/N_o)_R + k + T_s - G_{TDRS} + L_{fs} + L_x \quad (3-15)$$

where

- $(\frac{C}{N_o})_R$ = carrier-to-noise density required to support the link
- k = Boltzmann's constant
- T_s = system noise temperature
- G_{TDRS} = TDRS antenna gain
- L_{fs} = free space path attenuation
- L_x = extraneous losses

Table 3-16. Return Link Power Requirements for MDR Service

Description	Frequency - S-Band	
	Service	
	10 kbps	1000 kbps
C/N_o , required (ΔPSK , BER = 10^{-5})	49.9 dB-Hz	69.9 dB-Hz
TDRS antenna gain dB	30.9	30.9
ΔCNR degradation, dB	1.0	1.0
FEC coding gain(1) dB	4.7	4.7
Boltzmann's constant, k	-228.6 $\frac{dBw}{Hz-^{\circ}K}$	-228.6 $\frac{dBw}{Hz-^{\circ}K}$
TDRS system temp, (2) T_s , dB		
Path loss, L_{fs} , (2) dB	191.1	191.1
Extraneous losses, (3) L_x , dB	0.6	0.6
Noise density, dB-Hz	-202.6	-202.6
System margin db	3.0	3.0
$EIRP_{user}$	7.6 dBw	27.6 dBw
(1) R = 1/2, K = 7, convolutional code with Viterbi Decoder (2) Selected at point where T_s and L_{fs} have maximum effect (3) Polarization and pointing.		



To support 10 kbps and 1000 kbps, with 3 dB margin, the user spacecraft requires an EIRP* of 7.6 dBw and 27.6 dBw, respectively. If the MDR user spacecraft were to have a transmit power, P_T , of 6 watts (~ 8 dBw), then the 10 kbps service can be provided through an omnidirectional antenna, whereas, the 1000 kbps service would require an antenna gain of approximately 20 dB (2.1 ft).*

3.5.3 TDRSS Tracking Performance

3.5.3.1 Position Location of the Tracking and Data Relay Satellite

It is of interest to determine the precision with which a tracking and data relay satellite position can be known from the ground. To do this, a hypothetical tracking system consisting of three ground stations implemented as shown in Figures 3-42 and 3-43 were selected. The stations are located at Rosman, Mohave, and Santiago, and the TDRS were placed at 11°W and 143°W . The stations have approximately symmetrical latitudes with respect to the equator, and the triangle formed by these stations represents a reasonable geometry. Shown in Tables 3-17 through 3-20 are the results obtained from NASA's P-CON Error Analysis when all three stations are performing range and range rate measurements or trilaterating on a TDRS. From the data shown in Tables 3-17 through 3-20 it is concluded that the primary sources of error are those associated with the ground stations σ_G and the propagation σ_B and in order to precisely track a synchronous TDRS, these errors must be minimized. The last case, however, as shown in Table 3-20, indicates that after a 24-hour period, with reasonable ranging errors, bias errors, and ground station errors, that a tracking and data relay satellite can be position located to within an error of 40 meters with an inconsequential velocity error.

Position location errors of the ground stations have in the past been the fundamental limitation in the remote positioning of a spacecraft. However, technology is being developed to locate ground stations very precisely. For example, a technique has been developed by NASA using a Mariner probe whereby range rate data is used to reduce the ground station location errors (geodetic bias unresolved) to approximately 5 meters in the x-y dimensions. Furthermore, Transit satellite technology has evolved to where station location errors on the order of one meter (geodetic bias unresolved) has been reported and very long baseline interferometry promises to reduce station location uncertainties to less than 1 meter. To reduce the absolute position of ground stations to three meters, improvements in geodesy are required. This is being accomplished under the TIPS program by APL where both satellite gravity and atmospheric drag coefficients will be separated and measured so that more refined geodesy can be accomplished with the Transit satellite technology. It is anticipated that the TIPS program will refine bias errors in station locations to within two meters and with the precision of the existing Transit technology station locations can be determined absolutely to within a three-meter error.

* Based on S-band support, if Ku-band support is provided, then required antenna gain is 10 dB (~ 0.4 ft (0.12m)).

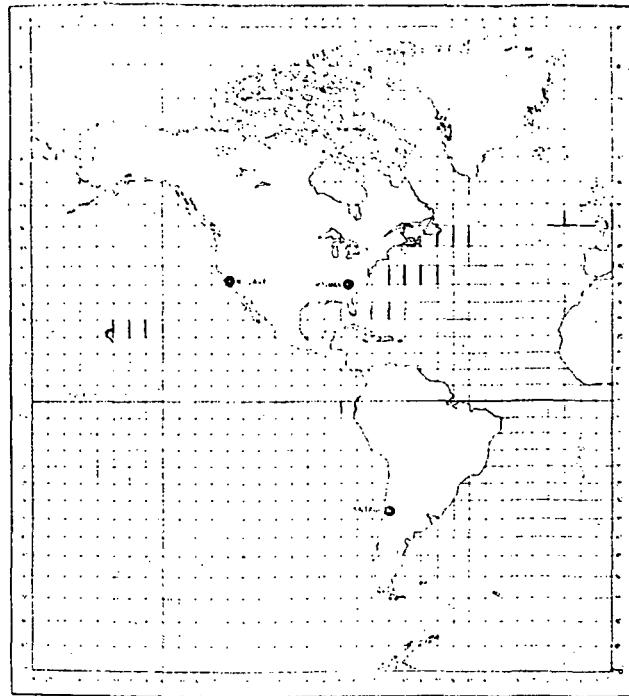


Figure 3-42. Assumed Locations for the TDRS Ranging Stations

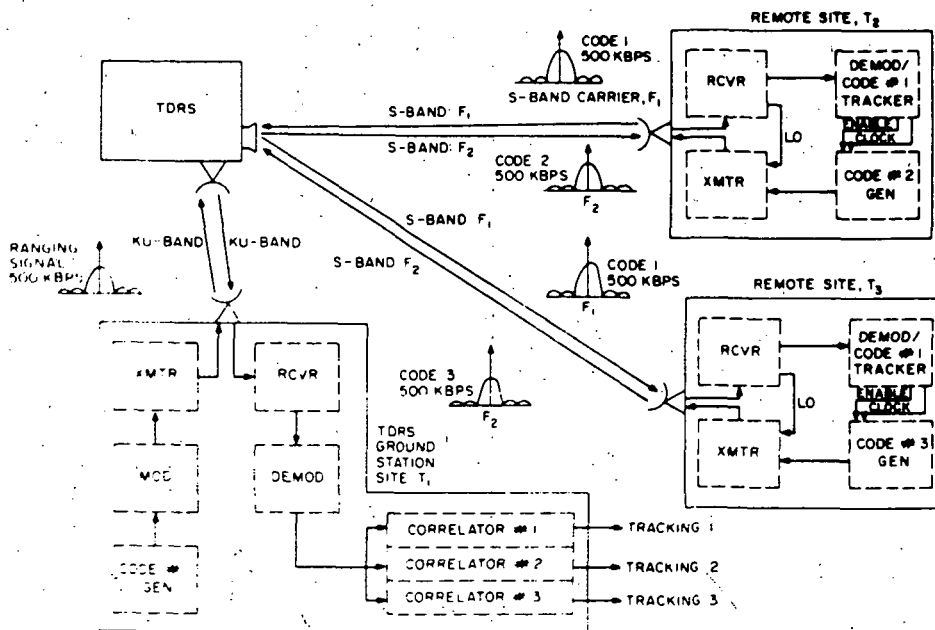


Figure 3-43. Functional Design of the TDRS Ranging Concept

Table 3-17. TDRS Location Accuracy (TDRS at 11°W)

Assumptions			
Tracking Uncertainties			Station Elevation Angle
	Noise	Bias	Rosman: 6° Mohave: cannot participate Santiago: 16°
	Range	3 m	
Range rate	.01 cm/sec	.02 cm/sec	Station location = 27 m uncertainty

Inclination	Position Error	Velocity Errors	Comment
0°	257 m	.019 m/sec	
3°	203 m	.015 m/sec	Rosman off 3 hrs.
5°	182 m	.013 m/sec	Rosman off 7.5 hrs.
10°	160 m	.012 m/sec	Rosman off 10 hrs.

Table 3-18. TDRS Location Accuracy (TDRS at 143°W)

Assumptions			
Tracking Uncertainties			Station Elevation Angle
	Noise	Bias	Rosman: 15° Mohave: 40° Santiago: 16°
	Range	10 m	
Range rate	.01 cm/sec	1 cm/sec	Station location = 9 m uncertainty

Inclination	Position error	Velocity Errors	Comment
0°	292 m	.02 m/sec	
3°	252 m	.019 m/sec	Santiago off 8 hrs.
5°	251 m	.019 m/sec	Santiago off 9.5 hrs.
10°	257 m	.02 m/sec	Santiago off 11 hrs.

Table 3-19. TDRS Location Accuracy (TDRS at 143°W)

Assumptions			
Tracking Uncertainties			Station Elevation Angle
	Noise	Bias	
Range	3 m	6 m	Rosman: 15°
Range rate	.01 cm/sec	.02 cm/sec	Mohave: 40°
			Santiago: 6°
			Station location = 27 m uncertainty
Inclination	Position Error	Velocity Errors	Comment
0°	97 m	.007 m/sec	
3°	98 m	.007 m/sec	Santiago off 8 hrs.
5°	99 m	.007 m/sec	Santiago off 9.5 hrs.
10°	99 m	.007 m/sec	Santiago off 11 hrs.

 Table 3-20. TDRS Location Accuracy (TDRS at 143°W)
 (After 24 Hours of Tracking)

Assumptions			
Tracking Uncertainties			Station Elevation Angle
	Noise	Bias	
Range	3 m	6 m	Rosman: 15°
Range rate	.01 cm/sec	.02 cm/sec	Mohave: 40°
			Santiago: 6°
			Station location = 3 m uncertainty
Inclination	Position Error	Velocity Errors	Comment
0°	40 m	.0029 m/sec	
3°	39 m	.0028 m/sec	Santiago off 8 hrs.
5°	38 m	.0028 m/sec	Santiago off 9.5 hrs.
10°	38 m	.0027 m/sec	Santiago off 11 hrs.

The results in Tables 3-17 through 3-20 are summarized in Figure 3-44. The position error of the TDRS is virtually independent of inclination angle when all three stations participate fully and the ground station position errors and bias errors are minimized.

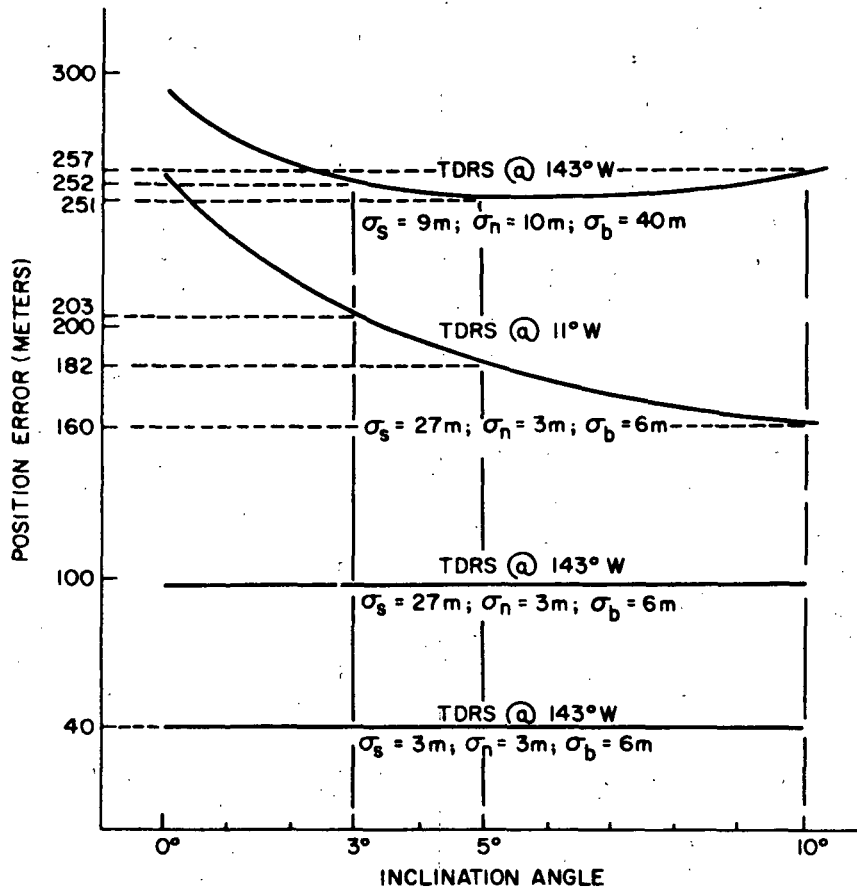


Figure 3-44. TDRS Position Location as a Function of Inclination Angle

Table 3-21 indicates that trilateration of a TDRS by three ground stations imposes a negligible amount of power drain on the TDRS. A nominal 10 dB TDRS antenna gain is assumed and precise ranging can be accomplished with an expenditure of .5 watt RF power at S-band from the TDRS.

Table 3-21. S-Band Ranging Power Budgets

Path loss @ S-band	191 dB
TDRS antenna gain	15 dB (peak; 14.3 dB at edge)
GS antenna gain 30' (9.1 m) dish	43 dB
Other losses	1.0 dB
P_t TDRS	1.0 watts = 0 dBw
Δ CNR Loss	0.5 dB
T_g ground station (150°K)	21.8 dB

$$\Delta R_{PN} = \frac{\pi}{5} \frac{T_c \cdot C}{\sqrt{2 \left(\frac{S}{N}\right)_L}}$$

$T_c = 2 \times 10^{-6}$ sec - (500 Kchip/sec)

$\left(\frac{S}{N}\right)_L = 71.8$ dB (1 Hz loop bandwidth)

 $\Delta R = 7 \times 10^{-2}$ meters

3.5.3.2 Tracking the User Satellite

There is no requirement to determine the position location or orbit of either an LDR or MDR. However, roundtrip range and range rate error requirements for both MDR's and LDR's for a single TDRS link are given in Table 3-22.

Table 3.22. User Spacecraft Tracking Requirements

LDR	Range error:	10 Meters Systematic 15 Meters Random
	Doppler (random):	10 cm/sec 1 sec integ. 1 cm/sec 10 sec integ.
MDR	Range error:	6 Meters Systematic 2 Meters Random
	Doppler (random):	.6 cm/sec 1 sec integ. .06 cm/sec 10 sec integ.



In the previous section it was noted that the TDRS's can be tracked to a 40-meter range uncertainty and a .003 m/sec velocity uncertainty after 24 hours of tracking by three ground stations. Cooley (Reference 3-9) with the aid of the NAP III computer program has estimated the uncertainties in a user's orbit when the TDRS uncertainty is 500 meters and the random range rate error is .03 m/sec. His results indicate that the user position uncertainty for two TDRS's tracking a user with \dot{R} measurements only is 113 meters after a 10 minute tracking period. Thus, we conclude that Cooley's estimate can be easily achieved if the TDRS's uncertainties are 40 meters and .003 m/sec and both TDRS's participate in the \dot{R} measurements.

Based on Cooley's results, John Bryan (Reference 3-9) conceived of the one-way range and range rate concept for tracking a user satellite via two TDRS's. Magnavox has evaluated this approach to determine if \dot{R} errors are within those required to meet Cooley's prediction for tracking a user via two TDRS's with \dot{R} data only.

3.5.3.3 One Way Range Rate Tracking of the User Spacecraft

The system configuration and ranging signal propagation are illustrated in Figure 3-45. The TDRS's are assumed to be phase-locked to a Ku-band up-link signal generated at synchronized ground stations, the user is assumed to originate a VHF downlink (user/TDRS) ranging signal fully derived from an incoherent L.O. present in the user spacecraft, and the two TDRS's relay such downlink signals to ground at Ku-band by side-stepping the VHF received signals with the mixing references being derived from the TDRS VCO's phase-locked to the uplink ground signal. The possibility of a direct GS/TDRS/GS beacon signal turnaround for TDRS tracking or Ku-band doppler compensation purposes is illustrated by the dotted line, and its effects will be discussed.

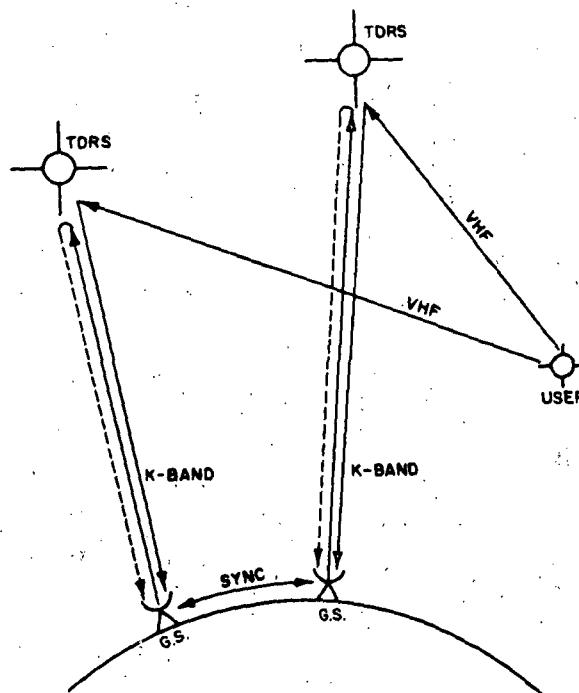


Figure 3-45. One-Way Ranging System



When both TDRS's are in simultaneous contact with the user, the received ground signals can be processed to extract either one-way range difference ($1\Delta R$), one-way range rate ($1\dot{R}$) or one-way range rate difference ($1\Delta\dot{R}$) data in real time, which in turn can be used in an ODP (orbital determination program) to track the user orbital motion. If the TDRS/user geometry is such that only one TDRS maintains contact through certain time intervals, then the tracking data would be limited to one-way range rate during those intervals. When both TDRS-relayed signals are available, the ground receivers have the option of independently extracting the tracking signals and then combining them to generate the $1\Delta R$ or $1\Delta\dot{R}$ data, vs first performing the signal combination and then extracting the tracking data from the composite signal thus obtained. The actual choice involves subsystem realization and signal processing complexity considerations, including compatibility to the ODP logistics to account for the aforesaid loss of coverage by one of the TDRS employed.

To derive quantitative performance results, the system specifications listed below will be assumed, though any changes from these value can be logically accommodated in the performance analysis that follows through the parametric formulation employed:

Orbital dynamics: $\dot{R} = 1 \text{ m/s}$ and $\ddot{R} = 1 \text{ mm/s}^2$ for TDRS
 $\dot{R} = 7 \text{ km/s}$ and $\ddot{R} = 10 \text{ m/s}^2$ for user

Power budget: $\frac{C}{N_0} = 40 \text{ dB-Hz}$ for user/TDRS link

Doppler Signal Extraction. The 1-way doppler signal propagation is illustrated in Figure 3-46. If we assume that the GS receiver has no additional information when processing the TDRS-relayed user-signal, then the doppler reproduction potential is limited to a term of the form

$$\underbrace{(2LD_t)}_{\text{2-way Ku-band GS/TDRS/GS doppler effect}} \pm \underbrace{N(D_0 + D'_0)}_{\text{1-way VHF User/TDRS/GS doppler effect}} = \underbrace{(2LD_t \pm ND_0)}_{\text{net doppler effect due to GS/TDRS and TDRS/GS link}} \pm \underbrace{(ND'_0)}_{\text{net doppler effect due to User/TDRS link}}$$

and the conditions $2LD_t \ll N(D_0 + D'_0)$ and $D_0 \ll D'_0$ are required if the doppler signal is to effectively reflect the user orbital motion relative to the TDRS. The condition $D_0 \ll D'_0$ will be met except at nil user relative velocities, but the condition of nil 2-way Ku-band link doppler is more restrictive and should be verified since the TDRS doppler is essentially emphasized by the Ku-band/VHF ratio relative to the user doppler. The maximum doppler conditions correspond to $2LD_t \sim 100 \text{ Hz}$ and $N(D_0 + D'_0) = 3.5 \text{ kHz}$ so that the doppler signal should indeed reflect the user relative motion except at rather small user relative velocities.

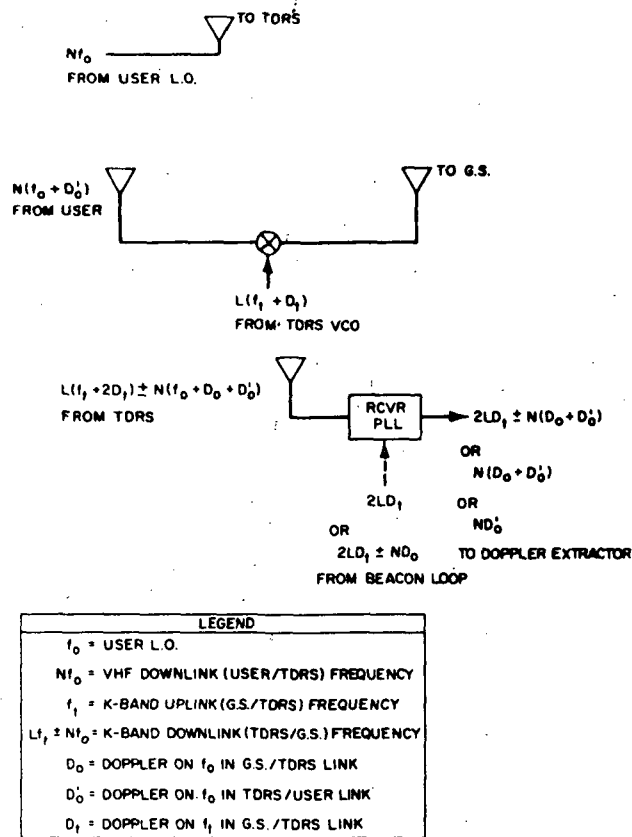


Figure 3-46. Doppler Signal Extraction

It should still be understood that the disregard of the $2LD_t$ term is tantamount to introducing a bias 1-way range rate error of

$$\mu_R^* = \frac{c}{Nf_0} (2LD_t) \sim 200 \text{ m/s maximum} \quad (3-16)$$

which is in general small when compared to the true range rate (7 Km/s maximum) yet may predominate over other error sources and effects to establish error performance bounds in any given ODP (orbital determination program). The 2-way Ku-band link doppler (or the net GS link doppler) can be compensated by the inclusion of a direct GS/TDRS/GS beacon/Turnaround signal whose scaled doppler can provide the desired compensation as illustrated in the figure, in which case the aforesaid bias error is removed and the ODP error performance is improved.

The interest in using the turnaround beacon signal is further emphasized by oscillator noise compensation considerations. The beacon signal is, of course, derived from the TDRS VCO, and hence, will contain the (TDRS-loop filtered) phase noise contributions of the TDRS VCO and of the uplink ground master. These oscillator noise contributions are then



present in the TDRS/GS downlink carrier and beacon signals and ideally differ only by the carrier/beacon frequency ratio so that they can be eventually compensated at the ground receiver when the beacon signal is referred to the carrier frequency for doppler compensation purposes, provided that both downlink carrier and beacon signals exhibit nil differential propagation delays (e.g., essentially same ionospheric delays) as well as equivalent filtering (e.g., same carrier and beacon loop receiver design) to preserve phase noise time-correlation. Moreover, the oscillator noise in the ground receiver RF reference should be uncorrelated to the retransmitted phase noise even though a common master is used (due to roundtrip propagation delays). Its (Rcvr-loop filtered) Ku-band phase noise should be accounted for in any system error analysis; i.e., the user oscillator should be more unstable than the ground master but the latter contributes Ku-band phase noise vs VHF phase noise for the former. The use of a common receiver RF reference in both carrier and beacon extractions plus identical loop designs also would provide local-reference RF (Ku-band) phase noise compensations when the carrier and beacon signals are subtracted for doppler compensation purposes. The ground oscillator noise contribution would then be limited to the IF bias frequency accompanying the doppler signal, thus making it nil relative to the user VHF oscillator noise contribution.

In summary, the inclusion of the turnaround beacon signal is recommended both for doppler and oscillator noise compensation, and, of course, can be used to provide 2-way range rate data on the TDRS/GS link itself for TDRS tracking purposes. The oscillator noise compensation potential of the TDRS beacon turnaround approach is a direct consequence of the user 1-way range rate system and would not be applicable in 2-way ranging systems. The retransmitted oscillator noise in the TDRS/GS downlink carrier would still include ground master and TDRS VCO effects in user 2-way ranging systems, but they would not exhibit the TDRS/user/TDRS roundtrip propagation delay (say, 0.25 sec), while the beacon signal would not propagate through the user link so that the downlink carrier and beacon signal would have uncorrelated phase noises, even assuming an ideal coherent transponder at the user (an effective width greater than 10 Hz is representative of oscillator phase noise spectral content so that effective correlation times smaller than propagation delays are characteristic). The carrier and beacon phase noise effects would then add mean-square wise rather than compensate each other, as a consequence of the TDRS/user/TDRS propagation inherent in 2-way ranging systems.

Inclusion of the beacon turnaround approach in 1-way ranging provides ground oscillator noise compensation making such error source nil relative to the user oscillator noise, but doubles the mean-square contribution of the ground receiver VCO noise since the carrier and beacon loop effects will be independent and no compensation should be expected. Hence, the two basic oscillator noise processes to be considered for range rate purposes are the user VHF oscillator noise and the ground carrier + beacon (loop) VCO noise, all of them filtered by the receiver loop error transfer

function, and it is not a priori evident which process predominates due to the different oscillator type and frequency bands involved.

Error Analysis. The 1-way raw range rate data samples are assumed to be derived using conventional cycle-counting measurements on the 1-way doppler signal extracted at the ground receiver. The (average) doppler measurement f_d is used to compute (average) range rate according to $\dot{R} = cf_d/Nf_o$, so that errors may be contributed by the doppler measurement itself (e.g., any phase noise or time jitter accompanying the doppler signal or introduced during the measurement operation), or by using incorrect values of the arithmetic constants c and Nf_o involved in the computations (e.g., uncertainty in the velocity or light or user oscillator drift). The doppler measurement itself may involve incorrect computation constants (e.g., bias frequency drifts) used to convert the measured parameters (number of cycles counted or their time duration) to a doppler value f_d , and such errors will also induce range rate errors to be accounted for.

1. Systematic Errors. An uncertainty δc in the velocity of light represents an uncertainty

$$\delta \dot{R} = \frac{f_d}{Nf_o} \delta c = \frac{\delta c}{c} \dot{R} \quad (3-17)$$

in range rate, so that $\delta c/c = 3 \times 10^{-7}$ yields $\delta \dot{R} \approx 2$ mm/s maximum. A long-term (relative to the propagation time) frequency drift δf_o in the user L.O. in turn implies that the measured doppler should be referred to the unknown transmitted frequency $N(f_o + \delta f_o)$ rather than the nominal value Nf_o used in the computation to convert doppler into range rate data, so that a net systematic error of

$$\delta \dot{R} = \frac{cf_d}{Nf_o} - \frac{cf_d}{N(f_o + \delta f_o)} \approx \left(\frac{\delta f_o}{f_o} \right) \frac{cf_d}{Nf_o} = \frac{\delta f_o}{f_o} \dot{R} \quad (3-18)$$

is introduced. For example, a long-term user oscillator instability (relative to the link propagation delay) of 10^{-6} or better would be required to maintain this error within 1 cm/s, and make it commensurable to the velocity of light uncertainty effect.

An effect in the long-term drift of the ground oscillator will appear in the bias frequency accompanying the doppler signal. The doppler measurement approach is based on counting bias plus doppler cycles and arithmetically subtracting the nominal bias value to get doppler only, so any bias drift δf_b will be incorrectly preserved as a measured doppler and contribute an error.



$$\delta \dot{R} = - \frac{c}{Nf_o} \delta f_b = - \frac{\delta f_b}{f_d} \dot{R} \quad (3-19)$$

However, this error can be essentially compensated in the doppler measurement operation if the high frequency reference used as time standard is also derived from the same ground oscillator thus exhibiting a proportionate drift. For example, a doppler measurement based on counting N_1 cycles of bias plus doppler $f_b + f_d$ and measuring the counting time T with a high-frequency reference f_r essentially measures the number N_2 of reference cycles corresponding to this time (i.e., it quantizes time to $1/f_r$ sec units) and yields doppler from the arithmetic computation $f_d = (N_1/N_2)(f_r - f_b)$. A joint drift $f_r \rightarrow f_r + \delta f_r$ and $f_b \rightarrow f_b + \delta f_b$ would imply that the true doppler should be computed using these unknown values instead, thus introducing a net bias error of

$$\delta \dot{R} = \frac{c}{Nf_o} \delta f_d = \frac{c}{Nf_o} \left(\frac{N_1}{N_2} \delta f_r - \delta f_b \right) \quad (3-20)$$

where $\delta f_r/f_r = \delta f_b/f_b$ if a common ground oscillator is used so that this expression reduces to

$$\delta \dot{R} = \frac{c}{Nf_o} \left(\frac{N_1}{N_2} f_r - f_b \right) \left(\frac{\delta f_b}{f_b} \right) \approx \frac{cf_d}{Nf_o} \left(\frac{\delta f_b}{f_b} \right) = \left(\frac{\delta f_b}{f_b} \right) \dot{R} \quad (3-21)$$

which differs from the first result derived ignoring the time standard reference drift. It is evident that under these conditions the user oscillator drift will predominate over the ground oscillator drift effects since $\frac{\delta f_o}{f_o} \gg \frac{\delta f_b}{f_b}$ should prevail.

2. Random Errors. The thermal noise processes added to the signal through the propagation links of Figure 3-45 eventually appear as phase noise in the doppler signal extracted at the ground receiver. The downlink additive thermal noise has contributions from both the user/TDRS and TDRS/GS links, but the latter may be neglected assuming typical signal-to-noise density conditions. Also, the uplink GS/TDRS additive noise becomes phase noise at the TDRS tracking loop and is scaled and retransmitted as such to ground when side-stepping the user signal with the TDRS VCO for ground relay purposes. Such phase noise essentially will be reproduced by the ground receiver loop since its bandwidth should be larger than that of the TDRS loop due to the larger doppler dynamics to be tracked, and should also be negligible relative to the downlink user/TDRS thermal noise effect due to both the larger GS/TDRS signal-to-noise density and the narrower TDRS



loop bandwidth (even assuming the latter to be somewhat wider than tracking requirements to permit unaided signal acquisition at the TDRS). Of course, the inclusion of the beacon turnaround compensation would introduce further retransmitted and received thermal noise processes in general uncorrelated to their carrier signal counterparts due to different spectral occupancy, but again their effects will be negligible relative to the user/TDRS thermal noise contribution with its predominant noise-to-signal density.

The rms one-way doppler and range rate errors may be evaluated from the expression

$$\sigma_R^* = \frac{c}{Nf_o} \sigma_D = \frac{\sqrt{2} c}{2\pi Nf_o T} [R_\phi(0) - R_\phi(T)]^{\frac{1}{2}} \quad (3-22)$$

where T is the doppler counting time and $R_\phi(\cdot)$ is the phase noise autocorrelation function given by the inverse transform

$$R_\phi(T) = \int_{-\infty}^{\infty} \frac{\phi}{2S} |H_\ell(j\omega)|^2 e^{j\omega T} \frac{d\omega}{2\pi} \quad (3-23)$$

where ϕ/S is the noise-to-signal density and $H_\ell(s)$ is the tracking loop transfer function. If the loop bandwidth is wider than the data sample rate (as is often the case) then $|R_\phi(T)| \ll R_\phi(0)$ and the one-way rms error expression reduces to

$$\sigma_R^* = \frac{c}{Nf_o} \sigma_D = \frac{c}{2\pi Nf_o T} (\text{SNR})_\ell^{-\frac{1}{2}} \quad (3-24)$$

where $(\text{SNR})_\ell = \frac{S}{\phi B_n}$ and $B_n = \int_{-\infty}^{\infty} |H_\ell(j\omega)|^2 \frac{d\omega}{2\pi}$ is the loop bandwidth.

A lower bound on the loop bandwidth is established from phase dynamic tracking requirements (doppler rates, short-term oscillator instabilities). If a conventional 2nd-order loop design with a damping factor of $1/\sqrt{2}$ for the receiver loop is assumed, the doppler rate tracking error will be given by

$$\phi_e(\text{doppler rate}) = \frac{405D}{B_n} \text{ deg} \quad (3-25)$$

and since the predominate doppler rate contribution is $ND_o = 5 \text{ Hz/s}$ maximum then a loop bandwidth B_n 15-45 Hz is required to maintain the locking error below 1-10 deg. The bandwidth constraint due to the short-term instabilities of the user L.O. is, in turn, accounted for by representing the power spectral

density of the oscillator phase noise in the parametric form

$$S_{\phi}(\omega) = \frac{A}{\omega^3} + \frac{B}{\omega^2} + \frac{C}{\omega} + D \quad (3-26)$$

where the constants depend on the type and quality of the oscillator in question. The rms locking error contribution is then evaluated from the expression

$$\phi_e(\text{osc noise}) = \left[\int_{-\infty}^{\infty} S_{\phi}(\omega) \left| 1 - H_2(j\omega) \right|^2 \frac{d\omega}{2\pi} \right]^{\frac{1}{2}} \text{ rad rms} \quad (3-27)$$

for a given loop transfer function. The A and B term have been found to predominate for 2nd-order loops having a deamping factor of $1/\sqrt{2}$ and $B_n < 100$ Hz when typical spacecraft oscillators are considered (Reference 3-10), in which case the approximation

$$\phi_e(\text{VHF osc noise}) \sim \frac{1}{20 B_n} \left(1 + \frac{B_n}{400} \right)^{\frac{1}{2}} \text{ rad rms for } B_n < 100 \text{ Hz} \quad (3-28)$$

has been verified to be effective so that $B_n > 3$ Hz would be required to maintain the rms locking error within 1° . The doppler rate bound thus predominates over the spacecraft oscillator jitter bound when the typical spectral parameter values are assumed for the latter.

It should be acknowledged that the local receiver oscillators used for mixing purposes, the uplink signal retransmitted by the TDRS downlink relay, and the TDRS and GS loop VCO's also contribute oscillator phase noise and should be accounted for in the bandwidth constraint determination. The ground-originated processes (TDRS retransmitted or Rcvr reference L.O.'s) can be compensated using the beacon turnaround approach and the carrier + beacon loop VCO effects need only be considered. As previously stated, these VCO's may exhibit Ku-band phase noise filtered by the loop error transfer function, to be compared to the user VHF phase noise identically filtered and the predominant error source is not evident. In the absence of definite data on VCO spectral decomposition to aid in an error evaluation analogous to that performed for the user L.O., we will limit ourselves at this stage to recognize the need for a closer look at this problem and to cite that VCO closed-loop locking errors in existing tracking systems have been specified as 3° in 10 Hz loop bandwidth, so that the bandwidth range under consideration seems to be adequate and $B_n = 15$ Hz will be used in the discussion that follows based on the doppler rate and user oscillator noise locking error analysis.



The 40 dB-Hz user/TDRS link budget may not be fully applicable to the range rate signal due to the possible presence of carrier phase modulation for LAR ranging purposes. The corresponding loop SNR for the two cases of no carrier attenuation (no modulation) and -3.5 dB carrier attenuation (e.g., a 1.2 rad PM sidetone) using $B_n=15$ Hz are then

$$(\text{SNR})_{\ell} = \begin{matrix} 28.2 \text{ dB (no attenuation)} \\ 24.7 \text{ dB (3.5 dB attenuation)} \end{matrix}$$

which represent locking errors within 2.5° rms. The corresponding rms range rate errors as a function of output data rate $1/T$ for $B_n=15$ Hz are now summarized for the two cases in question.

<u>T(sec)</u>	<u>σ_R^* (cm/s, no carrier atten)</u>	<u>σ_R^* (cm/s, 3.5 dB carrier atten)</u>
10	0.12	0.18
1	1.2	1.8

and the use of higher data rates would question the $B_n T \gg 1$ assumption used to neglect the R (T) contribution to σ_R^* , and a detailed characterization of the phase noise correlation introduced by the loop filtering would then be required for quantitative results.

The effect of short-term oscillator instabilities can be evaluated from the formula

$$\sigma_R^* = \frac{c}{Nf_o} \sigma_D = \frac{c}{2\pi Nf_o} \left[\int_{-\infty}^{\infty} S_{\dot{\phi}}(\omega) \left(\frac{\sin \omega T/2}{\omega T/2} \right)^2 \frac{d\omega}{2\pi} \right]^{\frac{1}{2}} \quad (3-29)$$

where $S_{\dot{\phi}}(\omega) = \omega^2 S_{\phi}(\omega)$ is the power spectral density of the oscillator frequency jitter. ϕ If we assume a predominant B-term in the spectral decomposition, the previous expression reduces to

$$\sigma_R^* = \frac{c}{Nf_o} \sigma_D = \frac{c}{2\pi Nf_o} \left(\frac{2B}{T} \right)^{\frac{1}{2}} \quad (3-30)$$

where in our case the oscillator in question is a mixture of the user VHF L.O. contribution and the carrier + beacon receiver VCO contributions. The user L.O. contribution may be evaluated assuming typical spectral parameters for spacecraft oscillator noise as

$$\sigma_R^* (\text{user osc noise}) \sim \frac{1}{9\sqrt{T}} \text{ cm/s rms} \quad (3-31)$$

or

<u>T(sec)</u>	<u>σ_R^*(cm/s, user L.O.)</u>
10	0.035
1	0.111

so that the thermal noise error contribution predominates over the user L.O. jitter effect.

The above analyses show that the expected \dot{R} errors are well within those required to reach the results predicted by Cooley for tracking a user spacecraft via two TDRS's with \dot{R} data only.

More extensive analyses of both the forward and return link range and range rate errors at VHF and UHF are given in the next section to further substantiate the accuracy claims.

3.5.3.4 LDR Forward and Return Link Range and Range Rate Performance

To evaluate the impact of the specified chip rates on forward and return link range rate accuracies the link power budgets used to evaluate data rate capacities were assumed.

The expression for the rms range error due to noise can be expressed as, (on a worst case basis):

$$\Delta R_{\text{rms}} = \frac{\pi}{5} \frac{C T_c}{\sqrt{2 \left(\frac{S}{N}\right)_L}} \quad (3-32)$$

where

C = velocity of light

T_c = PN chip duration

$\left(\frac{S}{N}\right)_L$ = code loop SNR = $\left[\frac{C}{N_o} \left(\frac{1}{B_L}\right)\right]$

B_L = the one sided code loop bandwidth



Therefore, either equation 3-13 or 3-14 which is used to evaluate the carrier-to-noise density for the forward and return links respectively can be inserted into equation 3-32 to determine the forward and return link rms range error. Thus, the estimates of range error includes all potential loss, RFI, multipath, other user signals, and expected ambient Gaussian noise at the receiver.

In Figures 3-47, 3-48, and 3-49 the forward link rms range error at VHF and UHF are presented. Figure 3-50 depicts the return link range error at 136 MHz. In all cases range error is compared with RFI density with chip rate as a parameter; other conditions assumed are the same as those (for the forward and return links) in Sections 3.5.1 and 3.5.2, except where noted in the figures.

The range rate rms error in the forward and return links can be determined from the standard range rate error equation which has been developed in the multipath/modulation study for the tracking and data relay satellite (Reference 3-11), namely

$$\Delta \dot{R}_{rms} = \frac{C}{2 \sqrt{2\pi} T_{ob} f_c \sqrt{(S/N)_{CL}}} \quad (3-33)$$

where

C = velocity of light

T_{ob} = observation time

f_c = carrier frequency

$\left(\frac{S}{N}\right)_{CL}$ = carrier tracking loop SNR $\left[= \left(\frac{C}{N_o}\right) \left(\frac{1}{B_{CL}}\right)\right]$

B_{CL} = carrier tracking loop bandwidth

As in the aforementioned case, equations 3-13 or 3-14 are inserted into equation 3-33 to obtain an indication of the expected $\Delta \dot{R}$ for the forward and return link. Presented in Figures 3-51, 3-52, and 3-53 is the expected forward link rms range rate error at VHF and UHF. In addition, the range error is estimated for the return link (i.e., 136 MHz) and is shown in Figure 3-54.

3.5.4 Pseudo-Random Code Acquisition and Tracking

Pseudo-random code (hereafter referred to as PN code) modulation is used in the communication links to both the LDR and MDR user satellites. In the LDR user satellites, PN modulation is used to:

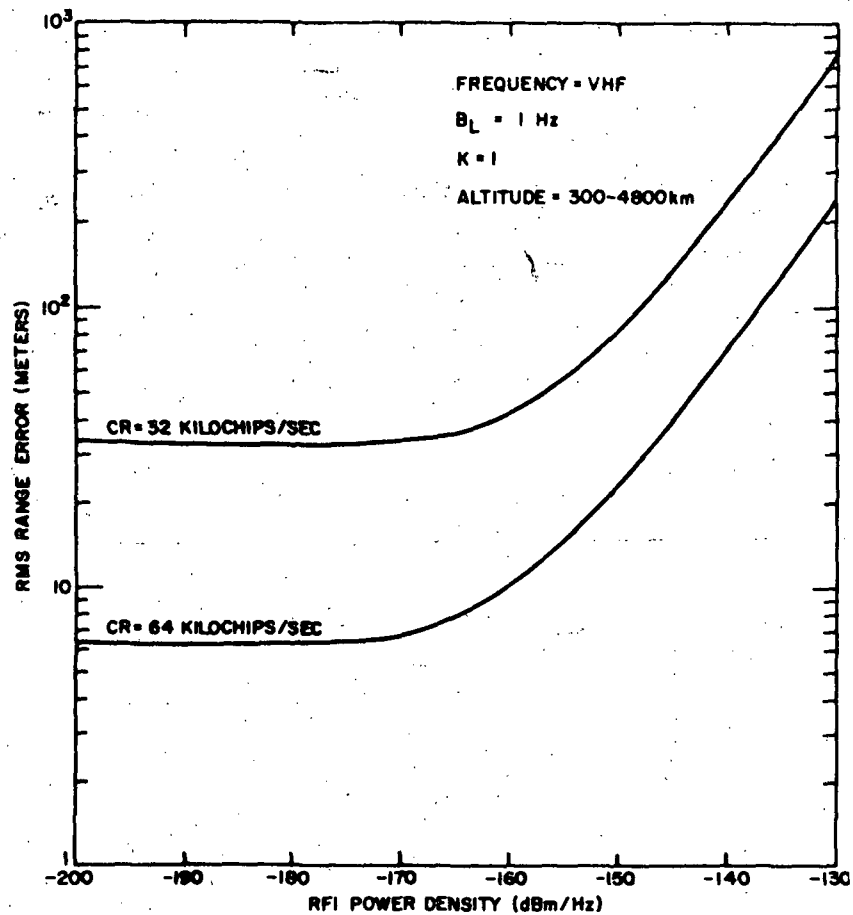


Figure 3-47. Forward Link RMS Range Error Versus RFI Power Density at VHF

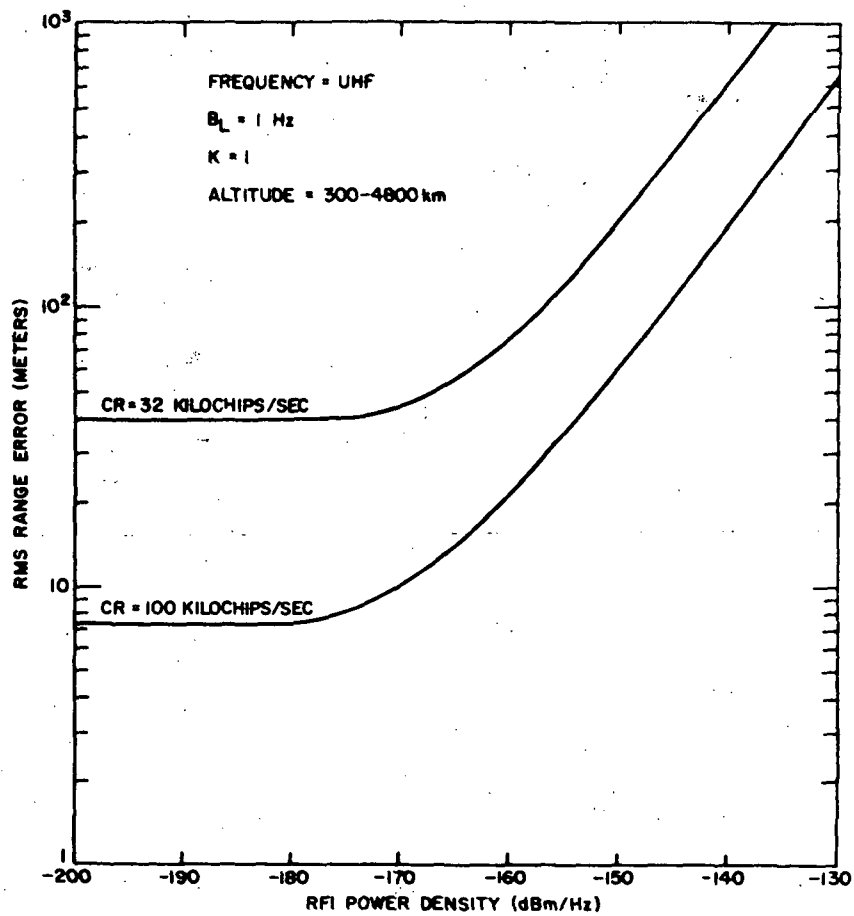


Figure 3-48. Forward Link RMS Range Error Versus RFI Power Density at UHF



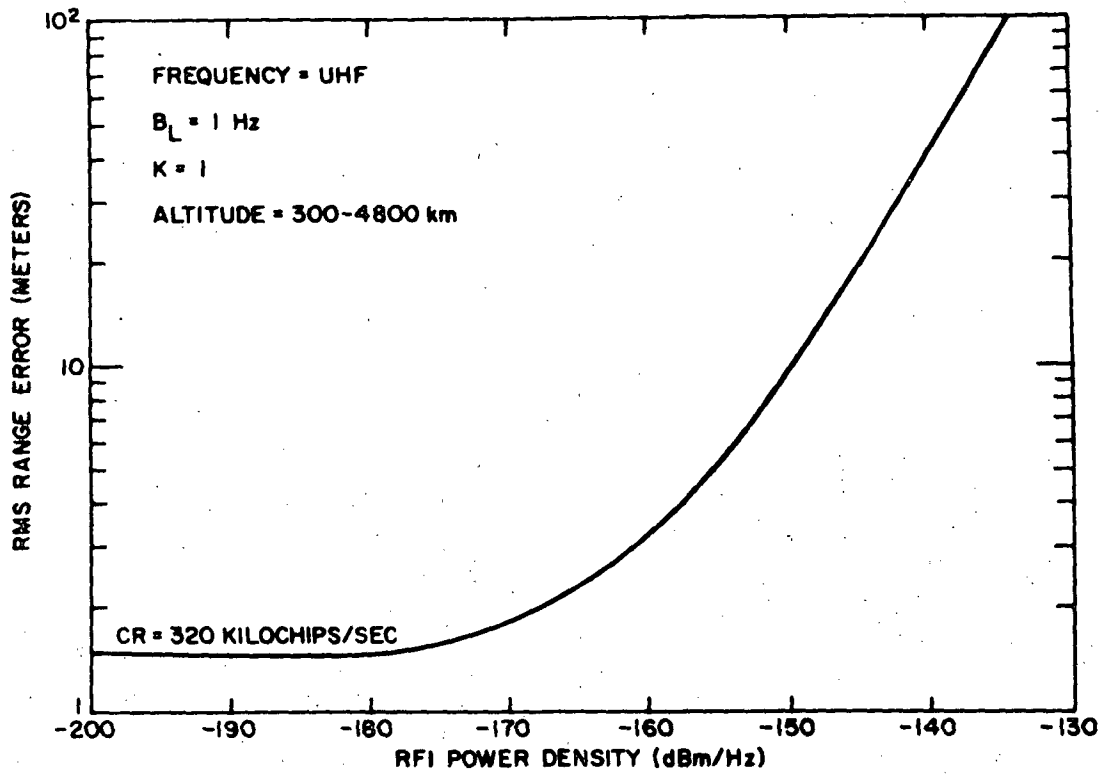


Figure 3-49. Forward Link Range Error Versus RFI Power Density--Chip Rate = 320 Kilochips per Second

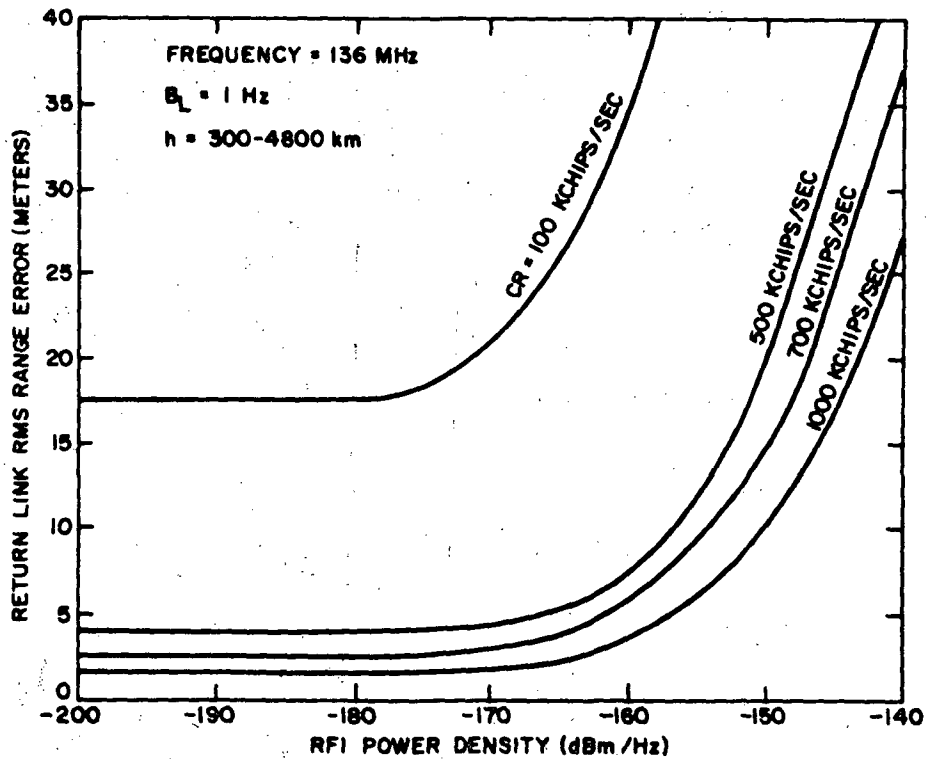


Figure 3-50. Return Link RMS Range Error Versus RFI Power Density at 136 MHz

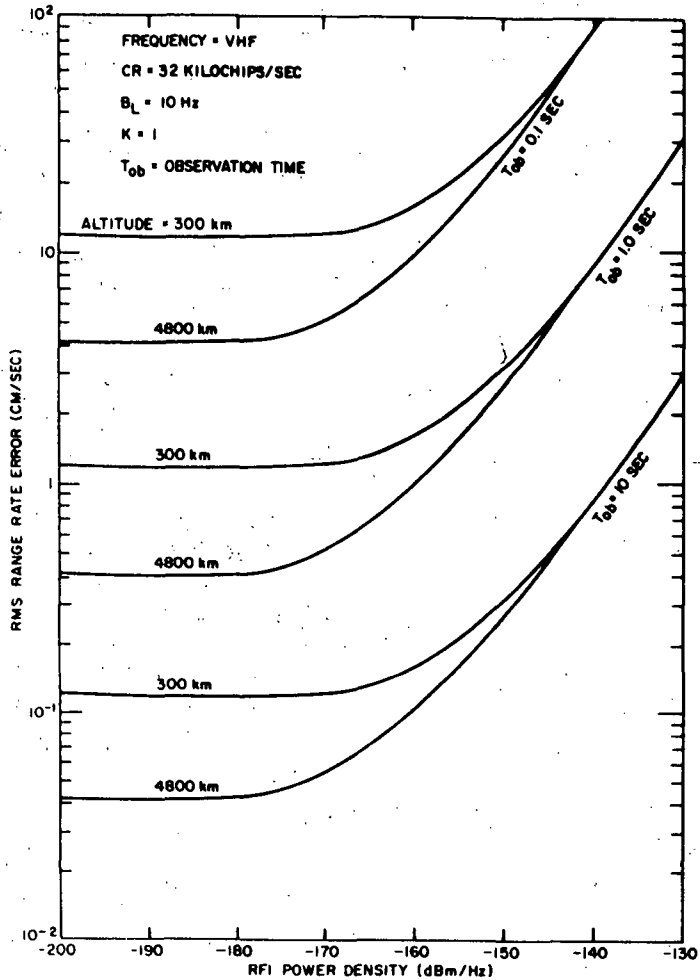


Figure 3-51. Forward Link Range Rate Error at VHF - Chip Rate = 32 Kilochips per Second

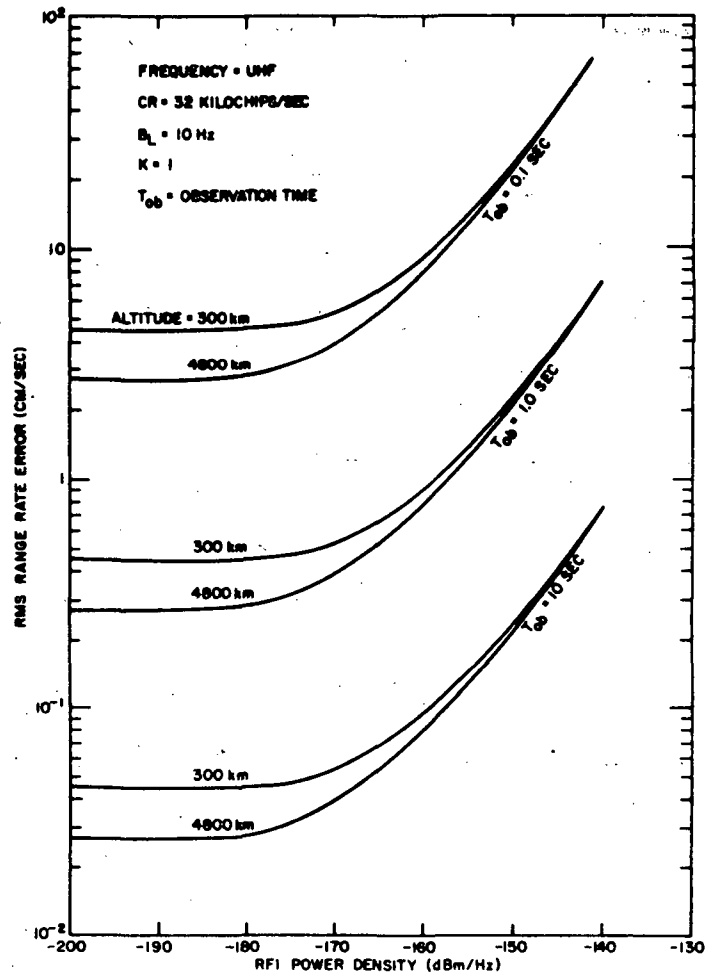


Figure 3-52. Forward Link Range Rate Error at UHF - Chip Rate = 32 Kilochips per Second



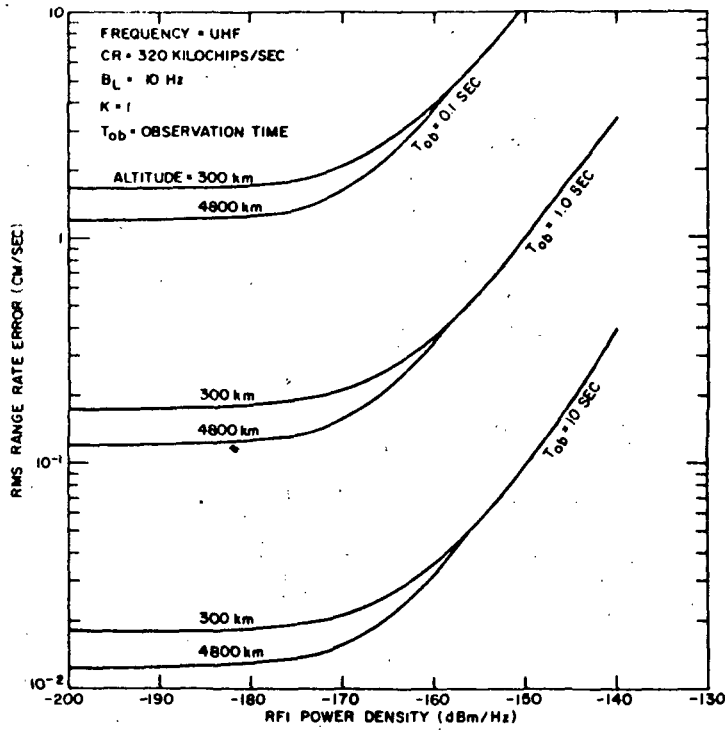


Figure 3-53. Forward Link Range Rate Error at UHF -
Chip Rate = 320 Kilochips per Second

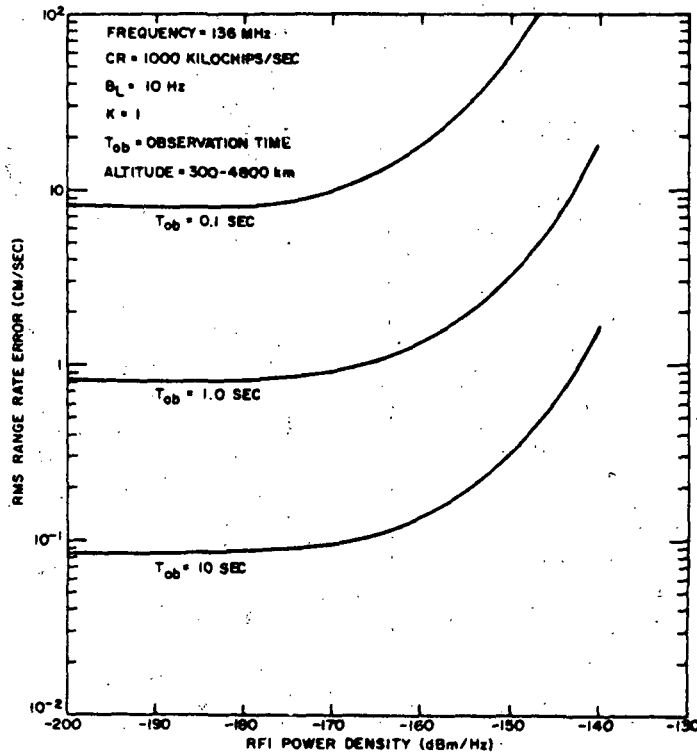


Figure 3-54. Return Link Range Rate Error at 136 MHz -
Chip Rate = 1000 Kilochips per Second



1. Distribute the signal energy emanating from the TDRS to the user over a bandwidth such that the signal flux density at the earth will conform to the requirements of the IRAC (these requirements are presented in Table 3-11 of Section 3.3 of this report).
2. Discriminate against the multipath signals which will exist in the LDR case because of the omni-antennas.
3. Provide code division multiplexing from 20 users on the return link. Each of the up to 20 users will have a unique PN sequence to permit signal differentiation.
4. After synchronization has been accomplished, the two-way range information from TDRS to user is contained in the relationship between the transmitter and receiver PN code generators.

The need for PN modulation for the MDR type user satellite is for conformance with the IRAC flux density requirements and for ranging.

The use of PN modulation necessitates a synchronization procedure which must meet several requirements and is constrained by number of parameters. Synchronization is achieved in two steps: initial acquisition (i.e., synchronizing the received and reference coded to within a bit) and tracking (i.e., pulling into correlation after initial acquisition and maintaining this correlation of the two codes). Acquisition can be implemented in a number of ways and the choice is dependent primarily on the time allowed to acquire.

The time required to acquire a received PN code is a function of the amount of frequency and time uncertainty which must be resolved. The frequency uncertainty is a function of the doppler and the time uncertainty is due to the unknown transit time from transmitter to receiver. The procedure used here is to search the total frequency uncertainty region (max. approximately ± 12 kHz at 400 MHz) for each increment of the time uncertainty. If the signal is not present then the search is advanced to the next time increment and the frequency search repeated. This procedure is repeated until the signal is found within a particular time interval (in terms of the PN code chips) and frequency interval. The decision as to whether the signal is found is based on the magnitude of the signal of a given frequency cell relative to the average level (multiplied by a fixed threshold factor) over the total frequency uncertainty band.

The procedure illustrates that the time to acquire the received code will be based on the number of uncertainty cells (both frequency and time) searched and the dwell time per cell. The number of time cells to be searched is dependent on the length of the PN sequence which is in turn dependent on the PN code rate and the time length of the code to provide unambiguous ranging.



3.5.4.1 Frequency Search

The frequency search is accomplished by the doppler processor. A functional block diagram of the processor is included in the overall LDR receiver block diagram of Figure 3-55. A detailed description of the LDR and MDR transponders is presented in Section 11.0. A basic approach would be to sweep over the frequency uncertainty range. A better approach from a standpoint of saving time is a bank of parallel matched filters centered at intervals of the data rate. This in effect is what the doppler processor does.

The doppler processor performs a digital spectral analysis of the input signal over the frequency uncertainty range. At 400 MHz the maximum doppler which will be experienced will be ± 12 kHz. Assuming two modes of operation (i.e., 100 bps and 1000 bps data rates) the doppler processor is mechanized in the following manner. At 100 bps, samples are taken for a period of 10 ms with a frequency resolution of 100 Hz and 240 frequency slots in the frequency uncertainty range. The Fourier coefficients for each of the 240 frequency slots are computed sequentially. This procedure is functionally represented by the squaring and integration block in the block diagram. As each set of coefficients is computed they are compared with the previous set and the largest set retained until all 240 sets of coefficients have been computed and compared. This largest set is then compared against an average level. A decision that the signal has been acquired is based on the peak set of Fourier coefficients exceeding the average level by some threshold factor. The value of this threshold setting will depend on the desired probability of acquiring false lock and the bandwidth of the baseband circuitry preceding the doppler processor while operating in the acquisition mode.

Thus, the dwell time for each frequency cell is a function of the number of computations performed to compute a set of Fourier coefficients. The total time for each frequency search (over total frequency uncertainty range) is the reciprocal of the data rate or 10 ms and 1 ms corresponding to 100 bps and 1 kbps.

3.5.4.2 Time Search

After each frequency search if the PN code has not been acquired the reference PN sequence is retarded by 1/2 bit and the entire process repeated until acquisition is made. The choice of 1/2 chip shifts in the reference code is made because even under the worst case phasing relationship (no worse than a 1/4 chip displacement) the cross-correlation of the received and reference PN codes will be down only 1 dB from the ideal autocorrelation peak. The steps could have been made smaller but the acquisition time would be increased proportionally.

3.5.4.3 Acquisition Time

The maximum one way unknown range increment which could exist is 20,000 km. The IRAC requirement for 400 MHz is that the signal flux density on the earth shall not exceed -150 dBw/meter² in a 4 kHz frequency band. These requirements indicate that the 30 dBw EIRP from the TDRS to the LDR user

3-74
SD 72-SA-0133

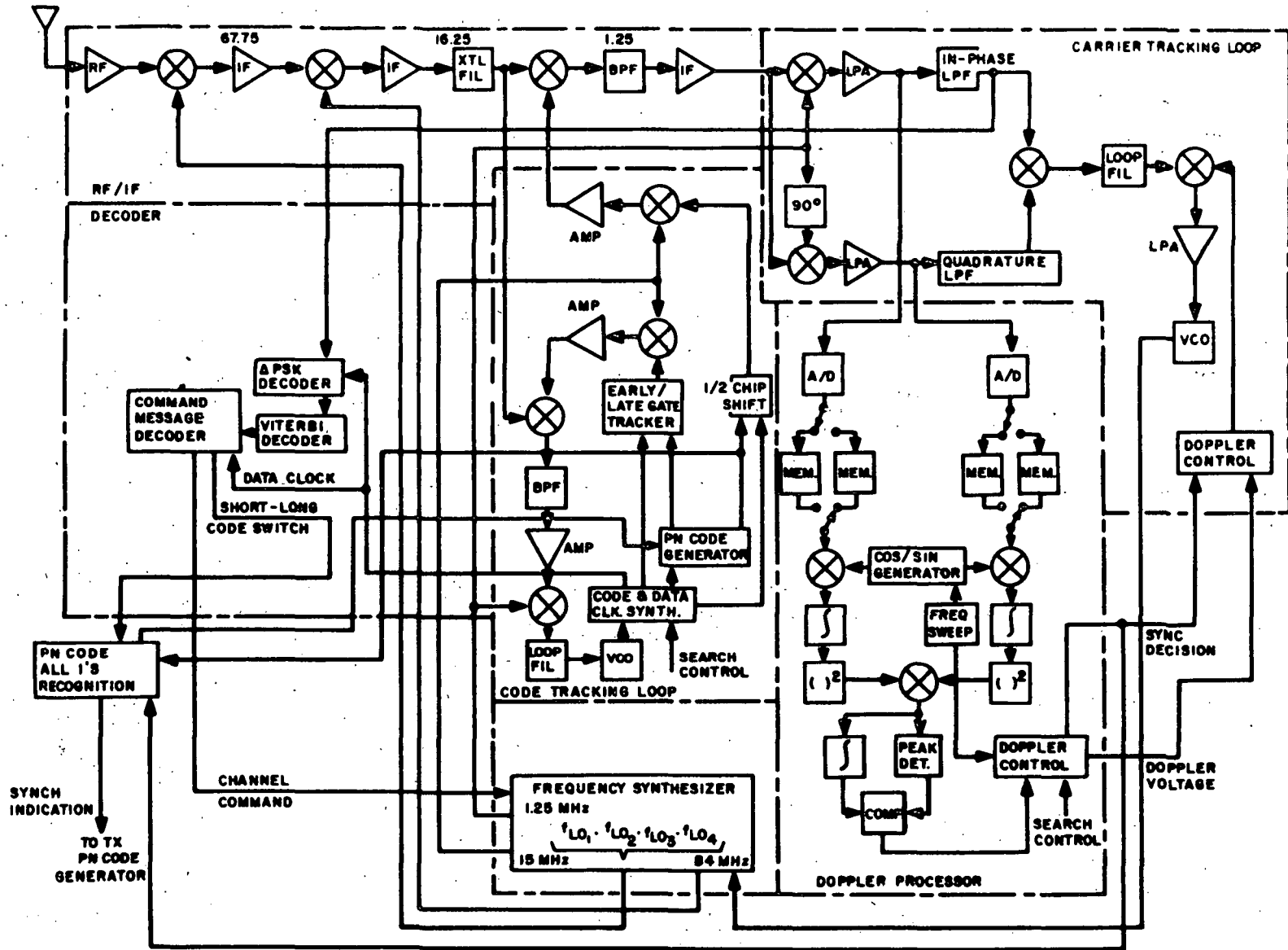


Figure 3-55. LDR Receiver



must be uniformly distributed over 250 kHz. Using a one side receiver filter bandwidth-to-PN code chip rate ratio of 1.5, the minimum chip rate will be 167 kilochips/sec. At this minimum allowable chip rate the code length necessary for two-way unambiguous ranging over the 40000 km uncertainty will require a code length of 22222 chips since at 167 kilochips/sec each chip represents 1800 meters in range. This will require a maximal length sequence of 32767 chips.

The acquisition time based on 1/2 bit shifts, 32767 chip code length, and 10 ms frequency search time results in a total maximum acquisition time of 655.3 secs. The problem is six times as bad in the return link because of the maximum 1 Mchip/sec required. This is an unacceptably long acquisition time. Assuming a 40-sec acquisition as reasonable, the curves of Figure 3-56 show that for a 100 bps data rate a 2047 chip code is the maximum length which can be used. This can be increased to a 4095 code by going to 1 chip shifts but at a 3 dB cost required C/N. Given that 2047 is the maximum code length for the acquisition mode the following concept has been used to resolve the two contradictory problems, i.e., short acquisition time and large range uncertainty.

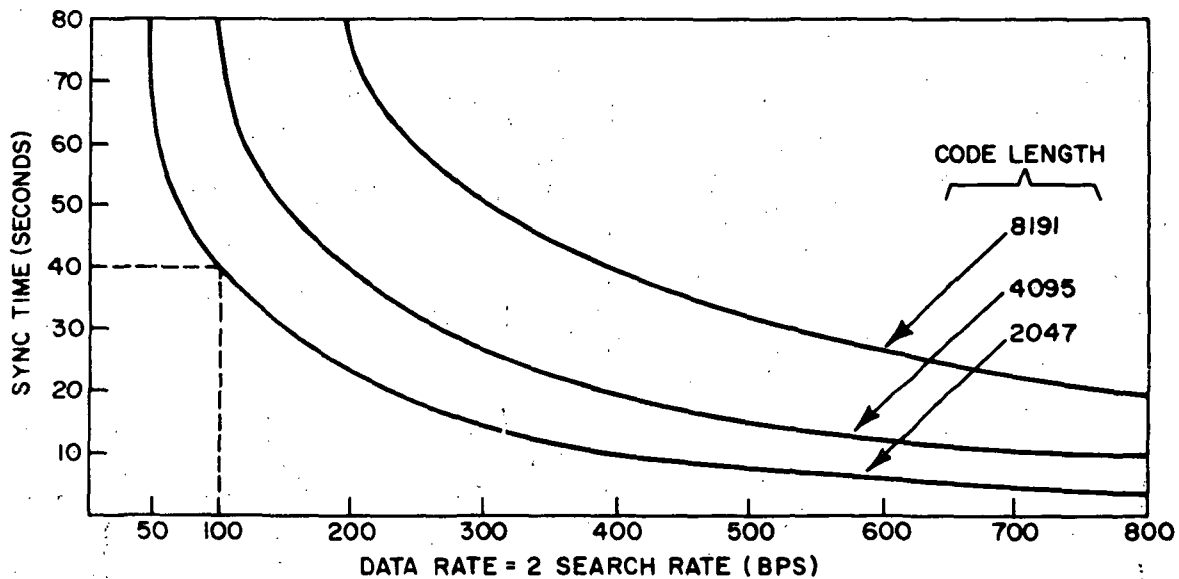


Figure 3-56. PN Synchronization Time



The ground station initially will transmit a short code to the user satellite which will take a maximum of 40 secs to acquire. Acquisition of the received code in the user will initiate the transmitter and the PN code generator in the transmitter. Since the code sequences in the receiver and transmitter will be different, the all one's point in both the received and transmitted sequences will be synchronized to avoid a time uncertainty. The PN code chip rate for the return link is six times faster than the forward link rate which means that during the acquisition mode the six sequences of the 2047 sequences will be transmitted for each sequence received but the all one's vector of the received code will be correlated with every sixth sequence transmitted. The transmitted signal must be acquired in the ground station. Using the same basic acquisition procedures an additional acquisition time will be required, again a maximum of 40 seconds. Now the user and TDRS ground station are completely synchronized in both the forward and return links. Data can now be transmitted to and from the user. However, to resolve the range ambiguity problem the PN code must be lengthened. This will be done by changing the PN sequence structure at each code interval. Since a minimum of 22222 chips are required for the unambiguous ranging eleven 2047 length codes, each a different sequence, can be sequentially transmitted to achieve a total length of 22517 chips. With 20 possible users and an increase rate of 1 Mchip/sec, 320 unique codes are required for the return link and eleven for the forward link. There are 2049 Gold codes of length 2047.

3.5.5 Manned User Performance

Although not a specific item in the program work statement, the manned user support is implied by virtue of the requirement for voice link support. At this time the postulated manned user in the TDRSS during the first several years of operation is Space Shuttle. Since no specific support requirements for a manned user have been stipulated, the Shuttle requirements will be used as an example of typical manned user support.

The specification for the link support required for Shuttle are given in Table 3-23.

Table 3-23. Space Shuttle Requirements and Constraints

°Data Rate
Forward link = 2 kbps
Return link = 76.8 kbps
°Voice
Forward link = 19.2 kbps (1 or 2 channels)
Return link = 19.2 kbps (1 or 2 channels)
°Bit Error Rate
Data = 10^{-4}
Voice = 10^{-3}
°System Margin = +3 dB
°Shuttle Antenna Gain = +3 dB



The voice and data for Shuttle on both the forward and return link are time-division-multiplexed. The voice modulation is adaptive-delta-modulation. It was shown in Section 3.4 that the required C/N₀ to support a voice link with a BER = 10⁻³ and greater than 90% intelligibility is on the order of 49 dB-Hz. The data modulation is assumed to be ΔPSK, for which a BER = 10⁻⁴ requires an E_b/N₀ of approximately 8.7 dB, so that the required C/N₀ is on the order of 41.7 dB-Hz (no margin).

In the sections that follow the TDRS forward and return link requirements to support Shuttle will be discussed.

3.5.5.1 Forward Link Support

As stated, the forward link support for Shuttle consists of one 2 kbps data link and a minimum of one, but preferably two, voice links multiplexed with the data. The available carrier-to-noise density into a 3 dB Shuttle antenna is, depending on the system temperature assumed, between 50.1 dB-Hz and 52.5 dB-Hz. The discrepancy evolves from a difference in MSC estimates (T_s = 30 dB) and those of NR/AIL/Magnavox (T_s = 27.3 dB). A typical power budget is presented in Table 3-24, and reflects the difference.

Table 3-24. Forward Link Power Budget for Shuttle

Description	MSC	NR/AIL/Magnavox
EIRP, dBw	41.0	41.0/47.0*
Transponder Loss, dB	0.5	0.25
Path Loss, dB	192.0	192.0
Other Losses, dB	---	0.6
G _{Shuttle} , dBi	3.0	3.0
Boltzmann's Const., dBw °K-Hz	-228.6	-228.6
System Temp., dB	30.0	27.3
C/N ₀ , dB-Hz	50.1	52.45/58.45

*Increased EIRP used for voice only.

The carrier-to-noise densities required to support the links of interest (see Table 3.23) have been computed for a system margin of 3 dB, and are listed in Table 3.25.



Table 3-25. Carrier-to-Noise Density Required for Shuttle Support in Forward Link

Link	Margin	Required C/N ₀
Data (ΔPSK; BER = 10 ⁻⁴)	3 dB	44.7 dB-Hz
Voice (Δ-Mod; BER = 10 ⁻³)	3 dB	51.8 dB-Hz
Data + 1 voice	3 dB	52.58 dB-Hz
Data + 2 voice	3 dB	55.44 dB-Hz

When the C/N₀ requirements of Table 3-24 are compared to the C/N₀ available in Table 3-25, and estimate of the additional gain required to support the link can be made. Estimates of additional signal gain required to support Shuttle are presented in Table 3-26. In that table the estimates based on MSC link assumptions are compared with those made by NR/AIL/Magnavox.

Table 3-26. Estimates of Additional Gain Required to Support Space Shuttle in Forward Link

	MSC			NR/AIL/Magnavox		
	Data	Data +1 Voice	Data +2 Voice	Data	Data +1 Voice	Data + 2 Voice
C/N ₀ , available (includes +3 dB margin)	50.1	50.1	50.1	52.8	52.8	52.8
C/N ₀ , required	44.7	52.58	55.44	44.7	52.58	55.44
Additional gain required, dB	--	+2.48	5.34	--	--	2.99

The table indicates that a minimum additional forward link gain of approximately 2.99 dB is required. Depending on which set of assumptions is used, support with that minimum additional gain can be given to either a data + 1 voice link (MSC), or a data + 2 voice link (NR/AIL/Magnavox). If the MSC

assumptions are used then an additional gain of 4.84 dB is required for the data + 2 voice link. This improvement can be achieved through the use of forward error control (see Section 3.4). A rate one-half ($R = 1/2$) convolutional code with constraint length of seven ($K = 7$), coupled to a Viterbi (maximum likelihood) decoder can provide the gain margin needed. A recent editorial in an IEEE Journal indicates that at this time a 20 kbps Viterbi decoder ($R = 1/2$; $K = 6$) has size, power, and weight characteristics of 9 in.³ (150 cm³) 6.8w, and 0.5 lb (.2 kg), respectively, (estimated price = \$5000); projections of these characteristics to the year 2000 indicate size, power and weight of one integrated circuit, 0.6w, and negligible weight (cost = \$200).

An alternative to forward error control is to increase the TDRS transmit power (say by 6 dB) during voice transmission. If a voice transmission duty cycle of 25% is assumed, the average transmit power remains at 41 dBw; the net result, however, is a system margin for 1 data + 2 voice of about 6 dB.

3.5.5.2 Return Link Support

As indicated in Table 3-1 return link support requirements for Shuttle are a data rate 76.8 kbps ($BER = 10^{-4}$) and one (acceptable) or two (preferable) delta modulated voice links at 19.2 kbps each ($BER = 10^{-3}$). The carrier-to-noise density required for return link support of Shuttle is shown in Table 3-27.

Table 3-27. Carrier-to-Noise Density Required for Shuttle Support in Return Link

Link	Margin	Required, C/N ₀
Data: 76.8 kbps (Δ PSK; $BER = 10^{-4}$)	3 dB	60.59 dB-Hz
Voice: 19.2 kbps (Δ -Mod; $BER = 10^{-3}$)	3 dB	51.8 dB-Hz
Data + 1 voice	3 dB	61.17 dB-Hz
Data + 2 voice	3 dB	61.50 dB-Hz

In the table a +3 dB system margin has been included. Table 3-28 provides an indication of the return link power budget (namely the required transmit power) for shuttle support.

Table 3-28 indicates that under the MSC assumptions the amount of power required to support the link is quite large. Under the NR/AIL/Magnavox assumptions, however, the additional power gain can be achieved with forward error control as described in Section 3.5.5.1.



Table 3-28. Return Link Power Budget for Shuttle

Description	MSC			NR/AIL/Magnavox		
	Data	Data +1 Voice	Data +2 Voice	Data	Data +1 Voice	Data +2 Voice
C/N ₀ , dB-Hz (required; with 3 dB margin)	60.59	61.17	61.50	60.59	61.17	61.50
Path loss, (1) dB	192.0	192.0	192.0	191.1	191.1	191.1
TDRS trans- ponder loss, dB	0.5	0.5	0.5	0.5	0.5	0.5
G _{TDRS} (S-band), dBi	30.1	30.1	30.1	30.9	30.9	30.9
G _{Shuttle} dBi	3.0	3.0	3.0	3.0	3.0	3.0
Losses (TDRS), dB	3.0	3.0	3.0	0.6	0.6	0.6
Boltzmann's constant, $\frac{dBw}{K-Hz}$	-228.6	-228.6	-228.6	-228.6	-228.6	-228.6
System temp, dB(1)	30.0	30.0	30.0	26.8	26.8	26.8
EIRP required, dBw	24.39	24.97	25.30	19.49	20.07	20.40
Add. gain reqd with P _T =40w(2) (16 dBw)	8.39	8.97	9.3	3.49	4.07	4.40

(1) The values for path loss and system temperature in the NR/AIL/Magnavox case were computed at the point where the sum of their effect is maximum.

(2) P_T = transmit power into the antenna.



3.5.5.3 Combined Voice and Data Transmission

Simultaneous transmission of voice and data can be accomplished efficiently by three techniques; frequency-, time-, and phase-multiplexing. Of the three, phase-multiplexing is the preferred technique. The phase-multiplexing concept as applied to delta-modulated voice and straight binary data can be relayed in a concept referred to as quadrature modulation (i.e., a quadrature carrier multiplexing). The system is fully digital with the exception of audio processing and filtering circuits and provides for transmission of a constant envelope signal.

As mentioned, quadrature modulation provides a channel for continuous constant envelope simultaneous transmission of voice and data. Since the voice and data channels have different performance requirements (10^{-3} and 10^{-4} respectively) the channel power must be varied accordingly. By adjusting the inphase and quadrature signal vectors one can keep the total transmitted power constant while increasing or decreasing the power in the voice or data channel alone.

3.6 REFERENCES

- 3-1 Jenny, J. A., and Weiss, S. A., "The Effects of Multipath and RFI on the Tracking and Data Relay Satellite System," prepared under NASA Contract No. NAS5-20125, 19 March 1971.
- 3-2 Jenny, J. A., and Shaft, P., "The Effects of Multipath and RFI on the TDRSS Command and Telemetry Links - A Final Report," prepared under NASA Contract No. NAS5-20228, 9 March 1972.
- 3-3 Ploussios, G., et al., "Noise Temperature of Airborne Antennas at UHF," Technical Note ESD-TR-66-237, Lincoln Laboratory, Massachusetts Institute of Technology, 6 December 1966.
- 3-4 Birch, J. N., "Multipath/Modulation Study for the Tracking and Data Relay Satellite System," Final Report Contract NAS5-10744.
- 3-5 GSFC Document No. X-520-69-38, "Range and Velocity Components of TDRS Multipath Signals," by T. Golden, February 1969.
- 3-6 Viterbi, A. J., "Orthogonal Tree Codes for Communication in the Presence of White Gaussian Noise," IEEE Trans., Vol. COM-15, No. 2, April 1967, pp. 238-242.
- 3-7 Birch, J. N. and Getzin, N. R., "Voice Coding and Intelligibility Testing Study," Final Report, prepared for NASA/GSFC, Contract NAS5-20168, April 1971.



- 3-8 Birch, J. N., "Multipath/Modulation Study for the Tracking and Data Relay Satellite System," Final Report Contract NAS5-10744, prepared by The Magnavox Company, Silver Spring, Maryland.
- 3-9 Flight Mission Analysis Branch, NASA/GSFC.
- 3-10 Grant, T. L., and Cramer, R. L., "Effect of Oscillator Instability of Telemetry Signals," NASA/AMES TN-D6442, July 1971.
- 3-11 Birch, J. N., Op. Cit.



4.0 TDRS TELECOMMUNICATION SUBSYSTEM

This study supports a plan by NASA to launch two operational Tracking and Data Relay Satellites (TDRS) into geosynchronous orbit in the late 1970's to continuously service and provide real-time support for low-altitude orbiting spacecraft (below 5000 km). The two TDRS satellites plus an in-orbit spare will be used as shown in Figure 4-1 to provide multiple-access service to a variety of user spacecraft at different orbital altitudes with a wide range of link performance requirements and physical configurations. For this study, the users have been categorized with respect to their return data rate (H) needs where for a low data rate (LDR) $H = 10^2 - 10^4$ bps, for a medium data rate (MDR) $H = 10^4 - 10^6$ bps, and for a high data rate (HDR) $H \geq 10^6$ bps including TV. This section covers the Part I phase of the study which describes:

- Design goals and criteria
- Design requirements and constraints
- Detailed description of the recommended design
- Spaceborne system and subsystems
 - Link analysis and tradeoffs
 - Mechanization tradeoffs
 - Detailed description of the recommended design
 - Performance specification
 - Size, weight, and power

Each TDRS satellite must simultaneously support 20 LDR users and at least one MDR user in the return link (user to TDRS to GS), and two LDR users and at least one MDR user in the command link (GS to TDRS to user). The 2914 Delta will be the TDRS payload launch vehicle.

To meet these design requirements, this telecommunication study analysis has stressed an overall design goal to maximize the simultaneous support of user spacecraft and link performances consistent with the high reliability requirements of unattended five-year life in space. In addition, minimum size, weight, and power for the TDRS spacecraft as well as minimum impact at the user spacecraft terminal are emphasized. High reliability is achieved through full block redundancies of all critical components/subassemblies, functional redundancies employing back-up via entire functional chain, and/or multiple operating channels which provide high reliability through graceful degradation. The recommended design reflects a state-of-the-art technology, yet is consistent with the need to provide flyable hardware in 1977 with minimal or no need for advanced research and development of hardware.

To support the low altitude orbiting users, the TDRS satellite must provide a multiple access relay space-to-space interface with the users; and a space-to-ground interface with the ground station.

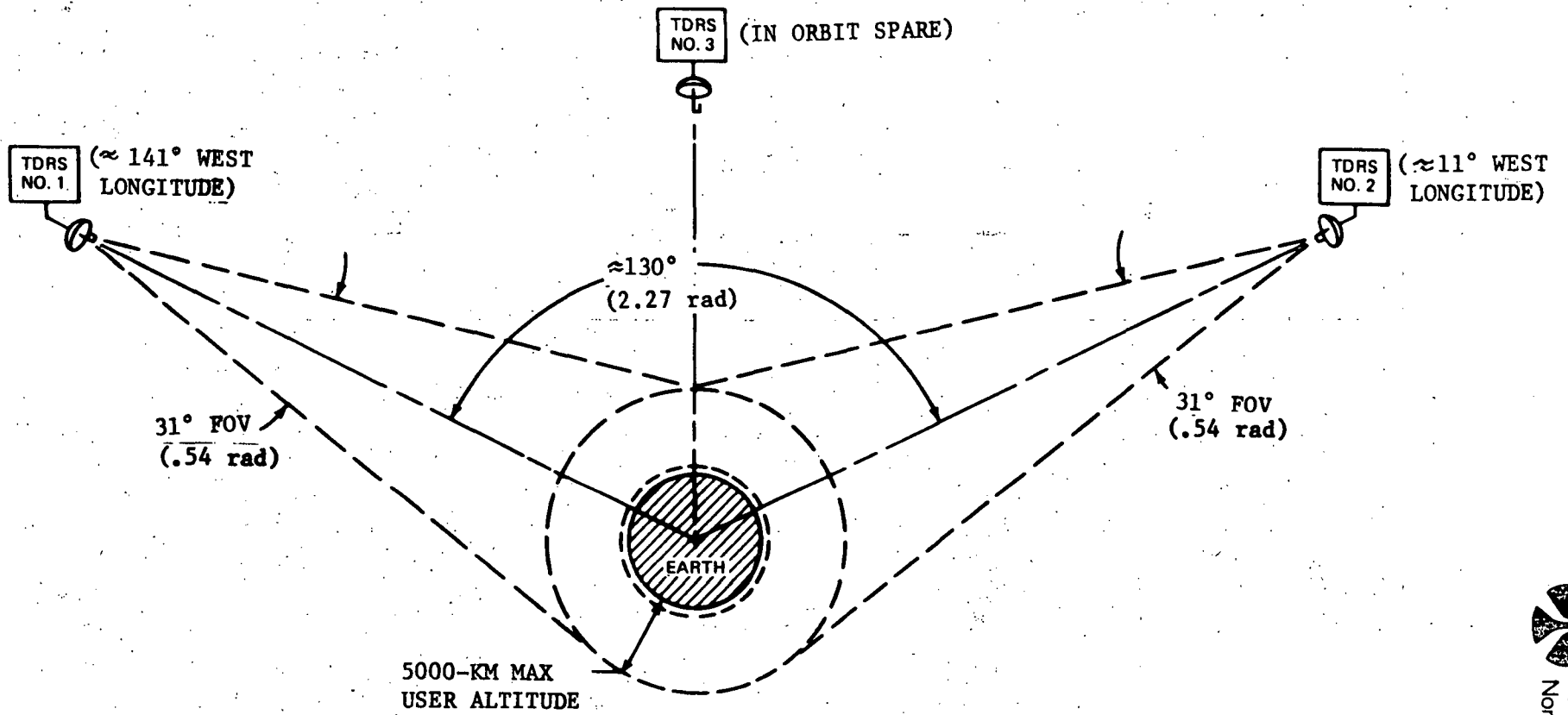


Figure 4-1. Space Geometry for Two Satellite TDRSS Network



The LDR space-to-space links (both return and forward) are subject to intentional interference resulting from direct signals emanating from other in-band users, as well as multi-path introduced by earth surface reflection from both the desired as well as other users. The unintentional interference signals, referred to herein as RFI, result primarily from earth-based in-band emitters and urban "trash noise" emitted from various urban machineries/generators. Although accurate RFI power densities for the present and future operational environment do not appear truly predictable, existing library catalogs of domestic and foreign emitters indicate potential levels can totally disrupt the entire link if adequate precaution is not taken during the early design phases.

In the LDR return link, the TDRS transponder sees nearly an entire hemisphere of RFI emitters, its level being potentially 20 to 40 dB greater than the desired user signal. To combat the high RFI environment, an Adaptive Ground Implemented Phased Array (AGIPA) has been conceived which adaptively employs spatial filtering and polarization discrimination of RFI emitters to optimally maximize the signal-to-interference ratio (SIR). As the name AGIPA implies, the spaceborne phased array conducts all of its beam steering/beam shaping and other signal processing functions at the ground station (GS). As a result, all advantages of the phased array are achieved without placing the complexities of the multi-beam processing functions aboard the TDRS. AGIPA provides an independent beam and signal processor for each user, employing a mini-computer at the GS to provide the iterative SIR optimization process.

For this Part I phase, it is conservatively recommended that a four-element phased array be used with AGIPA whose antenna characteristics are the same as a fixed field-of-view (F-FOV) approach which sees the entire 31-degree FOV.

Comprehensive analysis has been conducted to compare the performance of AGIPA with a F-FOV approach for the LDR return link. Since AGIPA is an adaptive system, it was essential to create typical realistic RFI models to compare and assess the performances of the two approaches. A computer program was developed to assess their performances in typical user spacecraft orbits. For both the Atlantic and Pacific scenarios representing TDRS satellites at 11 degrees west and 141 degrees west longitude, AGIPA has been shown to provide nominally 5 to 15 dB of improvement in link performance as compared to a F-FOV approach. It also shows a capability when combined with wide band PN of achieving the specification requirement of 10 kbps in relatively high RFI density. In contrast, a F-FOV approach becomes limited to less than 100 bps; and in the presence of a large jammer (e.g., 20 kw emitter), the F-FOV becomes totally inoperative. AGIPA adaptively utilizes spatial and polarization filtering to discriminate the large emitter along with the other RFI emitters, thus optimizing the SIR, with relatively minor degradation in link performance.



The results of the comparative analysis not only show that processing gain is necessary to achieve the specified link performance in the light of the expected RFI power density; they also indicate the shortcomings of the F-FOV in achieving the desired link performances and more significantly, the potential of becoming totally disabled in the presence of a single large RFI emitter.

For the LDR return link, eight wideband (2.0 MHz) linear channels are used to relay the vertically and horizontally polarized components from the four antenna elements. The loss of any channel or channels causes graceful degradation and merely represents reduced performance, thereby providing high reliability.

This AGIPA concept is in hardware development at AIL under NASA-GSFC Contract Number NAS5-21653 for demonstration in an anechoic test chamber at a scaled frequency at S-band. This demonstration will include an RFI model including 10 RFI emitters.

The LDR command or forward link is also subject to RFI, but contrary to the return link, it is the user spacecraft receiver which is confronted in the interference signals. Since user spacecraft can be more than 200 times closer to the RFI emitters than the TDRS spacecraft, the TDRS transponder must overcome this large differential space loss to provide an adequate signal-to-noise ratio (SNR) at the user. This link was evaluated for operation at VHF, UHF, and S-band. The link analysis and TDRS hardware implementation impact support the recommendation to operate this link at UHF. The relatively large implementation impact at S-band eliminates it for this Part I phase. In comparing VHF and UHF in this RFI limited link, the link performance of both bands are equivalent. The 10 dB additional space loss at UHF becomes immaterial since the desired as well as the RFI signals suffer the same additional space loss. Although a definitive assessment of the RFI power level cannot be identified at VHF and UHF, it appears that the RFI power density can exceed the desired signal by approximately 30 to 40 dB; and the existing data tend to indicate that the density is less at UHF. In addition, the effective isotropic radiated power (EIRP) is limited in both VHF and UHF to +30 dBw to maintain the flux density below the IRAC established guidelines. As a consequence, the relative performance of these links can be evaluated for the same EIRP. By employing high gain backfire antenna elements collinearly stacked on each of the four VHF array elements, the hardware implementation tradeoff has shown that UHF band can provide the maximum link performance for the minimum size, weight, and power impact at the TDRS. The TDRS will form two beams on the satellite which will simultaneously support two command links to one or two independent LDR users.

In the design of the MDR space-to-space link, considerable thought and analysis have been given to (1) insure flexibility to handle the transition between current and future needs, (2) provide operational flexibility to meet the frequency format of potential users, and (3) encompass the varying requirements of the TDRS specification as well as the Space Shuttle. Tradeoff analyses have shown that this link can optimally meet the above needs by employing a dual frequency S/Ku-band capability: S-band to meet the needs of current low performance ($H = 10^4 - 10^5$ bps) users, and Ku-band to meet the



needs of the high performance ($H \geq 10^5$ bps) user, including future TV requirement for the Space Shuttle. The TDRS satellite will provide two dual frequency MDR transponders to simultaneously support two independent users; both operating at S-band, both at Ku-band, or one at each frequency band. Link analyses show that the TDRS specifications as well as Space Shuttle requirements can both be supported employing 6.5' (2 m) parabolic dishes. In the return link, both receivers will be designed with an alternate mode to operate as a 10-MHz channelized receiver, tunable in 20 discrete steps over the entire 100-MHz bandwidth; however, one of the receivers will be designed wide open with a 100-MHz bandwidth at S- and Ku-band to provide a true bentpipe repeater at the TDRS with a growth capacity to handle TV. In addition, at Ku-band, each receiver is tunable in four discrete steps over a 400-MHz bandwidth. This combination of a wide open/channelized receiver provides operational flexibility for the user signal format and frequency consistent with the weight and power limitations. In the forward link, each transmit channel will be designed wideband; wide open at 95 MHz channels at S-band, and 100 MHz channels tunable in four discrete steps over a 400-MHz bandwidth at Ku-band. In addition, one of the MDR transponders will be designed so that either/or both the 6.5' (2 m) dish and the transceiver can functionally provide a backup for the TDRS/GS link at S-band as well as Ku-band.

The Ku-band TDRS/GS link provides the interface not only between the space-to-space links and the ground station, but also the ancillary functions that are necessary to support and service the TDRS satellite itself; viz., the coherent reference for the on-board frequency source, and tracking, telemetry, and command functions. Tradeoff analysis of multiplexing approaches shows that a FDM/FM technique trading power and weight for increased bandwidth, will meet the design goals to provide frequency flexibility, maximum link performance and minimum size, weight, and power. In fact, to achieve the wide open operating flexibility in the MDR links, the Ku-band frequency spectrum for the space-to-space and ground links overlap; however, because of the spread spectrum (FM) used in the space-to-ground link, this signal will be below the user receiver noise level and will not degrade its performance. Link analysis shows that this link can operate with a 3' (.9 m) dish on the TDRS satellite in conjunction with a 60' (18.3 m) dish at the ground station to provide a 99.97 percent probability of successfully establishing the link in a 25 mm per hour rainfall rate in the Washington, D.C., areas. The baseline design provides a rain margin of 17.5 dB. In addition, one of the two 6.5' (2 m) dishes can be used for this TDRS/GS link to provide an additional 6.5 dB of gain, or a total of 24 dB of margin for operation in rain.

The on-board TDRS/GS link transmitter output is adaptive, such that a 10 dB final RF power amplifier is inserted only for operation of this link in inclement weather. Consequently, the average power requirement can be maintained at a low 5.1 watts (dc) level for normal operation.

In the forward TDRS/GS link the ground station has additional flexibility to generate high RF power; consequently, the on-board receiver is designed with a mixer front end. The RF front end is wide open (500 MHz wide) and subsequently down-converted and demultiplexed to provide the individual channelized data for relay to the users or for on-board coherent reference, tracking, telemetry, and command functions.



A common frequency source locked to a pilot tone transmitted from the ground station is used to generate the coherent signal references required on the TDRS. A central frequency generator is used initially to generate key reference signals which are subsequently used to lock-in remote voltage-controlled oscillators (VCO). This approach (1) minimizes the transmission of numerous RF reference signals throughout the on-board telecommunication system, (2) allows each VCO to operate incoherently as a backup mode, and (3) minimizes the generation and filtering of spurious signals. In addition, the frequency source is designed fully redundant, and also will be designed with an additional backup capability to become the prime reference source, such that the ground source can lock-in to the spaceborne reference.

In addition to the primary relay functions, the TDRS must provide tracking, beacon, order wire, telemetry, and command for the TDRS. An S-band transponder provides (1) trilateration ranging, (2) an MDR acquisition beacon, and (3) an order wire for service. A Ku-band beacon is used for acquisition and tracking of the TDRS by Ku-band MDR users with high-gain antennas. For telemetry and command (T&C) functions, a digital approach with a central multiplexer/processor is recommended. All command functions will be pre-programmed into a read-only memory device which can be commanded or scheduled to operate as required. The total spaceborne telecommunication system will weigh 240 pounds (109 kg), including support booms for the antennas.

Comprehensive tradeoff analyses have led to a recommended TDRS telecommunication system design and configuration that meets NASA future operational needs to continuously service and support in real time low-altitude orbiting spacecraft with state-of-the-art technology, but consistent with a launch in mid 1970's and the need for high reliability and unattended space application. Special emphasis has been given to constantly maximize user support as well as link performance, commensurate with a need to minimize overall network cost. Some of the key features of the recommended design are:

1. AGIPA: A unique adaptive phased array approach is recommended for the LDR return link which provides a practical means to: (a) combat the large RFI environment anticipated in the VHF band, (b) provide the required link performance, and (c) provide multiple access service to 20 users.
2. AGIPA can operate as an F-FOV system in the backup mode.
3. Satellite steered array approach is recommended for the LDR command link, operating in the UHF frequency band. This phased array approach using high-gain antenna elements minimizes the transmit power requirement and consequently the overall effective weight.



4. Dual frequency S/Ku-band transponder is recommended for the MDR space-to-space link. This approach offers the flexibility to service the current and future MDR users and also to optimally service the low and high performance MDR users.
5. Two MDR transponders are offered to simultaneously service and support two independent MDR users.
6. With a 6.5' (2m) dish, the TDRS can support the space shuttle requirements at S-band.
7. One of the MDR transceivers is designed to provide a functional backup to the TDRS/GS link transceiver.
8. One of the MDR 6.5' (2m) dishes can be used to provide an additional 6.5 dB margin for operating the space-to-ground link in rain.
9. MDR transponders are designed wide band to offer high degree of flexibility in user signal format and operating frequency.
10. FDM/FM multiplexing technique is recommended for the space-to-ground link. This approach trades bandwidth for size, weight, and power and, in addition, allows the satellite transmitter to have an all solid-state design.
11. TDRS/GS link transponder is adaptive, inserting a 10 dB RF power amplifier only when needed to combat rain in the TDRS/GS link. This minimizes the average power requirement for this link.
12. LDR dual frequency quad array uses a collinearly stacked VHF-UHF backfire element. These antenna elements are designed for deployment on station using extensible stem units; they stow in a compact package for launch.

4.1 TELECOMMUNICATION SYSTEM REQUIREMENTS

4.1.1 Design Goals and Criteria

Consistent with the requirements for space application and with a planned launch in late 1977, key design goals and criteria have been established to guide the analyses and recommended design for the TDRS telecommunication system. These design goals and criteria reflect an overall aim to provide a recommended design, including state-of-the-art technologies, consistent with the planned launch date and an operational 5-year life in space. The guidelines are described individually; however, they obviously are closely dependent and interrelated.



° MAXIMIZE USER SUPPORT AND CAPABILITY

After the necessary spacecraft and auxiliary spacecraft support subsystems were sized, the remaining physical constraints (size, weight, and power) were effectively used to maximize the service and support that the telecommunication subsystem can offer to the low-altitude orbiting users. Comprehensive tradeoffs have been used (1) to maximize the support of simultaneous users, and (2) to maximize link performance, both in the presence of high interference signal environment as well as to maximize the link data rate (H) capacity.

In the LDR space-to-space link, unique adaptive spatial and polarization discrimination techniques are employed to provide optimum return link performance in the presence of high intentional and unintentional interference signals.

In the MDR space-to-space link, two dual frequency (S/Ku) transponders are used to simultaneously support two independent users.

° MINIMIZE SIZE, WEIGHT AND POWER

Special emphasis has been placed to employ design and implementation techniques to minimize size, weight, and power consumption. Extensive use has been made of advanced hardware technology developed for space systems, including design techniques developed on a NASA-GSFC contract¹ for a multi-beam S-band retrodirective array. Unique deployable techniques, within the state of the art, were employed to compactly stow the equipments for launch. Otherwise, nonerectable techniques requiring less space operation were used for high reliability.

° MAXIMIZE FLEXIBILITY/VERSATILITY

The links are designed to maximize the operational flexibility and versatility of the TDRS relay transponder to meet the needs of current and future TDRS users. Recommended frequency and bandwidths have been selected to serve the currently planned users and to handle the transition period for future high-performance users.

The LDR link provides a service to the bulk of smaller, austere users as well as a back-up capability to the more sophisticated, larger spacecraft. In addition, the spaceborne return transponder is multiaccess with all demultiplexing of user signals conducted on the ground. Since all user receiver channels on the ground need not be included initially, additional channels can be added later as needed.

In the MDR link, considerable flexibility has been included in the selection of both frequency and operating bandwidth. A dual frequency (S/Ku) transponder offers a current need to meet existing S-band users; and Ku-band offers a transition phase to support present and future high-performance users prior to inclusion of a complete HDR support capability. The transceivers are designed broadband to handle existing and planned signal format and frequency; viz. at S-band both receivers will be 10-MHz wide but discretely tuneable in 5-MHz steps over the entire 100-MHz bandwidth. In addition, one receiver will be designed with an alternate "wide open" mode to handle future TV, as well as to provide a back-up capability to the on-board TDRS/GS link transponder. The Ku-band return link will be 100-MHz wide and tuneable in four discrete steps to support users over a total 400-MHz band. In the forward link, S-band mode

¹ Retrodirective Phased Array for the Data Relay Satellite, NASA Contract No. NAS5-10689.



is wide open to support any user frequency within the allocated 95-MHz band; and Ku-band bandwidth is 100-MHz and tuneable over a 400-MHz band. This approach offers considerable flexibility to support signal format and operating frequencies of current and future MDR users.

° HIGH RELIABILITY

Commensurate with a 5-year unattended space application, careful design consideration has been given to high reliability. Almost without exception, high reliability is incorporated via 100 percent component or block redundancies and, where possible, functional redundancies through alternate channels have been included. Where multiple channels normally are employed, high reliability is achieved through graceful degradation; in particular, the following reliability approaches are included:

1. Block redundancies of complete transmit/receive channels, TT&C logic and transceiver, frequency source, and antenna drive electronics
2. Component redundancies where block redundancies are not pragmatic, such as antenna drive motor
3. Functional redundancy of alternate mode such as:
 - . MDR transponder to back up the TDRS/GS link transponder
 - . MDR 6.5' (2m) dish to back up the ground link 3' (.9m) dish, providing an additional 6.5 dB rain margin
 - . Two MDR transponders to simultaneously support two users
 - . Frequency source is designed with an alternate mode to become the prime coherent reference in the event the pilot reference from the ground station is not available. In this event, the ground station will lock in to the spaceborne reference. When neither of the terminals can become a coherent reference source, the spaceborne frequency source is designed to operate incoherently, thereby providing a third degree of operational reliability.

° MINIMIZE IMPACT ON USER TERMINAL

Where feasible and practical, design approaches have stressed the need to minimize the impact on the user terminal, both from the need to simplify the equipment requirements for the small austere users but also from the standpoint of an overall TDRSS cost effectiveness. Impact on the user not only must be multiplied in cost by the total number of potential users, but also the implementation and designs frequently require special tailoring to each user spacecraft. In general, it becomes most cost-effective to put the cost into the TDRS relay spacecraft or ground terminal rather than into each user terminal.

° COST EFFECTIVENESS

Emphasis has been placed on employing design and implementation techniques leading to an overall TDRSS cost effectiveness commensurate with the link performance and reliability goals. When possible, cost burdens were placed on the TDRS spacecraft or the ground-based terminal rather than on the user terminal, since the terminal impact is limited to a few systems rather than many

as for the user terminals. Typical examples are the use of:

1. Uncooled paramp at the TDRS spacecraft
2. Forward error control processor at the ground station in lieu of a higher EIRP at the user

4.1.2 Requirements and Constraints

Section 3.1 described in depth the overall link requirements and established the requirements and constraints for the design and implementation of the spaceborne telecommunication system. These requirements and constraints not only incorporate the TDRS specification requirements but also include the results of system and subsystem tradeoff analyses to establish the on-board transponder designs as well as the designs of the ancillary equipments. These requirements and constraints are summarized in Table 4-1, including the applicable source.

Table 4-1. Summary of TDRS Telecommunication Implementation Requirements and Constraints

Parameter	Forward Link	Return Link	Remarks
1. Low data rate • Frequency, MHz • Data rate, bps • Bit error prob. • Flux density, dBw/m ² / 4 kHz • No of channels/users • Polarization • Transceiver type • EIRP, dBw • G/T _s , dB/K • Signal format Data Voice • PN chip rate • RF bandwidth, MHz • RFI	400.5 to 401.5 10 ² to 10 ³ 10 ⁻⁵ -150 2 Circular Linear freq. translation +30	136 to 138 10 ² to 10 ⁴ 10 ⁻⁵ 20 Linear - 2 ortho Linear translation Determine in study	• Tradeoff/Spec • Spec • Spec • IRAC • Spec • Spec • Spec • IRAC flux density and frequency tradeoff • NASA-NR meeting 2/2/72 • Tradeoff • Tradeoff • Tradeoff • Tradeoff • Not clearly definable
2. Medium data rate • Frequency, GHz (flux density, dBw/ m ² /4 kHz) • Data rate/P _e Spec, bps Space shuttle, bps • Voice Spec Space shuttle • No. of users • Polarization • Transceiver type • EIRP, dBw • G/T _s , dB/K • Signal format Data Voice • PN chip rate, Mcps • RF bandwidth, MHz	2.025-2.120/14.6-15.2 (-154)/(-152) (10 ² - 10 ³)/10 ⁻⁵ 2 x 10 ³ /10 ⁻⁴ A Δ M A Δ M @ P _e = 10 ⁻³ (≥ 90% intelligibility) 2 Circular Linear frequency translation Determine in study WBPB-PCM- Δ PSK WBPB-A Δ M-PSK 5.0 95 at S-band, 100 at Ku-band	2.2-2.3/13.6-14.0 (10 ⁴ - 10 ⁶)/10 ⁻⁵ 76.8 x 10 ⁻³ min 256 x 10 ⁻³ & TV max A Δ M A Δ M @ P _e = 10 ⁻³ (≥ 90% intelligibility) 2 Circular Linear freq. translation Determine in study WBPB-PCM- Δ PSK WBPB-A Δ M-PSK 0.5 10/100	• IRAC • IRAC • Spec • MSC • Tradeoff • MSC • Tradeoff • Spec • Spec • NASA-NR meeting, 2/2/72 • NASA-NR meeting, 2/2/72 • Tradeoff • Tradeoff • Tradeoff • Tradeoff (dual mode)
3. TDRS/GS link • Frequency, GHz Primary mode Backup mode • Flux density, dBw/m ² / 4 kHz • Polarization • Transceiver type • Grazing angle • Site location • Rain margin, dB	13.4 to 14.0 2.2 to 2.29 Circular Linear frequency translation ≥ 10 degrees Greenbelt/Rosman	14.6 to 15.2 2.025 to 2.11 ≤ 154 Circular Linear freq. translation ≥ 10 degrees Greenbelt/Rosman	• Spec • Spec • IRAC • Spec • Spec • Spec (also assess impact of White Sands/Mojave) • NASA-NR meeting
4. Telemetry and command • Frequency, MHz • Bandwidth, kHz • Transmit power, kw	148 to 149.9 30 5.0	136 to 138 30	• IRAC • IRAC • IRAC
5. TDRS tracking orderwire • Frequency, GHz • PN chip rate, kcps • Bandwidth, MHz	2.066 500 1.0	2.249 500 1.0	• Tradeoff • Tradeoff • Tradeoff



4.2 TELECOMMUNICATION SYSTEM DESIGN DESCRIPTION

4.2.1 Frequency Plan

The frequency plan for the TDRS system is based upon the spectrum available for TDRS operation, providing the maximum flexibility in the TDRS design for growth and operational flexibility, and minimizing the size and weight impact on the TDRS communication system.

The frequencies evaluated for use on TDRS during the study are shown in Table 4-2. These numbers differ from the original specification, but are based on redirection by the GSFC project office due to allocations provided by the IRAC committee. Table 4-2 is divided into two parts. The upper section defines those frequencies and channel allocations which were available for consideration during the study. The lower portion delineates the selected frequency for each application.

Table 4-2 considers the three major data handling links; LDR, MDR, and TDRS/GS. Starting with the LDR segment, the forward link alternatives were S-band, UHF, or VHF. UHF was selected and the system provides two 1-MHz channels unrestricted in the manner in which they are utilized. The LDR forward link, from ground station to TDRS UHF transmitter output, provides two channels each with 1-MHz bandwidth capability. To obtain two channels, the available options are:

- . Utilize a different frequency on each channel
- . Employ unique PN codes on each channel at either different or the same frequencies

The advantage of providing both channels with 1-MHz bandwidth is that complete flexibility is provided to the ground controller to select the desired operating frequency without constraint by the TDRS transceiver.

On the VHF return link, similar logic results in the selection of 2 MHz as the channel bandwidth. Since RFI on this link will vary with time, it is possible to use the entire 2 MHz or operate over smaller segments of the band where RFI is less of a problem. Additionally, returning the entire 2-MHz band to the GS permits narrow banding, and any other processing where it is most easily adapted to the changing RFI scenario.

For the medium data rate user the choices available for evaluation were S-band, X-band, and Ku-band on both the forward and return segments of the link. The selections made were S-band and Ku-band. It was decided to provide modes of service for two reasons (1) to minimize design constraints on user S/C and to provide an interface that allows for growth to support higher performance user S/C, and (2) S- and Ku-bands also are the assigned bands for the TDRS/GS link. The MDR links can serve as back-up for the TDRS/GS link. Since the TDRS design proposed includes the capability to service two MDR users per TDRS at either S-band or Ku-band, the spectrum available at Ku-band has to be shared between potentially four MDR users and two TDRS/GS links. Additionally, it is desirable to transmit and receive data at any frequency in one of the four 100-MHz Ku-band channels, and similarly at any place in the 2200 to 2300 MHz

Table 4-2. TDRS Frequency Plan

	Low Data Rate User		Medium Data Rate User		TDRS to Ground Station Link	
	Forward (Command)	Return (Telemetry)	Forward	Return	Forward	Return
Specified frequency allocation	VHF(108 to 132 MHz) or UHF (400.5 to 401.5 MHz) or S-band (2.025 to 2.12 GHz)	VHF (136 to 138 MHz)	2025 to 2120 MHz or 8.4 to 8.5 GHz or 14.6 to 15.2 GHz	2200 to 2300 MHz or 7.7 to 7.9 MHz or 13.4 to 14.0 MHz	Primary 13.4 to 14.0 GHz Backup 2200 to 2290 MHz Launch 148 to 150 MHz	Primary 14.6 to 15.2 GHz Backup 2025 to 2110 MHz Launch 136 to 138 MHz
Specified channel allocation	VHF (2-100 kHz) or UHF (2-0.5 MHz)	1 or 2 MHz	(S-band) 4-10 MHz each (X-band) 4-50 MHz each (Ku-band) 4-100 MHz each	(S-band) 4-10 MHz each (X-band) 4-50 MHz each (Ku-band) 4-100 MHz each	As required	As required
Selected frequency utilization	UHF (400.5 to 401.5 MHz)	VHF (136 to 138 MHz)	2025 to 2120 MHz and/or 14.6 to 14.8 MHz and 15.0 to 15.2 MHz	2200 to 2300 MHz and/or 13.6 to 14.0 GHz	Primary 13.4 to 13.64 GHz Backup 2200 to 2290 MHz Launch-148.26 MHz	Primary 14.6 to 15.2 GHz Backup 2025 to 2110 MHz Launch 136.11 MHz
Selected channels	2-1 MHz BW	2 MHz BW	(S-band) - Any center frequency in 2025-2120 MHz band with data BW equal to or less than channel BW (Ku-band) - Same as above in each of four 100-MHz channels.	(S-band) MDR 1 - 100-MHz channel divided into 20 10-MHz steps or -100 MHz channel. MDR 2 - 100-MHz channel divided into 20 10-MHz BW steps. (Ku-band) MDR's 1 and 2 same as above with four 100-MHz steps.	Primary 240 MHz BW Backup 90 MHz BW	200 MHz (2-10 MHz MDR; LDR; TT&C; OW) or 600 MHz (1-10 MHz MDR; 1-100 MHz MDR, LDR; TT&C; OW)

4-13

SD 72-SA-0133



Space Division
North American Rockwell



S-band allocation. The system selected to provide the required flexibility while balancing the impact on the TDRS is shown in Figure 4-2, which illustrates the worst case for the selected spectrum allocation. In this situation, all four MDR users in the network would simultaneously be operating at Ku-band. In Figure 4-2 (A), the four MDR channels are shown to occupy 14.6 to 14.8 GHz, and 15.0 to 15.2 GHz for the transmission of narrowband command data to the user.

The TDRS/GS link is shown as occupying the center 200-MHz segment from 14.8 to 15.0 GHz band for retransmission of two 10-MHz MDR channels to the GS, or the full 600-MHz bandwidth for retransmission of a 10-MHz channel for one MDR, and a 100-MHz television channel from a second MDR. The second TDRS is also at the identical center frequency for the TDRS/GS link. The advantages of this spectrum allocation are that all three TDRS can be identically designed, which results in a cost-saving, and makes it possible to have an identical spare TDRS since whichever satellite the spare replaces operates on the same frequency.

Although there are spectral overlaps between the two space-to-ground links, and between the space-to-ground and Ku-band space-to-space links, careful design precautions have been exercised to eliminate any interferences between these links. To operate these links to provide an overall SNR of 9.9 dB, all interfering signals must be reduced to at least 25 to 30 dB below the desired signal.

Figure 4-3 illustrates the first case where both TDRS/GS links are operated at a common frequency, illuminating both ground antennas. Since the ground antennas are pointing in opposite directions at different TDRS satellites, the two links can be sufficiently isolated to eliminate any cross-interference by: (1) designing each antenna with high front-to-back lobe ratios, and (2) locating the ground antenna out of the line of sight to the other TDRS satellite.

In the initial approach, commercial antenna technology current can provide over 70 dB of front-to-back lobe ratio.* In the second approach, the antennas can be installed below ground level (Figure 4-3) or by constructing a screen between the two antennas. Either technique can provide over 30 dB of link isolation; however, the below grade installation has the advantage that it minimizes the reception of urban "trash noise" produced by machineries, generators, etc. Consequently, it is conservatively estimated that the use of the above techniques can provide 50 to 60 dB of isolation between the two links, which more than meets the required isolation requirements.

A second mode of interference between the space-to-space and space-to-ground transmission is the possibility of either the main or sidelobe of the TDRS MDR antenna illuminating the ground antenna through its main lobe. For example, with reference to Figure 4-2, this occurs when MDR-1 is commanded at 14.65 GHz while the TDRS/GS link in either Figures 4-2(B) or (E) is receiving a wideband television transmission. For this situation, opposite sense polarization will reduce the interference by 25 to 30 dB. In addition, for this interference to occur, the MDR must pass through the boresight angle between the

* { Andrews Bulletin 1043, "Ultra High Performance Antenna," March, 1971.
Scientific Atlanta, "Ultra Directive Antennas," August, 1972.

SPACE-TO-SPACE LINK

FREQUENCY SPECTRUM

TDRS TRANSPONDER

DATA/CHANNEL

1. FORWARD (TDRS-TO-USER)

• LDR



1.0 MHz

ANY 2-290 KHz/TDRS

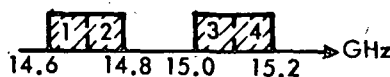
• MDR (S)



95 MHz

10 MHz TUNABLE IN BAND

(Ku)



4-100 MHz

ANY 2-100 MHz/TDRS

2. RETURN (USER-TO-TDRS)

• LDR



2.0 MHz

1.5 MHz

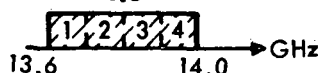
• MDR (S)



100 MHz

20-10 MHz STEPS OR
1-100 MHz WIDE OPEN

(Ku)



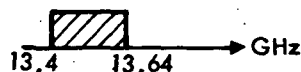
4-100 MHz

ANY 2-100 MHz/TDRS

SPACE-TO-GROUND LINK

1. FORWARD (GS-TO-TDRS)

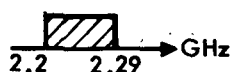
• PRIMARY (Ku)



240 MHz

SAME

• BACKUP (S)



90 MHz

SAME

• TDRS COMMAND (VHF)



2 MHz

≤ 30 KHz TUNABLE
IN BAND

2. RETURN (TDRS-TO-GS)

• PRIMARY (Ku)



200 OR 600 MHz

SAME

• BACKUP



85 MHz

SAME

• TDRS TELEMETRY (VHF)



2 MHz

≤ 30 KHz TUNABLE
IN BAND

Figure 4-2 Ku-Band Transmission from TDRS to Ground Station



TDRS satellite and ground antenna as illustrated in Figure 4-4. This would occur very rarely. In addition, since the ERP transmitted by the TDRS to the MDR is within 1 dB of that transmitted from TDRS to GS in the TV mode, the interference to the MDR is reduced by the bandwidth ratio of 100 MHz to 500 kHz or 23 dB. The worst case would occur for the MDR transmission illuminating the GS, and opposite sense polarization reduces this narrow-band signal 30 dB below the wideband channel and effectively eliminates interference between the space-to-space and space-to-ground links.

The Ku-band allocation represents the optimum utilization of the 14.8 to 15.2 GHz TDRS transmit band, while providing four 100-MHz MDR channels and either 300-MHz or 600-MHz TDRS/GS channels. In addition, there is the advantage of using identical TDRS designs, and to employ the MDR Ku-band antenna and transceiver as a backup for the TDRS/GS link.

When the MDR forward link operates at S-band, Table 4-2 shows the TDRS can transmit at any frequency in the 2025 to 2120 MHz band. Tuning is not required on the TDRS for the S-band forward link since the wide-open MDR transponder design provides complete flexibility in the selection of the operating frequency by the ground controller. The wide-open design places the burden on the ground transmitter in generating an adequate CNR in this bandwidth. The wide-open design is used for Ku-band mode also, with the exception that there are four selectable 100 MHz channels (Figure 4-2).

For the MDR return link, dual frequency operation at S-band and Ku-band has again been selected, and the frequencies are 2200 to 2300 MHz and/or 13.6 to 14.0 GHz. The objective in the design of the MDR links is to minimize the user and TDRS impact by providing unconstrained use of the entire S/Ku frequency bands available. Therefore, the two MDR channels can operate at any 10-MHz slot in the 100-MHz S-band spectrum. The 10-MHz slots can be set at any one of 20 locations in the 100-MHz band, permitting continuous coverage as shown in Figure 4-5. Any fine tuning for a specific S-band frequency can be accomplished within the 10-MHz bandwidth at the ground station. Since the data bandwidth is 1 to 2 MHz, fine tuning at the ground is entirely practical.

In addition to 10-MHz channel capability, one of the MDR's can switch to 100-MHz bandwidth. The system is designed to relay the entire 100-MHz bandwidth to the ground station for either television transmission, or for operation with a narrowband data transmission. For the latter case, narrowband filtering would be performed on the ground, again putting the complexity on the ground.

For Ku-band MDR operation, four 100-MHz slots are provided for each MDR as shown in Figure 4-5(A). Each of the 100-MHz channels can then operate as either a 20-step 10-MHz channel (on 5-MHz centers) as shown in Figure 4-5(B), or as a wideband channel as in Figure 4-5(C).

For the TDRS/GS forward link the channel allocation is shown in Figure 4-6. For each MDR a 95-MHz channel is available so that the ground has direct frequency control over an MDR channel, and is able to select any frequency in the 95-MHz bandwidth. The pilot, two LDR channels, and the TT&C channel are located as shown at the higher end of the spectrum.

For operation of the TDRS/GS forward link in the S-band back-up mode, the spectrum is as shown in Figure 4-7. For the back-up mode MDR-1 functions as the TDRS/GS link. Therefore, the 90-MHz bandwidth is divided as shown between

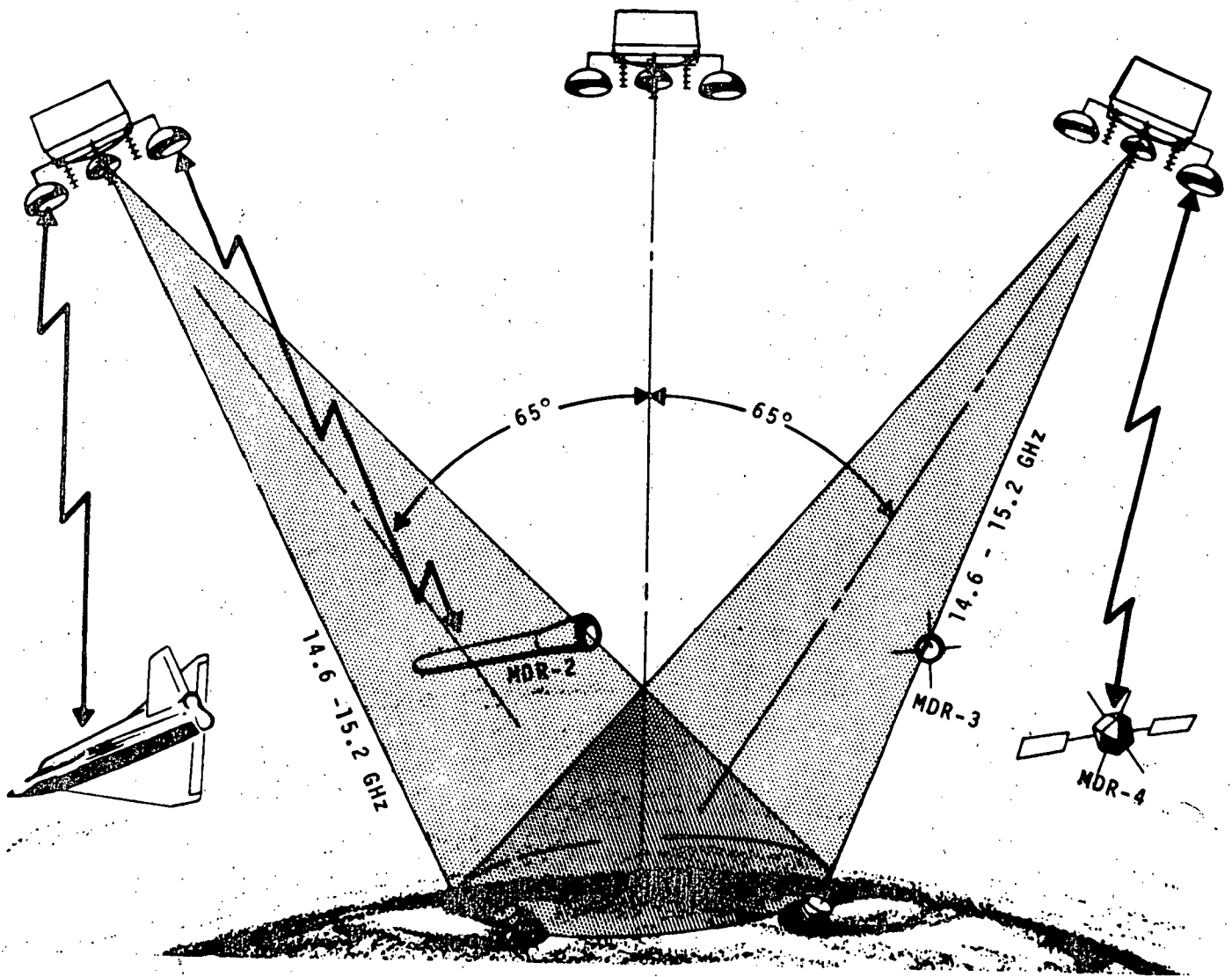


Figure 4-3. Ground Return Link Operating
at Common Frequency

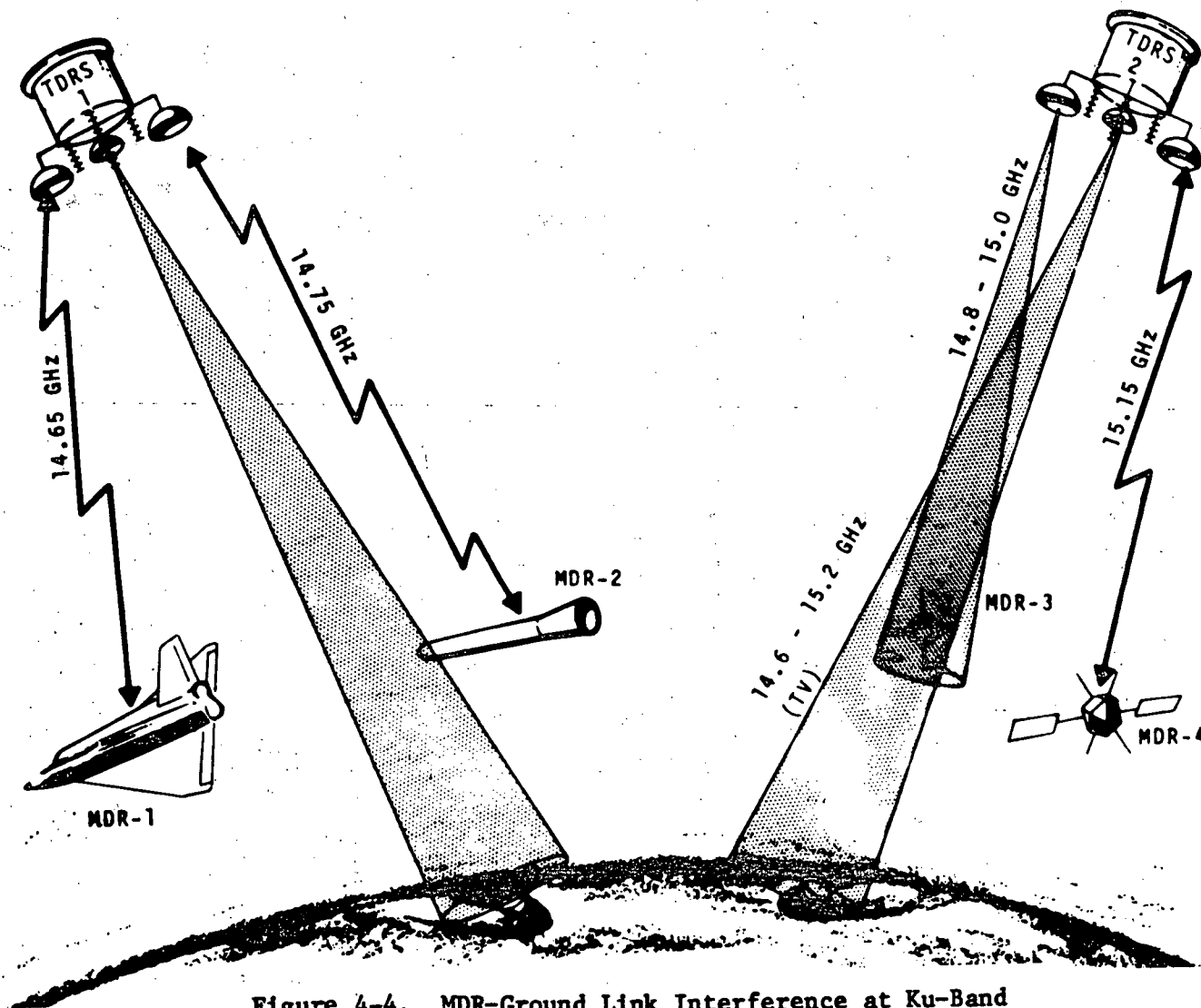
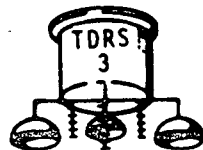
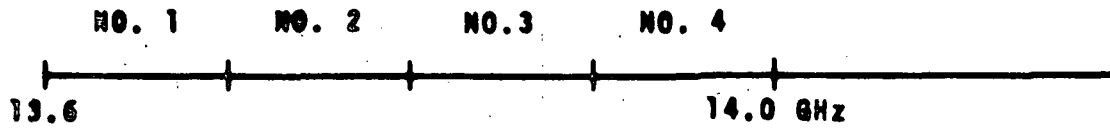
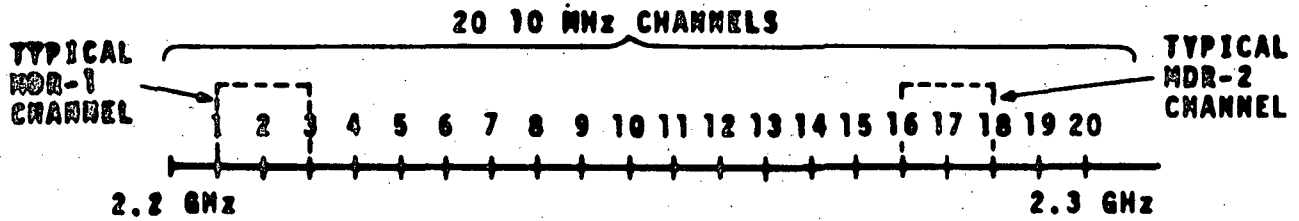


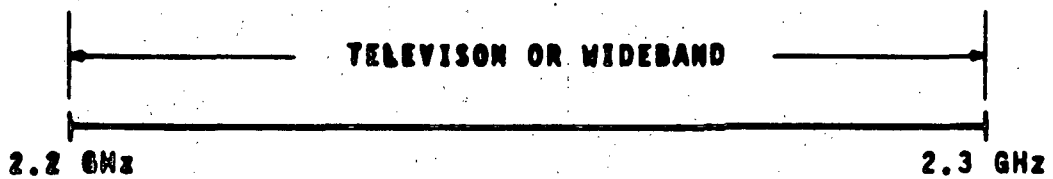
Figure 4-4. MDR-Ground Link Interference at Ku-Band



(A) MDR RETURN LINK K_u -BAND CHANNELS



(B) MDR RETURN LINK S-BAND CHANNELS



(C) WIDEBAND S-BAND CHANNEL FOR MDR-1 SYSTEM

Figure 4-5. MDR Return Link Frequency Plan

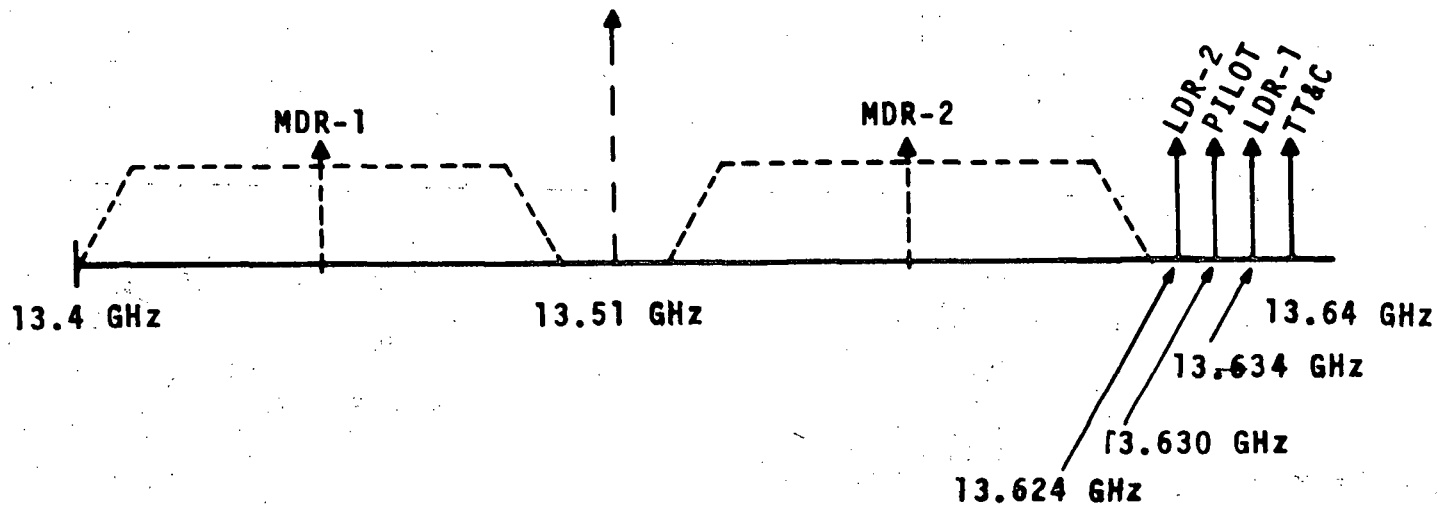


Figure 4-6. TDRS Forward Link Spectrum for Ku-Band Operation



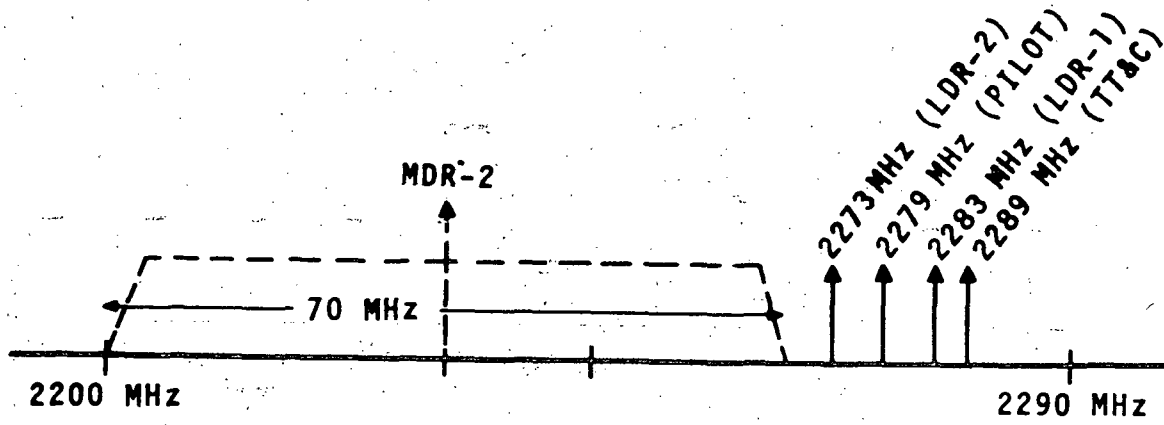


Figure 4-7. TDRS Forward Link S-Band Backup Mode



the MDR-2 and the LDR, pilot and TT&C functions. Therefore, almost full TDRS satellite capability is permitted in the backup mode in that both the specified LDR, MDR, and coherent ranging functions can be performed. This mode can also be used without disturbing the normal Ku-band allocation if additional network capability is desired by utilizing the in-orbit spare TDRS satellite.

The final column of Table 4-2 delineates the return link of the TDRS/GS. Normal operation was previously explained, and occupies either 200 MHz or 600 MHz of the 14.6 to 15.2 GHz band, depending on the reception mode of MDR-1.

For backup operation, the MDR-1 antenna and/or transceiver can replace the TDRS/GS antenna and/or transceiver, respectively, for operation at either S- or Ku-band.

For the TDRS/GS backup mode the spectrum is shown at S- or Ku-bands in Figure 4-8. For this mode only, 34.5 MHz of bandwidth is required to transmit the return link data to the GS. In this backup mode all specified functions are provided by dropping the MDR-1 system, which now functions as the ground-to-TDRS transponder.

4.2.2 Functional Description

4.2.2.1 General Description

The basic telecommunications subsystem components for the TDRS baseline design is shown in Figure 4-9. The subsystem contains an LDR, two MDR's and TDRS/GS transceivers, frequency source, S-band position location and order wire transceiver, Ku-band beacon, TT&C and an antenna farm. The LDR transceiver supports 20 LDR and 2 MDR users simultaneously on the return and forward links; and each MDR transceiver supports one MDR user operating at S- or Ku-band. All data received from the users are multiplexed onto a single line along with the TDRS telemetry data, and the S-band position location and order wire system.

The S-band position location system provides accurate tracking and position location of the TDRS satellite by trilateral range measurements between the main TDRS and two remote ground stations. A PN code is transmitted to each station, and a unique PN code is returned from each remote ground transponder via the TDRS/GS link to the main ground receiving terminal where the TDRS position is calculated. In addition to the location function, this system serves as a beacon and order wire for S-band users. Thus, a typical MDR user with a narrow-beam antenna could direct his antenna at the TDRS and send an order wire request to the ground control station. The ground controller would then point one of the 6.5 ft (2 m) dishes at the user. A Ku-band beacon is also provided for Ku-band users to acquire the TDRS.

To perform range and range-rate measurements through the TDRS, a frequency source is provided which is locked to a pilot signal transmitted from the ground station. All the transceivers and other RF processing systems in the TDRS derive their frequencies from references generated by the frequency source. A failure in the pilot link would still permit coherent ranging by using the on-board frequency source as the prime TDRS reference frequency. For this situation the ground station would receive the Ku-band beacon as the pilot and lock on to it.

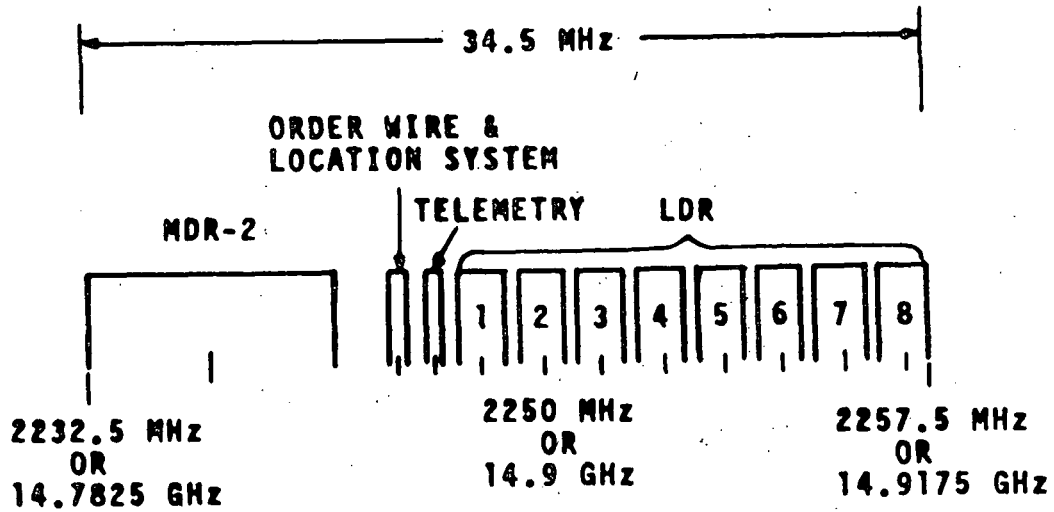


Figure 4-8. TDRS/GS Return Link Backup Mode Spectrum

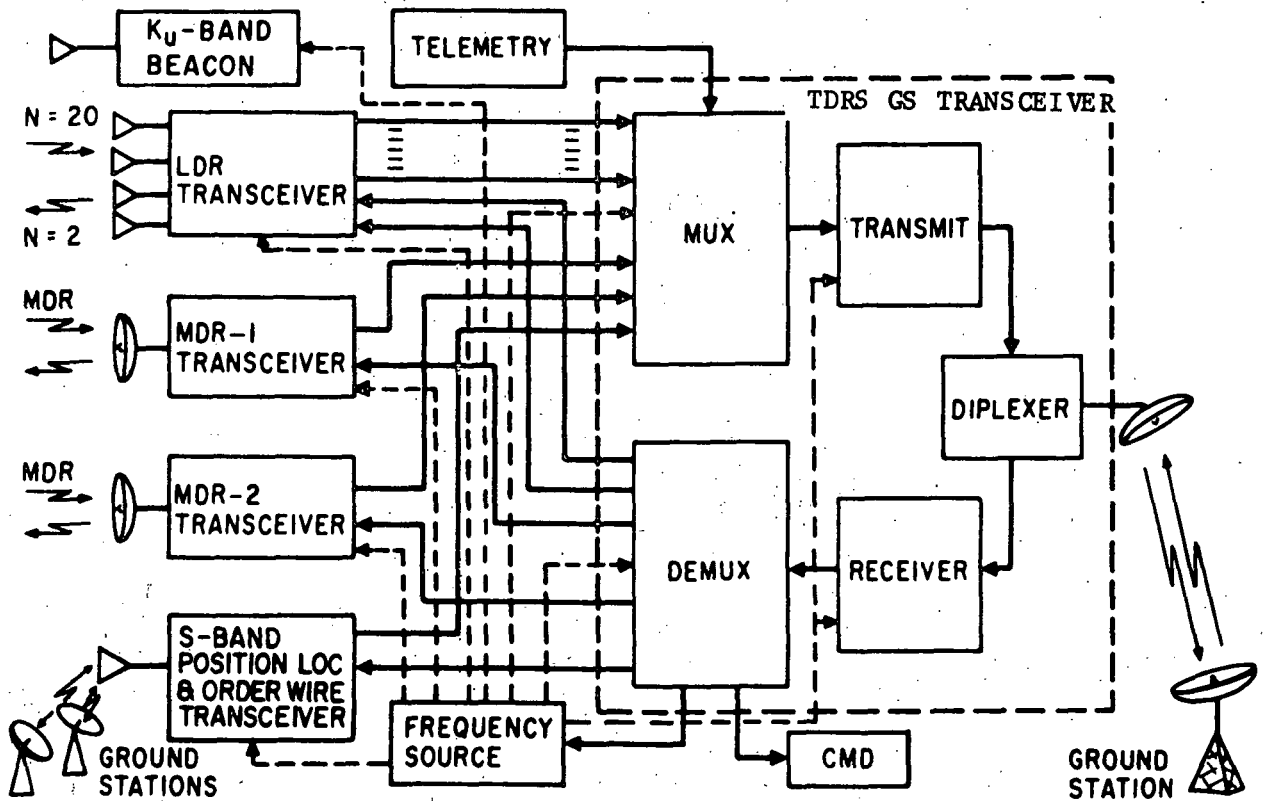


Figure 4-9. TDRS Telecommunications Subsystem



The remaining component of the telecommunication system is the TDRS Tracking, Telemetry and Command (TT&C) system which functions in conjunction with a VHF link or Ku-band TDRS/GS link to provide the TT&C function during in-flight transit and on-station phases, respectively.

4.2.2.2 Detailed Subsystem Description

Figure 4-10 shows the detailed block diagram of the TDRS telecommunication subsystem.

LDR signals are received from up to 20 users in a 2-MHz bandwidth from 136 to 138 MHz by the four-element VHF array. The antenna elements of the array each have 60° (1.05 rad) beamwidth, and the array provides adaptive coverage over the required 31° (0.54 rad) FOV with an element gain of 8.3 dB and an array gain of 14.3 dB at the 31° (0.54 rad) point. The array beam is formed on the ground by relaying the entire 2-MHz bandwidth from each vertical and horizontal outputs of the antenna elements, where a separate receive beam is formed for each LDR user. This approach places the complex signal processing equipment on the ground where adaptive beam processing always optimizes the received signal-to-interference ratio. The interference can be expected to be large for the VHF frequency band where the LDR return link operation is desired.

The signals received by the LDR-1 through LDR-4 receivers are code division multiplexed by a unique Gold code for each LDR user. Thus, the signal received over the eight channels consists of the 20 uniquely coded signals, the signal multipath, RFI, and thermal noise. The receiver will be designed to handle RFI levels of -92 dBm as shown in Figure 4-10. The eight receivers convert the composite antenna output signals to an IF frequency ranging from 50.0 MHz to 67.5 MHz so that the eight channels can be frequency division multiplexed for transmission to the ground station. The 50.0 to 67.5 MHz IF frequencies were selected based upon obtaining an operating point where filter components which are small and stable could be employed to obtain the required phase linearity needed to pass the 1 Mbps PN chip rate undistorted through the system. These IF filters only partially form the bandpass response for the LDR channels which also include demultiplexing and processing at the GS. Therefore, to achieve the desired amplitude and phase linearity over a 1.5-MHz bandwidth, a bandwidth of 2 MHz is employed in the TDRS. The signals are linearly amplified in the four receiver modules and summed at LDR-9, the receiver summing network. The composite FDM signal is then further down-converted to a 16.5-35.0 MHz band which is designated for the eight LDR channels. AGC is applied to the total FDM/LDR signal to maintain a constant drive level into the TDRS/GS FM modulator, regardless of RFI or noise fluctuations.

Each mixer in the LDR receivers is controlled by a phase-locked crystal VCO which is locked to a reference from the frequency source. Therefore, all mixing is performed coherently; in addition, the PLL/VCO is designed so that each one can be commanded to operate open-loop as a noncoherent local oscillator source should a malfunction develop in the pilot channel or frequency source reference.

LDR forward link transmission from the TDRS to the user is provided by a variety of operating modes, hardware capability and power-saving features in the subsystem design. Signals to be transmitted to LDR users are received from the TDRS/GS receiver by the LDR-10 transmitter divider at 50 MHz and 66 MHz

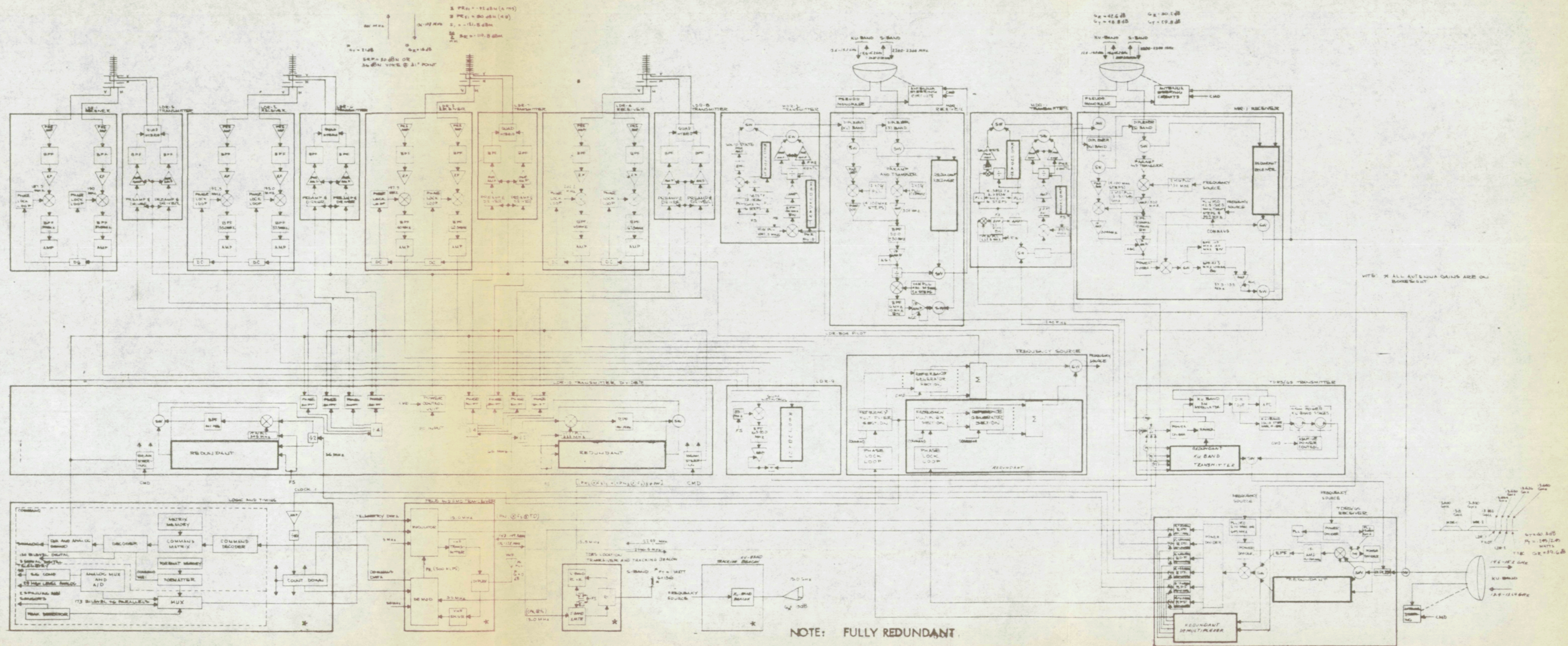


Figure 4-10. Telecommunications Subsystem Block Diagram



respectively for the two forward channels. These two signals are converted to the transmit frequency of 401 MHz. Both channels are sufficiently wide so that the ultimate transmit frequency on either of the two channels can be tuned on the ground between 400.5 and 401.5 MHz, the permitted transmission bandwidth at UHF. Thus, the two channels are completely flexible to operate with either two different frequencies, or two uniquely coded signals at the same frequency.

The mixer output signals at 400.5 to 401.5 MHz are filtered and divided four ways from one of the redundant upconverters. Each output of the four-way power divider drives a phase shifter which introduces the proper phase on each transmitter signal for steering the individually controlled beam by means of ground commands. The phase shifters drive separate transmitter chains in the LDR-5 through LDR-8 transmitter modules. Each transmitter chain amplifies the phase shifted signal to a level of 5.0 watts at the input to the quadrature hybrid port. Line and component losses reduce the radiated power to 4.0 watts per element per channel which results in an ERP of 30 dBw when combined with the remaining four transmitter outputs and the 18 dB of antenna gain over the required 31° (0.54 rad) FOV. The transmitter is a Class C design that can operate at either 18 vdc for 5 watts RF output or 28 vdc for 20-watt peak output. The 20-watt per element capability is designed for 25 percent duty cycle voice operation. Commands from the ground station switch the output voltage from either an 18 vdc bus or the normal 28 vdc bus in the LDR-10 unit. Therefore, capability is provided to transmit two separate beams at power levels of either 30 dBw, or 36 dBw with a 25-percent duty cycle using steered 90° (0.157 rad) beams for two separate users. Either voice and/or data can be (1) transmitted separately on either beam or (2) multiplexed onto either one or both of the two beams using quadrature techniques.

The LDR transponder provides an alternate capability to operate in a F-FOV mode. This mode can be used to provide simultaneous continuous coherent ranging on all users within the FOV, or to transmit commands to a user at a reduced data rate. In this mode, only one antenna element and its corresponding transmit channel are used with the RF amplifier operating at a 20-watt level. This provides an effective ERP of 27 dBw at the peak of the beam and 24 dBw at the 31° (0.54 rad) points for this F-FOV mode.

To summarize, the LDR forward link provides:

- . UHF operation of 400.5 to 401.5 MHz
- . Two separate high-gain (21 dBi peak) steered beams
- . Alternate fixed 31° (0.54 rad) FOV beam for illuminating all users simultaneously
- . Available ERP at 31° (0.54 rad) FOV points:
 - +30 dBw (or +36 dBw for voice with 25% duty cycle) using high-gain steered beam
 - +24 dBw using fixed 31° (0.54 rad) FOV beam

Dual frequency VHF/UHF operation reduces the duplexer difficulties at both the user and the TDRS, in addition to providing operation on the RFI limited LDR forward link where preliminary studies indicate less severe RFI level.

For servicing MDR users, two independent transmitting and receiving subsystems are provided. Each uses a 6.5 ft (2 m) parabolic reflector with dual S-band and Ku-band frequency selective feeds. Pointing of the dish is open



loop via ground commands at S-band and closed loop using pseudo-monopulse tracking circuits at Ku-band.

Referring to Figure 4-10, MDR-1 and MDR-2 are essentially identical designs with the exception that MDR-1 has some additional circuitry which permits it to act as a backup for the TDRS/GS link. Referring to the MDR-1 receiver, signals can be received at either S or Ku-band. The S-band section has a parametric amplifier followed by a transistor as the RF front end resulting in a noise figure of 2.3 dB. The S-band signal is converted to a 500 MHz IF by mixing with a 1750 MHz signal locked to a reference from the frequency source. The IF bandwidth is 100 MHz for receiving any signal in the 2200-2300 MHz band. Further amplification is provided and the 500 MHz signal is then down-converted to a center frequency of either 105 MHz or 42.5 MHz. The 42.5 MHz frequency is filtered by a 10 MHz bandpass filter, thus dividing the 100 MHz RF bandwidth into 20 discrete 5 MHz steps. This is accomplished by commanding the PLL/VCO over the 412.5 to 502.5 MHz. For operation in the wideband 100 MHz mode, the VCO is commanded to 395 MHz. The output of the MDR-1 receiver drives the TDRS/GS summing unit since the signal has been placed at the proper baseband location.

For Ku-band receptions a parametric amplifier front end with a noise figure of 2.9 dB is used. The Ku-band signal is converted to 500 MHz by PLL/VCO which can be stepped to any one of four frequencies locating the center of four 100 MHz segments of the Ku-band spectrum between 13.6 to 14.0 GHz in the center frequency of the 500 MHz IF. From that point on the Ku-band system functions identically with the S-band operation.

The MDR-2 receiver has the same capabilities to operate at S or Ku-band but only provides 10 MHz slots rather than 10 MHz and 100 MHz as does MDR-1. The MDR-2 receiver baseband output is at 6.0 MHz.

For transmissions to the MDR users, again S or Ku operation is provided in each unit. Signals from the TDRS/GS receiver drive the MDR-1 and MDR-2 transmitters at 240 MHz and 120 MHz, respectively. Similar to the LDR concept, each MDR IF is 100 MHz wide so that by ground frequency synthesis any frequency in a 95 MHz and 100 MHz band is available at S- and Ku-band, respectively. The 240 MHz or 120 MHz (+50 MHz) IF can therefore be converted to S-band with a fixed rather than variable PLL/VCO source.

At S-band the transmit signal is amplified to a level so that an ERP of +41 dBw is generated for data transmission or an additional 6 dB of gain can be added for peak transmission capability of +47 dBw ERP for voice. Again, the 25% duty cycle of voice transmissions permits the peak power to be raised by 6 dB while maintaining the average ERP at +41 dBw.

To conform with CCIR/IRAC flux density guidelines, the MDR forward link power must be spread over a 10-MHz bandwidth. This is accomplished by use of PN coding on the ground.

The outputs of the LDR receivers, MDR receivers, the telemetry system and the order wire are all summed and transmitted to the ground by means of the TDRS/GS transmitter. The baseband output of the combiner is located from 1 MHz to 47.5 MHz for two 10-MHz MDR's or from 1 MHz to 155 MHz for a 10 MHz and 100-MHz MDR. The baseband modules a VCO directly at the Ku-band center frequency of 14.9 GHz.



By utilizing FDM/FM, bandwidth can be traded for power so that the link power requirements can be satisfied for both the narrowband (200 MHz RF bandwidth) and wideband (600 MHz RF bandwidth) modes, using an all-solid-state Ku-band transmitter design. The transmit power required is 2.75 watts for a 17.5 dB rain margin. Since the 17.5 dB margin corresponds to a rain rate of 25 mm/hr adaptive power control is provided on the last two stages of the Ku-band power amplifier. During periods of clear weather or low rainfall, a 7.5 dB margin is provided by changing the bias control on the impact diodes of the power amplifier so that they appear to be open circuits to the circulators in the amplifier. Therefore, 0.245 watt is provided as the transmit power with the capability to switch to 2.45 watts during periods of high rainfall or other propagation anomalies. In addition, the TDRS/GS transmitter output can be switched from the normal 3' (.9 m) diameter parabolic antenna to the MDR 6.5' (2 m) dish to provide an additional gain of approximately 6.5 dB.

The combiner output of the TDRS/GS transmitter can also be switched to the input of the MDR-1 transmitter where it can be amplified at either S- or Ku-band for transmission to the ground station. Since the transmit signal is now FDM, backoff from saturation of 7 dB is provided to minimize intermodulation distortion.

Receptions from the ground station are received via the TDRS/GS receiver at the Ku-band frequency of 13.4 to 13.64 GHz. The antenna is a 3' (.9 m) parabolic reflector. Steering in two axes is provided by ground commands.

The antenna output signal of the forward link from the GS is converted by a mixer front end to an IF of 500 MHz. The RF spectrum is shown in Figure 4-10. Note the wide spectrum allocation for the MDRs permitting continuous on the ground tuning. In both the front end and frequency synthesis, the TDRS/GS receiver design takes advantage of the large ground station RF power generating capability to minimize TDRS weight, power and complexity.

The outputs of the TDRS/GS receiver provide forward link signals to the two LDR and two MDR transmitters as well as the frequency source and telemetry tracking and command system.

The TT&C signal at an IF of 50 MHz is delta PSK modulated by a PN_1 code and the TDRS command data. The PN_1 , 500 kbps chip rate is separate from the command data in the S-band telemetry and command transceiver. This PN_1 code, then, is modulo two added to the telemetry data (TD) for transmission to the ground via the TDRS/GS link and also PSK modulates a 15.0 MHz reference signal for transmission at S-band via the TDRS location transceiver and tracking beacon system. The S-band signal is received by two remote ground located turn-around transponders which transmit codes PN_2 and PN_3 to the TDRS at 2250 MHz. These codes are received by the S-band location system earth coverage antenna where they are processed along with any MDR order wire requests down to a center frequency of 13.5 MHz. The order wire, PN_1 , PN_2 , and PN_3 are then retransmitted to the ground station via the Ku-band TDRS/GS link.



The TT&C functions have several modes of operation. During the inflight transmit phase, the VHF space-to-earth link provides the prime and only link with the ground control center. After the TDRS satellite is on station, the TDRS/GS Ku-band becomes the primary link, and the VHF link becomes a back-up system. During this phase the VHF transmitter is placed in standby and only the VHF receiver is left on. The TT&C uses a PCM- Δ PSK format to receive command rate of 128 bps and to transmit telemetry data of 31 kbps, including a PN chip rate of 500 kcps used for position location of the TDRS satellite. In the VHF mode, a VHF transceiver is used to establish the space-to-earth link, but in the Ku-band mode, the TT&C data is multiplexed with the other data for transmission or reception through the TDRS/GS transponder.

The remaining TDRS telecommunication system component is the Ku-band beacon which is used to provide a signal that can be used by Ku-band MDR users employing high-gain directional antenna for acquisition and tracking the TDRS satellite. This transmitter provides an output of 1.4 watts at 15 GHz. In addition, this 15 GHz is coherently locked to the on-board frequency source and, consequently, to the rest of the on-board transceivers. Therefore, in the event that the TDRS frequency source cannot establish coherence with the ground station, the role can be reversed such that the ground station can establish coherence by locking into the Ku-band beacon signal.

4.2.3 Telecommunications Subsystem Size, Weight, and Power Summary

The size, weight, and power of each of the baseline components is summarized in Table 4-3. Detailed supporting data for these figures may be found in Appendix 4-B.



Table 4-3. Telecommunications Subsystem Size, Weight, and Power Summary

Subsystem	Size		Weight		Power	
	in.	cm	lb	kg	Peak	Average
LDR						
Receiver (4)	8x7x.5	20.2x17.8x1.27	7.6	3.5		7.93
I.F. Summing Network	4x7x0.5	10.2x17.8x1.27	1.3	0.6		1.14
Transmitter (4)	10x2.62x1.12	25.4x6.7x2.84	4.5	2.0	137.6	34.40
Trans. Divider Network	10x7.5x2.25	25.4x19.0x5.7	5.1	2.31		11.40
Antenna, incl stem unit and support link			31.6	14.35		
MDR NO. 1						
Receiver	12x8x4	30.5x20.4x10.2	8.8	4.0	6.2	6.2
Transmitter	6x4.50x10	15.3x11.4x25.4	13.0	5.9		
S-band					190.0 ¹	47.5
Ku-band						14.5
Antenna, incl. support strut			33.96	15.4	24.0	7.0
MDR NO. 2						
Receiver	12x8x4	30.5x20.4x10.2	8.8	4.0		6.2
Transmitter	6x3.75x10	15.3x9.5x25.4	11.0	5.0		
S-band					180.4 ¹	45.1
Ku-band						13.2
Antenna, incl. support strut			33.96	15.4	24.0	7.0
TDRS/GS						
Receiver	9x5x4	22.9x12.7x10.2	4.7	2.14		5.25
Transmitter	7x6.5x4	17.8x16.5x10.2	6.0	2.73	49.0 ²	11.0
Antenna			14.85	6.75	9.5	
FREQUENCY SOURCE	10x10x2	25.4x25.4x5.1	5.6	2.5		4.8
TT&C						
Processor	6.2x4.5x5.4	15.7x11.4x13.7	9.6	4.4	10.0	10.0
Transceiver	5.5x5.5x2.63	14x14x6.7	4.0	1.8	4.5 ³	0.5
Antenna			3.0	1.36		
TDRS TRACK'G/ORDER WIRE						
Transponder	8x4x0.5	20.3x10.2x1.3	5.4	2.5		7.9
Antenna			0.3	0.1		
Ku-BAND BEACON						
Beacon	4x3x3	10.2x7.62x7.62	3.6	1.6		8.3
Antenna			0.3	0.1		
DC CABLING			13.3	6.04		
RF CABLING	75 feet	(22.9 meters)	4.9	2.2		
WAVEGUIDE			5.0	2.3		
Totals			240.17	109.4		
Two MDR's in S-band						256.0
One MDR in Ku-band, one in S-band						224.1
Two MDR's in Ku-band						191.1
NOTES						
1	For voice operation					
2	During rain at ground station, add 10 dB to transmitter power					
3	Transmitter (4 watts) not used "on station"					



4.3 LOW DATA RATE LINK

4.3.1 Return Link

4.3.1.1 System Analysis and Trades

The LDR telemetry link must simultaneously support and service 20 low-altitude satellite (LAS) users. To provide this multiple access capability, previous TDRS Phase A studies^{1,2} have concluded that a fixed gain antenna with a broad beam covering the entire 31° (.54 rad) field of view (FOV) should be employed at the TDRS spacecraft. For such a link with a fixed gain antenna at each terminal, link analysis shows that the return link should be operated at the lowest practical frequency; henceforth this link requirement is specified to operate in the VHF band. Unfortunately, the VHF band is subject to numerous unintentional interference emitters and urban "trash" noise, both of which are referred to herein as RFI. In addition, this link incurs intentional interference signals resulting from direct signals emanating from other in-band LDR users, as well as multipath (earth reflected) signals from both the desired and other in-band users. A Magnavox multipath/RFI study³ demonstrates that a wide-band spread spectrum pseudo noise modulation (WBPN) technique provides the optimum means to minimize multipath, along with a convenient PN signal format for conducting range and range rate measurement of the user spacecraft.

The results of the RFI investigation presented in section 3.2 clearly shows the peak values of the total average power density to be approximately -90 to -80 dBm as seen at synchronous altitude with a 16 dB gain F-FOV antenna. Although this RFI data excludes RFI duty cycle, some domestic radars and foreign emitters, it does reflect that considerable caution must be exercised in the design of this link to include a capability to combat the RFI. Not only is it difficult to assess the current RFI environment, but it is equally difficult to anticipate and/or predict the RFI environment for the planned operational life time of the TDRS network. For the postulated nominal RFI level of -92 dBm, this can exceed the power level of the desired signal by 20 to 30 dB.

A unique adaptive phased array technique that incorporates the advantages of an electronically scanned phased array but implements the usual complexities of a phased array at the ground station was conceived to enable operation in an RFI environment. This approach has been coined AGIPA⁴ for Adaptive Ground Implemented Phased Array. AGIPA not only is an electronic scanned array, but

1. GSFC Mark I Tracking Data Relay Satellite System Concept, Phase A Study Report, November 1969, prepared by NASA-GSFC.
2. Tracking Data Relay Satellite Network, Final Study Report, 30 September 1969, prepared by JPL, California Institute of Technology.
3. Multipath Modulation Study for the TDRS, Contract Number NAS5-10744, dated January 1970, prepared by Magnavox-Advanced Systems Analysis Office.
4. AIL is currently under NASA-GSFC contract (NAS5-21653) to develop a laboratory hardware system for demonstration in an anechoic test chamber at a scaled S-band frequency.

utilizes a combination of adaptive spatial filtering and polarization discrimination to maximize the signal-to-interference ratio (SIR). The overall link functions are illustrated in Figure 4-11, and shows that the TDRS relay is merely a linear bentpipe transponder which transmits the information from each phased array element down to the ground station. In this case since both linear orthogonally polarized antenna components are utilized, two channels are required for each array element. It is at the ground station where all beam forming/beam steering as well as all adaptive signal processing functions (spatial filtering and polarization discrimination for optimum SIR) are performed with a minicomputer.

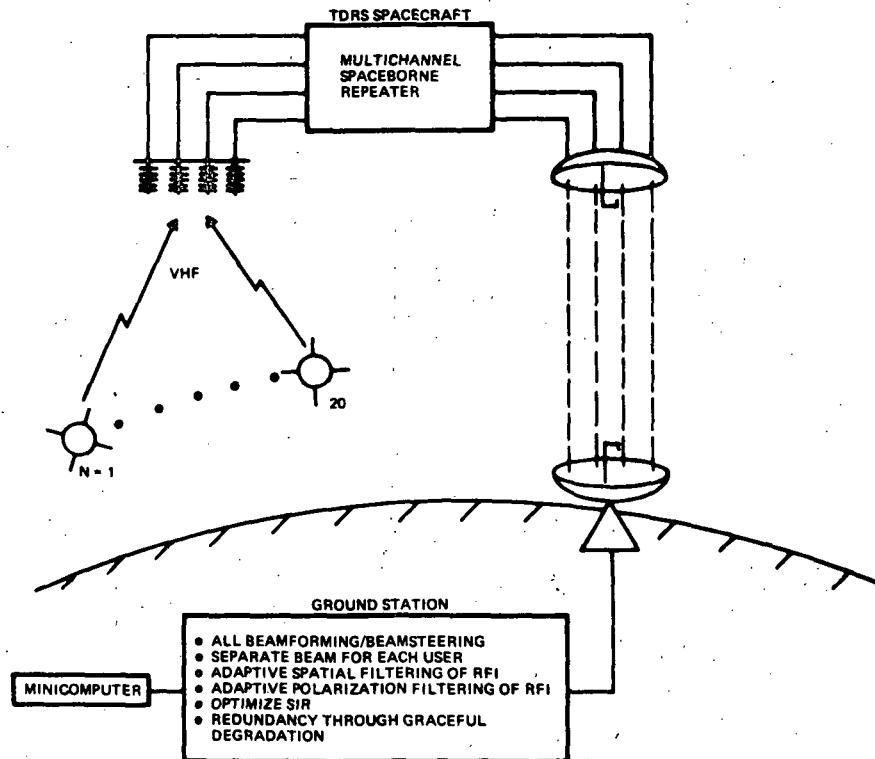


Figure 4-11. AGIPA Approach for LDR Return Link

For spatial filtering, AGIPA effectively uses the antenna pattern characteristics to place RFI emitters into pattern nulls. Consequently, the effectiveness of AGIPA to spatially filter RFI is a function of the number of elements and their spacing. The greater the number of elements, the greater is the beam shaping flexibility, while the spacing of the elements affects the beamwidth, Figure 4-12. Generally, the beamwidth is the most significant criteria; consequently, AGIPA has been evaluated and designed to operate with a ring array. A quad array providing a coverage of 31° (0.54 rad) is used, which employs the same antenna as the F-FOV approach. Figure 4-13 defines and compares the F-FOV and the AGIPA approaches.

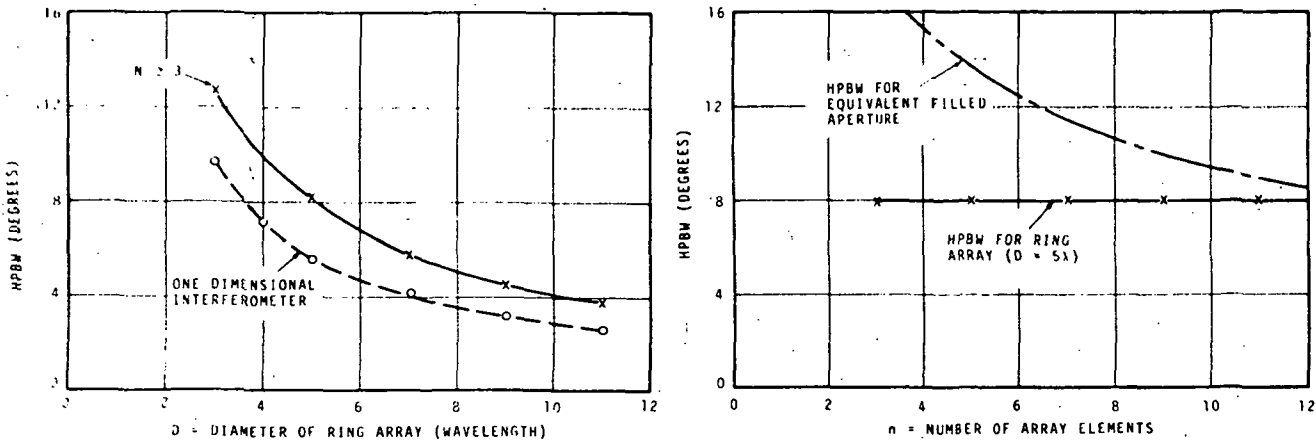
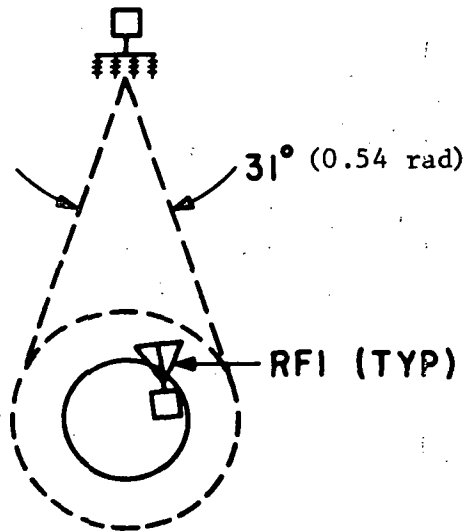
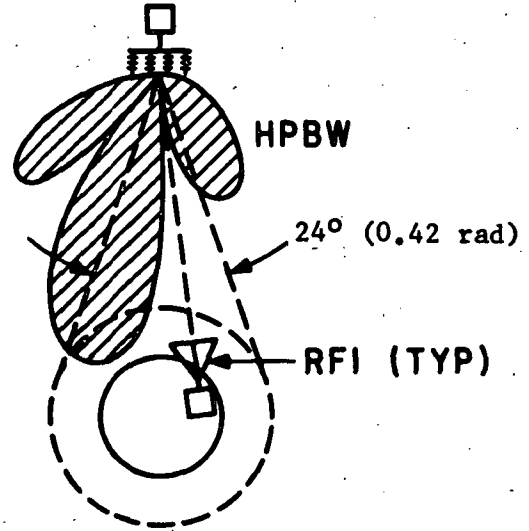


Figure 4-12. HPBW Characteristics of LDR Ring Array



F-FOV APPROACH

- FIXED BEAM COVERS ENTIRE FOV
- POLARIZATION DIVERSITY OF SIGNAL
- POLARIZATION FILTERING OF RFI



AGIPA APPROACH

- ADAPTIVE GROUND IMPLEMENTED PHASED ARRAY
 - ADAPTIVE SPATIAL FILTERING OF RFI
 - ADAPTIVE POLARIZATION FILTERING OF RFI
 - HPBW - AGIPA = 24° (0.42 rad)
- } FOR MAXIMUM SIR

Figure 4-13. LDR Return Link F-FOV vs AGIPA

A simplified functional block diagram of the AGIPA is shown in Figure 4-14 for a four-element phased array. To provide polarization diversity, this requires eight receive channels, four channels each for the vertically polarized (VP) and horizontally polarized (HP) signal components. Without going into the detailed algorithm, it can be shown that if the desired and interference signals are identified in the individual channels as well as after their summation, sufficient information is then available to compute the changes to be made to the weighting factors (amplitude and phase) to optimize the SIR*. Since the adjustments in weighting factor in the individual channels are interdependent, an iterative plunge routine has been developed using a minicomputer to calculate the magnitude and direction of each successive plunge. Since the computer can read-in only one source of information at a time, only one signal correlator and one interference correlator are used for the eight channels. Outputs are sequentially read-in and stored in the computer from one channel, and the correlators are sequentially switched to the other channels. After reading-in all eight channels, the computer determines the appropriate corrections to be made to each weighting network. The plunge routine is continued until the resultant SIR converges to a maximum; the entire optimization process is completed in less than one second. In actual operation the relative location of the interference signals are continuously but slowly changing; consequently the optimization process is continuously maintained for each user spacecraft. Since AGIPA processes both orthogonally polarized components of the desired and interference signals independently in its SIR optimization procedure, it has the complete flexibility to effectively utilize polarization as well as spatial information to discriminate and filter the undesired interference signals.

To evaluate the concept, a computer program was developed that simulates AGIPA in the presence of a variety of self-jamming and external RFI interference environments. The program has been designed with sufficient flexibility to enable system evaluation as design parameters and/or signal (desired and interference) environments are varied. The program was developed such that AGIPA's performance could be directly evaluated against a F-FOV approach.

Typical RFI models were developed as viewed from a geosynchronous TDRS satellite nominally located at 11 degrees west and 141 degrees west longitude for a performance evaluation of F-FOV and AGIPA approaches. In the Atlantic scenario, Figure 4-15, 20 RFI emitters were discretely located to typically represent the real environment, concentrating approximately 50 percent of the total average power along the United States coastline, 35 percent in Europe, and 15 percent scattered elsewhere. The total average power of the 20 RFI emitters was made variable; however, the distribution of the power was maintained as described. The relative polarization of each RFI emitter was picked from a random numbers table to realistically represent the random characteristic of the received RFI signals. In the Pacific scenario, Figure 4-16, 16 RFI emitters were used, with 50 percent of the total average RFI power concentrated along the North American Pacific coastline, 35 percent in Asia, and

* For detail discussion the readers are referred to the design reports issued in the Reference 1 contract.

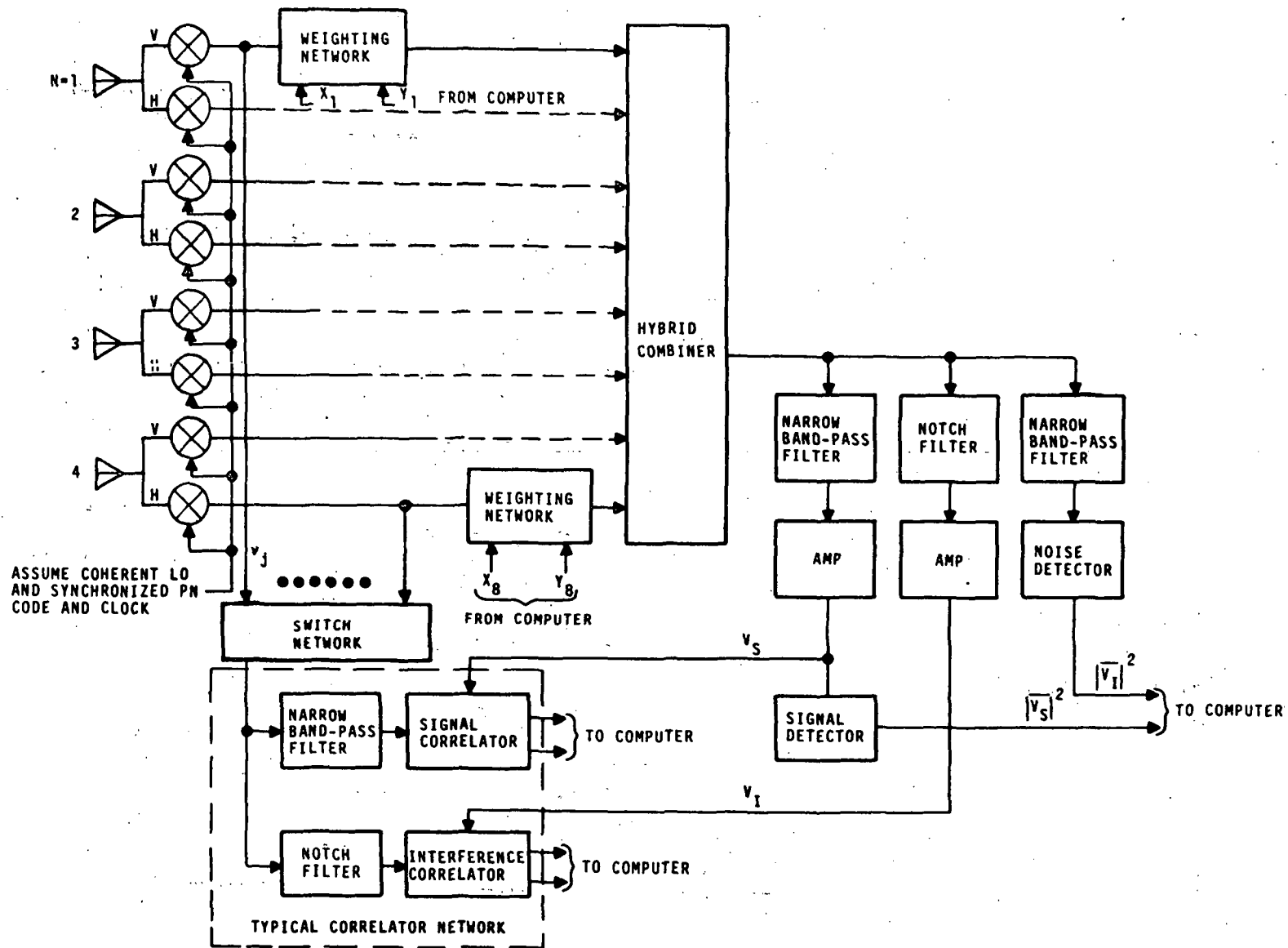


Figure 4-14. Adaptive Antenna for 8-Channel PN Receiver



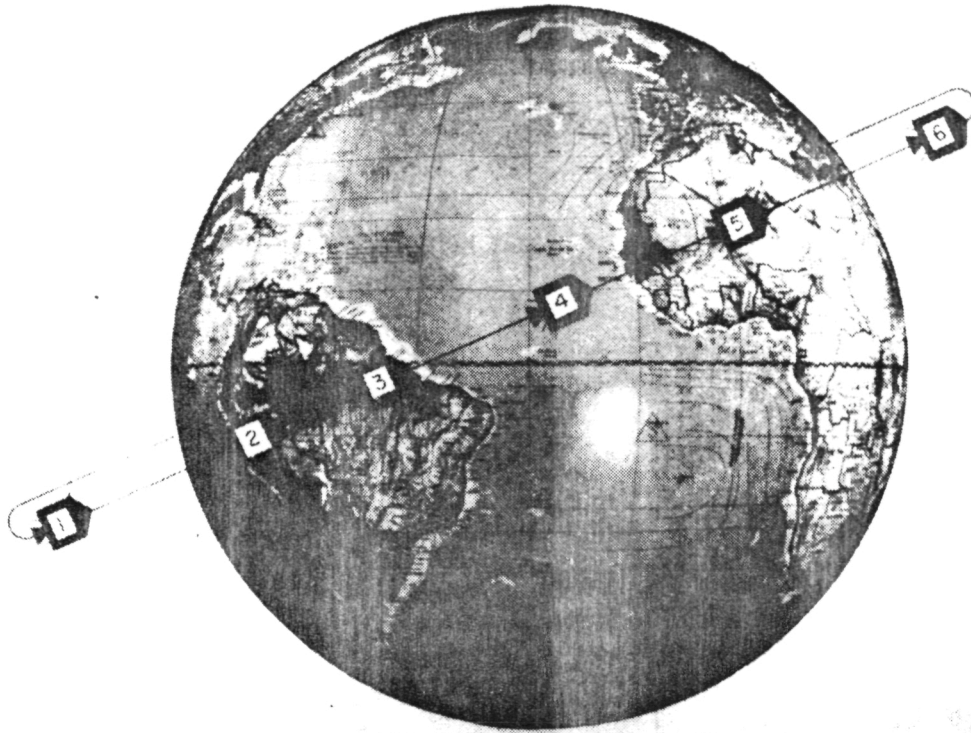


Figure 4-15. RFI Model for Atlantic Scenario

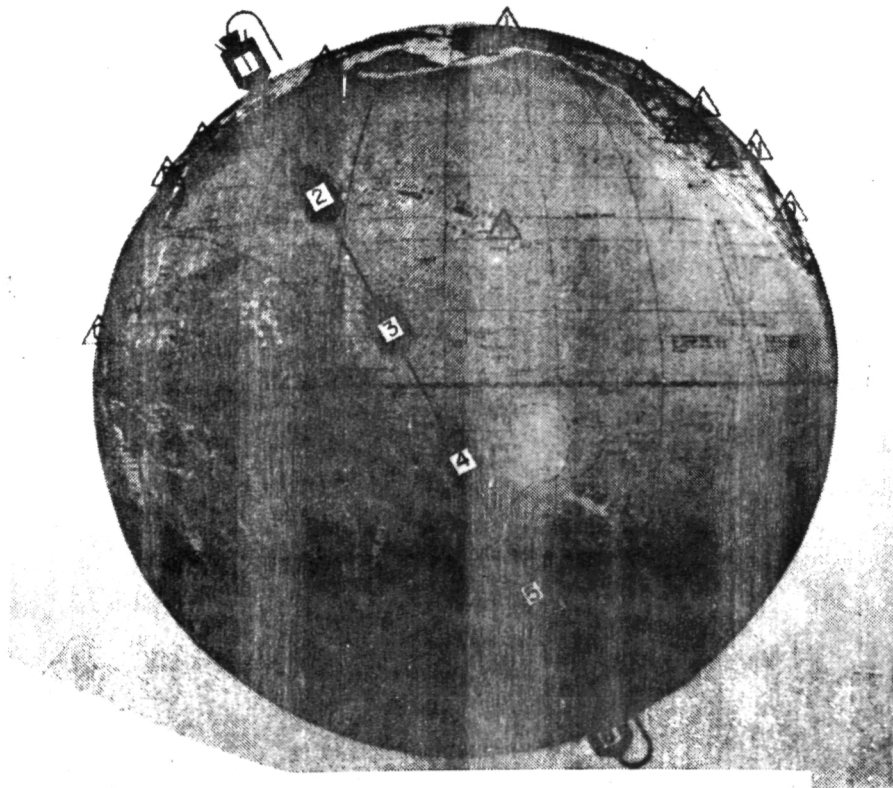


Figure 4-16. RFI Model for Pacific Scenario

15 percent elsewhere. In examining both scenarios, it is interesting to observe that the bulk of the RFI emitters are located near the perimeter of the earth disc coverage zone; therefore, it can be expected that the user will be in the relatively "clear" area most of the time such that even an AGIPA with a relatively broad antenna pattern can be expected to provide good spatial discrimination of RFI emitters.

The Atlantic scenario assumes a typical user spacecraft orbit with an inclination angle of 24° (0.42 rad). User performance was evaluated at six locations as shown in Figure 4-15. As a "worst case" the user was also located in the center of the European emitters. The Pacific scenario assumes a typical atmosphere explorer with an orbit inclination angle of 63° (1.1 rad).

A performance comparison of the F-FOV and AGIPA approaches were made using the same antenna for both approaches, providing an HPBW corresponding to the operational 24° (0.42 rad) FOV. For this analysis a quad-array of backfire elements as shown in Figure 4-17 was used. Since the F-FOV is nonadaptive, all RFI emitters are visible within the HPBW as typically shown in Figure 4-18 for the three-dimensional computer-generated antenna pattern for the Atlantic scenario.

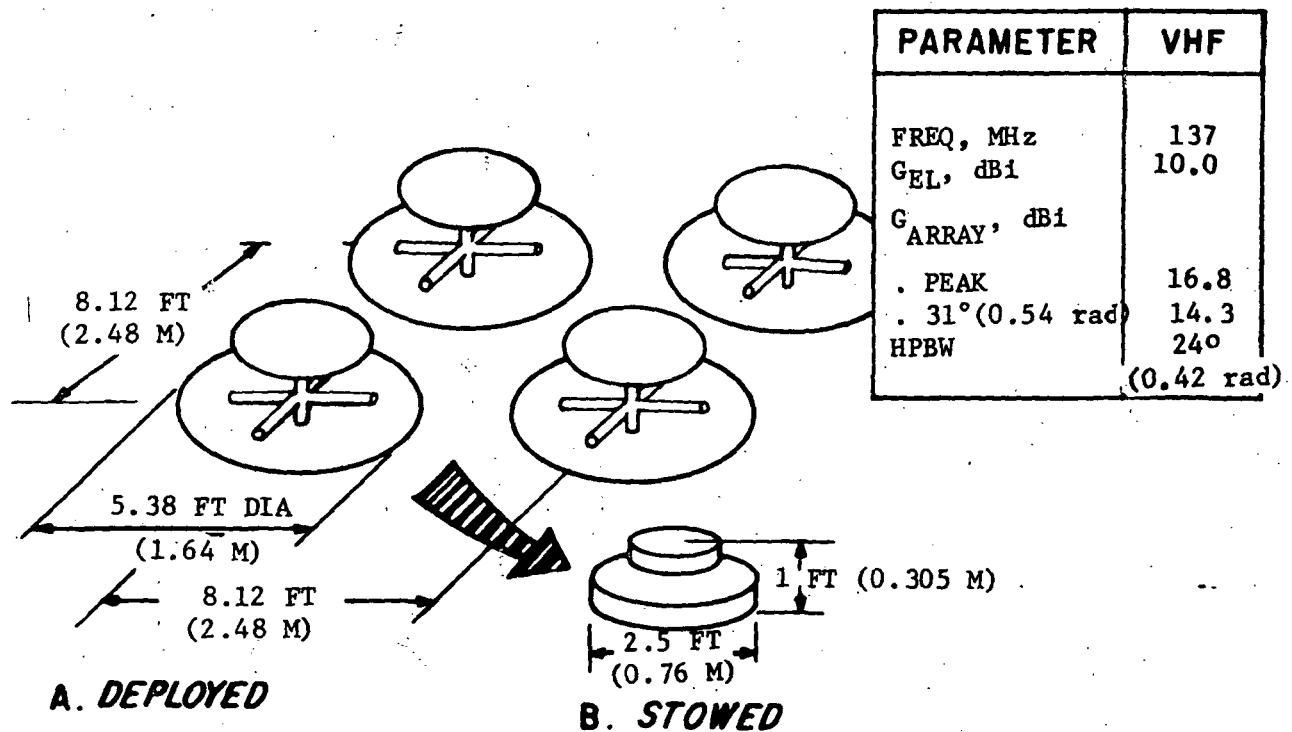


Figure 4-17. VHF Quad Array of Backfire Elements for F-FOV and AGIPA Approaches

INITIAL SIG/INT

ELEMENT NUMBER	LOCATION	RHO	THETA	MAG.	WEIGHT	DEGREES
1	HORIZ.	0.64	45	1.		45.
	VERT.			1.		45.
2	HORIZ.	0.64	135	1.		45.
	VERT.			1.		45.
3	HORIZ.	0.64	225	1.		45.
	VERT.			1.		45.
4	HORIZ.	0.64	315	1.		45.
	VERT.			1.		45.

SIGNAL DESIRED	RHO	THETA	J/N-WATTS	POLAR
----------------	-----	-------	-----------	-------

TOTAL RFI =

() = 0 TO 3DB . = 3 TO 6DB + = 6 TO 10DB
 9 = 10 TO 15DB \$ = 15 TO 20DB x > 20DB

SCALE RADIUS 16 DEGREES

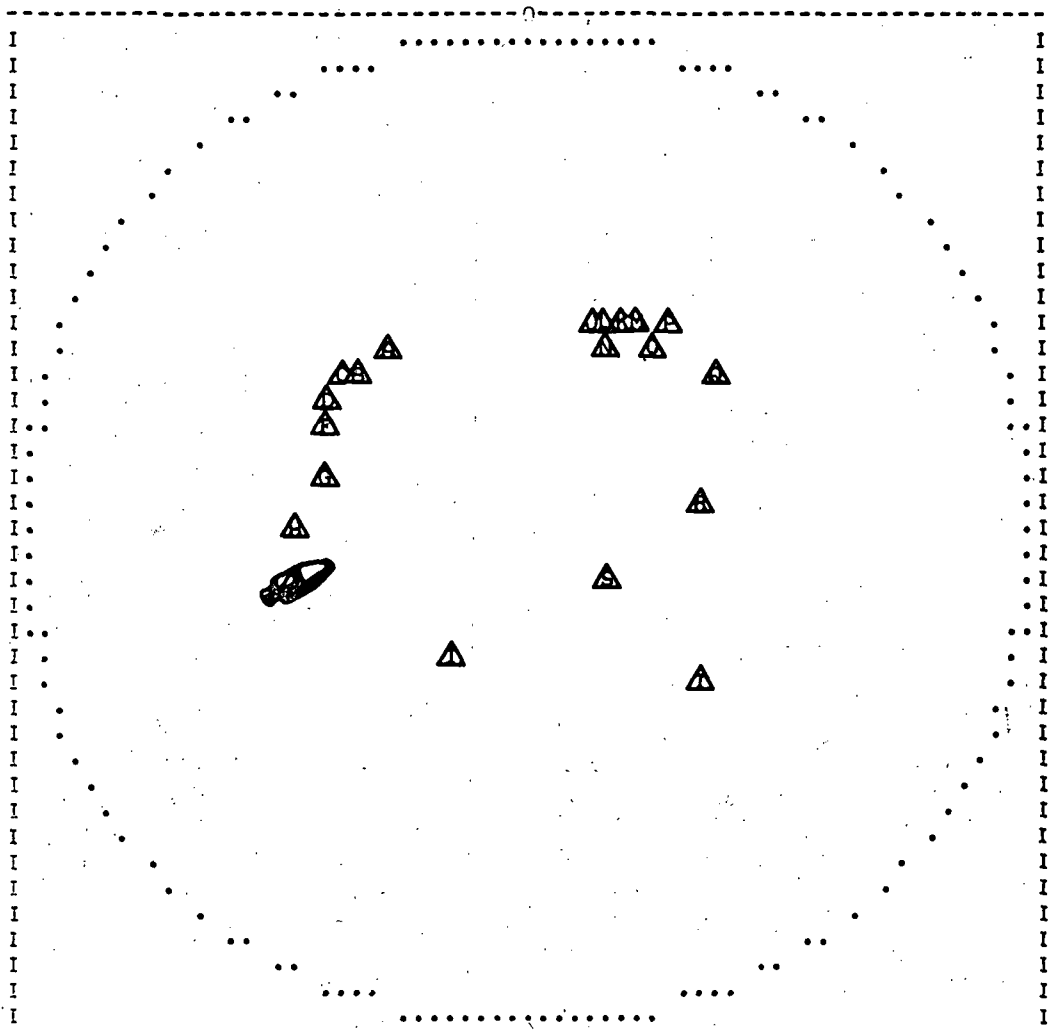


Figure 4-18. Atlantic View



The AGIPA concept utilizes the same quad-array of backfire elements as the F-FOV approach. Figures 4-19 through 4-25 represent the adaptive computer patterns for each of the seven user locations for the Atlantic scenario. The computer patterns show an expanded view of the earth disc FOV only in order to most effectively show its performance against the earth-based RFI emitters. The resultant adapted SIR is shown on each figure as the "Plunge N SIG/INT" value which represents that "N" iterative beam steering plunges or adaptations were taken to obtain the optimum SIR. The difference between the adapted "Plung N SIR" and the Initial SIR is the SIR improvement (Δ SIR) of the AGIPA over the F-FOV approach. The resultant Δ SIR is plotted in Figure 4-26.

Similar computer patterns were made for the Pacific scenarios and the resultant Δ SIR also tabulated in Figure 4-26. The improvement varies considerably, depending upon AGIPA's capability to adaptively discriminate against the RFI emitters. Even for the worst case (user located in the middle of the European emitters--Atlantic scenario), AGIPA eliminates more than 50 percent of the unwanted emitters.

The computer-generated antenna patterns, as well as the signal-to-interference ratio improvement (Δ SIR) of the adaptive AGIPA approaches were computed for a total average rms FRI power-to-signal received signal power (RFI/ P_r) ratio of 23 dB for typical Atlantic and Pacific RFI models. AGIPA employing the same quad-array or backfire antennas as the F-FOV approach, the SIR improvement (Δ SIR) has been shown to be significant.

This Δ SIR improvement can now be reflected in terms of improved link performance by examining the communication link equation for a multiple access spread spectrum system:

$$H = \frac{FEC}{CNR} \left[\frac{N_o}{P_R} + M_o + \frac{RFI_o}{P_R} \right]^{-1} \quad (4-1)$$

where:

- H = information data rate in bps
- $N_o = KT_s$ = receiver thermal noise density
- FEC = forward error control
- CNR = required carrier-to-noise ratio
- $M_o = \frac{\Gamma(3N/2)P_R}{B}$ = intentional in-band noise density due to direct and multipath signals from "N" users;
 Γ is reflection coefficient of multipath signal
- RFI_o = unintentional in-band noise density due to RFI
- P_R = desired user received signal power

If we assume that PCM -APSK modulation is used in this link, a CNR of 10.9 dB is required to provide the required bit error probability (P_e) of 10^{-5} , including a Δ CNR degradation of 1 dB through the TDRS transponder. In addition, employment of forward error control (FEC) of the form rate 1/2 (48, 24) non-systematic convolutional code constraint length seven with a Viterbi decoder results in an improvement of approximately 4.7 db.



INITIAL SIG/INT-20.05 DB
PLUNGE 15 SIG/INT-5.1 DB

ELEMENT NUMBER	LOCATION	RHO	THETA	MAG.	DEGREES
1	HORIZ.	0.64	45	2.03753	-10.1757
	VERT.			0.287955	45.
2	HORIZ.	0.64	135	1.89275	22.7218
	VERT.			0.287955	45.
3	HORIZ.	0.64	225	2.03753	-79.8243
	VERT.			0.287955	45.
4	HORIZ.	0.64	315	1.89275	67.2782
	VERT.			0.287955	45.

SIGNAL DESIRED #1	RHO	THETA	J/N-WATTS	POLAR
	12	252	5	0

TOTAL RFI = 1000 WATTS

() = 0 TO 3DB . = 3 TO 6DB + = 6 TO 10DB
@ = 10 TO 15DB \$ = 15 TO 20DB X > 20DB

SCALE RADIUS 8 DEGREES

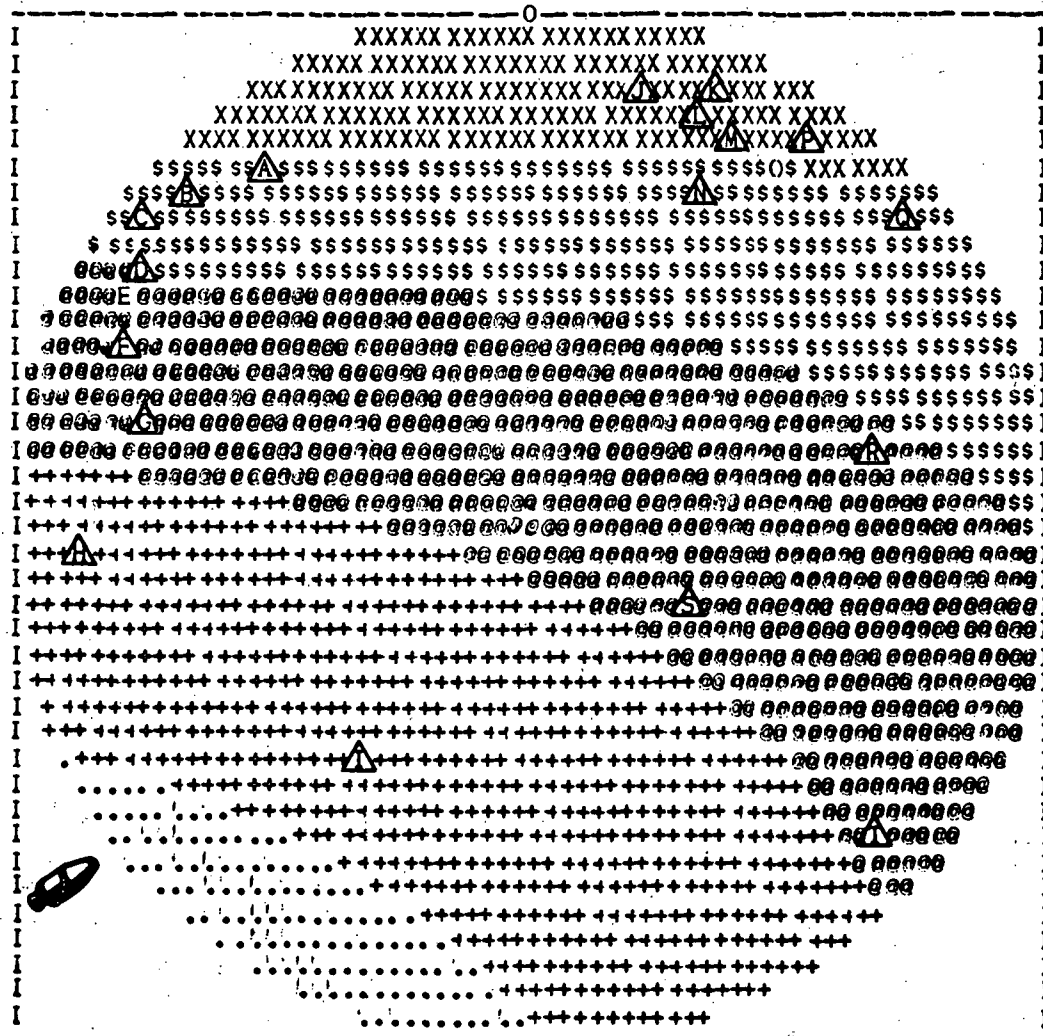


Figure 4-19. Atlantic View - Signal No. 1



INITIAL SIG/INT-19.09 DB
PLUNGE 15 SIG/INT-8 DB

ELEMENT NUMBER	LOCATION	RHO	THETA	WEIGHT MAG.	DEGREES
1	HORIZ.	0.64	45	1.95354	-21.2204
	VERT.			0.342884	45.
2	HORIZ.	0.64	135	1.82727	11.6599
	VERT.			0.342884	45.
3	HORIZ.	0.64	225	1.95354	-68.7796
	VERT.			0.342884	45.
4	HORIZ.	0.64	315	1.82727	78.3401
	VERT.			0.342884	45.

SIGNAL DESIRED #2	RHO	THETA	J/N-WATTS	POLAR
	8	255	5	0

TOTAL RFI = 1000 WATTS

() = 0 TO 3DB . = 3 TO 6DB + = 6 TO 10DB
 @ = 10 TO 15DB \$ = 15 TO 20DB X > 20DB

SCALE RADIUS 8 DEGREES

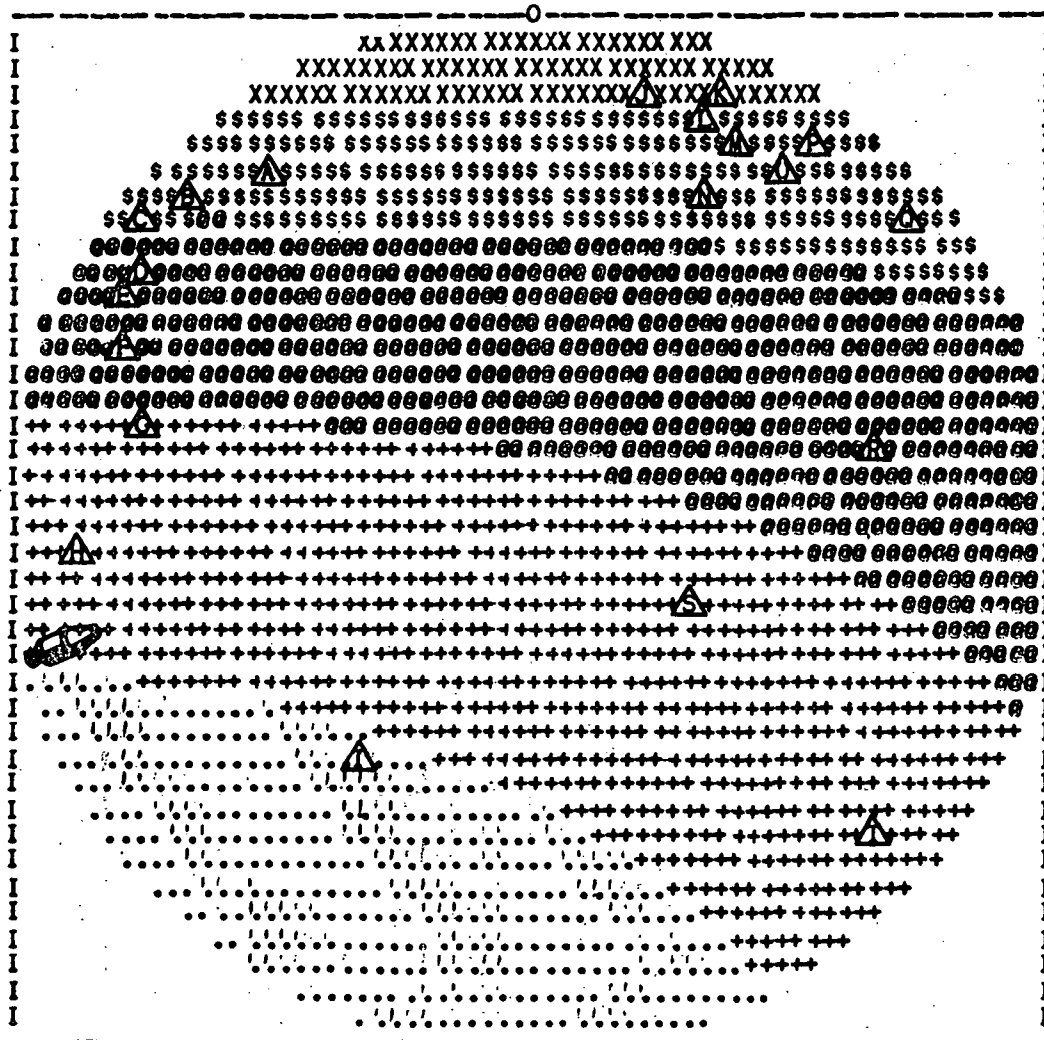


Figure 4-20. Atlantic View - Signal No. 2



INITIAL SIG/INT-18.53 DB
PLUNGE 15 SIG/INT-10.96 DB

ELEMENT NUMBER	LOCATION	WEIGHT			
		RHO	THETA	DEGREES	
1	HORIZ.	0.64	45	1.71058	-42.29
	VERT.			0.449179	45.
2	HORIZ.	0.64	135	1.72097	-9.03883
	VERT.			0.449179	45.
3	HORIZ.	0.64	225	1.71058	-47.71
	VERT.			0.449179	45.
4	HORIZ.	0.64	315	1.72097	-80.9612
	VERT.			0.449179	45.

SIGNAL DESIRED #3	RHO	THETA	J/N-WATTS	POLAR
4	4	263	5	0

TOTAL RFI = 1000 WATTS

() = 0 TO 3DB . = 3 TO 6DB + = 6 TO 10DB
 @ = 10 TO 15DB \$ = 15 TO 20DB X > 20DB

SCALE RADIUS 8 DEGREES

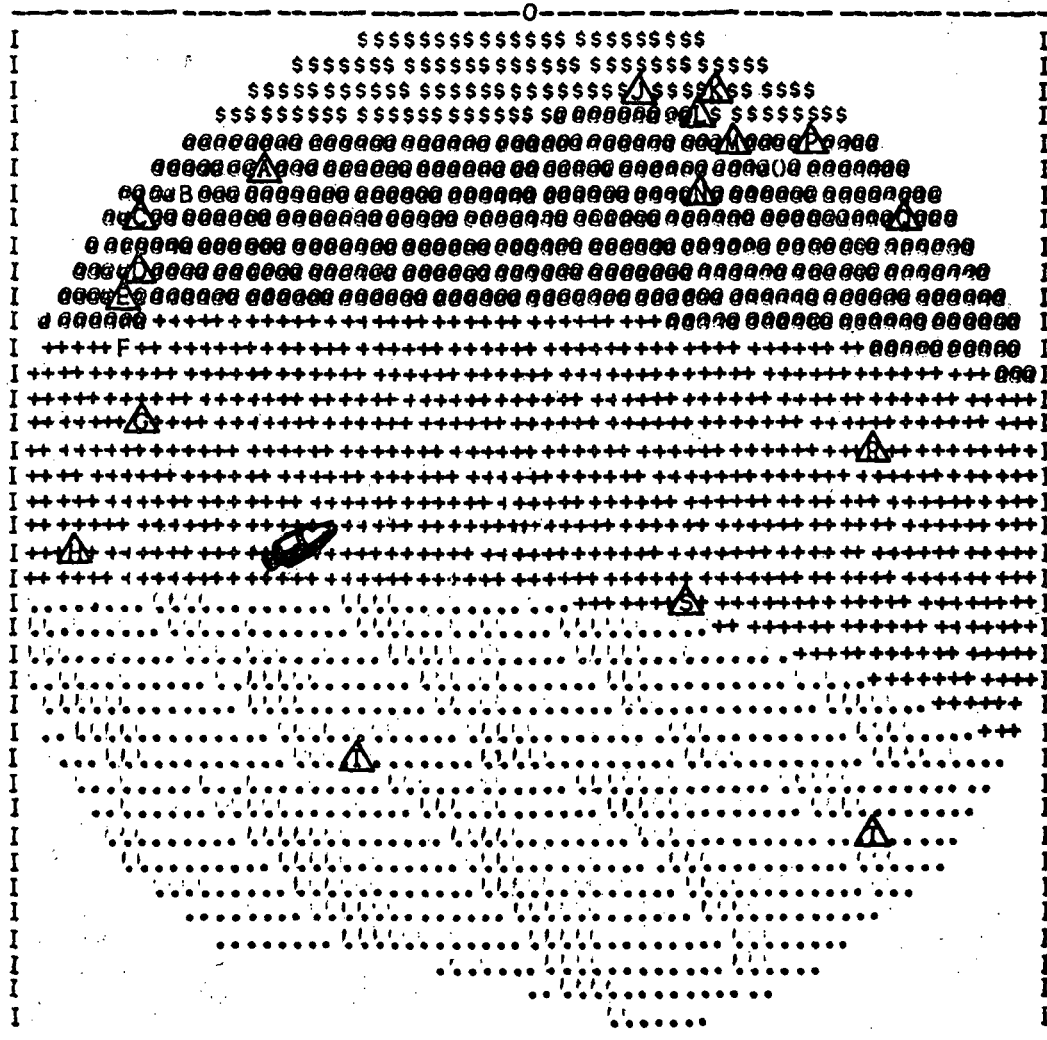


Figure 4-21. Atlantic View - Signal No. 3



INITIAL SIG/INT-18.37 DB
PLUNGE 15: SIG/INT-16.62 DB

ELEMENT NUMBER	LOCATION	RHO	THETA	MAG.	HEIGHT
1	HORIZ.	0.64	45	1.33529	-69.548
	VERT.			0.511429	45.
2	HORIZ.	0.64	135	1.82906	-29.5008
	VERT.			0.511429	45.
3	HORIZ.	0.64	225	1.33529	-20.452
	VERT.			0.511429	45.
4	HORIZ.	0.64	315	1.82906	-60.4992
	VERT.			0.511429	45.

SIGNAL DESIRED #4	RHO	THETA	J/N-WATTS	POLAR
	1.5	11	5	0

TOTAL RFI = 1000 WATTS

() = 0 TO 3DB . = 3 TO 6DB + = 6 TO 10DB
 @ = 10 TO 15DB \$ = 15 TO 20DB X > 20DB

SCALE RADIUS 8 DEGREES

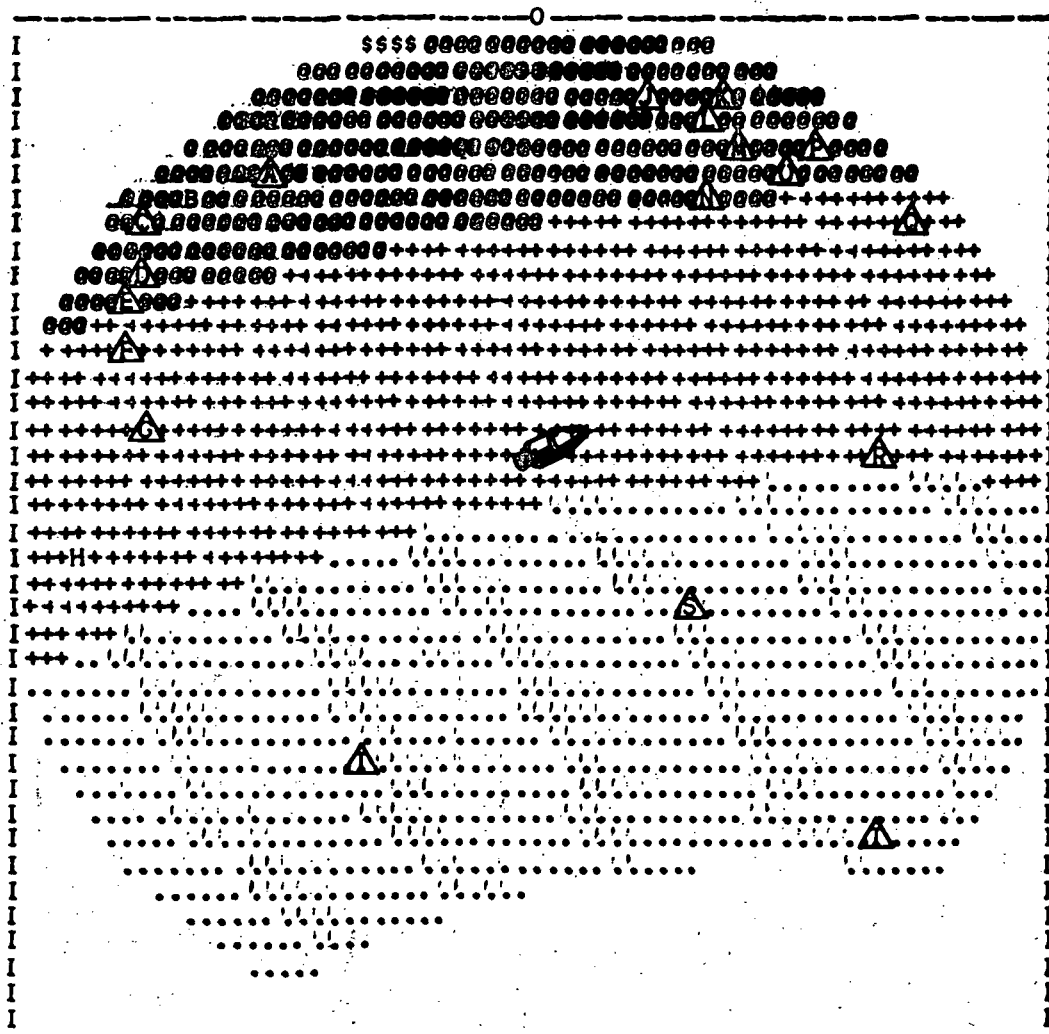


Figure 4-22: Atlantic View - Signal No. 4

INITIAL SIG/INT-18.73 DB
PLUNGE 15 SIG/INT-14.05 DB

ELEMENT NUMBER	LOCATION	RHO	THETA	WEIGHT	MAG.	DEGREES
1	HORIZ.	0.64	45	0.967302	0.42111	61.9361
	VERT.					45.
2	HORIZ.	0.64	135	2.23823	0.42111	-40.8736
	VERT.					45.
3	HORIZ.	0.64	225	0.967302	0.42111	28.0639
	VERT.					45.
4	HORIZ.	0.64	315	2.23823	0.42111	-49.1264
	VERT.					45.

SIGNAL DESIRED %	RHO	THETA	J/N-WATTS	POLAR
	5.8	55	5	0

TOTAL RFI = 1000 WATTS

() = 0 TO 3DB . = 3 TO 6DB + = 6 TO 10DB
 @ = 10 TO 15DB \$ = 15 TO 20DB X > 20DB

SCALE RADIUS 8 DEGREES

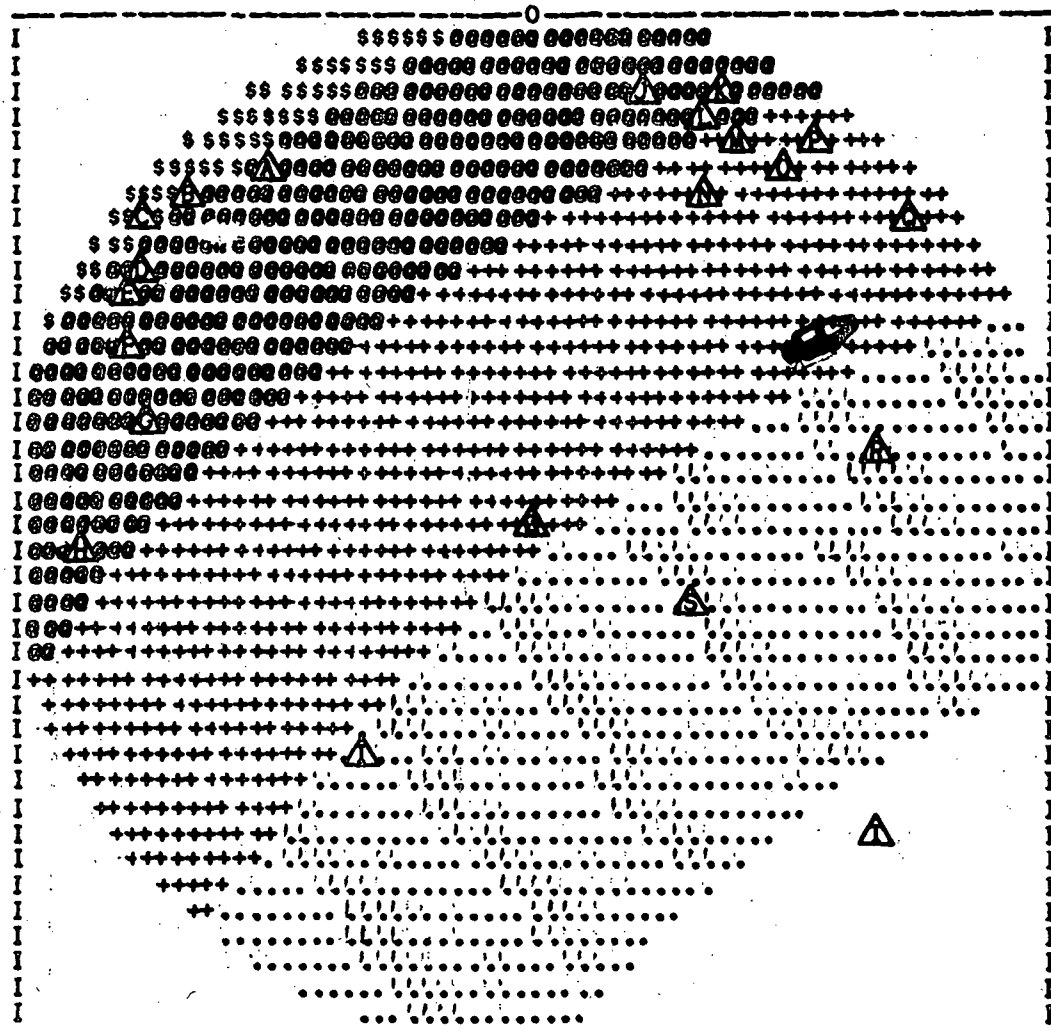


Figure 4-23. Atlantic View - Signal No. 5



INITIAL SIG/INT-19.76 DB
PLUNGE 15 SIG/INT-12.27 DB

ELEMENT NUMBER	LOCATION	RHO	THETA	MAG.	WEIGHT	DEGREES
1	HORIZ. VERT.	0.64	45	1.47989 0.31362		-56.5763 45.
2	HORIZ. VERT.	0.64	135	2.1844 0.31362		-16.681 45.
3	HORIZ. VERT.	0.64	225	1.47989 0.31362		-33.4237 45.
4	HORIZ. VERT.	0.64	315	2.1844 0.31362		-73.319 45.

SIGNAL DESIRED #6 RHO 11 THETA 61 J/N-WATTS 5 POLAR 0

TOTAL RFI = 1000 WATTS

() = 0 TO 3DB . = 3 TO 6DB + = 6 TO 10DB
@ = 10 TO 15DB \$ = 15 TO 20DB X > 20DB

SCALE RADIUS 8 DEGREES

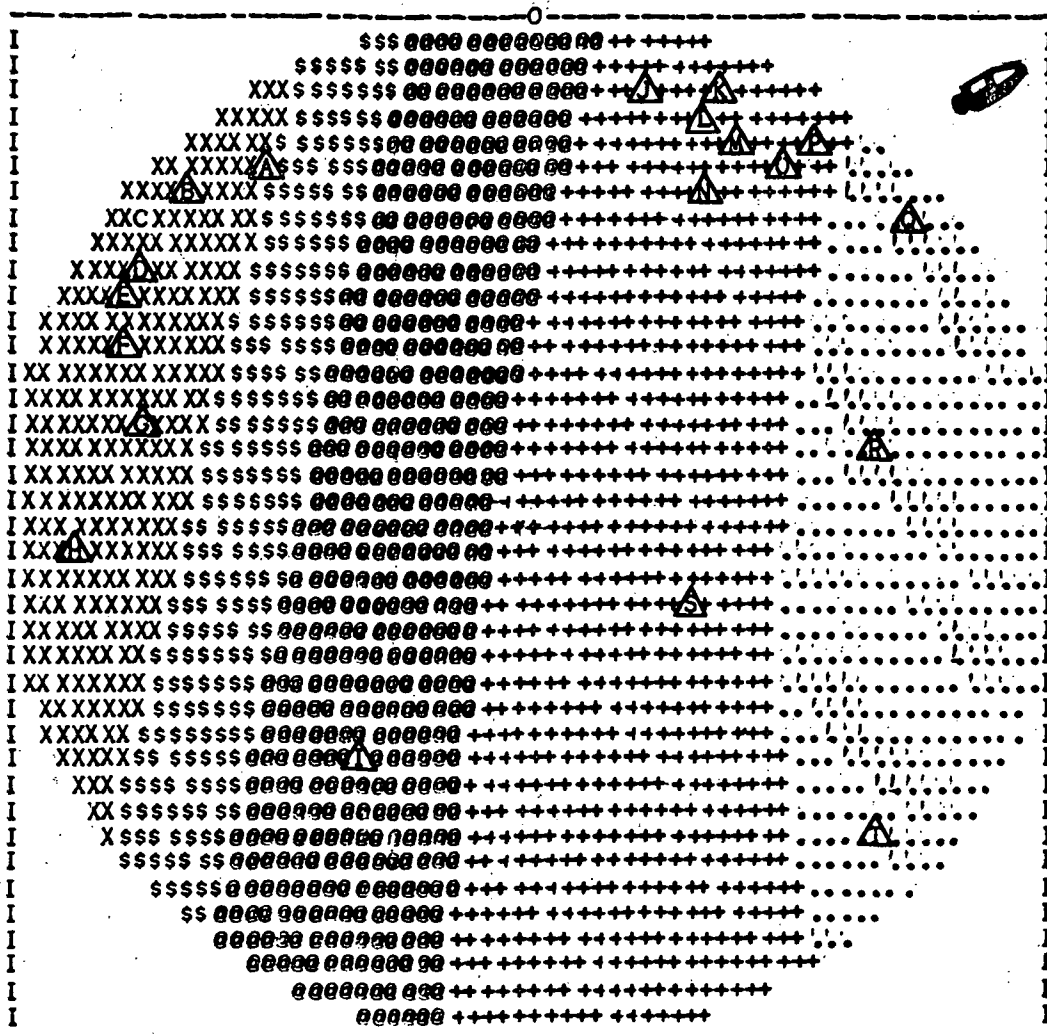


Figure 4-24. Atlantic View - Signal No. 6



INITIAL SIG/INT-18.99 DB
PLUNGE 15 SIG/INT-15.82 DB

ELEMENT NUMBER	LOCATION	RHO	THETA	WEIGHT	
				MAG.	DEGREES
1	HORIZ.	0.64	45	2.28578	-62.3153
	VERT.			0.35043	45.
2	HORIZ.	0.64	135	1.24831	-71.5213
	VERT.			0.35043	45.
3	HORIZ.	0.64	225	2.28578	-27.6847
	VERT.			0.35043	45.
4	HORIZ.	0.64	315	1.24831	-18.4787
	VERT.			0.35043	45.

SIGNAL DESIRED #7 RHO 7.5 THETA 22 J/N-WATTS 5 POLAR 0

TOTAL RFI = 1000 WATTS

() = 0 TO 3DB . = 3 TO 6DB + = 6 TO 10DB
@ = 10 TO 15DB \$ = 15 TO 20DB X > 20DB

SCALE RADIUS 8 DEGREES

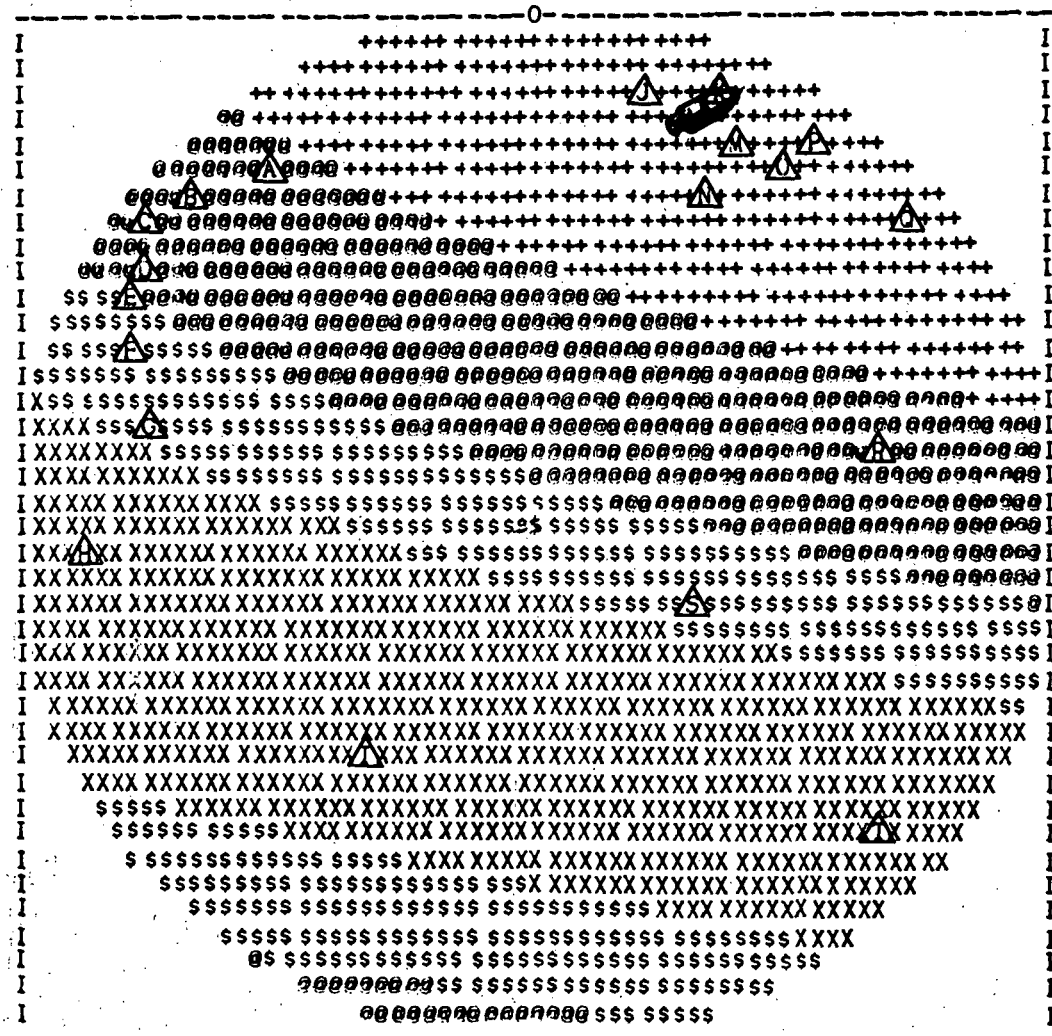
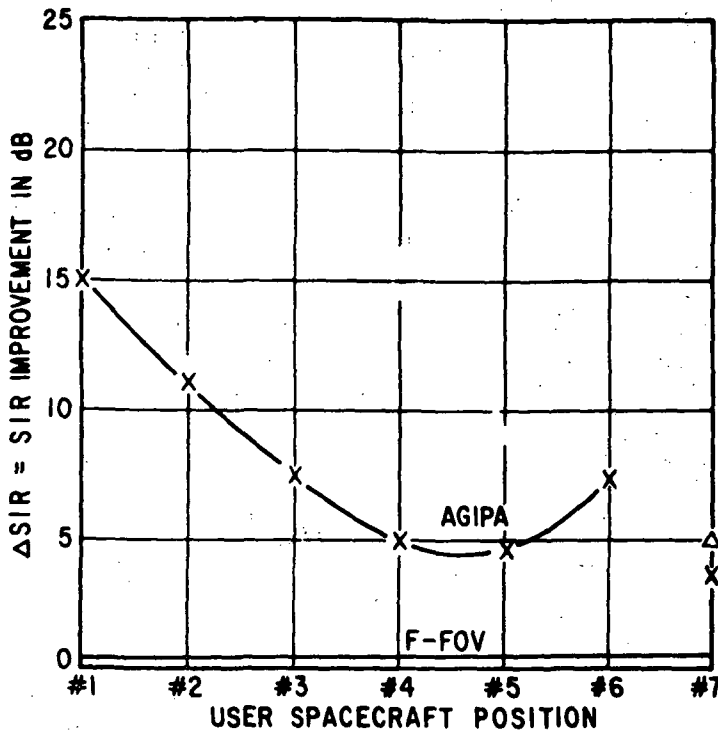
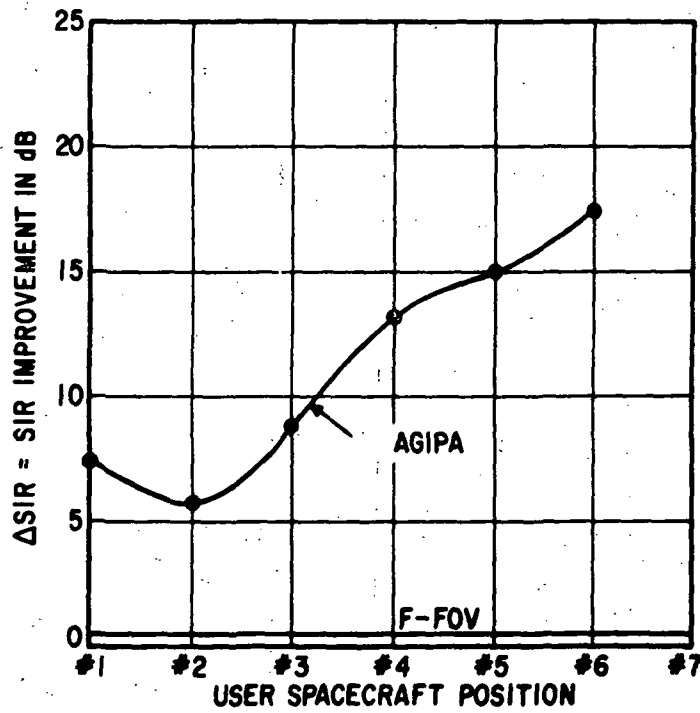


Figure 4-25. Atlantic View - Signal No. 7



A. ATLANTIC SCENARIO



B. PACIFIC SENARIO

Figure 4-26. SIR Improvement: F-FOV vs AGIPA



The antenna gain at the TDRS varies for both link approaches. Even though AGIPA utilizes the same quad-array of backfire elements, the effective antenna gain for AGIPA is 4.8 dB greater than the F-FOV approach. This can be explained by referring to Figures 4-27 and 4-28. Figure 4-27 describes the electrical and mechanical characteristics of the quad-array. The F-FOV combines the output of the four elements to provide an array half-power beamwidth (HPBW) of 24° (0.42 rad) as shown by the pattern in Figure 4-28. Its peak gain is 16.8 dB; and its 31° (0.54 rad) FOV (HPBW) gain is 11 dB. AGIPA electronically steers its beam. Consequently, its scan loss is determined by the element pattern characteristic. For elements with HPBW's of 45° (0.79 rad), this loss is only 1.0 dB. Therefore, at the edge of the field of view AGIPA can provide 15.8 dB as compared to 11.0 dB for the fixed field-of-view approach.

Equation 4-1 was then evaluated as a function of RFI/ P_R density for the F-FOV approach for a user transmit power of one watt. A plot of this equation is used as a reference to compare the AGIPA approaches in Figures 4-29a and 4-29b for the Atlantic and Pacific scenarios, respectively. The computer program used to generate the patterns and to compute the Δ SIR was extended to include other values of RFI/ P_R ratio in Equation 4-1; consequently, the improved H capacity can be readily calculated as a function of Δ SIR using Equation 4-1. The resultant H improvement has been calculated for each user position versus RFI/ P_R for both Atlantic and Pacific scenario, and superimposed on the curves of Figure 4-29 and 4-30 respectively. Since AGIPA's performance varies considerably (5 to 18 dB) depending on the user position, the overall data rate improvement is shown by the spread of dashed lines, representing user positions 1 through 6 in both scenarios. The threshold levels shown differ for each approach (F-FOV, and AGIPA) since they have different TDRS antenna gains. The threshold level represents the maximum H that the link can support in the absence of RFI.

In reviewing Figures 4-29a and 4-28, it is evident that for a total average rms RFI power level of -92 dBm or power density of -154 dBm/Hz (assume RF bandwidth of 1.5 MHz), that the F-FOV can support only a data rate of 80 bps/watt whereas with AGIPA the data rate capacity increases from 500 to 3200 bps/watt or a nominal improvement of ten times F-FOV. Even in this high RFI density, AGIPA can nominally support the required 10 kbps data rate with a user EIRP of 10 dBw.

As a further comparison, the impact of a large RFI jammer was assessed by letting one of the emitters radiate with an EIRP of 20 kw. The result was that the F-FOV was made completely inoperative; whereas AGIPA placed the jammer into a deep pattern null and suffered negligible SIR degradation.

In summary, it has been shown that the adaptive techniques offer considerable performance improvements over the F-FOV approach. In fact, AGIPA must be employed to meet the performance requirements in the evidence of the large RFI environment. Even though the magnitude of this large RFI density is not clearly defineable or predictable, sufficient design precaution must be implemented to insure its success and reliability for the planned operational period and life of the overall TDRS.

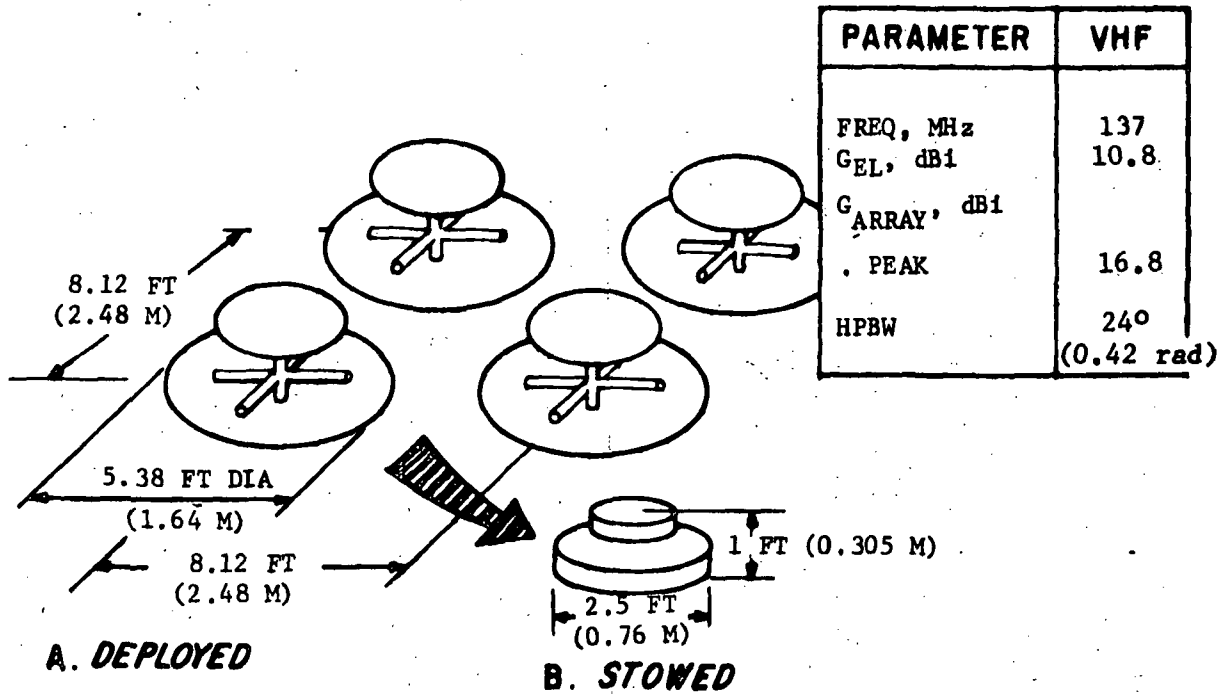


Figure 4-27. VHF Quad Array of Backfire Elements for F-FOV and AGIPA Approaches

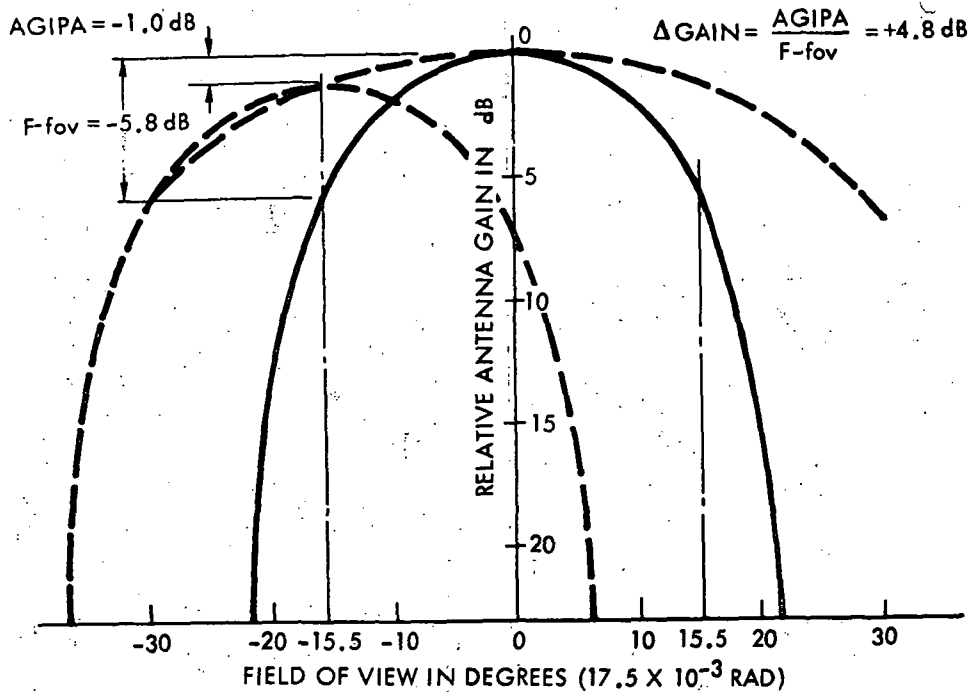
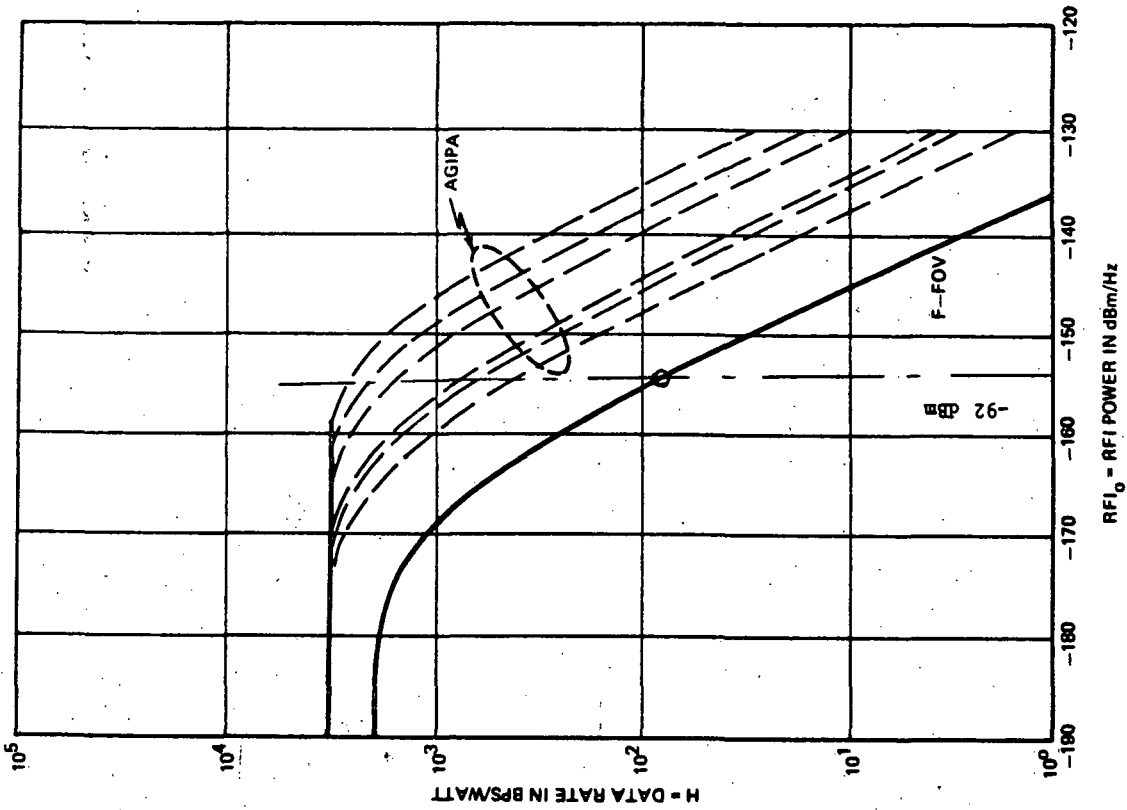
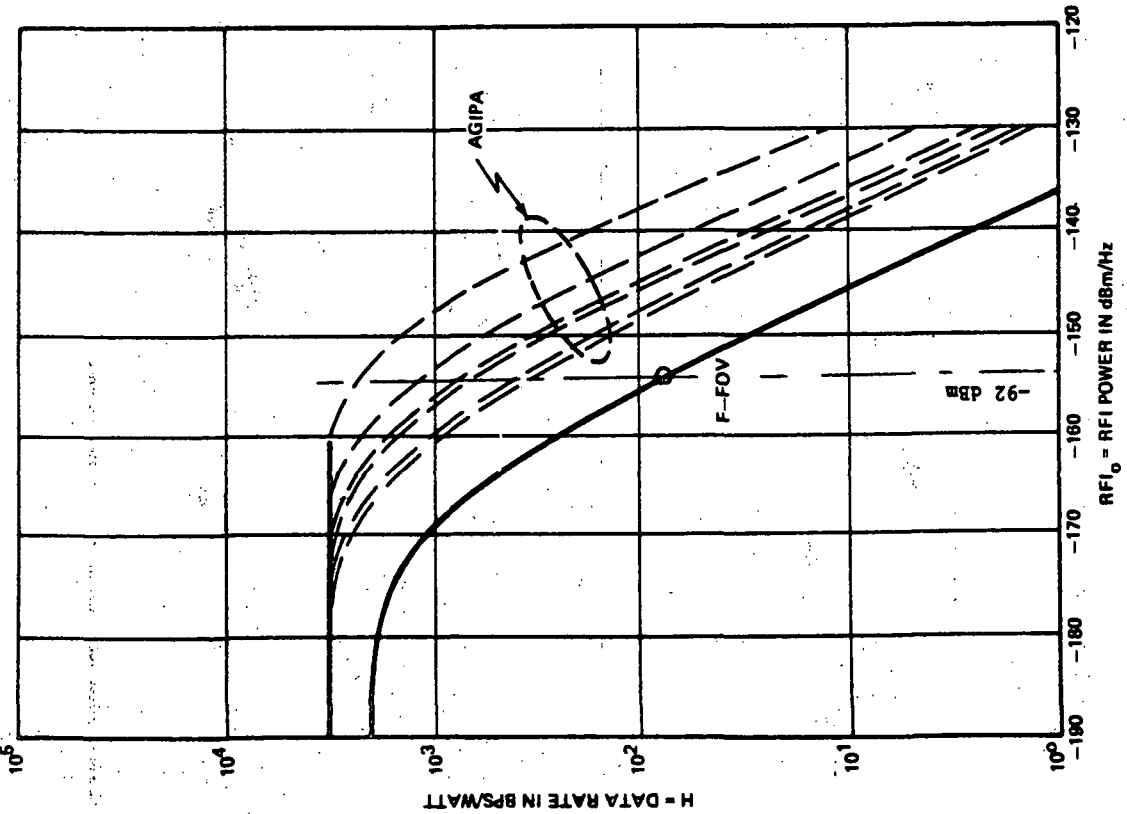


Figure 4-28. Scan Loss: F-FOV vs AGIPA



b. Pacific Scenario



a. Atlantic Scenario

Figure 4-29. LDR Return Link Performance: F-FOV vs AGIPA



4.3.1.2 LDR Forward Link Tradeoff Analysis

The design of the forward link for LDR users is based upon the requirement of providing two channels which can transmit either voice or data. The requirements and constraints of the analysis conducted for the forward link are summarized in Table 4-4.

Table 4-4. Low Data Rate Forward Link Requirements, Constraints

Frequency	VHF, UHF, S-band
Coverage	Users to 5000 km altitude - 31° (0.54 rad) FOV
ERP	Specified at VHF only to be 30 dBw over 26° (0.45 rad) FOV 28 dBw over 30° (0.52 rad) FOV
Flux density	Limited by CCIR: VHF - 144 dBw/m ² /4kHz UHF - 150 dBw/m ² /4kHz S-band - 154 dBw/m ² /4kHz
Channels	2
Information	1 kbps data at $P_e = 10^{-5}$ Voice
Duty cycle	Data - 100% Voice -25% "push-to-talk"

The tradeoff performed during the study consisted of evaluating the size and weight penalty imposed on the TDRS for achieving a specific performance level on the voice and data channels at the user. Data was developed for the three frequency bands of interest, VHF, UHF, and S-band using the variables in Table 4-5. The tradeoffs were performed in conjunction with the receiving LDR system, which was selected as a VHF four-element array with the AGIPA steering and processing concept.

The tradeoff performed on the F-FOV system, evaluated the use of a single antenna element versus multiple elements arranged in an array. The F-FOV is the reference used for comparison with all of the other mechanization alternatives.

Table 4-5. LDR Forward Link TDRS Implementation Tradeoff Matrix

System Alternative	Applicable Frequencies	Implementation
F-FOV with antenna gain of 15 dBi on boresight	VHF, UHF	Single element, four element array. Separate/single power amplifiers
Steered array with 15 dBi gain	VHF, UHF	Four/five elements Separate/single power amplifiers Satellite/ground steered array
Steered array with 21 dBi boresight gain	VHF, UHF, S-band	Four/five elements Separate/single power amplifiers Satellite/ground steered array
20 element retrodirective array	S-band	Number of elements

The second alternative is a low-gain four-element steered beam array, providing a peak array gain of 15 dBi. Each element has a HPBW of approximately 60° (1.05 rad) and a gain of 9 dBi. In addition to evaluating the ERP as a function of weight for the steered beam approach, the question of whether to perform the steering on the ground or in the satellite was evaluated. Steering from the ground is referred to as AGIPA even though the beam is pointed at the LDR using a priori knowledge of user position rather than adaptively positioned as in the receiver case.

The third system considered is a high-gain steered beam configuration. For this case the antenna element gain is increased from 9 dBi to 15 dBi, resulting in an array boresight gain of 21 dBi for four elements.

The final system evaluated was the use of a multibeam retrodirective array. Since the size of an S-band array is large for the required ERP the tradeoff was performed assuming that the retro would provide beams for the MDR user as well. A 20-element array requires that the MDR S-band function be combined as two beams with LDR forward link users. Therefore, the S-band antenna aperture would be shared for both LDR and MDR applications.

To evaluate the forward link implementation alternatives, the ERP was determined as a function of aspect angle between the TDRS and LDR user. Aspect angle changes as a function of the relative position between the user and the TDRS spacecraft and enables the consideration of losses in the actual dynamic TDRS situation.* These results are summarized in Table 4-6. The ERP's presented are for generating 40.5 dB-Hz at the input to the user receiver which is sufficient to support a bit rate of 1 kbps with an error rate of 10^{-5} . The link calculations include no margin for either RFI or equipment variations. The ERP's in Table 4-6 then became the basic requirements for initiating a preliminary design for each system at the three frequencies so that the weight of the electronics and power system could be determined as a function of link margin. For this analysis the power required was converted into weight at the rate of 35 lbs (.16 kg) per watt. The analysis was conducted at S-band only for Case 5 of Table 4-6 since the power required was otherwise prohibitive.

Table 4-6. LDR Forward Link ERP for Several Implementation Approaches

System Alternative	Peak ERP (&P _T) - dBw		
	VHF	UHF	S-Band
1. F-FOV (G _T = 15 dBi)	14.55 (-0.45)	23.75 (8.75)	40.75 (25.75)
2. AGIPA (G _T = 15 dBi)	14.85 (-0.15)	24.75 (6.75)	38.75 (23.75)
3. Low-gain steered beam (G _T = 15 dBi)	14.85 (-0.15)	24.75 (6.75)	38.75 (23.75)
4. High-gain steered beam (G _T = 21 dBi)	8.55 (-12.45)	17.75 (-3.25)	34.75 (13.75)
5. 20-element retrodirective array (G _T = 28 dBi)			27.75 (-0.25)

The results of the LDR implementation analysis are shown graphically in Figure 4-30. The equivalent weight is plotted as a function of margin for the various implementations and frequency bands. Where a system required a different antenna system than the VHF four-element needed for implementing AGIPA on the return link, the differential antenna weight was added to that required for the F-FOV system to make a comparison.

Each system was evaluated including the requirement for two separate channels; the curves labeled "quad" utilized quadrature modulation for this purpose. The numbers on each curve in Figure 4-31 refer to cases listed in Table 4-6.

* Third and Fourth Monthly Progress Report, TDRSS Configuration and Tradeoff Study, Tasks 9.2., 9.2.2, 9.2.3, 9.2.4, 9.2.5, in the third report, and Task 9.2.14 in the fourth report, April 15, 1972 and May 15, 1972, NAS5-21705.

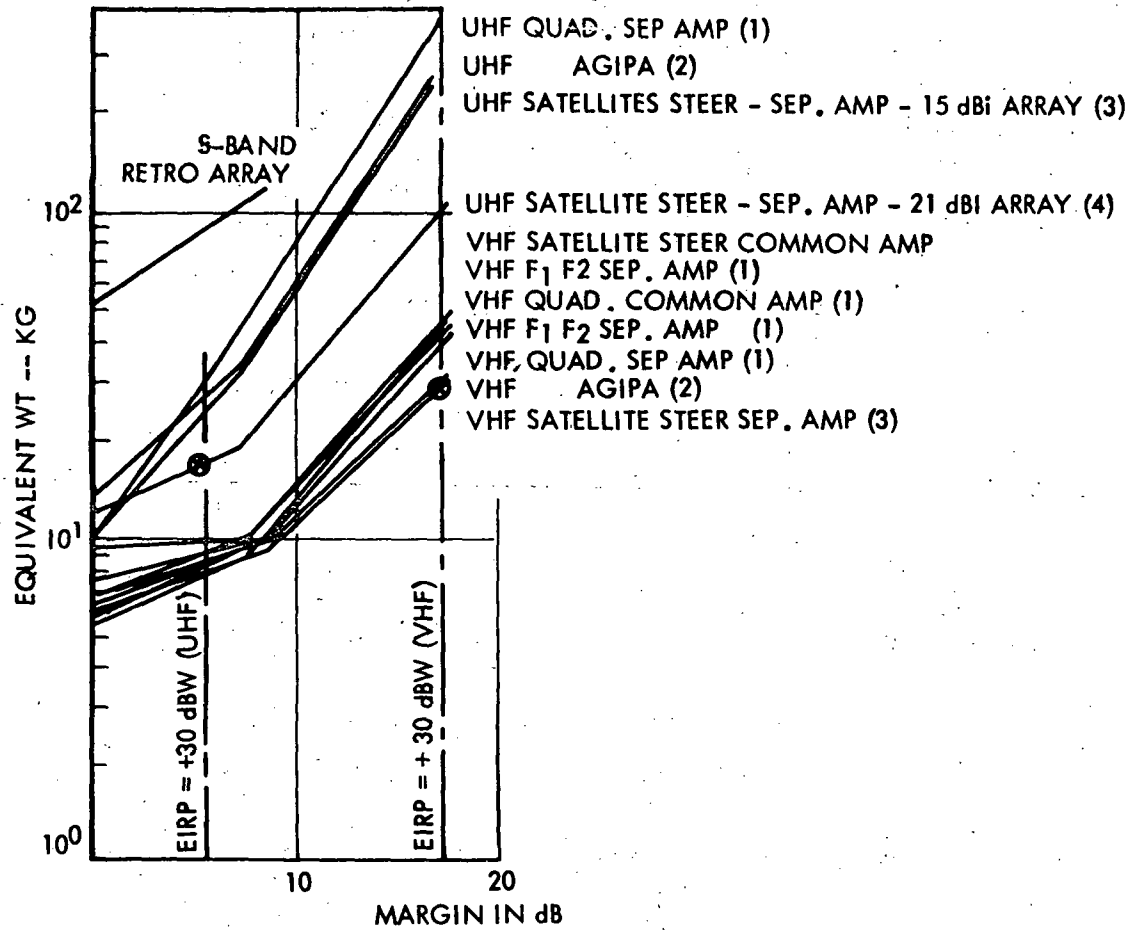


Figure 4-30. LDR Forward Link Transmitter Tradeoff



The curves show the most weight effective approach to provide the required ERP of +30 dBW is the high-gain satellite steered array operating at UHF. In summary, the advantages of operating at UHF are:

1. Wide channel bandwidth of 1 MHz
2. Reduced RFI levels requiring less system margin
3. Implementation of VHF/UHF TDRS antenna eliminates the difficult duplexing requirement at both TDRS and user
4. Ability to provide high TDRS antenna gain at UHF with small-sized elements

The particular implementation approach selected at UHF is a satellite-steered array using four high-gain (15 dB) elements, Figure 4-31. The selected approach is compatible with the VHF receiver array in that the spacing at VHF for 9 dB elements is close enough to that required at UHF for 15 dB elements so that the UHF elements can be co-located on top of the VHF element to mechanize the dual VHF/UHF approach.

Each element of the phased array is driven by a pair of power amplifiers whose sum develops a circularly polarized transmission. The two transmitted channels thus have orthogonal left-hand and right-hand polarizations. Phase shifting of the beam is accomplished at a low RF power level using digitally controlled varactor diode phase shifters. The controls are implemented via the command link for scanning the 9° (0.157 rad) beam over the 31° (0.54 rad) FOV.

4.3.1.3 LDR Transmit Power and Operational Considerations

The previous tradeoff considered the LDR transmitter power as a parameter of the study without selecting an operating point. Since the specification addressed only the VHF transmit power, the power at UHF is limited only by the IRAC/CCIR radiat-on flux density guidelines of -150 dBW/m² in a 4-kHz bandwidth. Calculations performed during this study show that an EIRP of +30 dBW spread over a 250-kHz bandwidth is the maximum power that the TDRS can generate on the LDR forward link and be consistent with the flux density constraint. The bandwidth selected corresponds to a 160 kcps chip rate and permits an operating configuration at UHF of four beams from two TDRS, each beam centered at a different center frequency using a common PN code. The LDR transmitter is, therefore, designed with a 1-MHz bandwidth and the frequency is controlled on the ground for any one of the four channels.

The transmitter output power for the +30 dBW limitation is $P_T = 30 - G_T = 30 - 18 = 12$ dBW per beam. For voice transmission, a push-to-talk mode of operation is recommended which is initiated either on the ground by keying the RF or by means of the TDRS command link. Since the transmitter design is Class C, the absence of an RF drive signal will power down the power amplifier and save satellite power. Using a duty cycle of 25 percent for the voice transmission, the ERP can be increased by 6 dB resulting in the same average dc power utilization. Therefore, each LDR beam is designed with a peak radiation capability of +36 dBW for voice, and +30 dBW for data.

4-57

SD 72-SA-0133

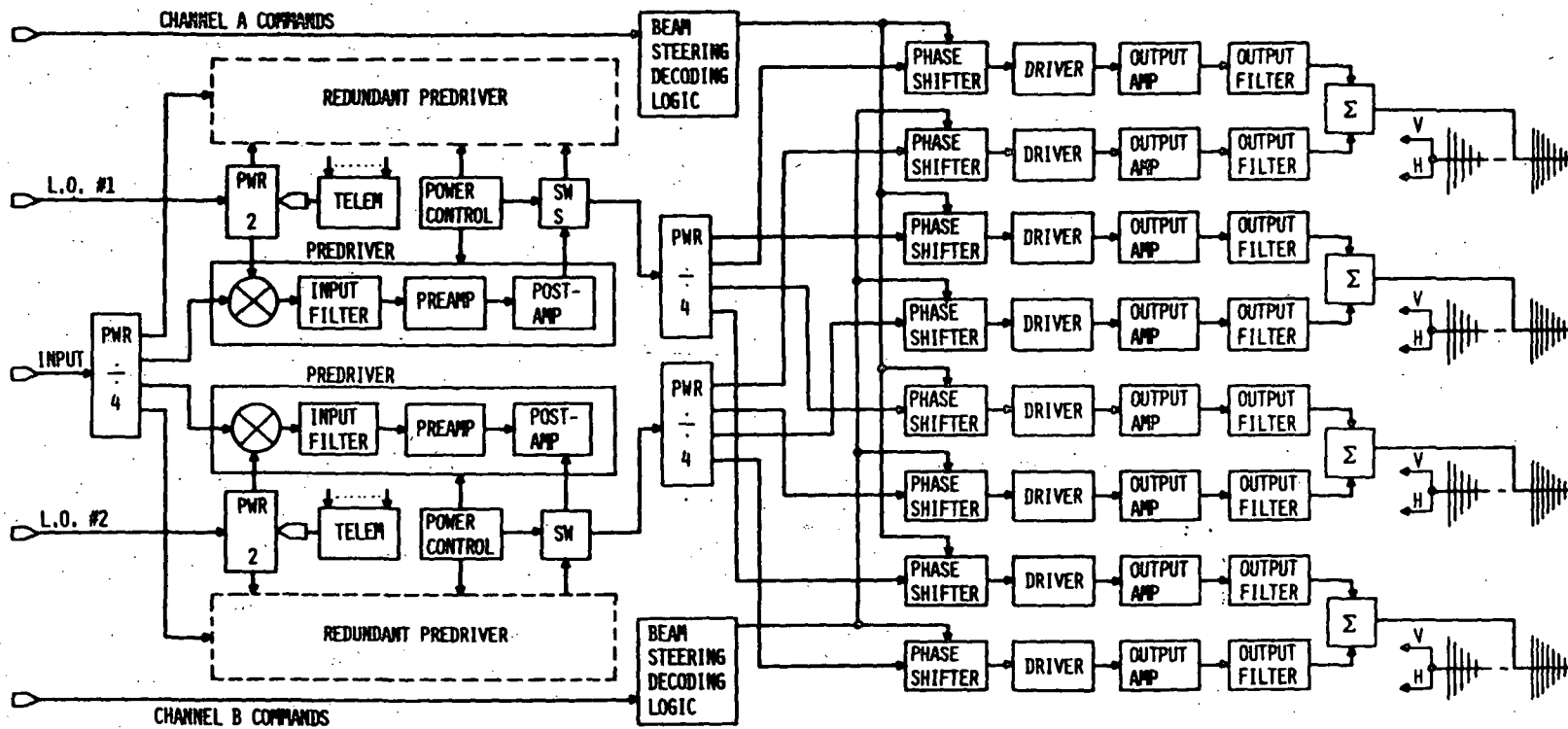


Figure 4-31. Block Diagram for UHF Satellite Steering-Separate Output Amplifiers



Long-term coherent tracking of many LDR vehicles requires simultaneous illumination of the entire FOV. This is accomplished by radiating from only one element of the array. For this mode the ERP would be +27 dBw on boresight and +24 dBw at the 31° (0.54 rad) FOV point. This mode could also be used to transmit a reduced command data rate to the users without steering the beam. Table 4-7 summarizes the design of the LDR transmitter demonstrating the flexibility and maximum utilization of TDRS capabilities in supporting LDR users, and Figure 4-32 compares the link performance versus RFI environment for both the steered array and the F-FOV approaches. The curves show the link performance at the peak of the beam and at its scan limits of 31° (0.54 rad). Even with the F-FOV approach, over 100 bps can be sent in a relatively high RFI power density of -165 dBm/Hz.

Table 4-7. LDR Forward Link Capabilities

- . Dual beam operation for transmission of either voice or data on each steered beam
- . ERP = +30 dBw for data on both steered beams
- . ERP = +36 dBw peak for 25% duty cycle push-to-talk voice channel on either one of the two channels
- . ERP = +24 and +25 dBw for simultaneous illumination of all users over a 30° (0.52 rad) and 26° (0.45 rad) FOV, respectively
- . Capability of two simultaneous voice beams, one high power (+36 dBw) and one low power (+30 dBw)
- . TDRS channel bandwidth of 1 MHz whose center frequency is controlled on the ground for handover and lockup purposes.

4.3.1.4 Recommended LDR Transceiver Approach

In the two previous subsections, the candidate LDR receiver and transmitter approaches were described and the results of approach versus relative weight tradeoffs are summarized in the matrix shown in Table 4-8. The trades indicate that the combination of the AGIPA for the receive function and a UHF ground controlled satellite steered array employing high gain (21 dB peak) quad array for the transmit function provide the most weight effective approach. Detailed performance analysis shows that the F-FOV will not meet the link requirements in the presence of RFI.

Therefore, in summary, the recommended design for the LDR transceiver from the performance and hardware implementation viewpoint is the AGIPA on receive and the ground-controlled satellite steered array on transmit. A functional block diagram of the recommended LDR transceiver is shown in Figure 4-33. Subsequent sections describe the mechanization tradeoffs and details of this recommended design.

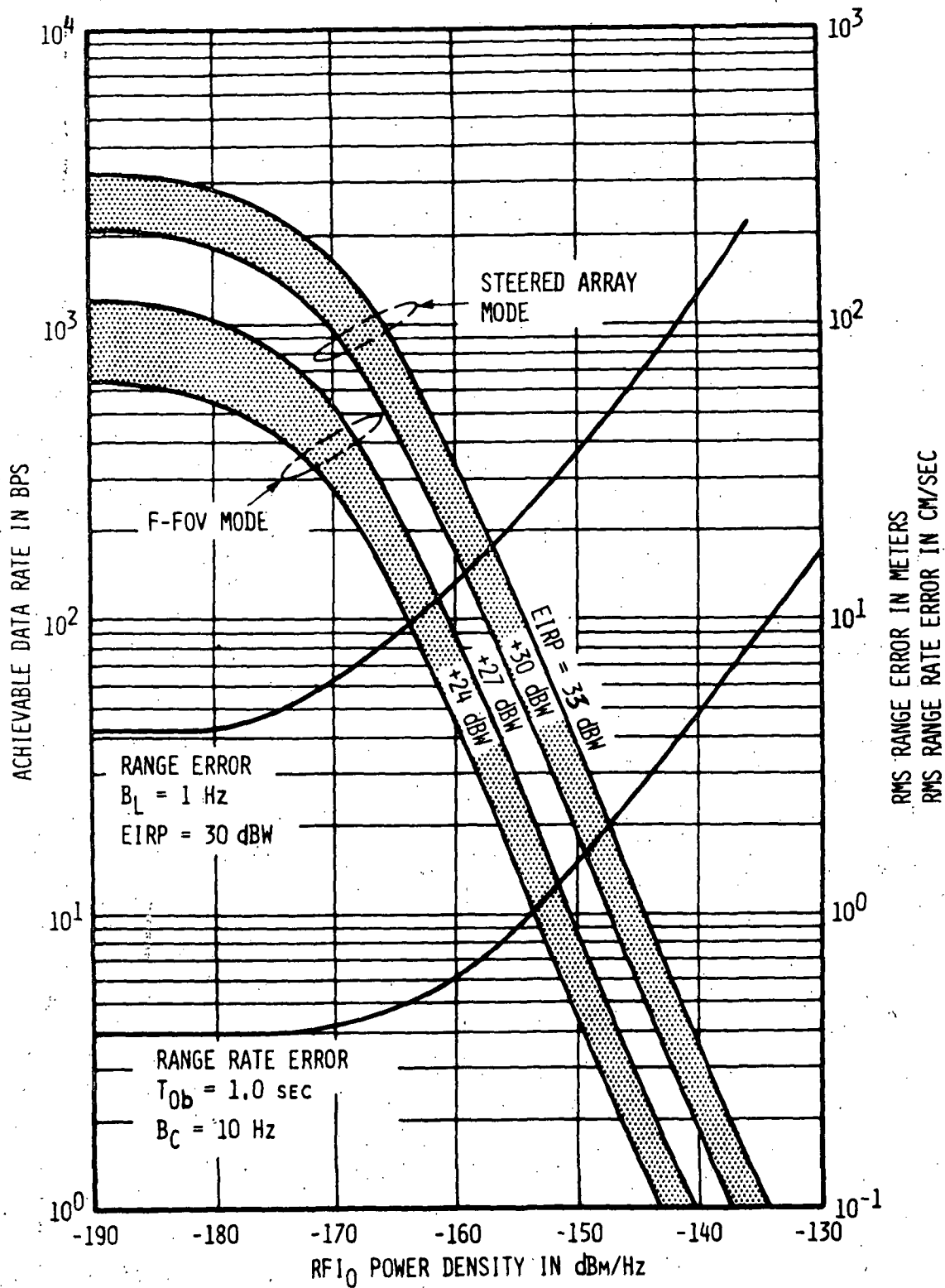


Figure 4-32. LDR Forward Link Performance Achievable Data Rate; Range Error and Range Rate Error

Table 4-8. Comparison of Candidate LDR Transceiver Approaches

Transmitter \ Receiver	Equivalent Weight *			
	F-FOV		AGIPA	
	Lb	Kg	Lb	Kg
1 - F-FOV				
VHF	110.0	49.9	108.0	49.0
UHF	71.0	32.2	69.2	31.4
2 - AGIPA				
VHF	80.2	36.4	78.5	35.6
UHF	64.2	29.1	62.6	28.4
3 - Satellite Steered Array				
VHF	78.2	35.5	76.5	34.7
UHF	55.6	25.2	53.9	24.5
4 - S-Band Retrodirective Array	161.0	73.1	159.0	72.2

Parameter	VHF	UHF	S-Band
ERP, dBw	30.0	30.0	41.0

*Does not include antenna but includes weight of trans. & power supply

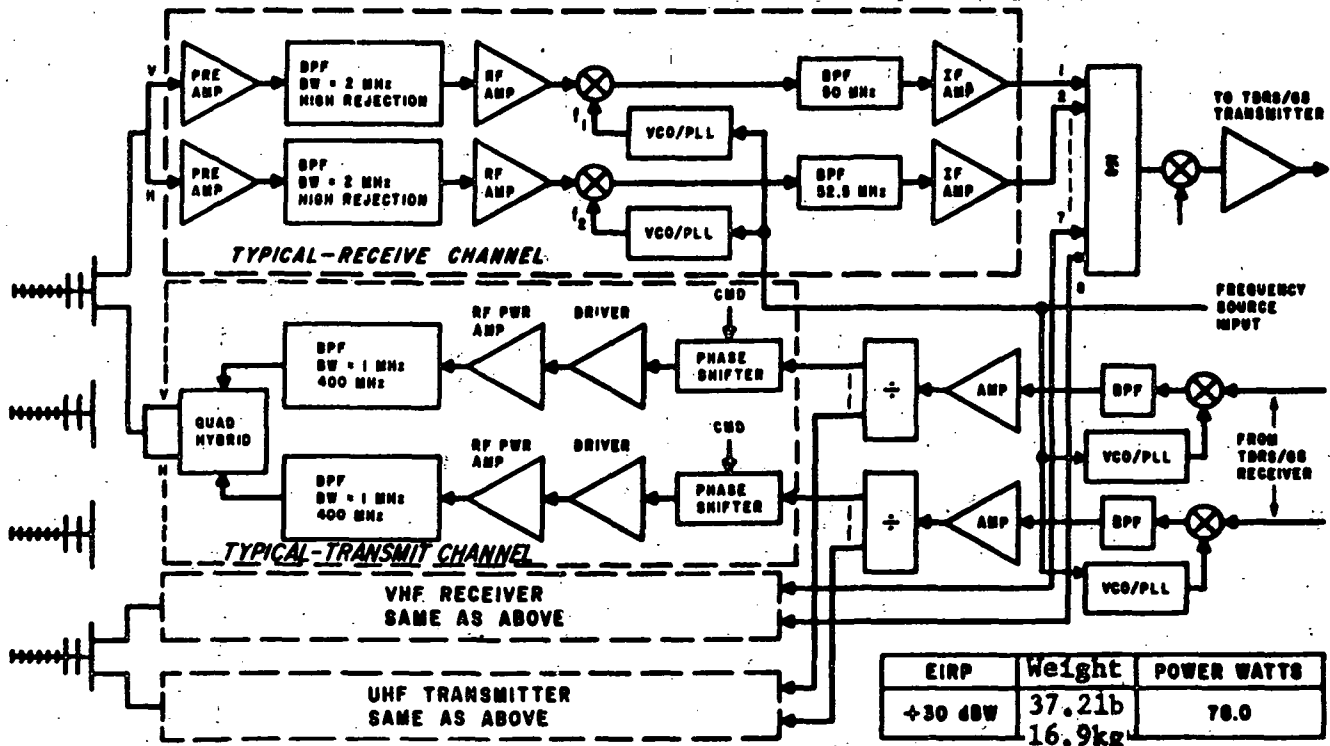


Figure 4-33. Recommended Dual Frequency LDR Transponder



4.3.2 LDR Antenna

4.3.2.1 Mechanization Trades

Link tradeoff analyses have shown that the requirements of this link can be optimally met by operating the link at VHF for the return link and at UHF for the forward link. S-band was discarded for use in the forward link due to the large implementation impact for the Part I phase. For these antenna trades, antenna array designs were considered for both the F-FOV and AGIPA approaches. Both F-FOV and AGIPA approaches use the same quad-array designs, providing a HPBW of 24° (0.42 rad) and peak array gain of 16.8 dBi.

In the initial tradeoff considerations for the LDR antenna, various element designs as shown in Table 4-9 were examined for relatively broad band operation in the VHF band (117.55 to 149.9 MHz). These elements were evaluated for use in the F-FOV and AGIPA (phased array) approaches. For these approaches the disc-on-rod surface wave structure provided the desired performance and the physical characteristics for compact storage during launch.

Subsequently, the scope of the LDR link was expanded to evaluate VHF in the return link but UHF and S-band in the forward link; however, the operational frequency bandwidths in the return and forward links were relatively narrow (less than a few percent). This change in direction opened up other element possibilities as identified in Table 4-10, including broadband devices such as the log periodic, and combination of individual narrowband elements operating at the two candidate frequencies which were previously eliminated for broadband use. The results of the trades demonstrate that a quad-array of backfire UHF elements collinearly stacked on the quad-array of VHF backfire elements as shown in Figure 4-34 provides the desired performance capability. The resultant characteristics of this dual frequency VHF-UHF configuration are shown in Figure 4-34.

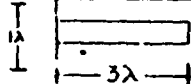
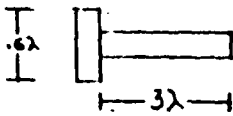
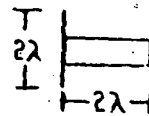
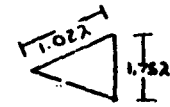
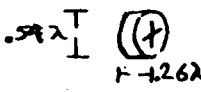
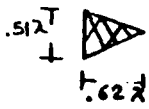
4.3.2.2 Detailed Design-LDR Antenna

The LDR frequencies have been assigned as follows:

Receive	VHF	136 to 138 MHz
Transmit	UHF	400.5 to 401.5 MHz

The selection of these narrowband operating frequencies made the consideration of yagi surface wave structures feasible. A prime advantage of disc-on-rod structures (wide bandwidths relative to yagi structures) was, therefore, minimized. The optimum configuration of a backfire element was selected providing the advantage over a disc-on-rod structure of reducing the axial length by a factor of three at the expense of nearly doubling the ground plane diameter. This reduction of axial length reduces the LOS blockage between antennas. Each antenna element operates at both UHF and VHF. The dual frequency VHF/UHF backfire array design is shown in Figure 4-34.

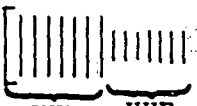


Table 4-9. Summary of Candidate LDR Antenna Configurations

Element Type	Nominal Bandwidth	Dual Freq. Operation 117 to 144 MHz	Polarization Diversity Capsule	Dual Freq. Operation 140 & 400 or S-Band	Number of Elements Req'd for 31° (0.54 rad) HP BW	Element Envelope (λ) Wavelengths	Comments
Helix	1.6:1	Yes	No	No	1		Does not provide polarization diversity
Disc-on-rod	1.3:1	Yes	Yes	No	1		Provides reasonable bandwidth and does not have critical alignment problems compared to a yage
Backfire yagi structure	1.1:1	No	Yes	No	1		Requires relatively large (2λ) ground plane reflector, also narrow band
Conical horn	≈2.0:1	Yes	Yes	No	1		Relatively large aperture - gain is 3 db lower than above elements
Cavity backed dipoles	1.3:1	Yes	Yes	No	7		Requires an array of seven elements to provide 15 db gain
Yagi	1.1:1	No	Yes	No	1	Same as disc-on-rod	Has a relatively narrow bandwidth
Log periodic	≈10:1	Yes	Yes	Yes	5		Requires an array of five elements to provide 15 db gain

4-62

SD 72-SA-0133

Table 4-10. Dual Frequency LDR Antenna Consideration

Parameter	Element Type		
	Co-Linear Disc-on-Rod	Co-Linear Backfire	Log Periodic
Configuration			
Element peak gain, dBi			
VHF	9.0	10.8	8.0
UHF	9.0	15.0	8.0
Quad array peak gain, dBi			
VHF	15.0	16.8	14.0
UHF	15.0	21.0	14.0
Comment	Total length becomes long.	Short backfire design permits high gain UHF antenna to be used. Design convenient for stowable configuration.	Low element gain makes antenna design undesirable.

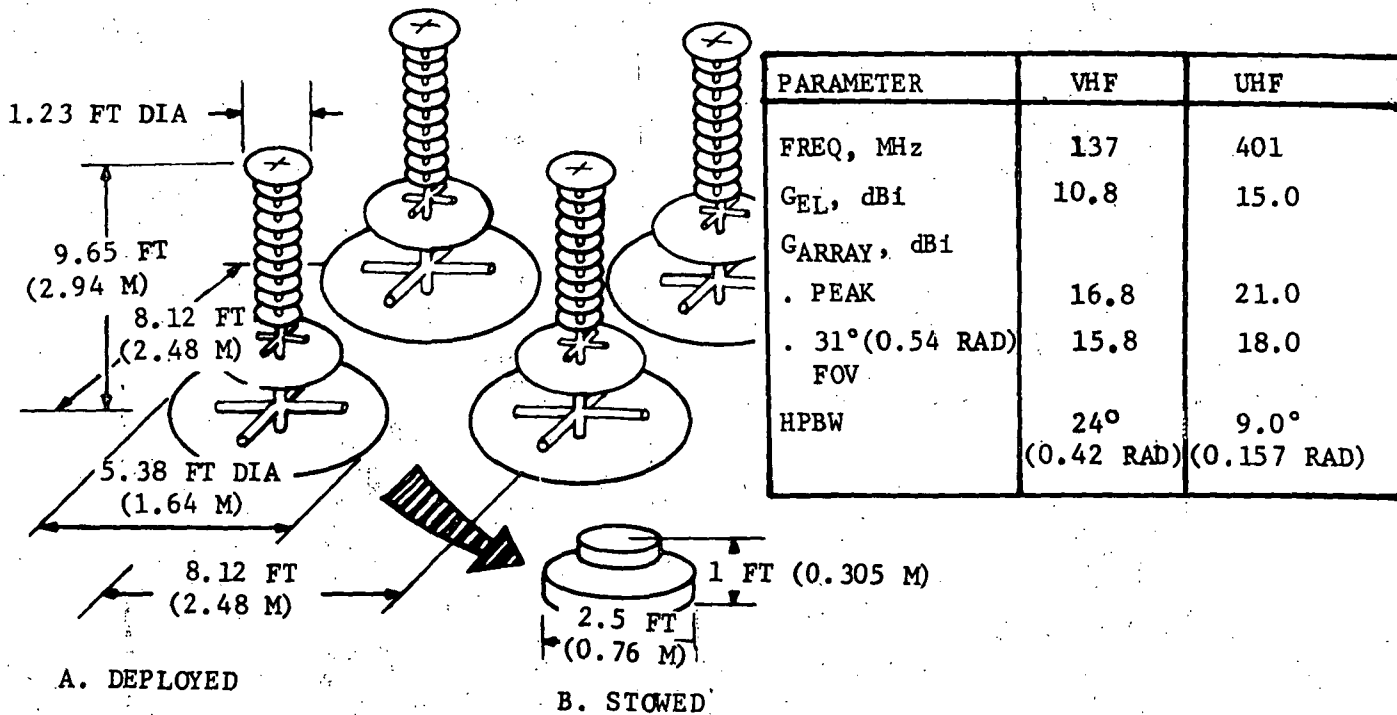


Figure 4-34. Dual Frequency (VHF-UHF) LDR Antenna

Antenna Element Design. The requirement of providing nominal gains of 9 dBi at VHF and 15 dBi at UHF with minimum length elements and narrow frequency bands of operation suggested the backfire antenna design. The design was optimized with the VHF structure having a length of $\lambda/2$ and a main reflector diameter of λ . The UHF element is placed in front of the VHF structure and has a length of 2λ and main reflector diameter of approximately 1.5λ .

The work of L. Dod* presents data for backfire antennas, but requires:

1. Extrapolation of data to provide gain information for a 1λ diameter main reflector
2. The assumption that the UHF element placement in front of the VHF element would not deteriorate VHF operation

To confirm these assumptions, a scale model was fabricated and tested. This antenna (operating at a scale frequency of 2400 MHz) consisted of an active backfire antenna representing the VHF antenna firing through a mock-up of the UHF antenna. The full-scale dimensions of this antenna (center frequency VHF equals 137 MHz, UHF equals 401 MHz) are shown in Figure 4-35 (Scale A). The UHF portion of the antenna was represented with metal disc elements. The VHF main reflector is 1λ in diameter and the smaller VHF reflector (also the main reflector for UHF) was optimized (for maximum VHF gain) as 0.43λ VHF or 1.25λ at UHF. This arrangement provided the following gain/beam-width data:

Test Frequency MHz	Scale Frequency MHz	Gain dBi ₁	Half Power Beamwidth degrees	
			E-Plane	H-Plane
2300	131	9.0	48	59
2350	134	9.1	45	56
2400	137	9.0	45	54
2500	143	8.9	43	53
2600	148	7.8	42	49

The center frequency E- and H-plane radiation patterns are presented in Figure 4-36. Sidelobe levels are 14 dB and the back lobe is approximately 13 dB. The gain measurements made above have been added to published data* and this summary is shown in Figure 4-37. To achieve the 9 dBi gain with a 1λ diameter reflector at VHF it was necessary to reduce the secondary reflector diameter to 0.43λ . This results in a UHF main reflector diameter of 1.25λ . Figure 4-37 indicates (through extending the 2λ curve) that the UHF gain would

* "Backfire Antennas for Telemetry and Tracking Applications", L. Dod, Goddard Space Flight Center, NTC Record, 1969.

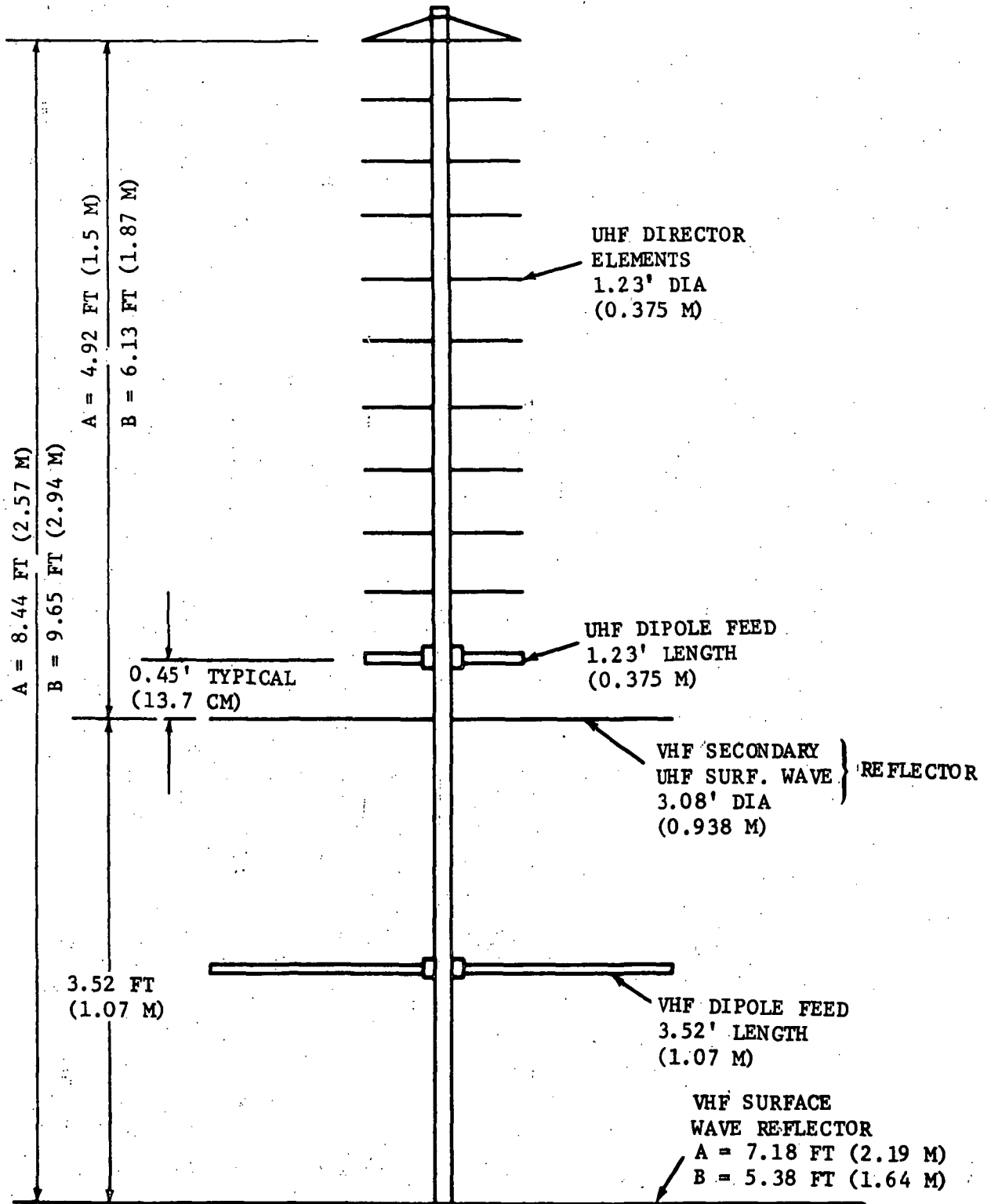


Figure 4-35. VHF/UHF Backfire Antenna Dimensions

4-66

SD 72-SA-0133

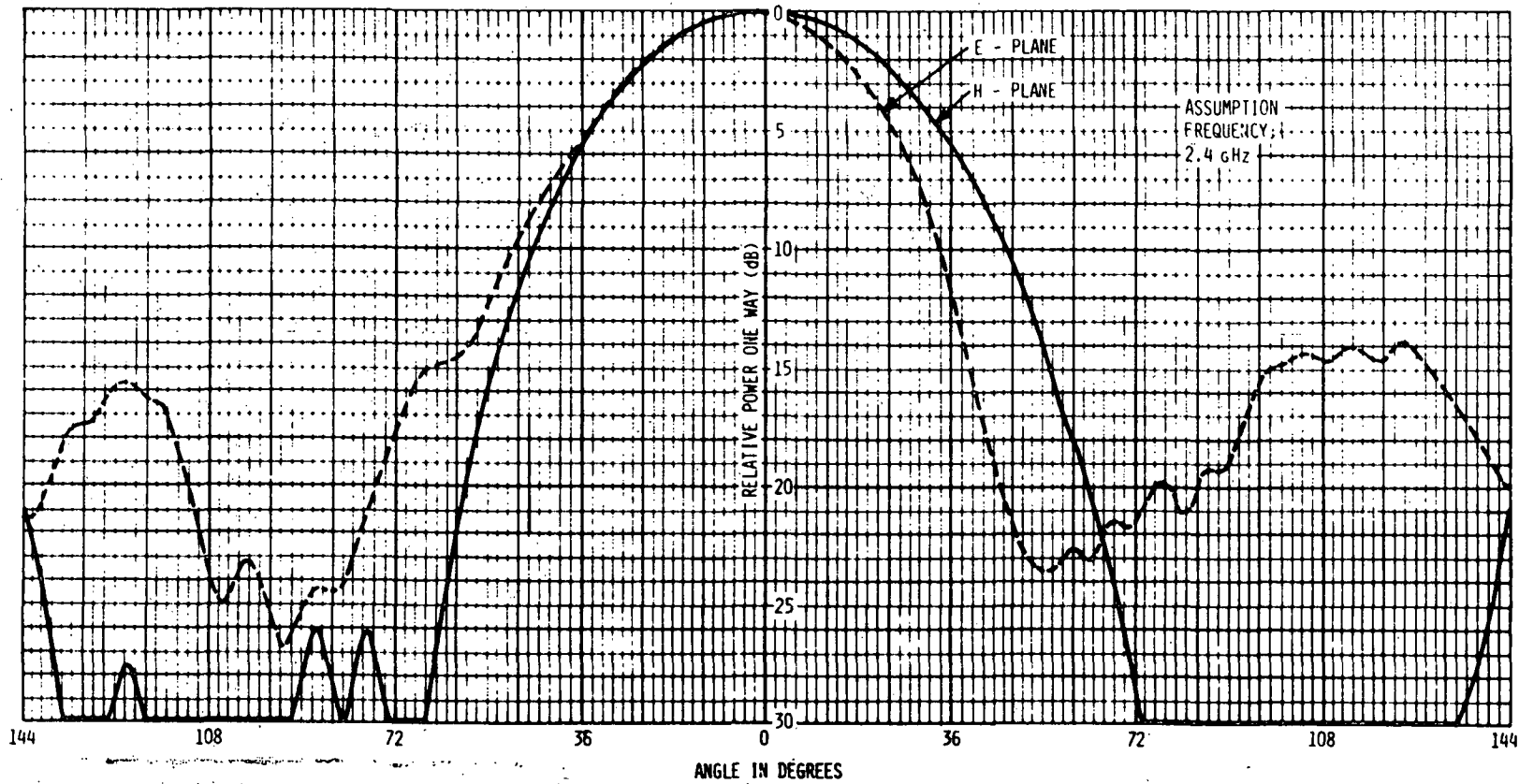


Figure 4-36. VHF Backfire Antenna Patterns

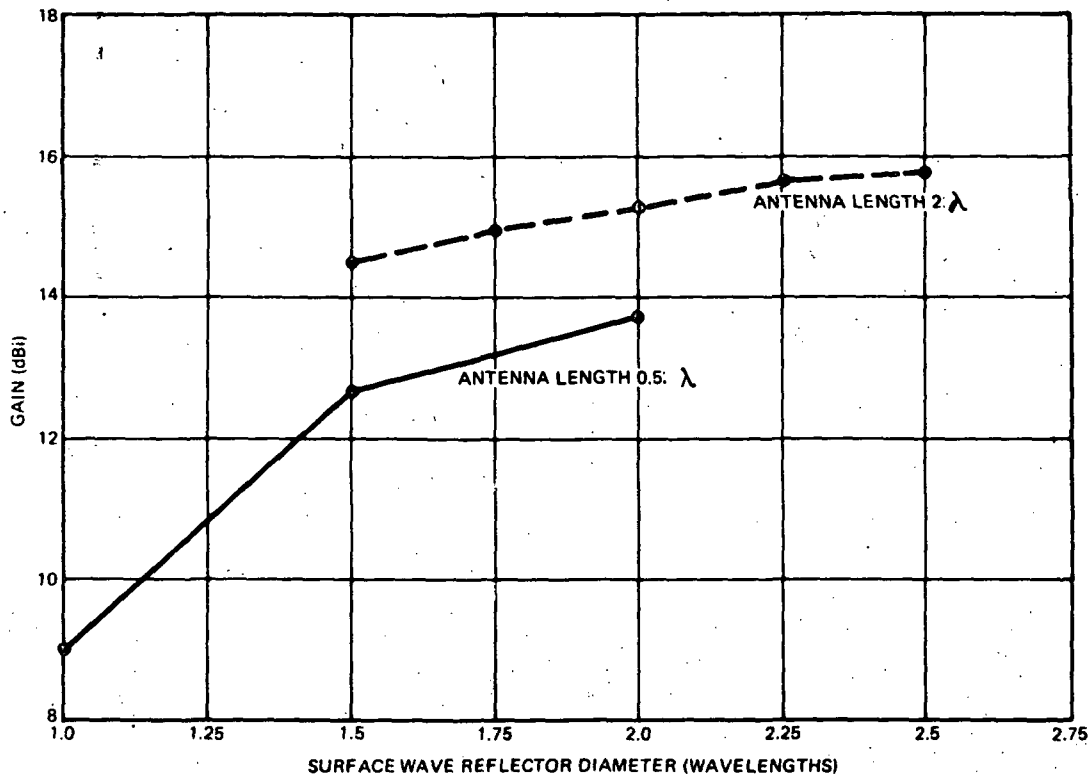


Figure 4-37. Backfire Antenna Gain Curves as a Function of Large Reflector Diameter

be approximately 14 dBi. This gain can be optimized at a single UHF frequency through experimental tailoring of the element lengths and secondary reflector diameter to achieve the desired UHF gain of 15 dBi. NASA-GSFC (L. Deerkowski) has also studied this co-linearly stacked (VHF/UHF) backfire design. These empirical results show that the VHF short backfire element can meet the desired performance characteristics with a ground plane diameter of 0.75λ rather than 1λ and provides peak element gain of 10.8 dBi. However, these data indicate that the UHF element must be approximately 1.21' (.37 m) longer, requiring two additional disc elements to achieve the desired 15 dBi peak element gain. The GSFC results confirm the need for additional element length at UHF. The resultant element design parameters are also shown in Figure 4-35 as Scale B. These new dimensions were included in the spacecraft layouts and in the antenna design.

Quad Array Considerations. The nominal 10.8 dB gain of the VHF antenna elements results in an element spacing between the phase centers of 6.4' (1.95 m) per side of a square array when the spacing considerations are determined by the condition that the effective area of the antenna elements shall not overlap. This calculation (based on $\text{Area (eff)} = G\lambda^2/4\pi$) would result in physical interference of the main reflectors. Increasing the spacing to 8.1' (2.47 m) (element separation based on an 11 dBi gain) prevents physical interferences of the ground planes and improves element-to-element isolation. Drawing an analogy



that the backfire antenna with orthogonal feeds and 10.8 dBi gain is similar to cavity-backed spiral, the coupling between elements for the 8.1'(2.48 m)(1.13 λ) spacing is estimated in the order of 30 dB. This estimate is with the 90°(1.57 rad) aspect angle power level 19 dB below the peak of the beam as shown in Figure 4-36. The 30 dB coupling results in a maximum gain error at the peak of the beam of 0.3 dB.

4.3.3 LDR Transponder

4.3.3.1 LDR Mechanization Trades

A functional block diagram of the LDR transponder was shown previously in Figure 4-33 and includes an eight-channel AGIPA and an eight-channel ground-controlled satellite steered LDR transmitter. Tradeoffs involved in each are described herein.

LDR Receiver Mechanization Trades. The mechanization trades in the LDR receiver are based primarily on the selection of techniques which provide adequate channel isolation and sensitivity to operate with signals which are buried below the level of expected RFI levels. A summary of these trades and the resultant recommendations are shown in Table 4-11.

LDR Transmitter Mechanization Trades. There are two types of signals being transmitted: (1) PSK data at 5 w cw per channel and (2) emergency voice with a 25 percent duty cycle which requires 20 w peak or 5 w average. For example, if the transmitter output stage is configured to provide a 20-watt peak capability but only has enough heat sink to handle a one-fourth duty cycle, then its output transistor must handle 22.8 w peak voice and 5.68 watts PSK cw. These two signals cannot be sent through the same amplifier with equal efficiency. There are three possibilities for a practical transmitter which are summarized in Table 4-12; and the recommended approach (as shown) is to design for 22.8 watts peak and reduce B+ voltage for reduced power operation.

4.3.3.2 Detailed Description of the LDR Transceiver

A functional block diagram of the LDR transceiver is shown in Figure 4-38. On receive, an eight-channel receiver is used to linearly translate both orthogonal components of the VHF quad array, and combined at a low baseband frequency (FDM) in the IF Summing Network for subsequent frequency modulation (FM) in the TDRS/GS transmitter.

On transmit, two independent forward links must be formed. The signal for each forward link is divided in the LDR transmitter divider network to feed the quad array. Since the beam is electronically steered, phase shifters are employed in each channel, prior to amplification in the LDR UHF transmitter assembly. Since there are two forward beams to be formed, a total of eight channels (four channels for each link) are required in the LDR transmitter.

Table 4-11. Summary of LDR Receiver Tradeoffs

Parameter	Tradeoffs	Recommendation
Receiver type	Superheterodyne - one versus two conversion	Superheterodyne used to provide good separation between 8 channels; double conversion used for good rejection of spurs
RF front end	Transistor preamp versus mixer	Transistor used to provide 1 dB noise figure for operation with negative SNR
RF filter	Filter before or after RF preamp	RF filter used after RF preamp to optimize noise figure; remaining filtering done after preamp
AGC	Usefulness of AGC in RF front end	AGC not used in RF preamp since RFI is greater than signal. AGC used after IF summing to maintain constant input to TDRS/GS transmitter
Design approach	Discrete versus integrated	Integrated approach used wherever practical to minimize size and weight

4-69

SD 72-SA-0133

Table 4-12. Summary of LDR Transmitter Tradeoffs

Parameter	Tradeoffs	Recommendation
Power amplifier	<p>Design for peak voice and absorb added inefficiency of cw operation</p> <p>Switch in 6 dB amplifier for voice operation</p> <p>Design for peak voice of 22.8 watts and reduce B+ voltage for 5.68 watts cw operation</p>	<p>Design for peak of 22.8 and reducing the B+ voltage provides the optimum approach with minimum impact on power consumption</p>

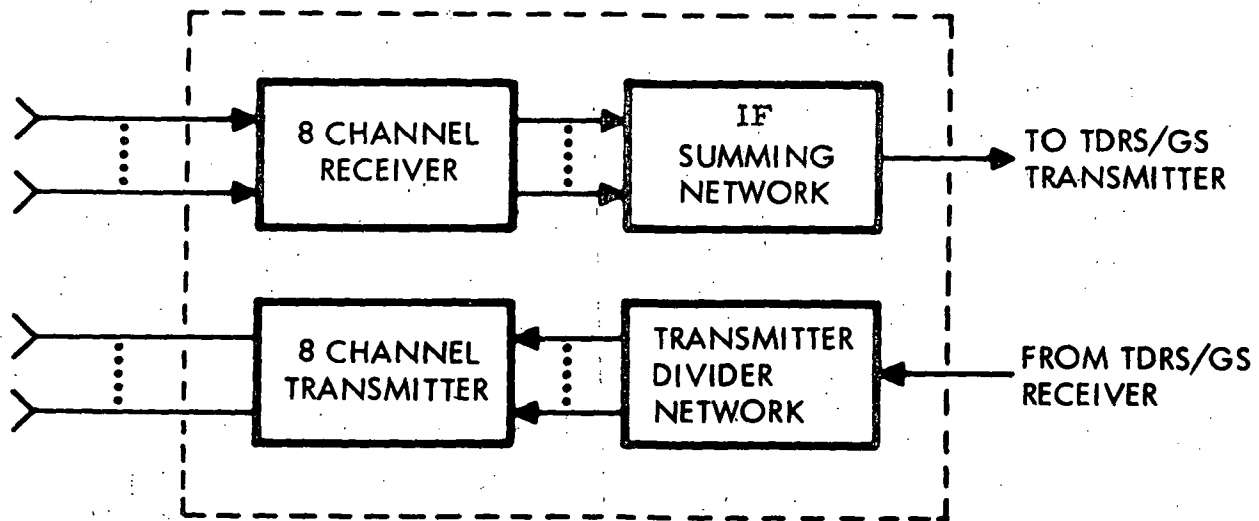


Figure 4-38. Functional Block Diagram of LDR Transceiver

LDR AGIPA Receiver and IF Summing Network. Two channels of the LDR AGIPA receiver eight-channel superheterodyne receiver are shown in Figure 4-39. Eight individual signals received at 137 MHz are down converted to individual IF's ranging between 50.5 MHz and 68.0 MHz. The overall IF spectrum of 19.5 MHz is then down converted to a baseband spectrum of 17 MHz to 34.5 MHz. This spectrum then is used to modulate the TDRS/GS transmitter.

Signals are received at a power level of -92 dBm at the input to the RF preamplifier. The design features a two-stage device using discrete transistors such as the 2N5650. The amplifier will be tuned to 137 MHz to optimize noise figure (1 dB) and gain (25 dB) as well as relieve the rejection requirement of the bandpass filter following the preamp. This design provides an overall device noise figure of approximately 1.0 dB with a total gain of 25 dB. The effective system noise figure is less than 2.0 dB, including second stage N.F. contributions and cable losses to the antenna. The maximum preamp output level is -55 dBm on 40 RFI peaks. The equivalent receiver noise input level is -109 dBm. A low pass filter is employed to keep the LDR transmitter power leak through in the linear region.

The signal is then (137 MHz) bandpass filtered to eliminate out-of-band signals and noise. Since the RF preamp is well within its linear region for all signals and noise, the filtering is performed after the preamp without loss of effectiveness. This configuration permits higher filter loss without sacrifice of noise figure. This approach simplifies the filter design with corresponding savings in size and weight. A six-pole lumped constant filter design having a linear phase characteristic and approximately a 3 dB insertion loss is used. Its bandwidth together with the other filters will produce a total link bandwidth of 2.0 MHz.

The RF amplifier will consist of two MIC amplifiers and deliver most of the overall receiver gain. The 1 dB compression point is approximately +2 dBm (maximum RFI level) which minimizes intermodulation products. The noise figure of this amplifier is not critical since system noise is established by the RF preamp.

The mixer will be a double-balanced plug-in type suitable for integrated operation in hybrid circuits. The mixer operates with +10 dBm L.O. drive to minimize conversion loss, signal compression and intermodulation distortion on RFI levels up to +2 dBm. Each mixer in the eight channels operates with different L.O. frequency to produce different IF's for each channel.

From the mixer the signal is fed to the bandpass filter. Each channel will have a separate IF ranging between 50.5 MHz and 68.0 MHz, a range selected for minimum filter size. This, in effect, takes the eight channels of information and places them into a spectrum 19.5 MHz wide. The channels are 2 MHz wide with 2.5 MHz center frequency separation. Each filter exhibits 6 dB insertion loss and provides 30 dB rejection at adjacent channel center frequencies. Lumped constant designs are used with components mounted directly on the same printed circuit board as the rest of the receiver. Compartmentalized construction is used to assure adequate RF isolation.

4-72

SD 72-SA-0133

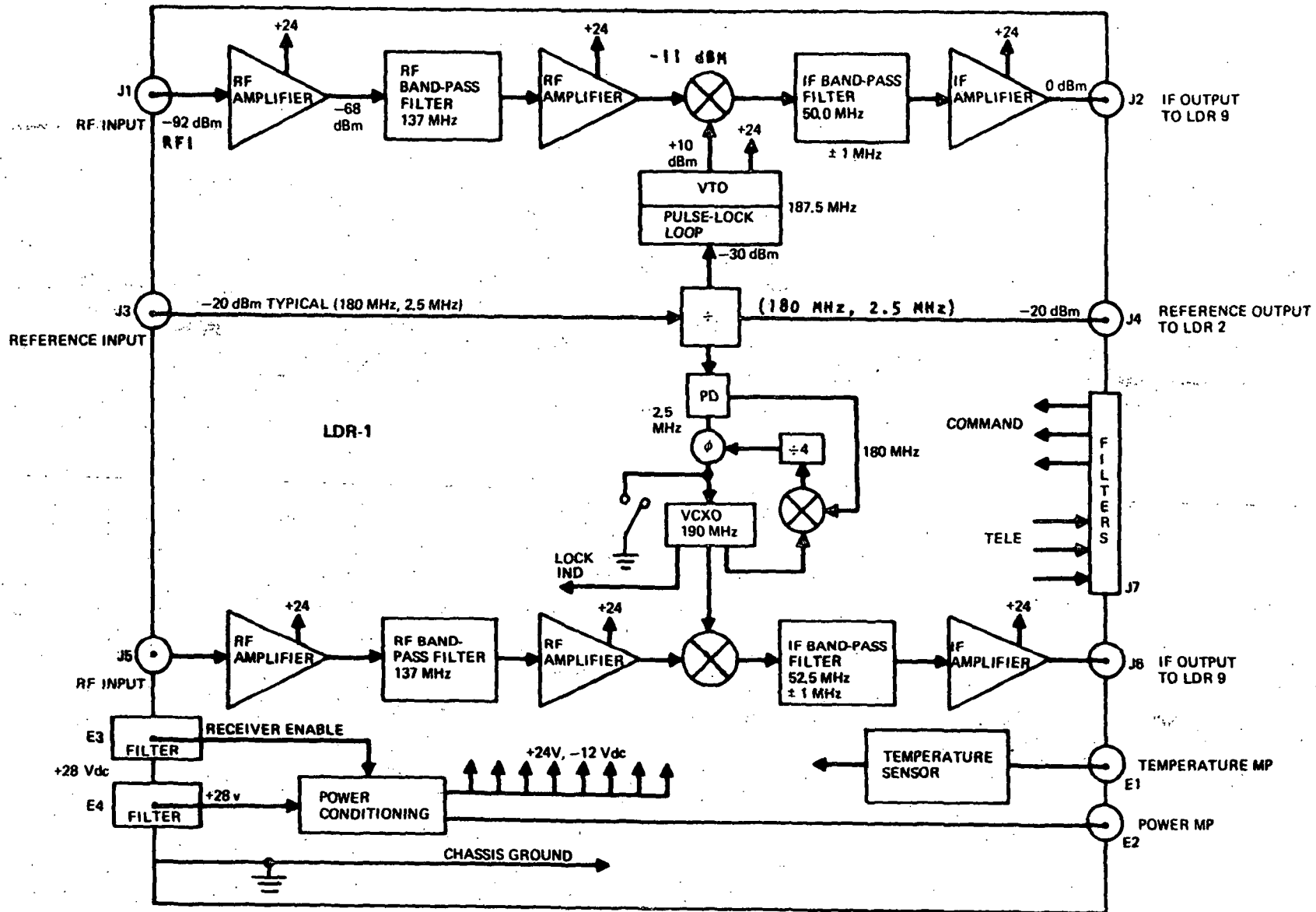


Figure 4-39. LDR Receiver Block Diagram

After filtering, the eight IF signals are amplified and summed together as shown in Figure 4-40. The function of this circuit is to combine the individual IF spectrums into a single output. Each IF signal receives a single stage of amplification (15 dB) and is resistively added into a common load. Pre-emphasis of the channels is performed in this unit. After summing, the IF signals are fed to the second mixer.

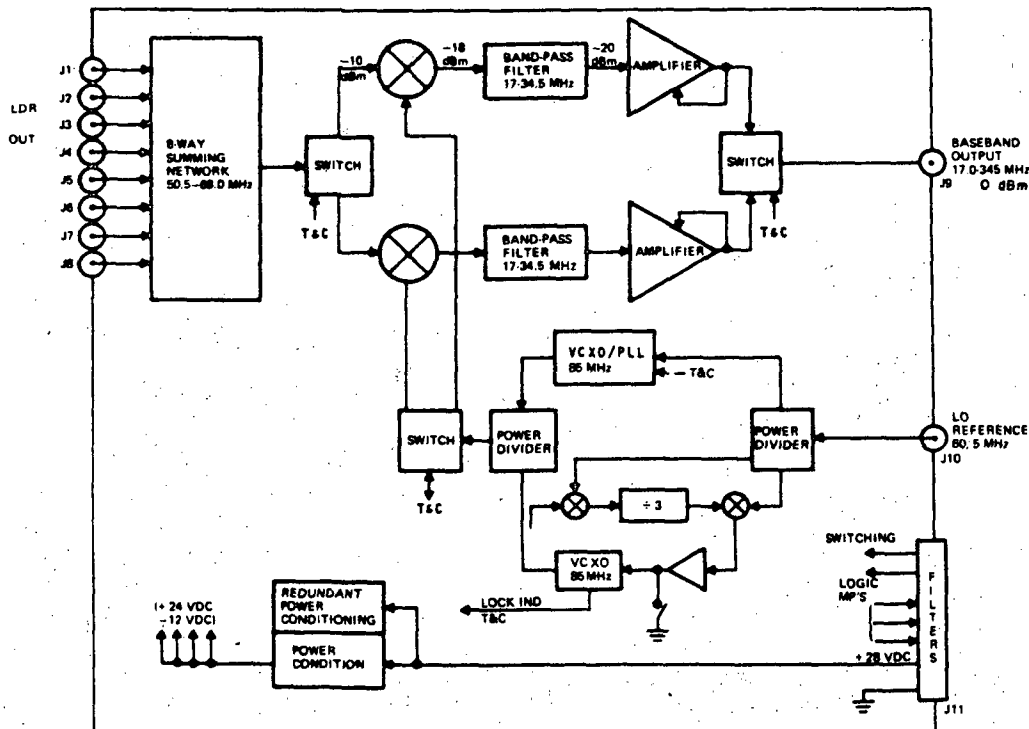


Figure 4-40. LDR Summing Network

The combined IF spectrum is down converted to a baseband of 16.5 to 35 MHz. This is achieved by mixing the 50.5 to 68.0 MHz band with a 85.0 MHz L.O. at +10 dBm producing the desired spectrum while maintaining linearity. After down converting to baseband the signal is filtered and amplified. The gain is sufficient to bring the RFI level to approximately -10 dBm before being fed to the TDRS/GS transmitter.

Since the receiver output level can change 26 dB, the last amplifier provides 26 dB of AGC range. The actual device gain is controlled from +14 to -12 dBm using pin diode attenuators. The amplifier is a linear integrated type with a 1 dB compression point of about +5 dBm. The second IF bandpass filter is lumped constant to reduce out-of-band noise. This portion of the LDR receiver is common to all eight receiver channels, and in order to maintain high reliability a redundant mixer amplifier and filter is used.



Due to the unique nature of the AGIPA principle, redundancy is not needed in each receiver. AGIPA redundancy is inherent in the fact that the eight channels are all handling essentially the same information. Loss of a channel merely reduces the resolution achievable in beam forming and in no way constitutes a catastrophic failure. The summer and second IF, which is common to all eight channels, will be 100 percent redundant.

Figures 4-41 and 4-42 show a layout of the recommended LDR receiver and IF summing network, respectively.

LDR UHF Transmitter Divider. The LDR-10 transmitter divider accepts the IF outputs of the TDRS/GS receiver, frequency source reference outputs and beam steering data. It provides four output signals at 401 Mz phase locked to the reference, with the proper phase shifts between the output signals to form a steerable antenna pattern when amplified and applied to the UHF antenna array.

As shown in Figure 4-43, the divider unit consists of two channels, 56 and 66 MHz, IF frequency inputs, each containing redundant phase lock loop local oscillators and mixers. The selected mixer output is divided four ways with in-phase hybrids and applied to varactor controlled hybrids to obtain the required 0 to 318.4-degree phase shift required for beam steering. Beam steering data is derived from seven-bit serial data applied to a seven-bit shift register controlling a 49-word, 16-bit-per-word, read only memory (ROM).

The phase locked local oscillator contains a voltage tunable crystal oscillator (VTCXO) with frequency multiplication to provide a +13 dBm signal at either 340 or 335 MHz. The output is split in a 3 dB hybrid and applied to the signal mixer and a mixer accepting the 360 MHz reference from the frequency source. The 15 or 25 MHz mixer output is amplified and drives a divider by 3 or 5 counter, whose output is applied to another mixer accepting a 5 MHz reference from the frequency source. This mixer output represents the phase error signal which is then amplified and filtered and applied as the control signal to the VTCXO to form the phase locked loop. The pulling range of the oscillator is as wide as required to overcome the frequency instability of the crystal oscillator over the operating temperature range which is typically 20 ppm, 7 kHz. Each oscillator may be commanded to run open loop by application of a signal ground to VTCXO control signal input. Telemetry monitoring points showing position of command and lock indication are provided for each phase locked loop and also indicates which phase locked loop and mixer assembly is in use.

The 0 dBm, 56 and 66 MHz, IF signals from the TDRS/GS receiver are split in two-way power dividers and mixed with the 4 L.O. outputs to provide the 401 MHz RF signals. The outputs of the redundant channels are selected with a latching relay, split four ways and applied to varactor-controlled hybrid phase shifters. The four outputs at a -20 dBm level are applied to the LDR5 through LDR9 transmitters through equal lengths of coax cable to maintain the proper phase relationship. The phase shifters have uniform phase shift with voltage characteristics and are mounted in one location so that the phase of each signal will track with changes in mounting plate temperature.

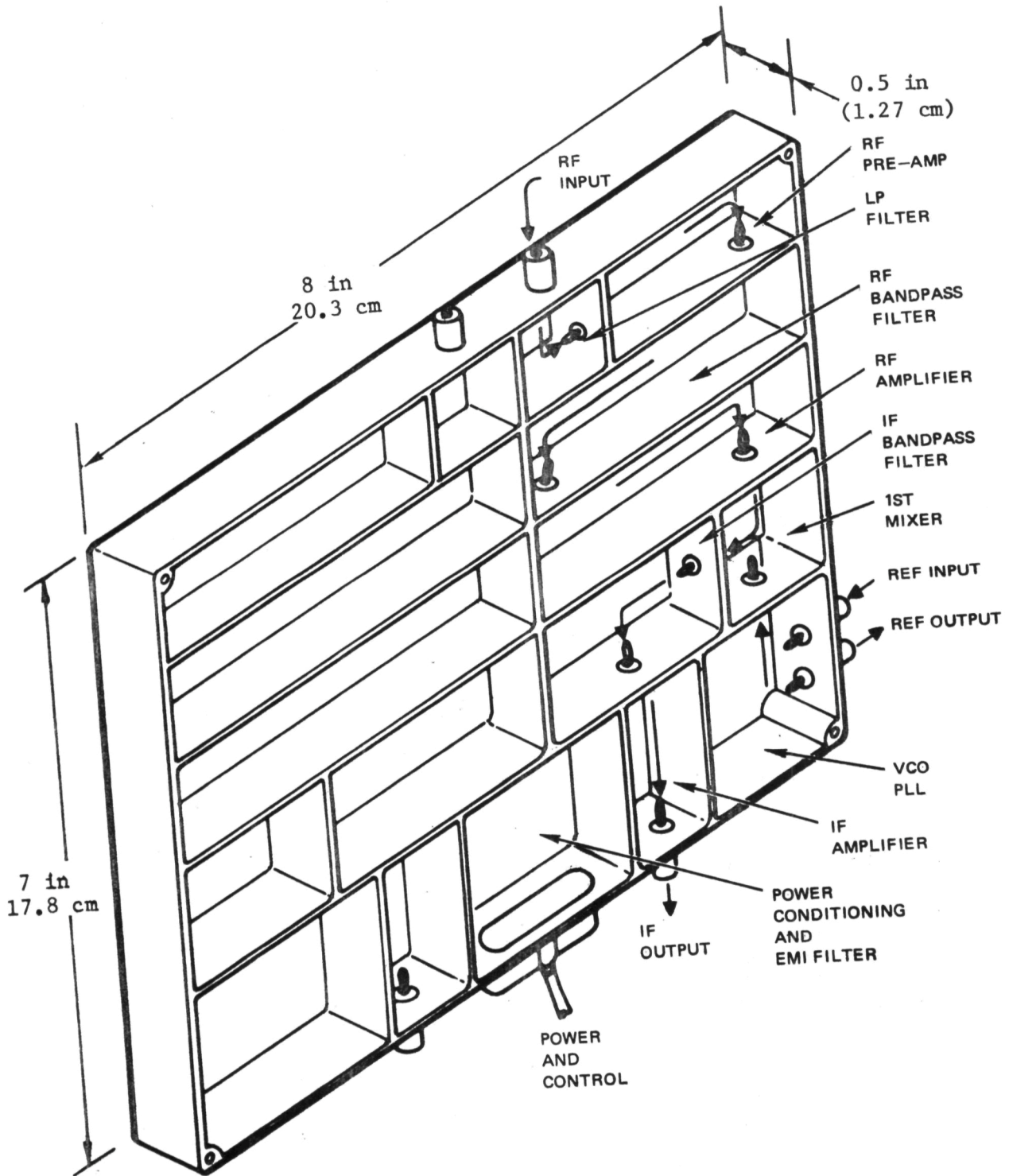


Figure 4-41. LDR Receiver (Two Channels)

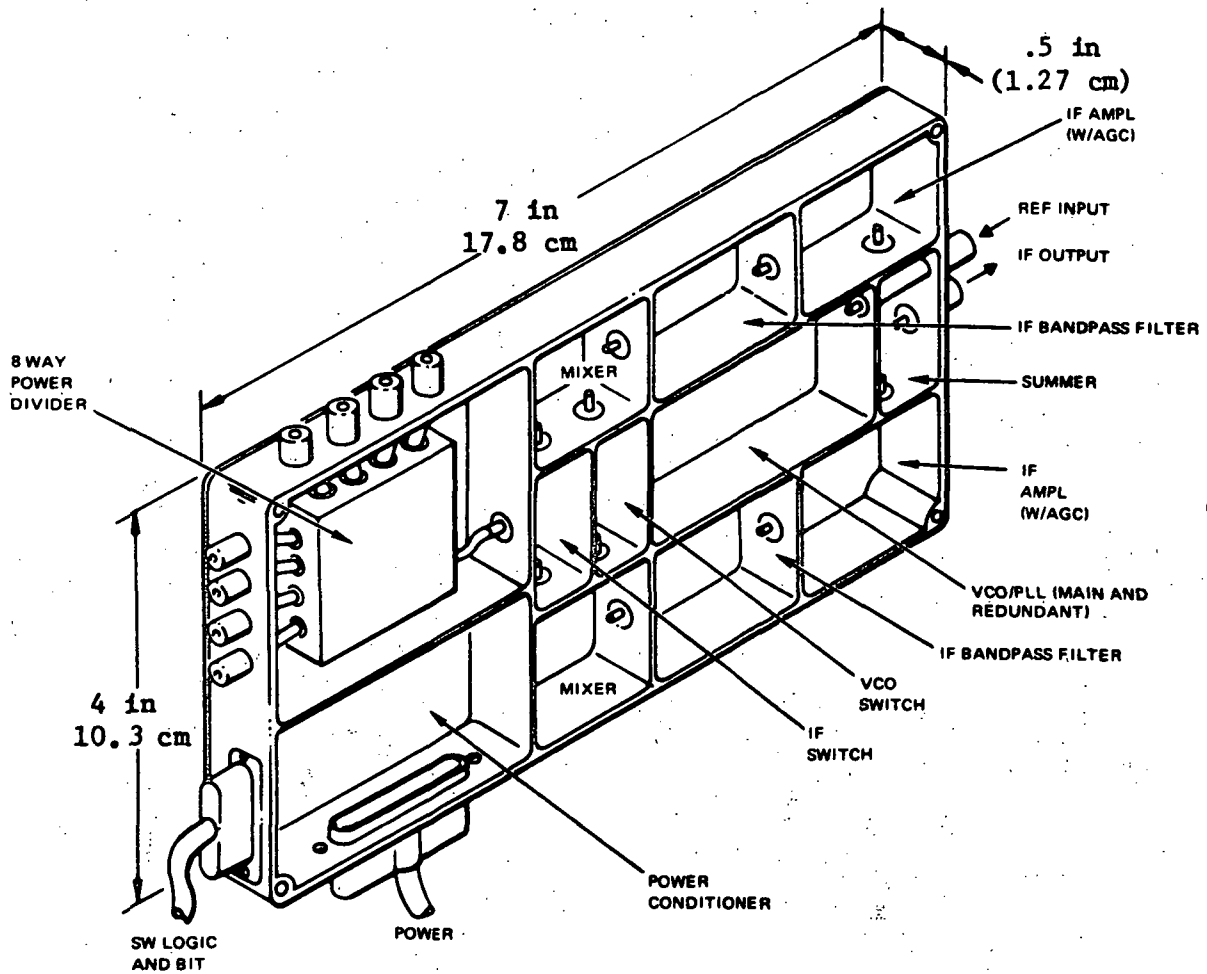


Figure 4-42. I.F. Summing Network

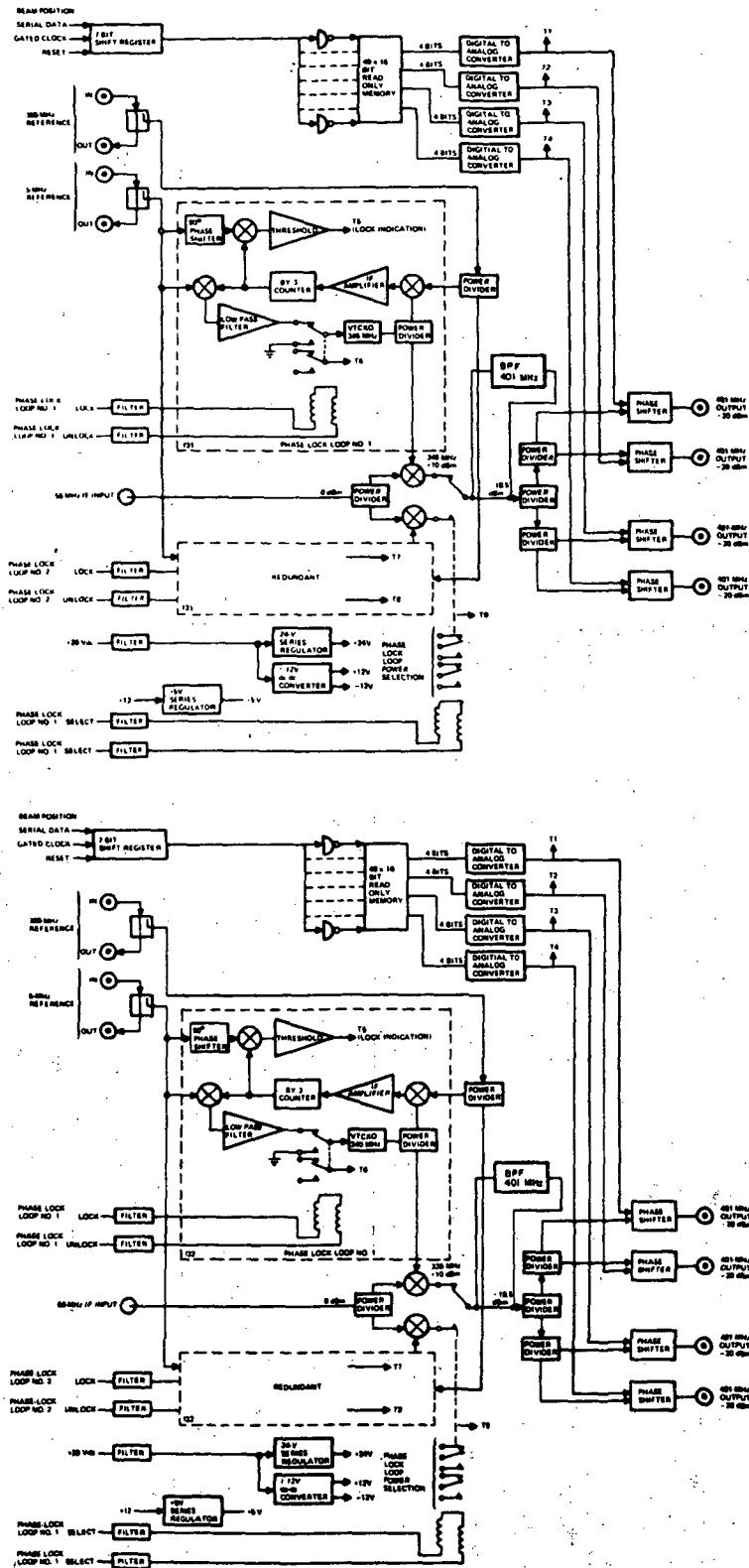


Figure 4-43. LDR Transmitter Divider Network



The varactor control voltage is derived from a digital to analog conversion of the 16-bit word read from the ROM. The 16-bit word is divided into four words of 4 bits each which are applied to four D/A converters. The D/A converter is a monolithic "IC" containing the current logic, current sources, ladder networks, and output operational amplifier on a single chip. The ROM is programmed to provide the digital equivalent of the voltage required to obtain the required phase shift from the 4 phase shifters at each of the 49 discrete positions. Telemetry monitoring of each D/A converter output is provided.

Spacecraft 28 volts is processed in three power conditioners per channel to provide the voltages, 24 v, +12 v, and 5 volts required by the phase locked loop and beam steering circuits. The 24 volts for the crystal oscillator is derived by series regulation of the input power. Plus and minus 12 volts are obtained from a dc to dc converter. The 5-volt logic power supply voltage is derived from the plus 12-volt line by series regulation in the third power conditioner. Total input power per channel is 5.7 watts.

The transmitter divider assembly, Figure 4-44, consists of two chassis mounted back to back with an aluminum plate sandwiched between them. Each chassis is an aluminum frame with dividers added for strength purposes. To the inside of each frame is mounted a microstrip P.C. board which acts as a mother board for all components. The beam steering circuits and the phase lock local oscillator are contained on multilayer boards which interconnect with the mother board forming one integral board assembly.

The complete transmitter divider assembly with its dividing plate in between and a cover on each outside surface forms a strong sectionalized assembly.

LDR UHF Transmitter. The LDR transmitter is straightforward in design. Each of four transmitter subassemblies has two identical channels with separate inputs whose outputs are combined in a quadrature coupler. The channel outputs are each 5 watts cw, or 20 watts peak voice, 25 percent duty cycle, with inputs of -23 dBm as shown in Figure 4-45. The output of the last amplifier is fed through a tubular filter with 60 dB rejection of the second harmonic of the 401 MHz fundamental. The output amplifier is a CTC-25-28 transistor capable of an output power of 25 watts and a gain of 7 dB. The amplifier is derated to provide no more than 22.8 watts, 25 percent duty cycle output for long life. The driver is a CTC-12-28 capable of 12 watts and 8 dB gain which is derated to 4 watts to provide long life. The CTC-C3-28 driver operates Class B at about 0.4 watts while the output stage is Class C. Each of the preamps use a 2N3866 transistor. The first three preamps operate Class A and the last is Class B with progressively less bias as the signal level decreases toward the front end. Interstage matching will be by means of a series L to rotate the normally low transistor input impedance, then a shunt C and then a series C to match to a higher resistance for presentation to the preceding stage. The impedance seen by each collector will progressively increase as the signal level to be handled decreases toward the input stages. The bandwidth of the transmitter is, however, broad enough to preclude system degradations because of bandwidth shifts due to component aging or temperature variations. The transmitter is powered directly from the

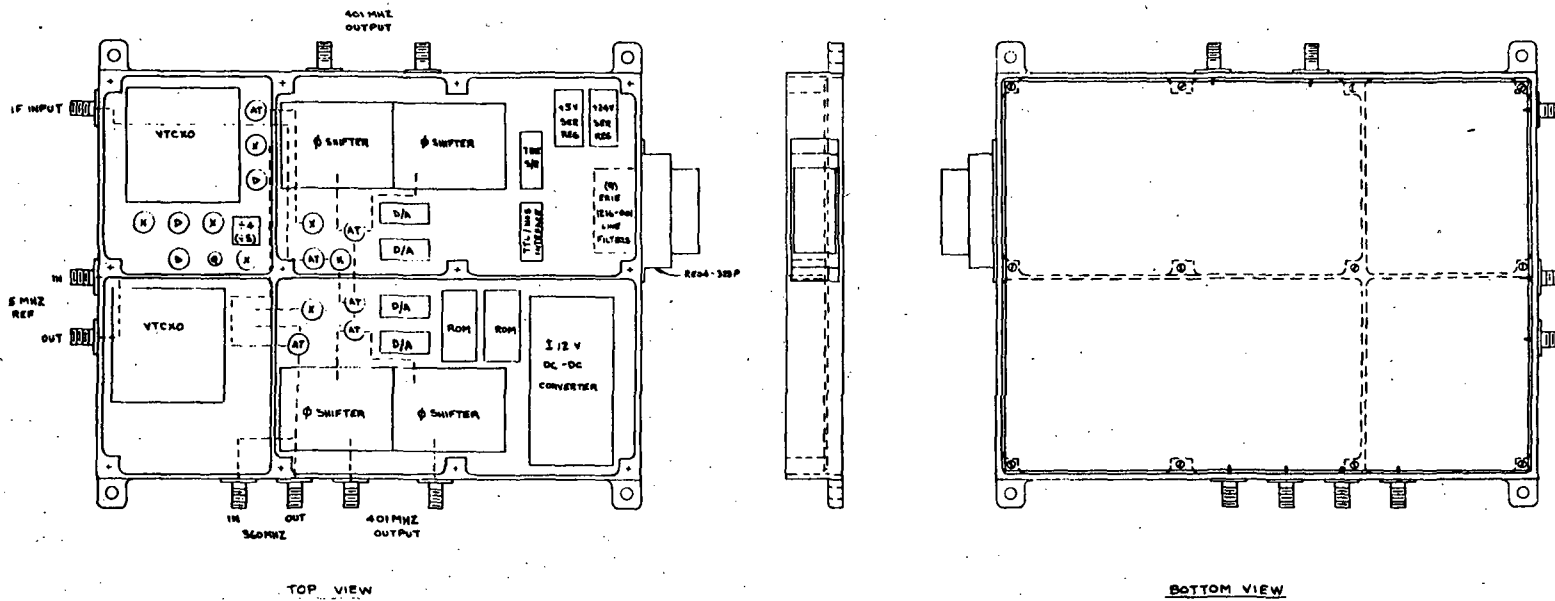
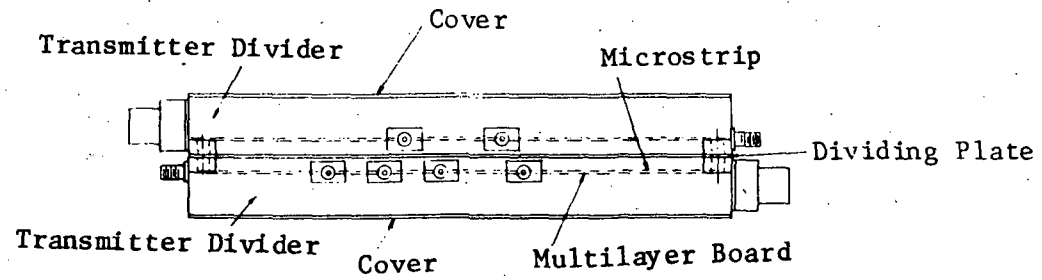


Figure 4-44. LDR Transmitter Divider

4-79

SD 72-SA-0133

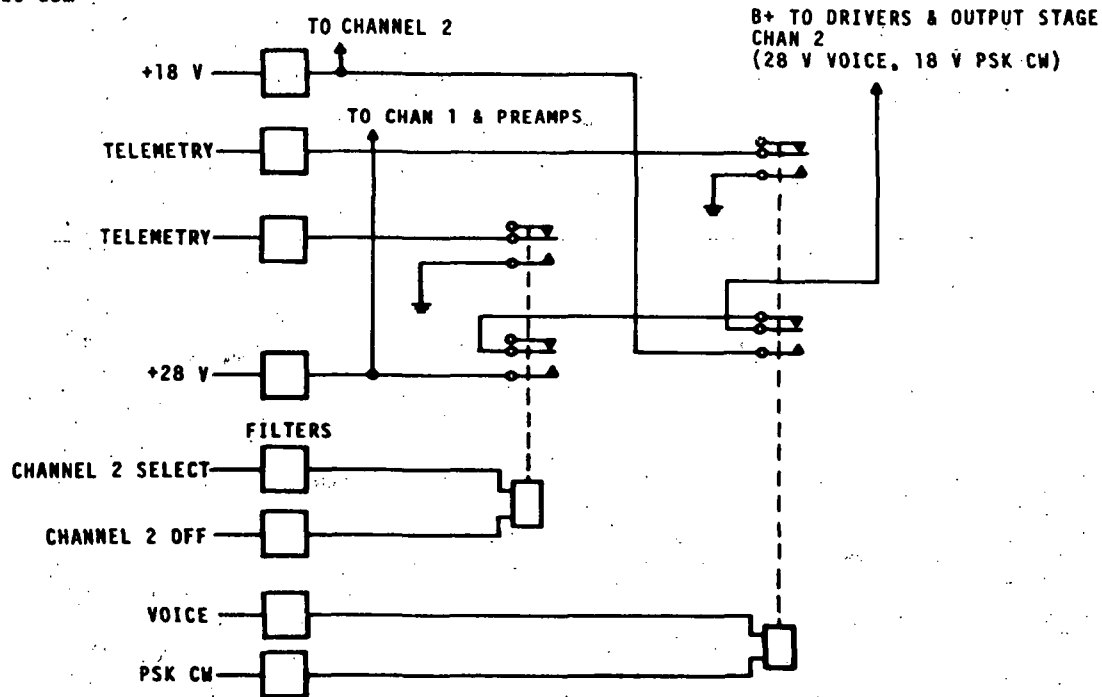
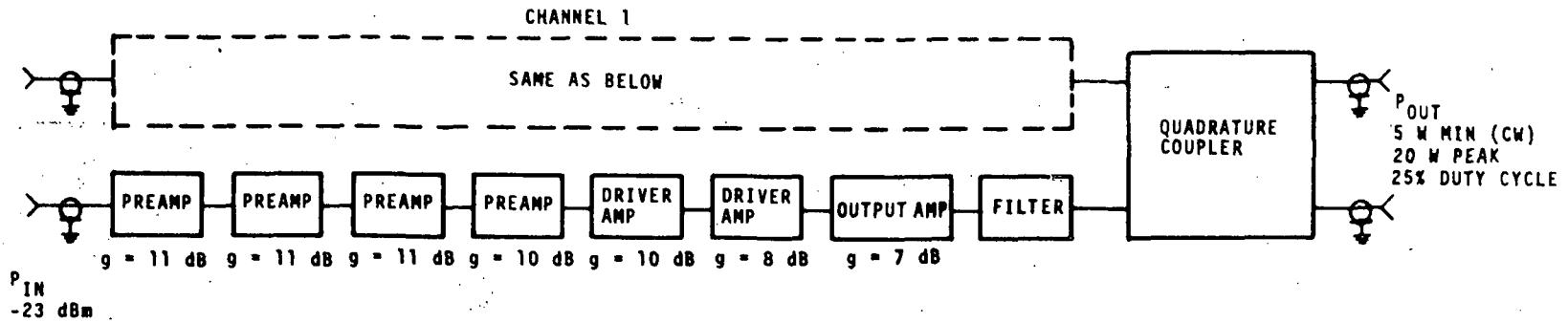


Figure 4-45. LDR Transmitter Block Diagram

4-80

SD 72-SA-0133



spacecraft 28-volt bus through a suitable relay control for turning transmitters on or off, or from +18 vdc to dc converter.

The transmitters will be constructed in a cellular metal structure with individual cells for each stage as shown in Figure 4-46. B+ for each stage will be brought in through the bottom of the cell by means of a feed through capacitor with B+ decoupling chokes, low frequency decoupling capacitors, and relays in a common enclosure below the amplifier cells. The structure will be used for thermal control within the transmitter and as such will conduct waste heat to the spacecraft equipment shelf structure for disposal. The transmitter assembly is shown in Figure 4-47.

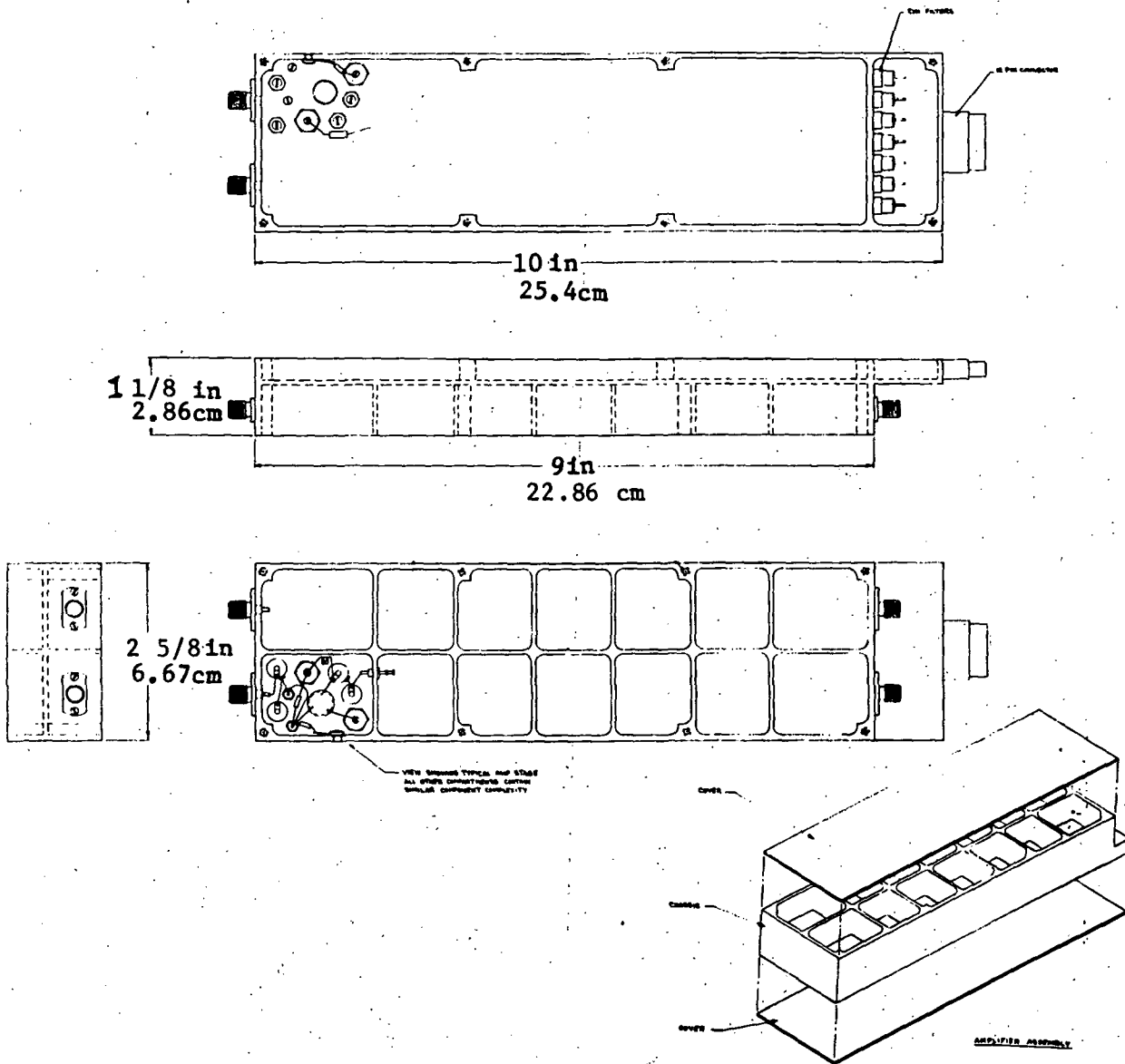


Figure 4-46. Driver-Output Amplifier Assembly

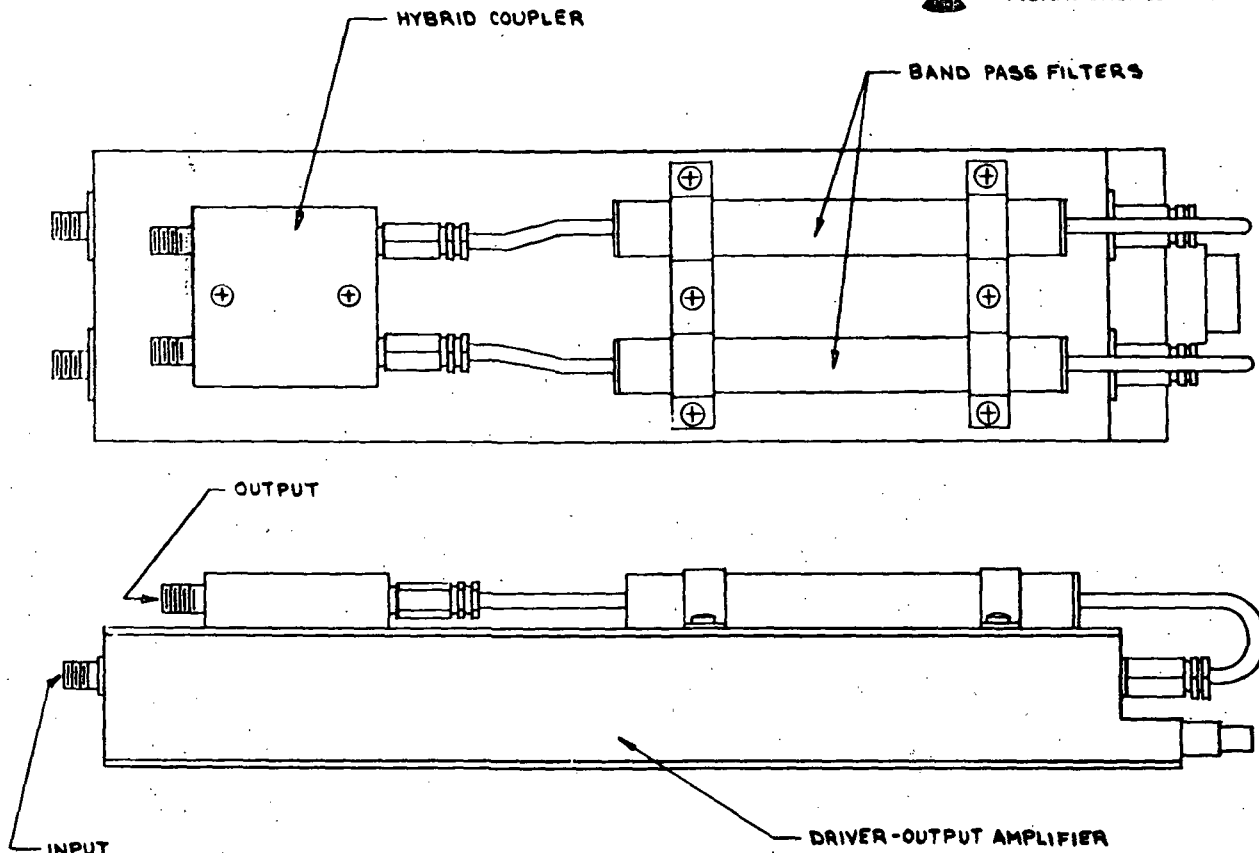


Figure 4-47. Transmitter Assembly

4.3.4 Performance Specification for LDR Transponder

4.3.4.1 Scope

This specification establishes the design performance requirements for the LDR transponder located on the TDRS satellite. This equipment provides the space-to-space interface between the LDR user spacecraft and the TDRS relay satellite.

4.3.4.2 Components

The major components of the LDR transponder are:

1. Dual frequency antenna
2. Receiver
3. IF summing network
4. Transmitter
5. Transmitter divider network



4.3.4.3 Design Requirements

LDR Antennas

Frequency Range

Receive (VHF)	136 to 138 MHz
Transmit (UHF)	400.5 to 401.5 MHz
Transmit avg. power	<16 watts

Polarization (VHF and UHF)

Each band	Orthogonal linear
-----------	-------------------

Isolation (between orthogonal linear polarizations)	>20 dB
---	--------

Element Type

VHF	} Colinearly stacked
UHF	

Input VSWR

<1.2:1

Peak gain (with respect to linear isotropic)

(VHF)	>10.8 dBi/element; 15 dBi/quad array
(UHF)	>16.8 dBi/element; 21 dBi/quad array

Side and back lobe levels

>13.0 dB

Half power beamwidth

VHF Element	>45 degrees (0.78 rad)
Array	>24 degrees (0.78 rad)
UHF Element	>31 degrees (0.54 rad)
Array	>9 degrees (0.54 rad)

Beam squint (determined from E- and H-plane average 3 dB beamwidth)

VHF	< +3 degrees (52.4 mr)
UHF	< +2 degrees (35.0 mr)

Size of VHF/UHF element

Erected - Diameter	< 6.0 feet (1.83 m)
- Height	<10.0 feet (3.05 m)
Stowed - Diameter	30.0 inches (0.76 m)
	12.0 inches (0.305 m)

Weight	{	Element 5.0 (2.27 kg)
		Stem unit 2.0 (0.91 kg)
		Strut 0.9 (0.41 kg)

7.9 pounds (3.59 kg)

Erection technique

Stored strain energy and elect. driven stem unit

LDR Receiver and IF Summing Network

RF frequency range	136 to 138.0 MHz
Receiver noise figure	1.02 dB
Receiver gain	Approximately 90 dB total
Instantaneous dynamic range	> 42 dB
Effective rec. bandwidth	2.0 MHz
Spurious rejection	> 50 dB (for out-of-band inputs, 50 dBm)
Baseband output level	-10 dBm
L.O. power	+10 dBm
IF frequency range	50.5 to 68.0 MHz
Baseband frequency range	17.0 to 34.5 MHz
AGC range	36 dB

LDR Transmitter

Inputs:

401 MHz \pm 7 -Hz, -20 \pm 2 dBm each channel

Prime power: 28v \pm 1v uncertainty, 137.6w peak/channel, 25% duty cycle for voice
18v \pm 1v, 38.8w min/channel, for data (Δ PSK)

Outputs:

20 watts peak, 25% max duty cycle/channel for voice
5.0 watts/channel cw on Δ PSK for data

Size: 10 x 2.62 x 1.12 inches } less connectors, max. each of 4
(25.4 x 6.67 x 2.84 cm)

Weight: 1.12 lb (0.51 kg) maximum each of 4: 4.5 lb (2.04 kg) total

LDR Transmitter Divider Network

Inputs:

56 MHz and 66 MHz IF	0 dBm
5 MHz and 360 MHz reference	-20 \pm 3 dBm
56 MHz and 66 MHz channel beam steering data	
7-bit serial data	TTL logic level
Gated clocks	TTL logic level
Clear	TTL logic level

L.O. and redundant channel select +28 volts plus
Input + 28 volts 11.4 watts

Outputs:

Eight 401 MHz \pm 7 kHz uncertainty -20 \pm 2 dBm

Phase accuracy between channels
 for position code 444 \pm 3 degrees (52.4 mr)
Overall phase stability \pm 5 degrees (87.3 mr)

Size: 10 x 7.5 x 2.25 inches (25.4 x 19 x 5.7 cm)

Weight: 5.1 lb (2.31 kg)



4.3.5 Size, Weight, and Power Summary for LDR Transponder

The size, weight, and power requirements are summarized below for the recommended LDR transponder Part I baseline configuration.

Component	Size in. (cm)	Weight		Power, watts	
		lb	(kg)	Peak	Avg
Antenna element					
Erected	64.5 dia x 116.0 (1.64 m dia x 2.94 m)	7.9	(3.59)		
Stowed	30.0 dia x 12.0 (0.76 m dia x 0.3 m)				
Antenna array ¹		31.6	(14.35)		
Receiver (4)	8 x 7 x 0.5 (20.2 x 17.8 x 1.27)	7.6	(3.45)	7.92	7.92
IF summing network	7 x 4 x .5 (17.8 x 10.2 x 1.27)	1.3	(0.59)	1.14	1.14
Transmitter (4)	10 x 2.62 x 1.12 (25.4 x 6.7 x 2.84)	4.5	(2.04)	77.6 ² 137.6 ³ 137.6	77.62 68.84 75.2 ⁵
Transmitter Divider network	10 x 7.5 x 2.25 (25.4 x 18.4 x 5.7)	5.1	(2.31)	11.4	11.4
Total		50.1	(22.76)		
2 data					98.1
2 voice					89.3
1 voice + 1 data					95.7

NOTES:

1. Includes weight of supporting links for each element
2. Both transmitters in data mode
3. Both transmitters in voice mode; however, it has been assumed that the peak voice requirements do not add up simultaneously
4. Assume 25-percent duty cycle for voice
5. 1 voice plus 1 data



4.4 MEDIUM DATA RATE LINK

4.4.1 MDR System Analysis and Trades

Comprehensive tradeoff analyses were conducted in the design of the MDR space-to-space link to arrive at a design that offers sufficient flexibility to support the variety of currently planned MDR users, and also to offer the versatility to support the transition to future high performance (HDR) users. Since the TDRS has an operational lifetime of five years, the initial TDRS system must offer a capability to support a host of low to high performance MDR users. An overall design goal was to maximize the number of independent MDR users that can be supported simultaneously by the TDRS satellite within the performance specification of the SOW, and to determine the optimum operating frequency (S- versus X- versus Ku-band). Candidate link approaches evaluated and compared during the study are shown in Table 4-13. The approach offering the greatest potential to encompass the design goals within the physical constraints of the 2914A Delta launch vehicle payload is the mechanically scanned dual frequency approach.

Table 4-13. MDR Link Approaches

Approaches	No. Users/ Aperture	Frequency Band		
		S	X	Ku
Electronic scan	2	*		
Mechanical scan				
Single frequency	2	*	*	*
Dual frequency	2	(S or X)	(S or Ku)	
Common apertures	2	(S & X)	(S & Ku)	
*Acceptable approaches				

Calculations were made for this space-to-space link to determine the antenna size necessary to support the TDRS specification as well as the space shuttle requirements as identified in Figure 4-48. Link calculations were computed using the following equation:

$$C/N_o = \frac{P_t G_t G_r \alpha_s}{K T_s} \text{ (FEC)} \quad (4-2)$$

where:

α_s = path losses

T_s = total system noise temperature

FEC = forward error control processing gain

It became apparent in examining the link equation that both α_s and T_s vary as a function of the TDRS-to-user spacecraft aspect angle (Ω) as defined in Figure 4-49, but most significantly these parameters do not maximize at the same aspect angle as shown in Figure 4-50. Consequently it is desirable to use the worst case combination of α_s and T_s , rather than the summation of individual worst cases.

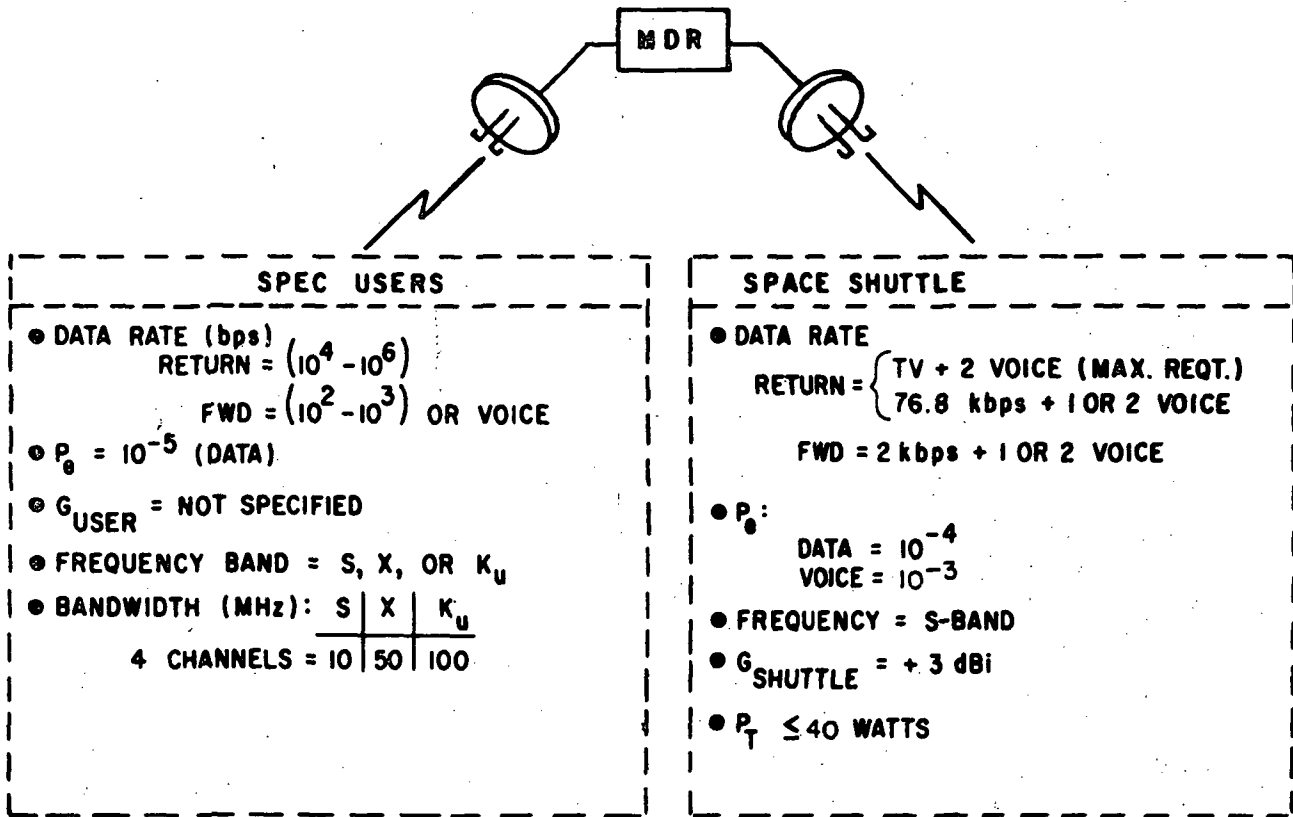


Figure 4-48. MDR Link Requirements and Constraints

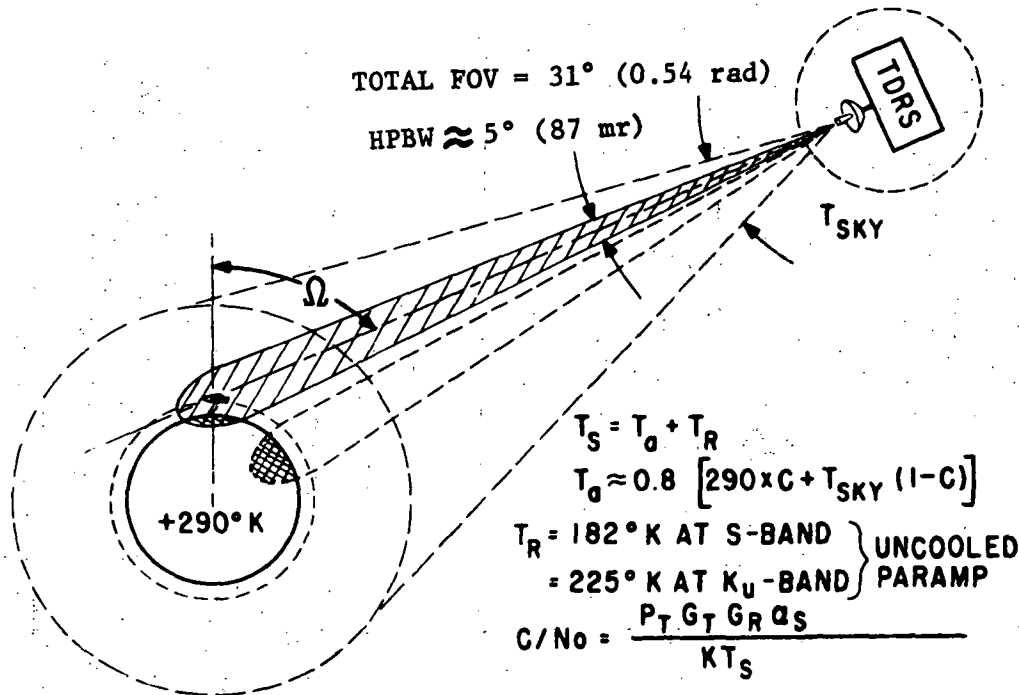


Figure 4-49. MDR Return Link: Space Geometry for T_s Calculation

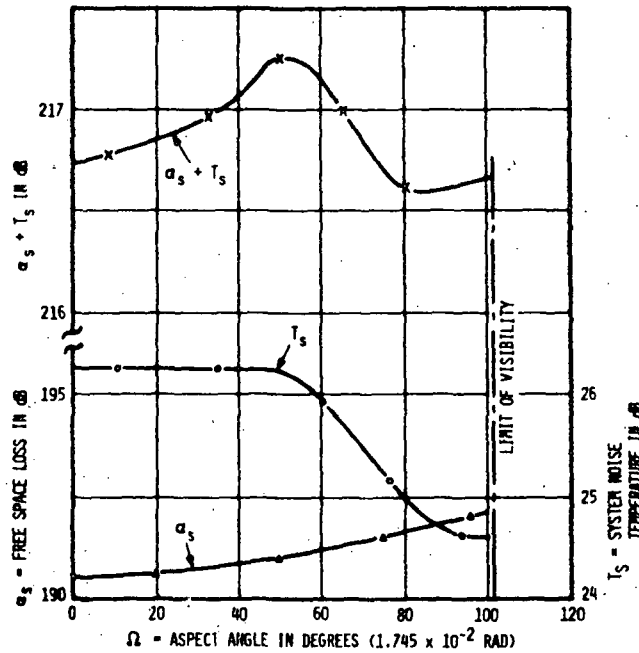


Figure 4-50. MDR Return Link, Space Loss T_s vs Aspect Angle

In computing the link requirements, uncooled paramps were considered in the TDRS receivers to minimize the impact on the users; in particular, the uncooled paramp is necessary to comply with the S-band return link requirements for the Space Shuttle within an antenna gain constraint of +3 dB and a maximum transmitter power allowance of +16 dBw¹.

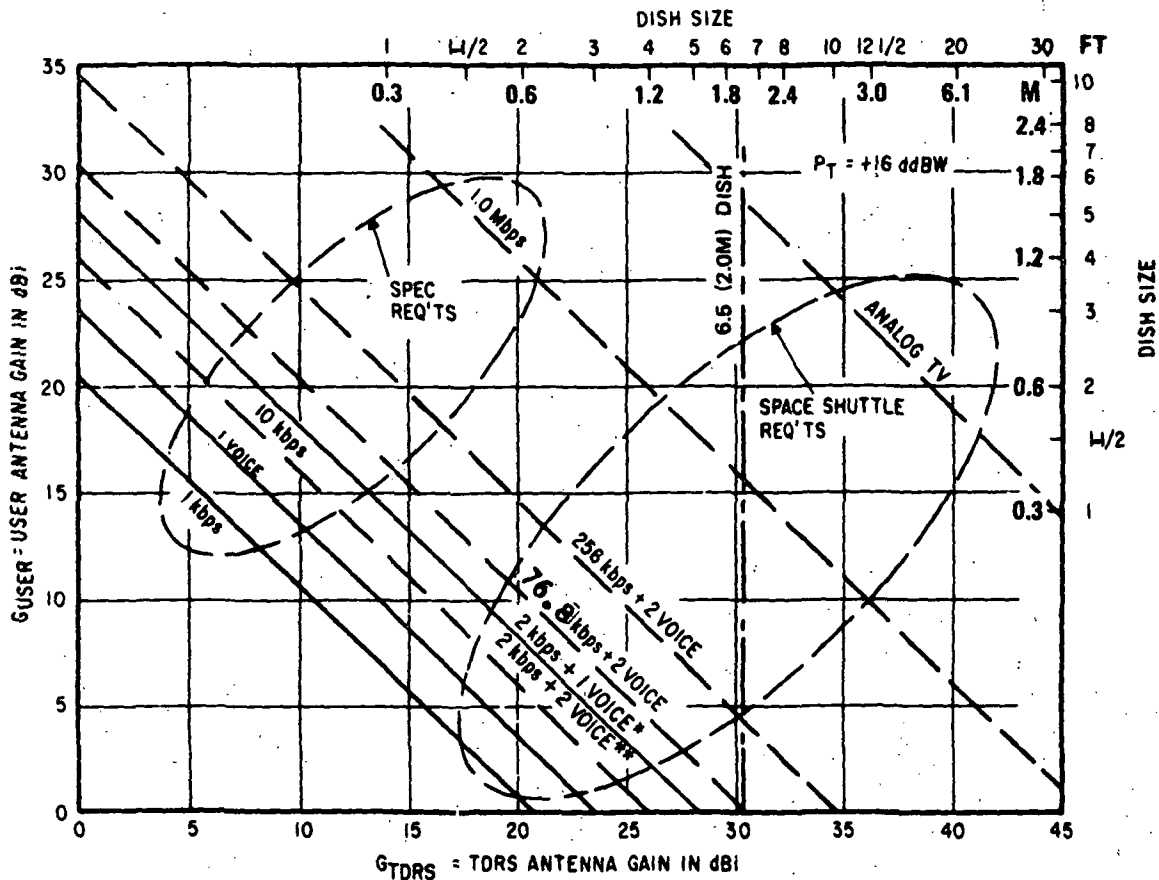
Using this link criteria, parametric curves of the antenna requirements at the user and TDRS spacecraft were computed for operation at S- and Ku-band frequencies as shown in Figures 4-51 and 4-52, respectively. The results indicate the MDR link is effectively independent of frequency for relatively austere low performance users employing nonsteerable (low gain) antennas. It is the higher efficiency in hardware implementation that results in their desire to operate at S-band. On the other hand, for the high performance users requiring a steerable antenna, the link performance improves directly as the square of the frequency; therefore, it is recommended that for operation of this link with a high performance MDR user, the highest candidate frequency or Ku-band frequency be used.

A comparison of the frequency-dependent components in the link equation

$$\frac{C}{N_0} = \frac{P_T G_T G_R \alpha_s}{K T_s}$$

shows the net gain in operating at Ku-band. These are compared below:

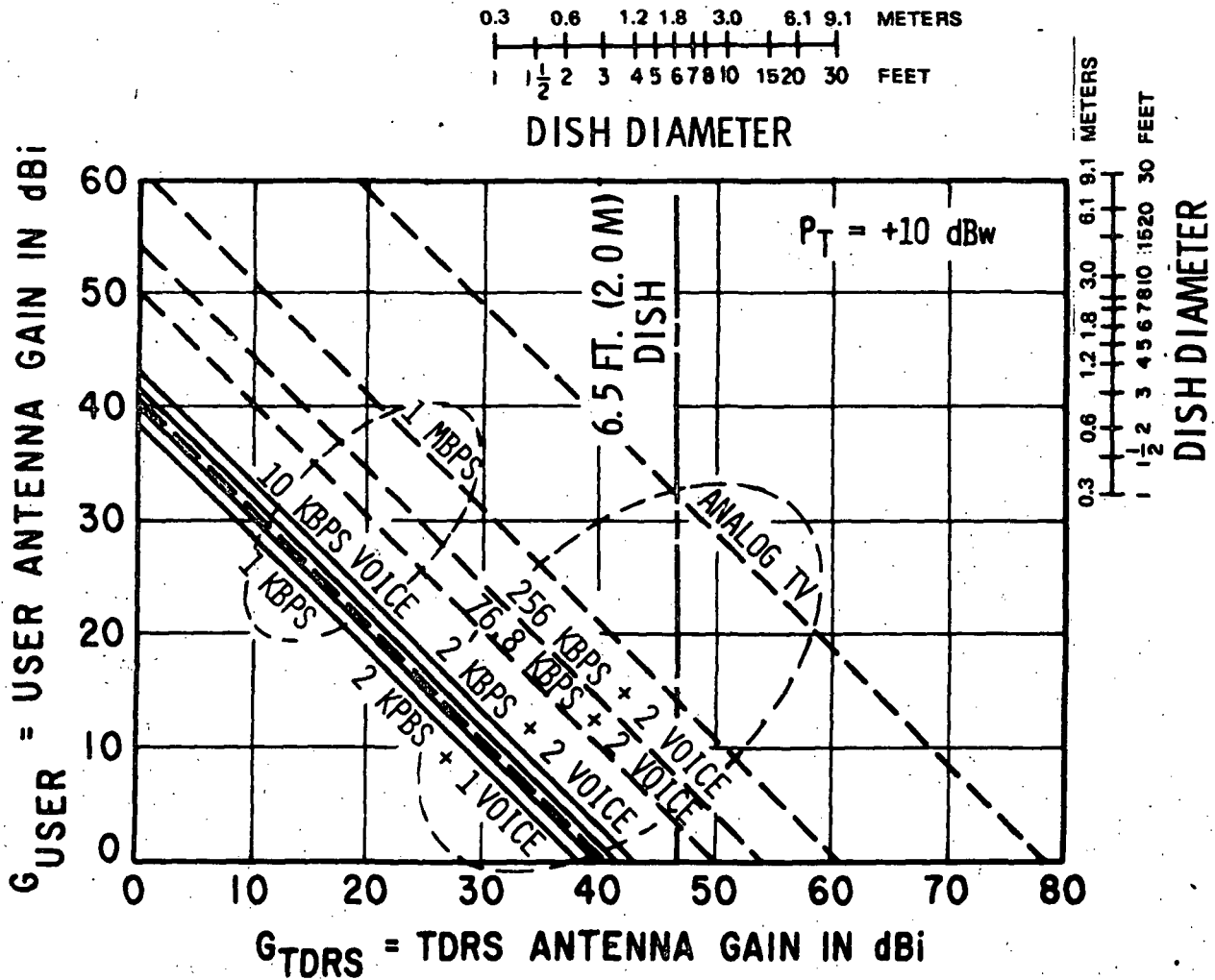
¹Private conversation with C. Dawson of MSC, 13 June 1972, recommending that a maximum of +16 dBw could be developed with minor impact on the power supply system.



NOTES:

1. ——— SOLID LINE = FORWARD LINK
 - - - DASHED LINE = RETURN LINK
2. SYSTEM NOISE TEMPERATURE (T_s)
 TDRS = 26.2 dB (UNCOOLED PARAMP)
 USER = 29.1 dB (SPEC) (TRANSISTOR)
 27.3 dB (SHUTTLE) (UNCOOLED PARAMP)
3. FORWARD ERROR CONTROL
 GROUND STATION = 4.7 dB
4. C/NO
 DATA = $9.9 + 10 \text{ LOG } H$
 VOICE = 48.8 dB-Hz (SPACE SHUTTLE REQUIREMENT)
 ANALOG TV = 88 dB-Hz
5. DESIGN MARGIN = 3 dB

Figure 4-51. MDR Link Antenna Requirements: S-Band



NOTES:

1. ——— SOLID LINE = FORWARD LINK
 - - - DASHED LINE = RETURN LINK
2. SYSTEM NOISE TEMPERATURE (T_s)
 TDRS = 27.0 dB (UNCOOLED PARAMP)
 SPECIFICATION USER = 33.5 dB (TDA)
 SPACE SHUTTLE = 27.4 dB (UNCOOLED PARAMP)
3. FORWARD ERROR CONTROL
 GROUND STATION = 4.7 dB
4. C/N_0
 DATA = $9.9 + 10 \log H$
 ANALOG TV = 88 dB-Hz
5. DESIGN MARGIN = 3 dB

Figure 4-52. MDR Link Antenna Requirements: Ku-Band



<u>Parameter</u>	<u>Ku/X</u>
1. TDRS antenna gain ratio	+5.3 dB
2. User antenna gain ratio	+5.3 dB
3. Space loss ratio	-5.3 dB
4. System noise temp ratio	-0.5 dB
5. Transmitter efficiency	
Solid-state amp	0 dB
TWTA	0 dB

In the above comparison, transmitter efficiencies used were approximately the same for the 1975 time period for both the solid-state amplifier and the TWTA. This net gain of approximately 5 dB in operating at Ku-band rather than X-band can be used to reduce the antenna gain at the user by an equivalent amount (or to reduce his aperture size). Additional contributing factors for selection of Ku-band rather than X-band for these users are: (1) operation of this space-to-space link in the same band as the space-to-ground link enables the MDR antenna and transceiver to provide a vital functional redundancy to the TDRS/GS link antenna and transponder; and (2) the larger MDR dish will provide additional 6.5 dB margin for operating the TDRS/GS link in rain.

As an initial design point, a 6.5 ft (2 m) diameter dish on the TDRS is considered since it is the largest fully erected aperture that can be stowed within the payload shroud dimensions of the 2914A Delta. S-band operation supports the 10 kbps specification requirements (Figure 4-51) with a user ERP of approximately +10 dBW in the return link, as well as the Space Shuttle requirement of 76.8 kbps plus two-voice with a Shuttle EIRP of +16 DBW¹. Even a 12.5' (3.8 m) dish on the TDRS will not support the maximum specification or Space Shuttle requirements without employing steerable antennas on the Space Shuttle. For those users requiring high-gain antennas, it is desirable to operate at Ku-band.

The TDRS S-band forward link maximum EIRP (+41 dBW) is limited by the IRAC/CCIR flux density guidelines of -152 dBW/m² per 4 kHz. Figure 4-51 shows that the specification and Space Shuttle requirements of 2 kbps plus 1 or 2 voice that can be met.

To summarize the frequency relation for the MDR link, the users have been generally categorized in Figure 4-53 in accordance with their requirements; viz., TDRS specification or Space Shuttle. The recommended operating frequencies for these categories are also identified in the figure; and generally, the low performance users with nonsteerable antennas operate at S-band, and the higher performance users employing steerable antennas operate at Ku-band.

The link calculation shows that the TDRS with a 6.5 ft (2 m) dish will support the Space Shuttle requirements of 76.8 kbps + 2 voice in the return link with an EIRP of +16 dBW. In the forward link, an EIRP of +41 dBW at the

¹A guideline reference used by MSC for maximum EIRP that could be generated on Space Shuttle with minimal development. Private conversation with MSC - C. Dawson, 13 June 1972.

TDRS supports 2 kbps plus 2 voice. The impact of the Shuttle support is summarized in Figure 4-54 for each of the terminals. In the forward link, if the bit error probability (P_e) for voice is reduced from 10^{-3} to approximately 10^{-4} , the effective C/N_0 can be reduced from 48.8 to approximately 43 dBHz as shown in Figure 4-55 without discernable degradation in the voice intelligibility.

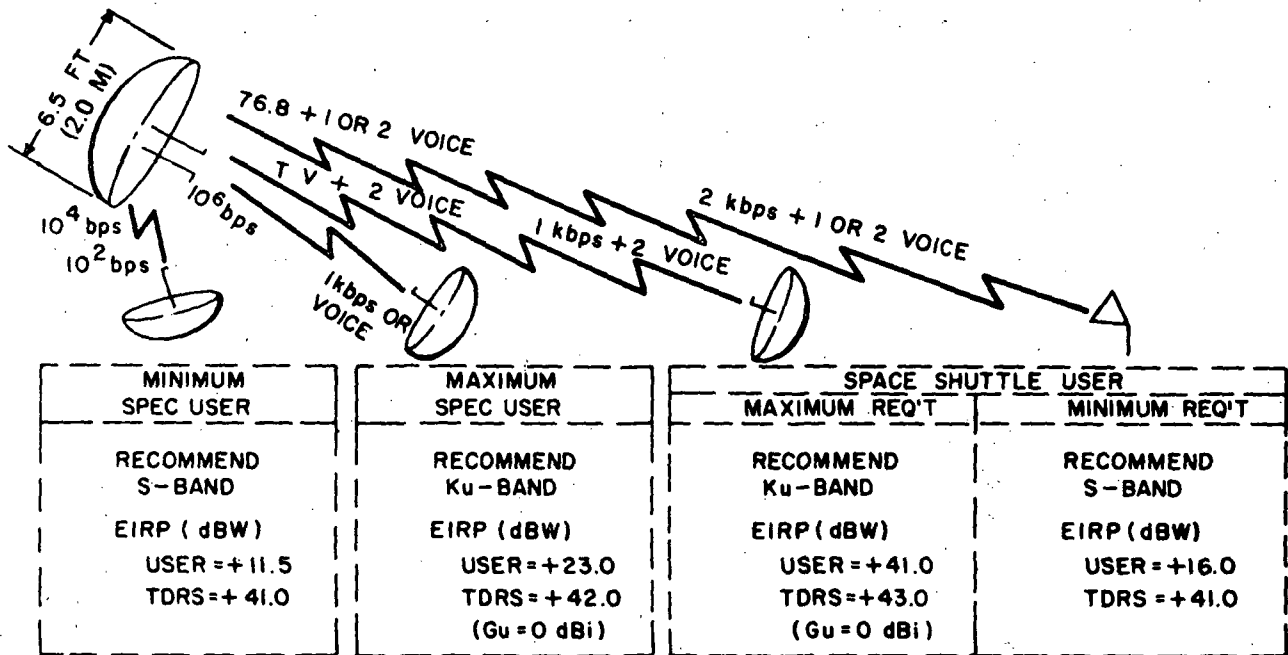


Figure 4-53. MDR Link Frequency Selection

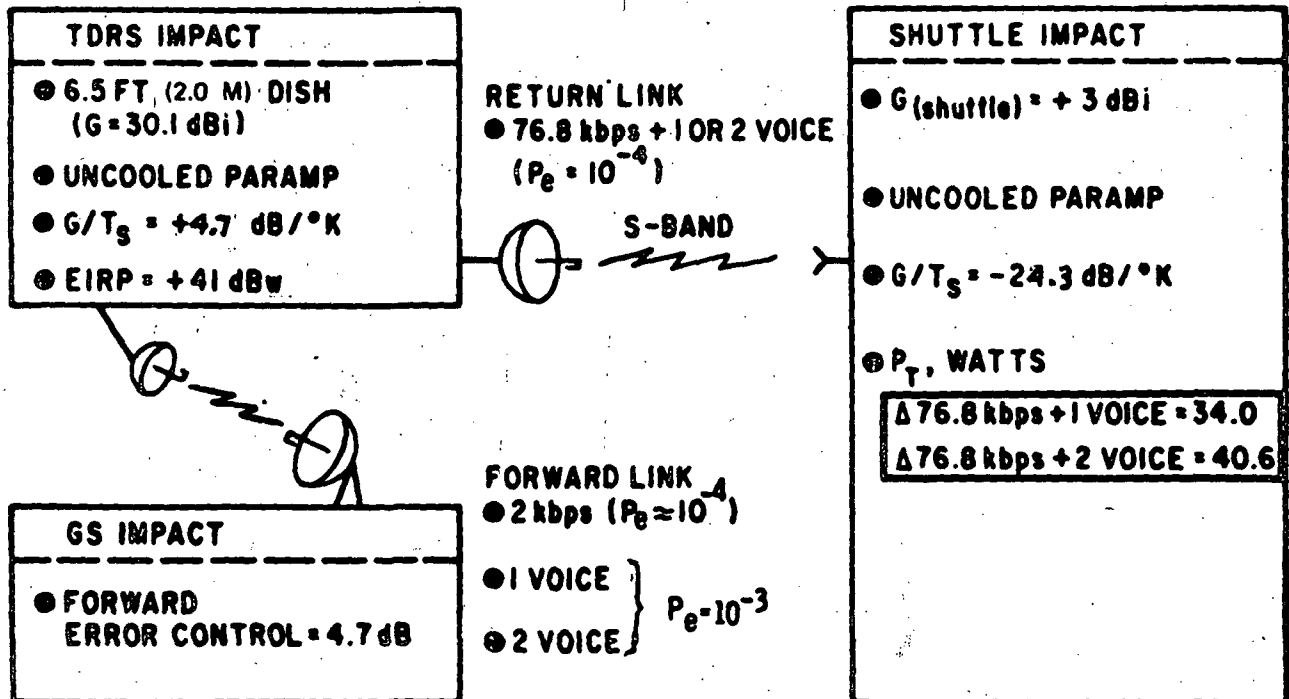


Figure 4-54. MDR Link Support of Space Shuttle

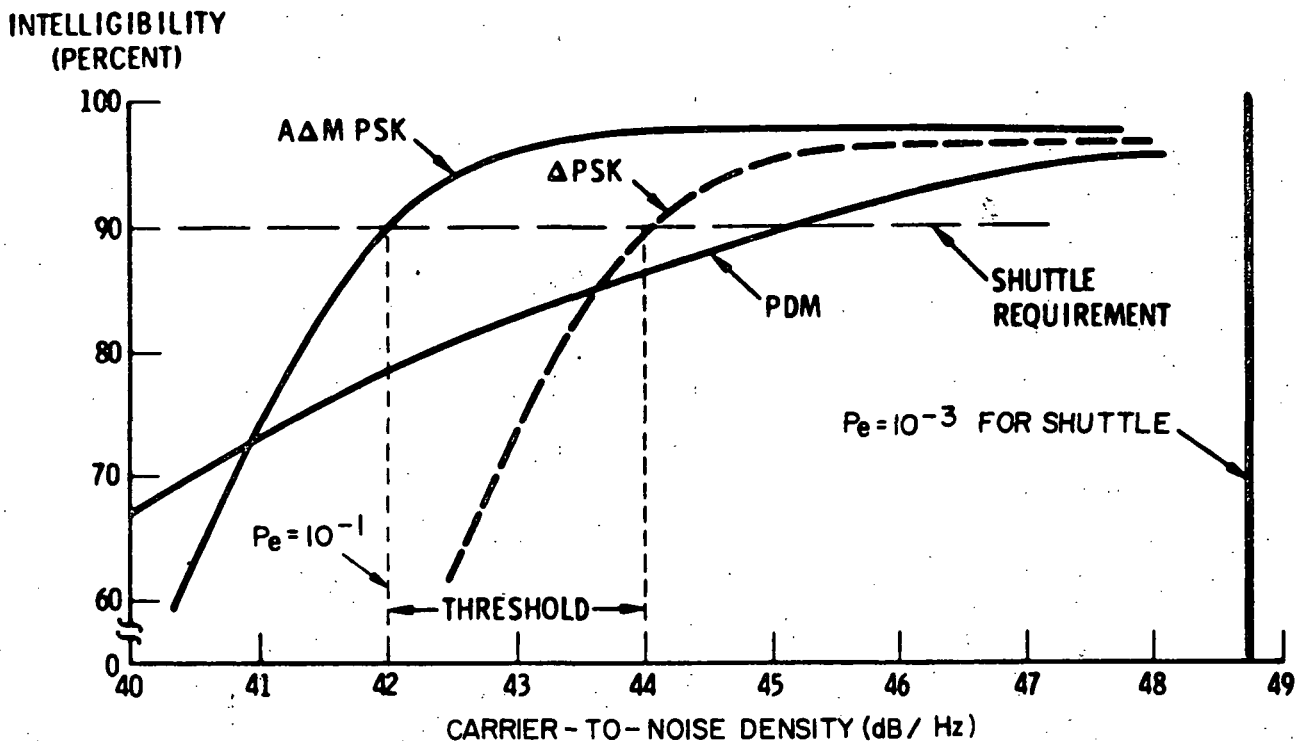


Figure 4-55. Comparison of PDM and Adaptive Delta-Modulation Voice.

In addition to the versatility to operate at S- and Ku-bands, the transponder receive and transmit channels have been designed with sufficient flexibility to accommodate users operating anywhere within the designated bands. In the receive mode, both MDR S-band channels have a 10 MHz bandwidth tuneable in 5 MHz steps over the entire 2200 to 2300 MHz range. However, one of these S-band channels will have an alternative 100 MHz "wide-open" mode to provide a bent-pipe capability at the TDRS, as well as to provide a future growth to handle TV for those users having sufficient EIRP. At Ku-band, the channel is 100 MHz wide and tuneable in four steps over a total 400 MHz band (again, the 100 MHz can handle future TV users). In the transmit mode, S- and Ku-band modes are 95 and 100 MHz wide, respectively, with a "true bent-pipe" capability. Although the "wide open" receive and transmit operation requires additional EIRP at the ground station to maintain the desired C/N_0 , link tradeoffs have shown that these EIRP's can be supported.

In summary, the recommended MDR transponder approach is:

1. Dual frequency (S- or Ku-band) transponder approach to optimally meet the current low performance/S-band user and future high performance Ku-band user.
2. A 6.5 ft (2 m) dish operating at S- or Ku-band to optimally support the specification and Space Shuttle requirements.
3. Tuneable 10 MHz-wide receive channels at S-band to provide the flexibility to service MDR users anywhere within the specified frequency range and range-rate formats. In addition, an alternate mode is provided for future wideband TV application. The Ku-band return link is 100 MHz wide, tuneable in four discrete steps over a 400 MHz total spectral range.



4. The forward link is 95 and 100 MHz wide at S- and Ku-bands, respectively, and will accept an S- or Ku-band signal anywhere within the band without tuning. In addition, there are four discrete 100 MHz bands available at Ku-band.

4.4.2 MDR Antennas

Table 4-14 broadly summarizes the various approaches considered in arriving at the MDR antenna design which consists of two 6.5' (2 m) diameter dishes. Each dish operates at both S- and Ku-band. S-band is open-loop, steered; Ku-band is closed-loop steered (autotrack). The antennas can be (1) either prime focus feed for both S- and Ku-bands, or (2) S-band can be prime focus with the Ku-band using a shaped Cassegrain system utilizing a frequency sensitive sub-reflector. The latter approach is somewhat more efficient and has been incorporated in the mechanical designs. Utilization of two separate dishes in the antenna farm for the MDR function provides a measure of redundancy.

Some of the weight/gain, weight/aperture size tradeoffs are summarized in Figures 4-56 and 4-57. Figure 4-56 shows the weight advantage (Ku-band operation) of the parabolic dish approach over a planar array approach for antenna gains over 25 dB. Gimbal and pedestal weights are not included in this figure. Figure 4-57 shows the weight advantage as a function of aperture size of the Radiation Inc. dual frequency design compared to a single frequency S, X and Ku-band planar arrays and an S-band self-focused phased array.

Figure 4-56 shows that the dual S/Ku design can be obtained for approximately the same weight as a dish operating at a single S-band frequency. The characteristics of the recommended S/Ku design are shown in Figure 4-58.

4.4.2.2 Detailed Design - MDR Antenna

Ku-band operation is achieved through use of a four-horn (closed loop) Cassegrain design. S-band operation is a prime focus (open loop) system.

The Ku-band Cassegrain feed design uses a frequency sensitive, shaped subreflector. S-band uses a cupped helix feed. The 6.5 ft (2 m) diameter reflector is a solid surface composite structure design. An X-Y gimbal system with redundant drive stepper motors and control electronics completes the system.

Feed/Microwave Design. The Ku-band system features a 12-wavelength diameter, dichroic(frequency sensitive), shaped subreflector and a single channel (pseudomonopulse) tracking waveguide circuit in which the sum channel is modulated sequentially by the X and Y axes error signals and uses much of the same waveguide transmission circuitry as the receive signal, but is diplexed before reaching the receive band comparator.

The S-band communications feed consists of an apex-mounted cupped helix. This type feed has a history of highly efficient illumination of the parabolic reflector.¹

¹Design was utilized by Radiation, Inc. on the UK-60 program as well as several other of their proprietary programs.

Table 4-14. Summary of Candidate MDR Antennas

Approaches	Frequency	General Antenna Type	Function	Considered Approaches	General Comments
Electronic scan	S	Array of high-gain elements	Forms multiple beams. Service two or more independent users	Retro directive phased array Self-focused phased array Computer-controlled phased array	Weight/complexity penalty Competitive in weight with dish for multiple users Weight/complexity penalty
Single frequency	S, X, or Ku	Planar array parabolic dish	Service a single MDR user	Planar waveguide arrays with polarizers vs. prime focus parabolic dishes	For aperture sizes considered - parabolic dish designs have weight advantage
Dual frequency	S and X S and Ku	Parabolic dish	Service a single user	Total prime focus system vs. combined and prime focus and Cassegrain systems	Total prime focus system has the disadvantage of reduced efficiency due to interlaced feeds when compared to the combined prime focus and Cassegrain system
Common aperture	S and X S and Ku	Parabolic dish One fixed prime focus feed One movable (S-band) feed	Service two independent MDR users at different freq.	Mechanically articulated feed and electromechanically scanned feeds	Scan losses (at S-band) are prohibitive for dish sizes under consideration

4-96

SD 72-SA-0133

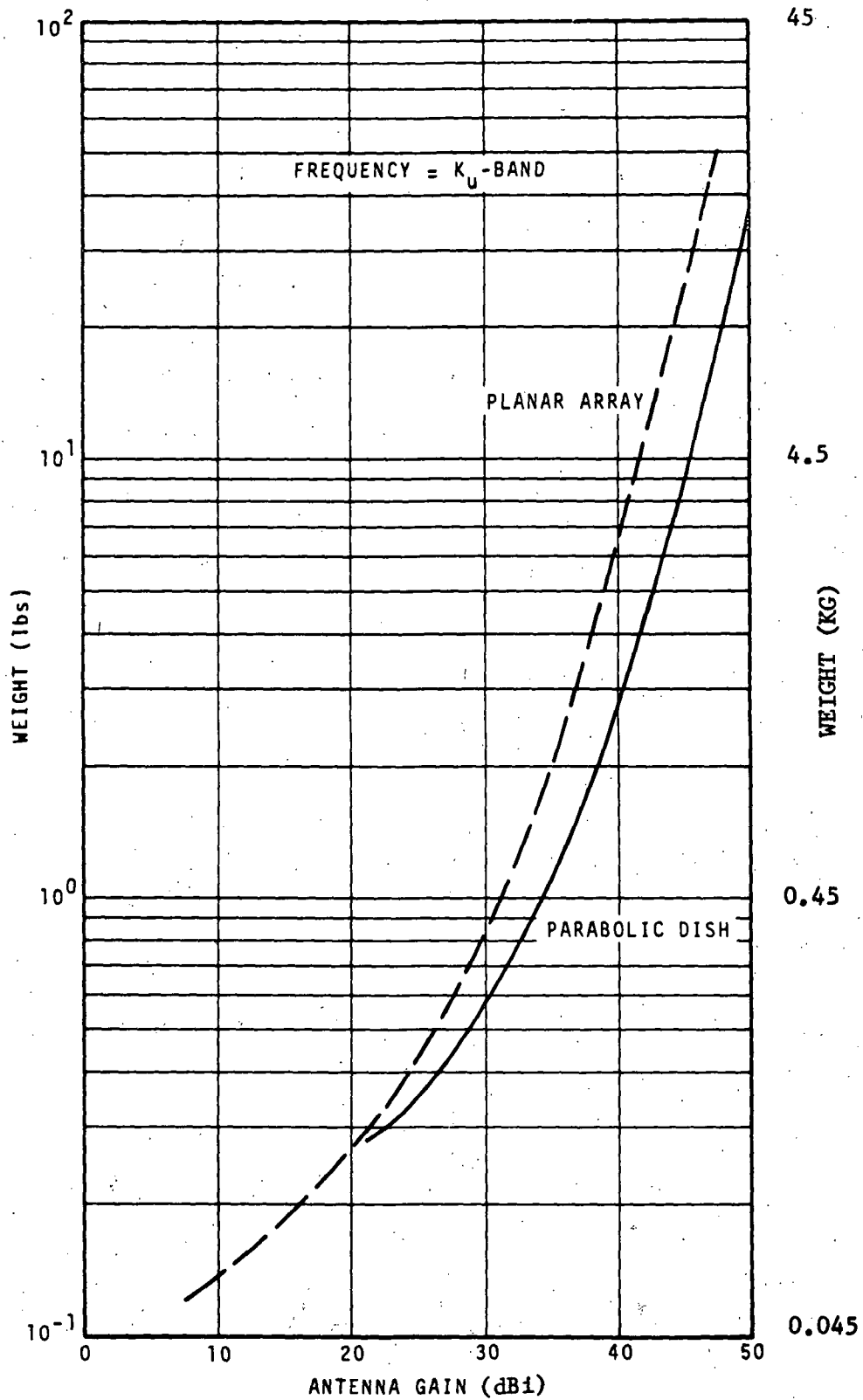


Figure 4-56. Comparison of Antenna Gain vs. Weight -
Planar Array Vs. Parabolic Dish

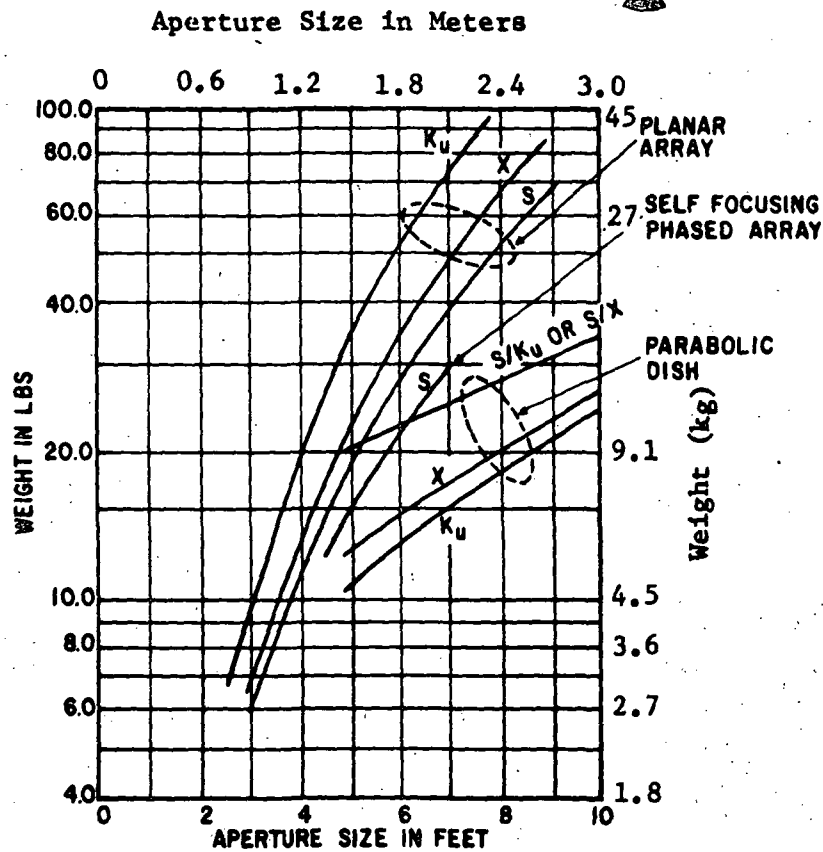
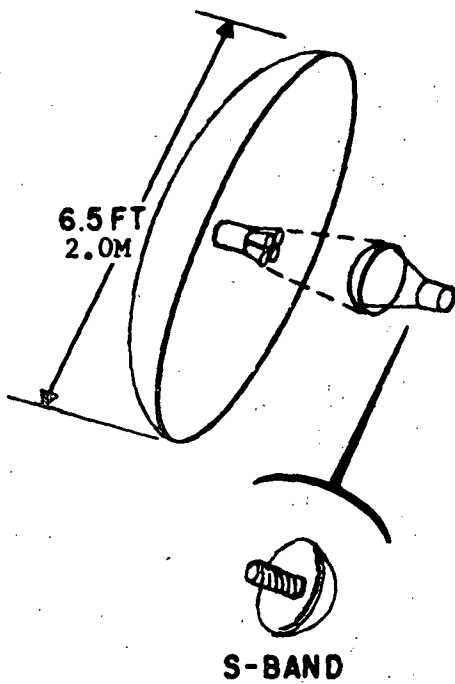


Figure 4-57. Weight vs Aperture Size for Planar Arrays and Radiation, Inc., Parabolic Dish Designs



PARAMETER	S	Ku
• APPROACH	• PRIME FOCUS	• CASSEGRAIN
• FEED	• HELIX IN CUP	• 4-HORN
• ACQ. & TRACK	• OPEN	• CLOSED DURING PSEUDO MONO-PULSE
• EFFICIENCY, %	52	65
• SUBREFLECTOR	• TRANSPARENT	• REFLECTS Ku-BAND, DOUBLY CURVED SURF.
• HPBW°	• ≈ 5.0	• ≈ 0.65
• GAIN, dB1	• 30.2	• 47.6
WEIGHT, LB (KG)	ANTENNA, INCL. GIMBAL, FEED & CONTROL ELECT.	28.26 (12.8)
(TOTAL SYSTEM)	SUPPORT STRUT	5.7 (2.59)
		33.96 (15.4)

Figure 4-58. MDR Link Dual Frequency Parabolic Dish Design

An important component in the system is the frequency sensitive subreflector (FSS). This type of subreflector has been developed and demonstrated by test to exhibit a maximum of 0.3 db loss in the reflective band (Ku-band) and less than 0.1 db loss in the transparent band (S-band). Another important feature of the design is the use of a shaped subreflector (rather than the conventional hyperboloid) to achieve an improved spillover/amplitude taper efficiency. Spillover/amplitude taper efficiencies in excess of 80 percent have been measured.

The requirements for one channel of S-band and two of Ku-band are handled at the antenna interface through the use of noncontacting rotary joints. One joint on each axis is a single Ku-band joint while the other is a dual concentric S- and Ku-band joint. Each joint has a center section of circular waveguide which is choke flange coupled to the rotating member. The S-band channel can be passed to the rotating member by either waveguide or transformer techniques concentric with the Ku-band section. The candidate design provides separation of the Ku-band transmit and receive channels to opposite sides of the gimbal system and results in a reduced coupling between these channels. Figure 4-59 shows the feed block diagram.

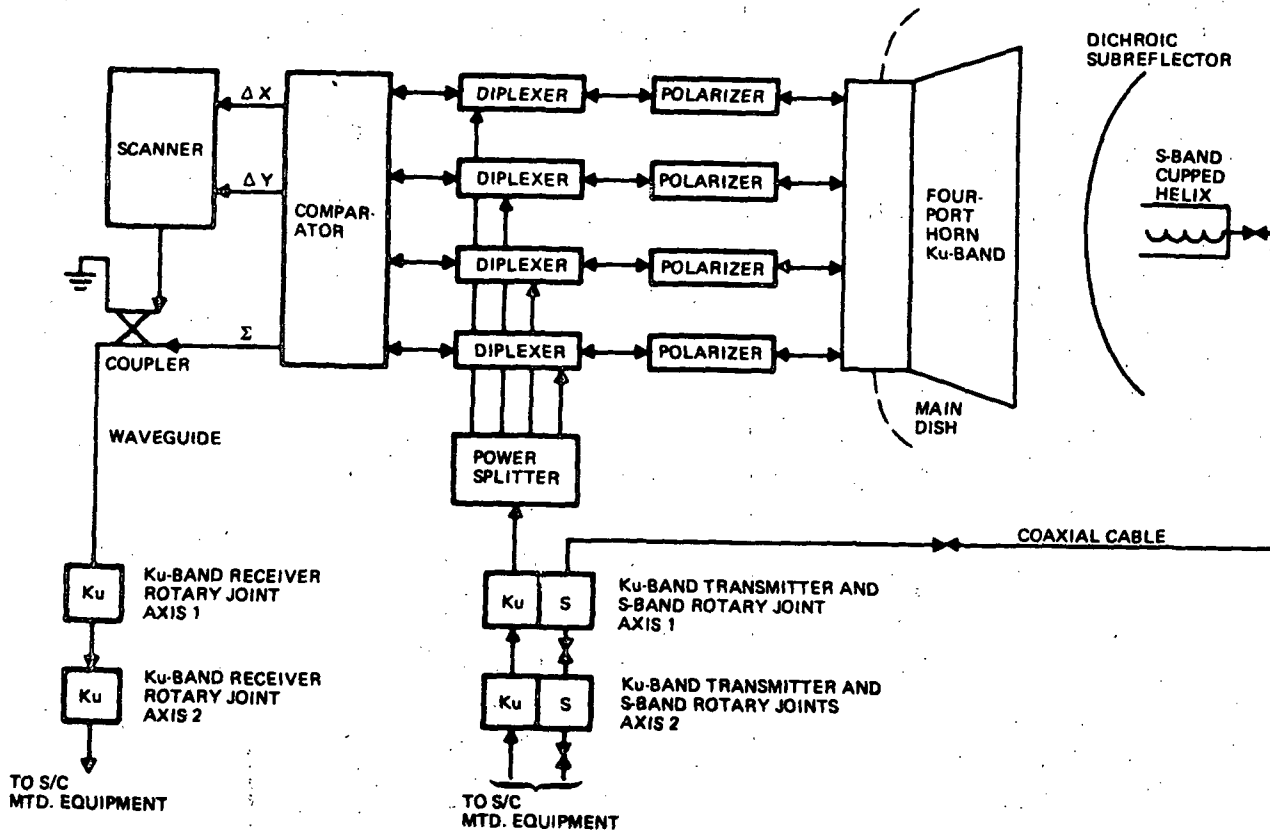


Figure 4-59. RF Block Diagram MDR Antenna Cassegrain Ku-Band/Apex S-Band



Table 4-15 presents the projected efficiency of the candidate system. The system is highly efficient with overall efficiencies of 65 percent and 52 percent for the Ku- and S-band frequencies, respectively. Table 4-16 presents a weight budget for the feed and microwave system. A weight and power budget summary for the S- and Ku-band antenna system is presented in Table 4-17.

4.4.3 MDR Transceiver

4.4.3.1 Mechanization Trades

The mechanization trades in the MDR transceiver are summarized in Figure 4-60. The trades are primarily in the

1. Receiver front end
2. Type of receiver
3. Transmitter amplifier
4. Dual frequency operation

In the receiver area, three tradeoff parameters were examined: the low noise amplifier, receiver type, and S/Ku-band operation. Three different types of front ends were considered: mixers, parametric amplifiers and tunnel diode amplifiers. The decision favored the paramps in both bands to guarantee maximum performance under all conditions and minimize the impact on the user terminal. TDA's and mixers did not provide sufficiently low noise temperatures in either band. The Ku-band configuration is a single paramp while the S-band uses a paramp and a transistor amplifier in cascade.

The MDR receiver provides dual band operation (S- and Ku-band). This configuration gives the best coverage and flexibility without adding much complexity. The combination of S- and Ku-band was selected because it provides the optimum transition of current and future users; provides back-up capability for the TDRS/GS transponder; and provides for making the TDRS compatible with existing hardware. As a result of the low baseband frequencies, double conversion is required to provide sufficient separation of signal and image frequencies. Single conversion and low I.F. frequency would combine to make the RF filtering an impossible task.

The first I.F. in the MDR receiver was selected at 500 MHz. This frequency represents an optimum blend of specifications. 500 MHz is low enough that ultra noise transistors are available, yet high enough to separate the RF image response by 1000 MHz, thereby easing the front-end design. The 500 MHz I.F. has an additional advantage in that it places the second L.O. in the UHF range, a convenient range for the frequency source.

All mixers in the MDR receiver are double balanced. This type of mixer is best when conversion loss and spurious responses must be kept low.

The entire MDR receiver with the exception of the paramps and the VCO/PLL circuits will be integrated on a single stripline circuit board. This type of construction is essential to small size and weight and improves reliability by reducing the number of interconnections.



Table 4-15. RF Efficiency Budget

	S-Band	Ku-Band
Spillover-amplitude taper efficiency	.650	.800
Primary phase efficiency	.970	.980
Blockage efficiency	.952	.975
Primary cross-polarization	.998	.990
Secondary cross-polarization	.978	.999
Dichroic loss efficiency	.980	.940
A. Illumination Efficiency (Product of above factors)	.574	.711
Surface tolerance efficiency	1.000	.994
RF reflectivity	.999	.990
B. Reflector Efficiency (Product of above factors)	.999	.985
Component insertion loss efficiency	1.000	.970
Cable insertion loss efficiency	.940	1.000
Mismatch loss efficiency	.970	.955
C. Loss Efficiency (Product of above factors)	.912	.927
Overall Efficiency (A x B x C)	52%	65%
Gain:		
Low band	29.8 dB	47.1 dB
Mid band	30.2 dB	47.6 dB
High band	30.9 dB	48.1 dB

Table 4-16. Feed/Microwave System Weight Budget

Item	Weight		Number/Item	Total Weight	
	lb	kg		lb	kg
Horn, polarizers, diplexers	1.25	0.57	1	1.25	0.57
Power splitter	0.5	0.23	1	0.5	0.23
Comparator	0.75	0.34	1	0.75	0.34
Scanner	2.5	1.14	1	2.5	1.13
Coupler	0.25	0.11	1	0.25	0.16
S-band/Ku-band rotary joint	0.75	0.34	2	1.50	0.68
Ku-band rotary joint	0.5	0.23	2	1.0	0.45
Dichroic subreflector	0.25	0.11	1	0.25	0.16
S-band cupped helix	0.25	0.11	1	0.25	0.16
Coaxial cable/connectors	0.5	0.23	1	0.25	0.23
Total				8.75	3.97

Table 4-17. Weight Budget and Power Summary for S- and Ku-Band MDR Antenna

Weight	Weight/Pounds	Weight/kg
Feed/microwave system (including rotary joints)	8.75	3.97
Reflector and feed support	11.26	5.11
Gimbal system	3.25	1.47
Drive electronics	5.00	2.27
Total weight *	28.26	12.8
Power - Peak	Power/Watts	
Motor drive (6 watts/axis)	12.0	
Motor clamping (4 watts/axis)	8.0	
Electronics	4.0	
Total peak power	24.0	
Power - Average		
Motor power slew	2.0	
Motor power - track (open or closed loop)	1.0	
Electronics	4.0	
Total average power	7.0	

* Plus support strut, 5.7 lb (2.59 kg)

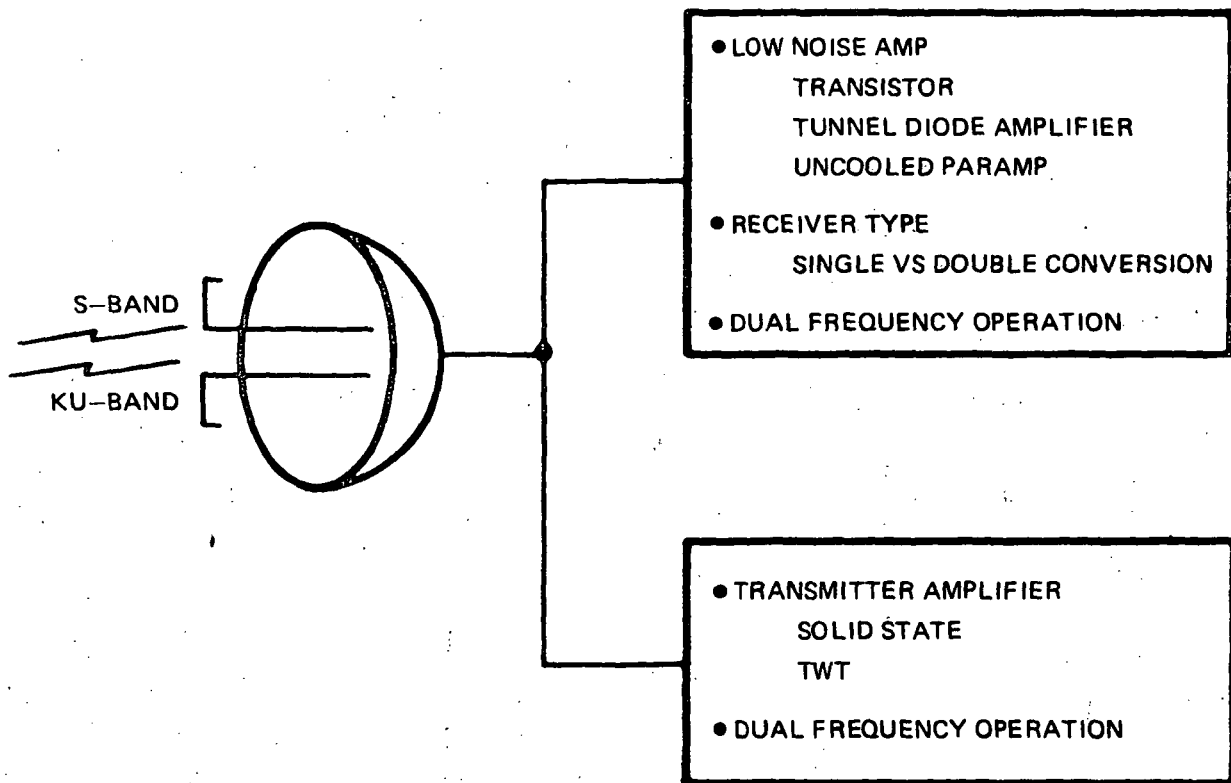


Figure 4-60. Summary of MDR Transceiver Mechanization Tradeoffs

The MDR receiver tradeoffs performed and the selected approaches summarized in Table 4-18.

In the MDR transmitter area, the tradeoffs were primarily in the selection of the power amplifier device, and in the optimization for dual S/Ku-band frequency operation.

In the power amplifier area, a study was made of a trade of solid-state devices versus traveling wave tube amplifiers (TWTA). For S-band operation, solid state is the obvious choice since the required power levels and its efficiency of approximately 44 percent for saturated operation is compatible with TWTA approaches but reliability is much higher. At Ku-band, current technology has not achieved the same level of proficiency as at S-band. Figure 4-61 compares the solid-state devices versus TWTA using the equivalent weight for comparison. Equivalent weight is the weight of the amplifier (including the high-voltage power supply for the TWTA) plus the weight of the prime solar panel (and batteries) required to support the amplifier). Figure 4-61 shows that for output power levels greater than approximately two watts, the TWTA is lighter than the solid-state device.

Table 4-18. MDR Receiver Tradeoff Summary

Tradeoff Consideration	Recommended Approach
Single conversion Double conversion	Double conversion
Dual band operation S-band/X-band S-band/Ku-band Single band operation S-band only Ku-band only	Dual band operation S-band/Ku-band
Paramp front end - Ku-band TDA front end - Ku-band Mixer - Ku-band	Paramp front end Ku-band
Paramp front end - S-band TDS front end - S-band Transistor front end - S-band Mixer front end - S-band Paramp transistor combination	Paramp transistor combination in S-band
I.F. frequency, 500 MHz Mixers - double balanced Integrated I.F.	From spurious analysis (optimum) Low loss, low spurs Small size and weight

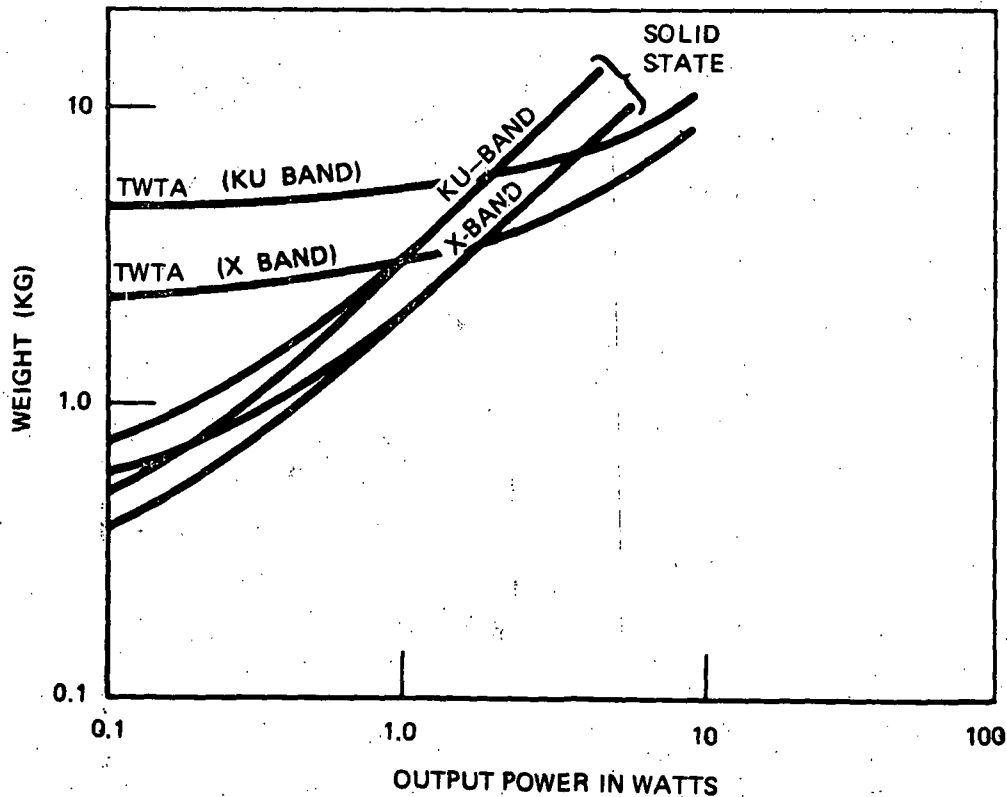


Figure 4-61. MDR Transmitter - Solid State versus TWTA



The selected approach uses a common driver amplifier up to S-band, and (1) power amplify for S-band mode, and (2) upconvert and amplify for Ku-band operation as shown in Figure 4-62.

The resultant dual frequency S/Ku-band transceiver is shown in Figure 4-63.

4.4.3.2 Detailed Description of MDR Transceiver

The two MDR receivers will handle transmissions at S-band (2200 to 2300 MHz) or Ku-band (13,600 to 14,000 MHz) from the user spacecraft to the TDRS. In addition to this primary function, one MDR receiver provides the backup coverage for the TDRS/GS receiver. The MDR receiver receives S- and Ku-band transmissions with a minimum of degradation and converts the individual spectrums to baseband frequencies suitable for modulation of the TDRS/GS transmitter.

MDR Receiver. The antenna output at -92 dBm is first fed through the diplexer to a parametric amplifier. The MDR receivers use paramp front ends in each band to assure maximum performance on low-level signals (See Figures 4-64 and 4-65. These ultra low noise devices guarantee the best possible performance regardless of other conditions. The S-band paramp noise temperature is 50 K and the Ku-band paramp is 100 K noise temperature. Both amplifiers have a gain of 16 dB. In S-band a transistor amplifier is used following the paramp. The low noise and extra gain of the transistor amplifier assures the best possible noise figure in this band. After being amplified, both S-band and Ku-band are down converted to the same 450 to 550 MHz I.F. band. In S-band this is accomplished with a single fixed L.O. In Ku-band, however, reception must be accomplished over a 400 MHz BW which requires tuning of the first L.O. in four 100 MHz steps, i.e., 13,150, 13,250, 13,350 and 13,450 MHz. Double conversion is employed in both bands to simplify the filter designs and reduce the spurious response levels. Both mixers are the double balanced type to further minimize the undesired responses. After mixing to the I.F. band, the signal is fed to a 500-MHz I.F. amplifier. Each 500-MHz I.F. after mixing receives amplification in the first I.F. amplifier to preserve noise figure. The Ku-band I.F. amp (A2) provides 25 dB gain while S-band (A4) only requires 15 dB gain. The outputs of both amplifiers are resistively summed and filtered. The 500 MHz bandpass filter following this amplifier aids in reducing spurious responses and out-of-band noise. The I.F. bandpass filter is immediately followed by an additional high-gain (+50 dB) AGC amplifier. This amplifier is common to the S- or Ku-band transmissions and maintains a uniform output. The device provides a 24-dB AGC range which compensates for variation in received signal levels or receiver gain. The amplifier output is maintained at -10 dBm, a comfortable level for the next device, the second mixer.

The second mixer converts the 500 MHz spectrum to base band frequencies of 6.0 MHz, 42.5 MHz or 105 MHz depending on which MDR receiver is used and whether TV transmission is being handled.

After mixing, the second I.F. signal is further filtered, depending on the selected mode, in either a 10 MHz or 100 MHz wide band pass filter if MDR 1 is being used. (MDR 2 has 10 MHz bandwidth only). After the filter, one final amplifier is provided to bring the output level up to -10 dBm. This device uses a single transistor stage to provide isolation.

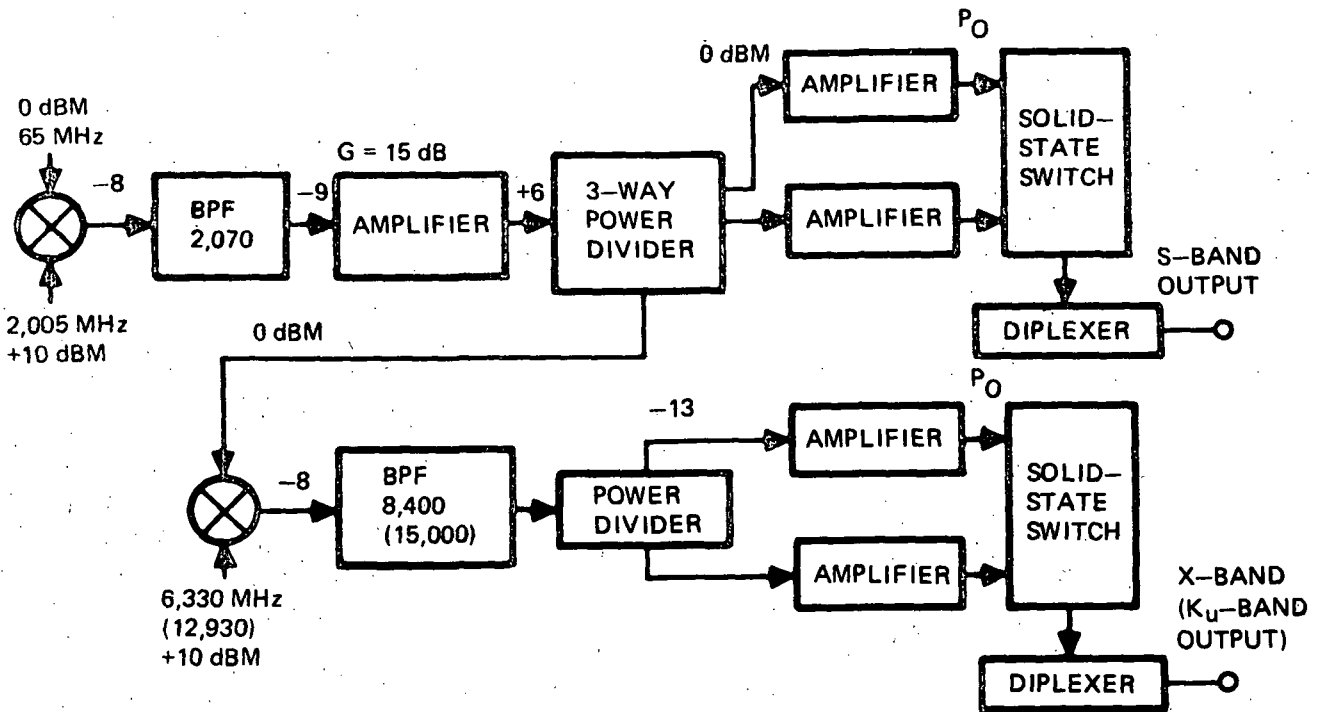


Figure 4-62. Dual Frequency MDR Transmitter

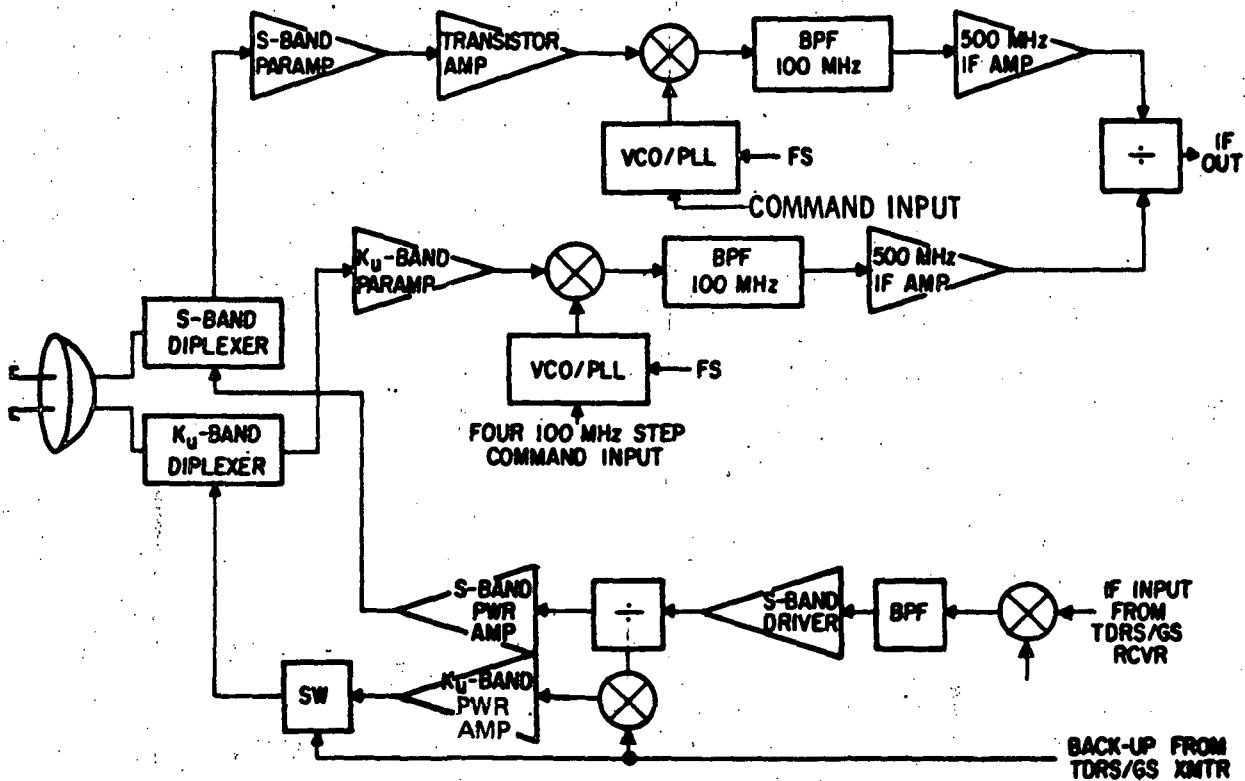


Figure 4-63. MDR Transceiver Block Diagram

4-106

SD 72-SA-0133

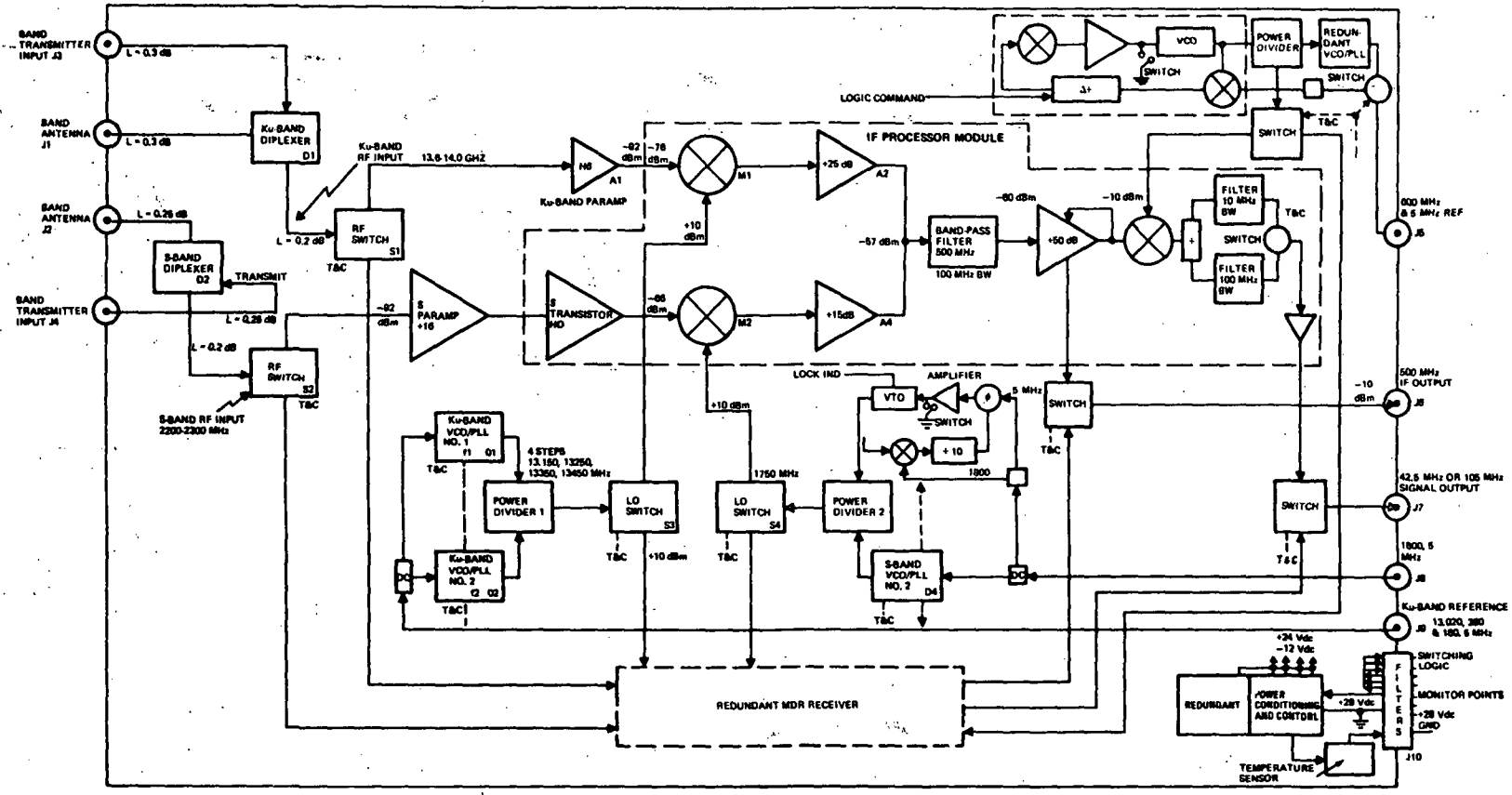


Figure 4-64. MDR No. 1 Baseline Receiver



Space Division
North American Rockwell

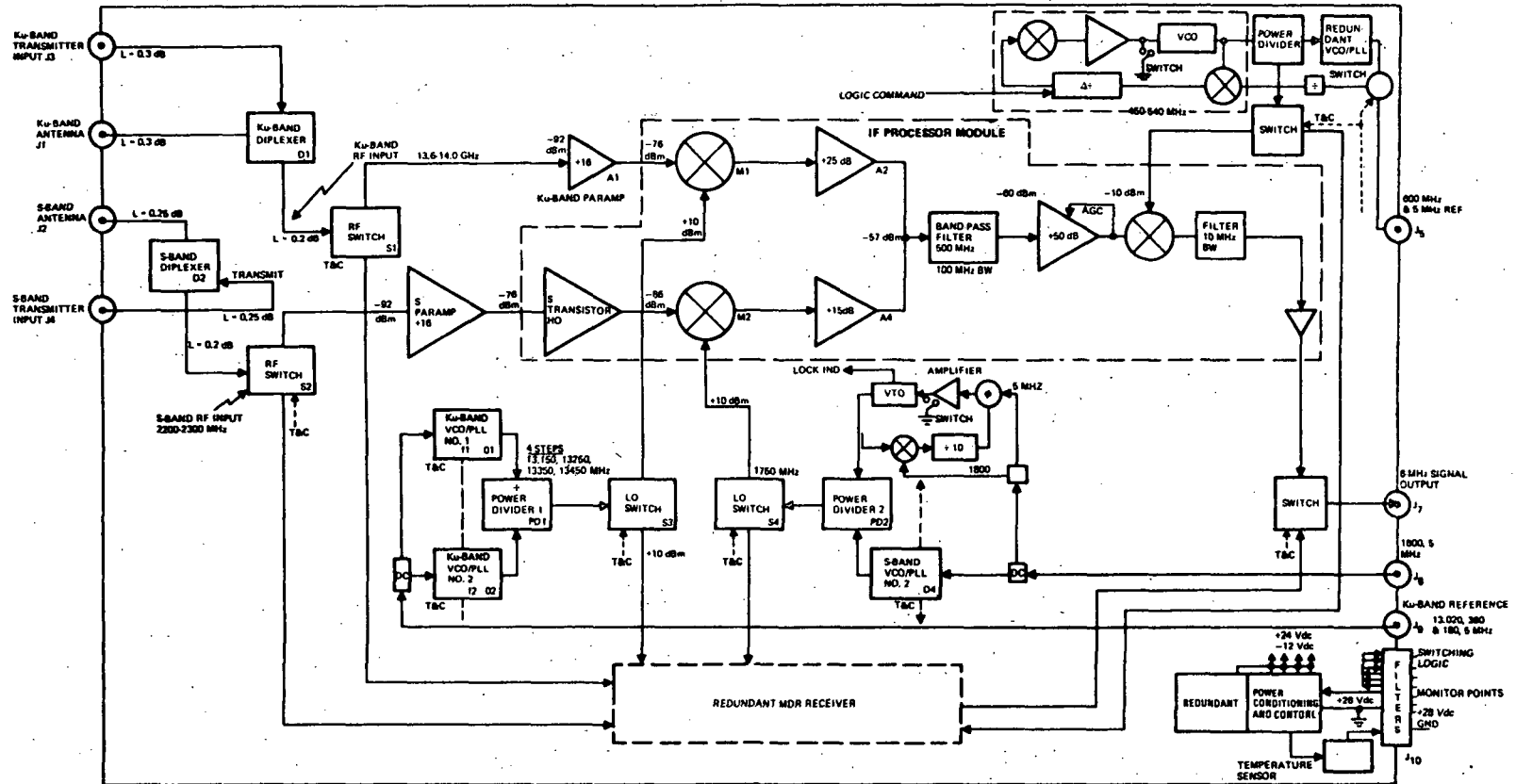


Figure 4-65. MDR No. 2 Baseline Receiver





The MDR receiver is totally redundant with the entire I.F. portion integrated in a hybrid design. Switching is accomplished at the input, following the diplexer, and at the output of the last amplifier. A layout of one MDR receiver is shown in Figure 4-66.

MDR Transmitter. The MDR transmitter accepts an input at 120 MHz (MDR 2) or 240 MHz (MDR 1), translates it to either S- or Ku-band and amplifies the resulting signal for transmission to the MDR user. The instantaneous bandwidth is 95 MHz and occupies the S-band region from 2025 to 2120 MHz. When transmitting in Ku-band, provision is made to select any four center frequencies, spaced at 100 MHz intervals between 14.6 to 14.8 or 15.0 to 15.2 GHz. The instantaneous bandwidth is 95 or 100 MHz at S- and Ku-band, respectively. All frequency translations are accomplished with phase-locked oscillators resulting in a completely coherent transmitter.

The S-band amplifier is transistorized with a nominal output of 14.1 watts (or 56.2 watts for voice transmission). Amplification at Ku-band is accomplished in a five-stage avalanche diode amplifier.

The MDR 1 transmitter is configured with an additional module to provide a backup unit for the TDRS/GS transmitter at either S-band or Ku-band.

MDR 1 Transmitter. Figure 4-67 is a detailed block diagram of the MDR 1 transmitter. The design features seven modules: two S-band, two Ku-band, 2 I.F., and the power control, conditioning, and telemetry module. The first three modules are supplied in pairs to provide 100-percent redundancy. The S-band module accepts a 240-MHz signal at 0 dBm level, up-converts it to 2067.5 MHz with an internally generated phase-locked oscillator, amplifies the resulting signal in a transistorized multistage amplifier, and provides a high-level signal (up to 56 watts) for S-band transmission, and a low-level signal (560 milliwatts) for Ku-band transmission. The low-level preamplifier stages are available today as complete integrated assemblies suitable for direct incorporation into strip line, or as packaged amplifiers in various configurations, including TO-5 cans. The high-level power stages are constructed from discrete components and are configured to be Class C amplifiers to obtain maximum efficiency.

The Ku-band module accepts an input signal at 2067.5 MHz, and up-converts it to Ku-band with an internally generated local oscillator phase-locked to the reference frequency. This signal can be at any of four frequencies between 12,782.5 and 13,082.5 MHz. The resulting Ku-band signal is amplified in a broadband five-stage circulator-coupled avalanche diode amplifier with an overall gain of 38.9 dB. This amplifier is constructed from strip line, with all stages utilizing a common substrate.

MDR-TDRS/GS Backup Mode. The I.F. module input is a video signal derived from the TDRS/GS transmitter. It contains signals in the frequency range from 1 to 35.5 MHz, representing MDR 2, orderwire, TT&C, and the LDR channels. The MDR 1 signal is not present, because its transmitter and antenna are dedicated to TDRS/GS as the backup function. The combined video signal is translated to 240 MHz with a locally generated phase coherent local oscillator and an image reject mixer. This type of mixer is required to suppress the lower sideband

4-109
SD 72-SA-0133

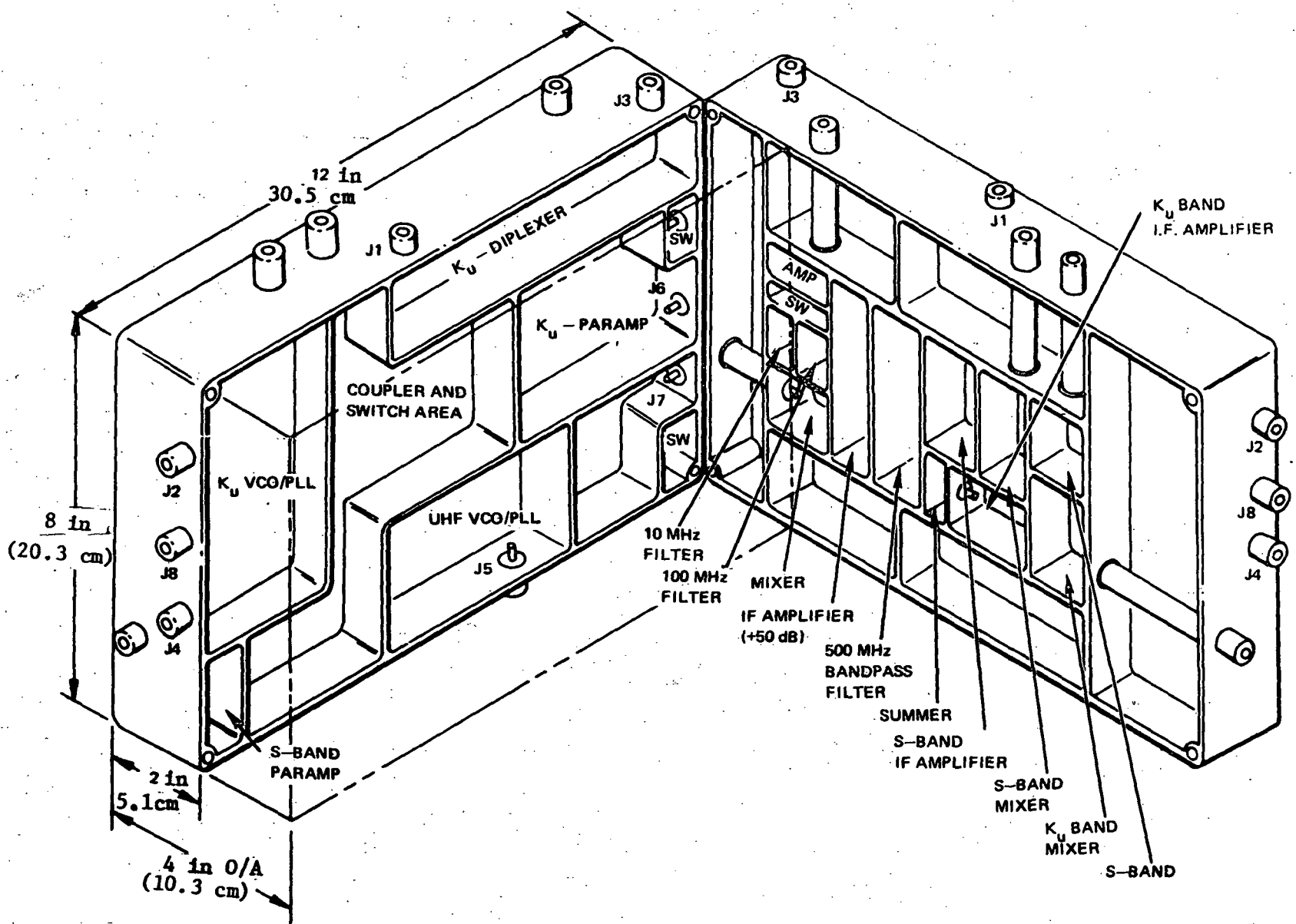


Figure 4-66. MDR Receiver Layout



because a bandpass filter will not provide sufficient rejection. A 240-MHz amplifier increases the signal to the proper insertion level for the S-band module. This level is 7 dB below the normal MDR 1 signal level. The necessity for reducing the signal for the TDRS/GS backup mode arises because the signal linearity requirement of the FDM format and amplitude information must be preserved. (The information in the MDR signal resides in its phase characteristics and not in the amplitude) Therefore, amplifier linearity is important and operation at saturation is not permissible. The backoff of 7 dB from saturation is sufficient to obtain adequate linearity and reduce intermodulation distortion to tolerable levels. The gain of the MDR antenna is approximately 7 dB higher than that of the TDRS/GS antenna; hence, the EIRP remains constant.

Command signals are used to configure latching relays to correspond to the desired operating mode. Telemetry outputs contain verification of the relay positions as well as monitoring output power, crystal currents, case temperature, and phase lock operation.

MDR 2 Transmitter. Figure 4-68 is a block diagram of the MDR 2 transmitter. The description for the MDR 1 transmitter is valid for the MDR 2 transmitter with the exception noted that the No. 2 unit does not have an I.F. module and so cannot function as backup for the TDRS/GS transmitter.

Physical Characteristics. Figures 4-69 and 4-70 show a layout of the S-band modules, primary and redundant unit. They are designed to nest together to form a rigid, compact assembly. The Ku-band module is constructed similarly and both sets of modules mount to a sturdy frame with the rest of the components.

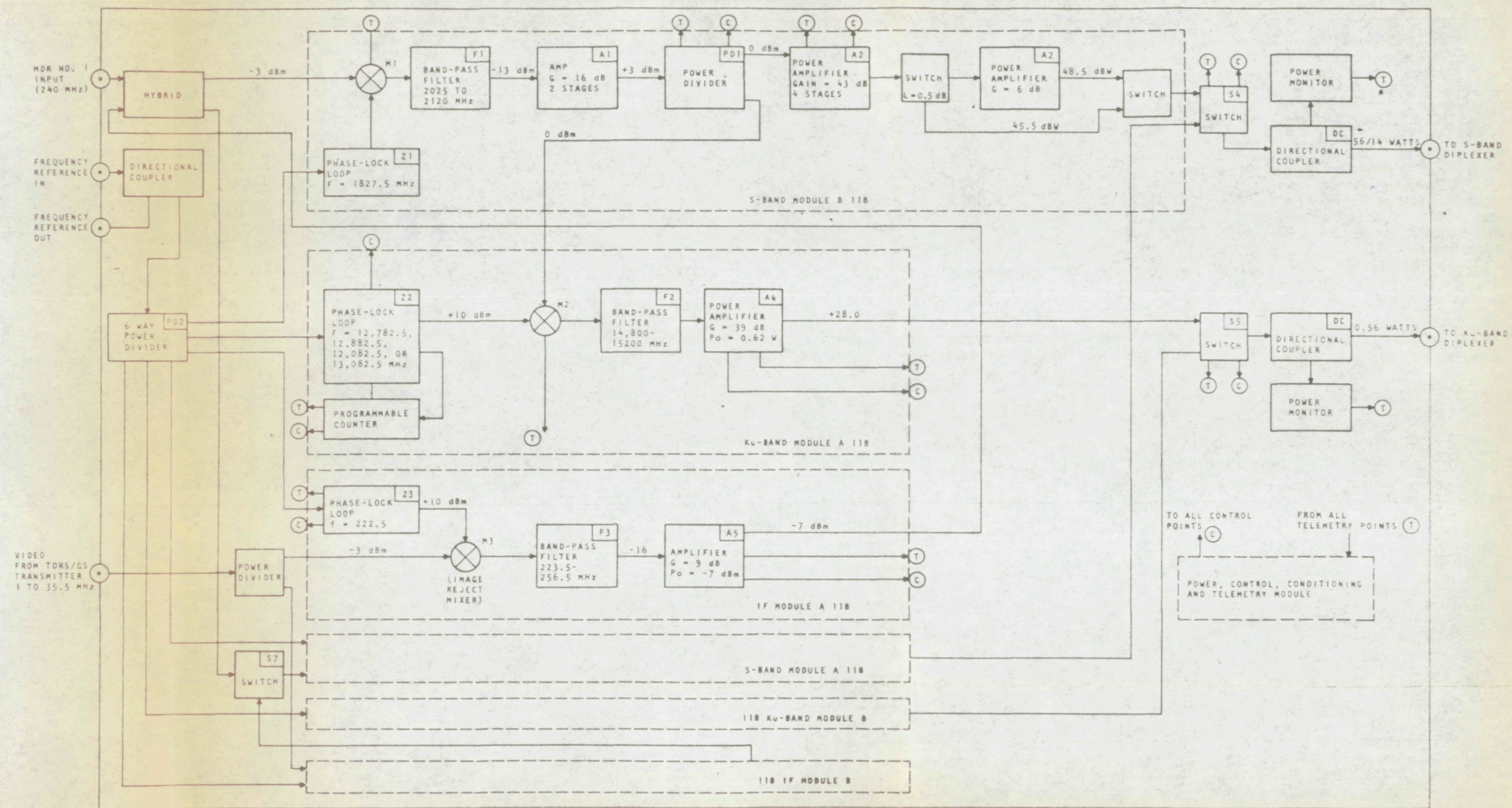


Figure 4-67. MDR No. 1 Transmitter Block Diagram

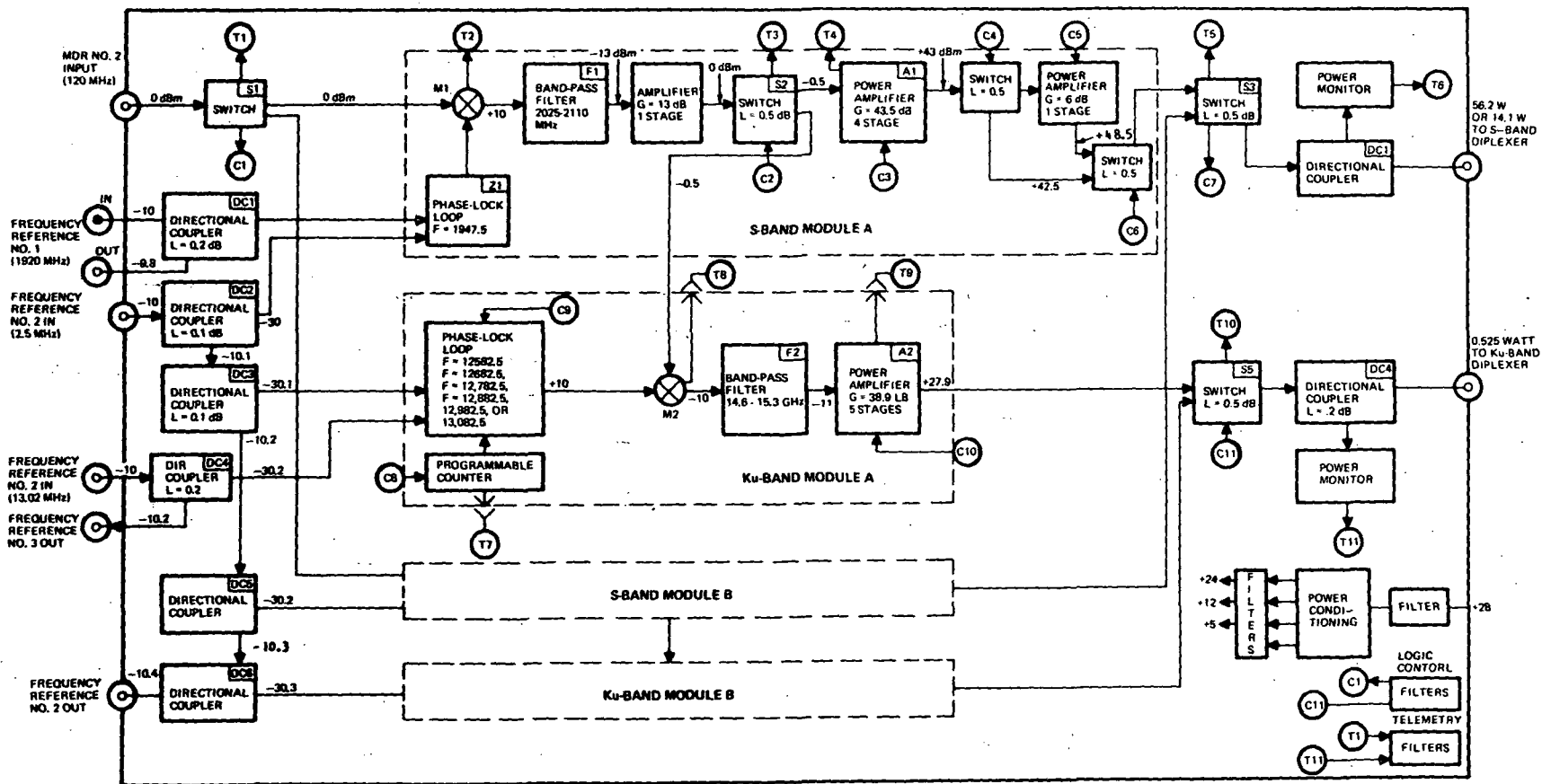


Figure 4-68. MDR No. 2 Transmitter Block Diagram

4-114

SD 72-SA-0133

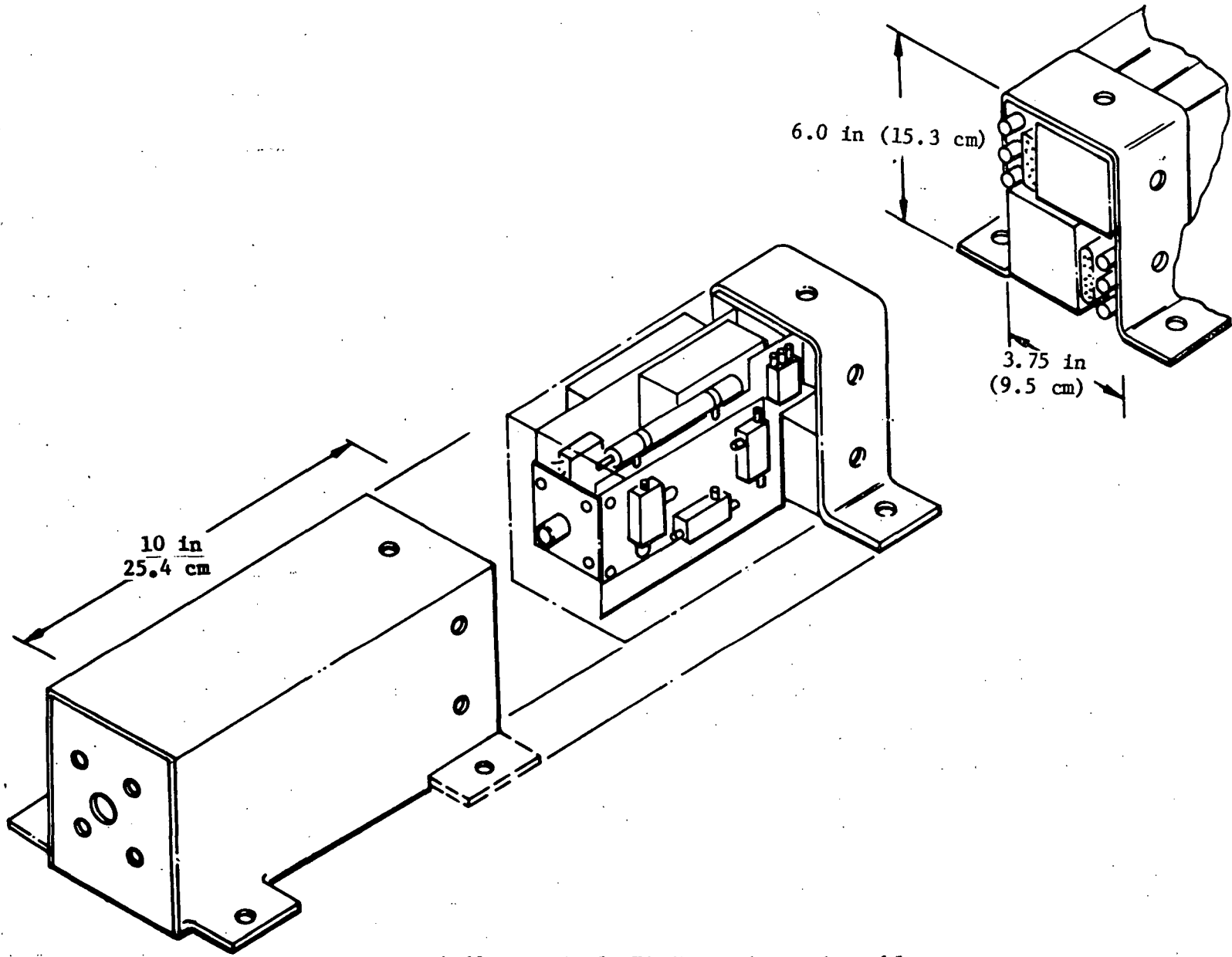


Figure 4-69. Typical MDR Transmitter Assembly

4-115

SD 72-SA-0133

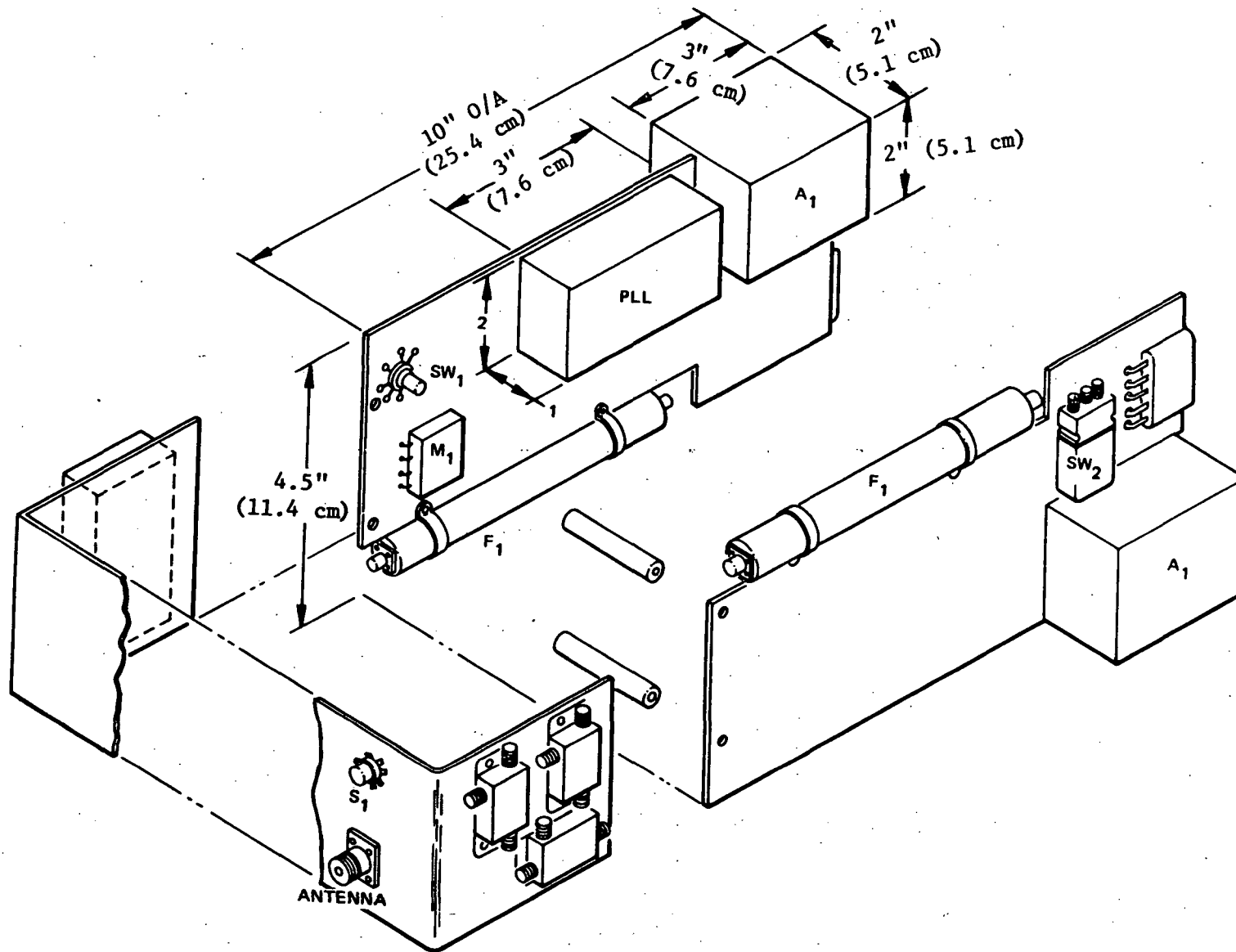


Figure 4-70. MDR No. 1 Module A



4.4.4 Performance Specification for MDR Transponder

4.4.4.1 Scope

This specification establishes the design performance requirements for the MDR transponder located on the TDR satellite. This equipment provides the space-to-space interface between the MDR user(s) and the TDRS relay satellite.

4.4.4.2 Components

The major components of the MDR transponder are:

- . Antenna
- . Receiver
- . Transmitter

4.4.4.3 Design Requirements

MDR Antenna - Dual Frequency S/Ku-Band

<u>Parameter</u>	<u>S-Band</u>	<u>Ku-Band</u>
Frequency, GHz		
Transmit	2.025 to 2.120	14.6 to 15.2
Receive	2.200 to 2.300	13.6 to 14.0
Antenna type	Parabolic dish	Parabolic dish
Antenna type	6.5 ft (2 m) dia.	6.5 ft (2 m) dia.
Feed type	Prime focal point	Cassegrain
Gain, dBi (midband)	30.2	47.6
HPBW, degrees (mr)	≈5.0 (87.3)	≈0.65 (11.3)
Polarization	RH or LHCP	RH or LHCP
Axial ratio, dB max	1.5	1.5
Input VSWR, dB	1.4:1	1.4:1
Side and back lobe levels, dB	≤ 17.0	≤ 17.0
Total antenna, eff., %	≥52	≥65 (sum mode)
Tracking configuration	Open	Closed (pseudo mono-pulse)
Tracking accuracy (3σ), degree (mr)		0.33
Pointing accuracy (3σ), degree (mr)	0.5 (8.7)	0.5 (8.7)
Gimbal step size, deg (mr)		0.03 (5.2)
Slew rate, deg/sec (mr/sec)	Nominal	1.0 (17.5)
	Maximum	5.7 (99.5)
Scan angle off boresight - 2-axis, degrees (rad)		15.5 (0.27)
Total weight - lb (kg), include: fee/microwave system (incl. rotary joints)		28.26 (12.8 kg)
Reflector & feed support Gimbal system		
Drive electronics Support strut		5.7 (2.59 kg)



<u>Parameter</u>	<u>S-Band</u>	<u>Ku-Band</u>
Total power - peak (watts) includes motor drive (6 watts/axis), motor clamping (4 watts/axis), electronics		24.0
Total power - average (watts) includes motor power slew, motor power - track (open or closed loop), electronics		7.0

MDR Receiver

Noise figure	2.5 dB	3.5 dB
Frequency range	2200 to 2300 MHz	13.6 to 14.0 GHz
First IF frequency	500 MHz	Same
First IF BW	100 MHz	Same
Spurious level	50 dB down	Same
Baseband freq., MHz	7.5, 42.5, 105	Same
Temperature	0 to 50 C	Same
Redundancy	100 percent	100 percent

MDR No. 1 Transmitter

Input Signals

MDR 1: $f_o = 240$ MHz, BW = 95 MHz, $P_i = 0$ dBm
 Frequency reference: 2.5 MHz, -10 dBm
 Video (TDRS/GS): 1 to 35.5 MHz, $P_i = 0$ dBm

Output Frequency

S-band: 2025 to 2120 MHz
 Ku-band: 100 MHz band centered on: 14,650, 14,750, 15,050 or 15,150 MHz

Output Power

S-band: 14 watts normal, 56 watts in voice mode
 Ku-band: 0.56 watt

TDRS/GS Backup Mode. Outputs reduced 7 dB to preserve linearity throughout system

Frequency Translation. Coherents, using phase lock loops

Redundancy: 100 percent
 DC input: 28 volts
 Volume: 4.5 x 6 x 10 inches (11.4 x 15.2 x 25.4 cm)
 Weight: 13 lb (5.91 kg)

MDR No. 2 Transmitter

Input Signals

MDR 2: $f_o = 120$ MHz, BW = 95 MHz, $P_i = 0$ dBm
 Frequency reference: 2.5 MHz, -10 dBm

Output Frequency

S-band: 2025 to 2120 MHz
 Ku-band: 100 MHz centered on: 14,650, 14,750, 15,050 or 15,150 MHz



Output Power

S-band: 14 watts normal, 56 watts in voice mode
Ku-band: 0.56 watt

Frequency Translation. Coherent, using phase lock loops

DC input: 28 volts
Redundancy: 100 percent
Volume: 3.75 x 6 x 10 inches (9.5 x 15.2 x 25.4 cm)
Weight: 11 lb (5 kg)

4.4.4.5 Size, Weight, and Power Summary of MDR Transponder

The size, weight, and power requirements are summarized below for the two MDR transponders on each TDRS satellite. Note that the transmitter configurations are slightly different for each MDR transponder

<u>Component</u>	<u>Size</u>	<u>Weight</u> lb (kg)	<u>Power (watts)</u>	
			<u>(Peak)</u>	<u>(Avg)</u>
MDR No. 1				
Antenna system	6.5 ft (2 m) diameter	33.96 (15.4)	24.0	7.0
Receiver	12 x 8 x 4 in. (30.5 x 20.3 x 10.1 cm)	8.80 (4.0)	6.2	6.2
Transmitter:				
S	6 x 4.5 x 10 in. (15.2 x 11.5 x 25.4 cm)	13.0 (5.9)	190.0*	47.5
Ku				14.5
MDR No. 1				
Antenna system	6.5 ft (2 m) diameter	33.96 (15.4)	24.0	7.0
Receiver	12 x 8 x 4 in. (30.5 x 20.3 x 10.1 cm)	8.80 (4.0)	6.2	6.2
Transmitter				
S	6 x 3.75 x 10 in. (15.2 x 9.5 x 25.4 cm)	11.0 (5.0)	180.4*	45.1
Ku			13.2	13.2
Total		109.5 (49.7)		
Two S-band				119.0
One S and One Ku				87.1
Two Ku				54.1

*Peak power for voice operation



4.5 TDRS/GS LINK

4.5.1 System Analysis and Trades

To define the TDRS/GS requirements it is first necessary to compute the link requirements and to establish the link and terminal parameters for this space-to-earth link. The overall losses are a combination of equipment losses, attenuation due to distance, and losses from weather conditions. Since this link sees the earth's atmosphere, its effect and impact on the spaceborne and ground terminal designs must be determined. To determine its impact, a model of the earth's atmosphere as developed by Holzer is used, Holzer's result agrees favorably with Altschuler's² model. The results agree closely with the test data from ATS-V experiment³.

The empirical formulas give constants for attenuation per kilometer as a function of the angle off the zenith. The results for the contribution of the atmospheric gases to the attenuation of a 15 GHz signal on a clear day is 0.4 dB. Clouds add 2.4 dB to give 2.8 dB of attenuation which can be expected before rain starts. Once the rain starts, it is measured in millimeters per hour and used in Holzer's formula:

$$A_r \text{ (dB)} = 0.07 R^{1.155} \text{ CSC}(\theta)$$

to find the attenuation as a function of the rate of rainfall, and the viewing angle off the horizon. This additional attenuation affects the signal by directly attenuating it, and by increasing the noise level. The system noise temperature is related to the total atmospheric attenuation and the receiver noise temperature by:

$$T_s \text{ (°K)} = \left(1 - \frac{1}{A}\right) 274.8 + T_r$$

The above relationships can be used to find the change in CNR caused by the presence of a certain rain rate. This change is referred to as the rain margin of the system, and relates to the rain rate according to:

$$M \text{ (dB)} = A_r + T_s \text{ (rain)} - T_s \text{ (clear)}$$

where $T_s \text{ (clear)}$ is the sky temperature found without any attenuation due to

1. Microwave Journal, page 119, March 1965.
2. AFCRL-65-566, August 1965.
3. Ippolito, Goddard Space Flight Center, November 1970.



rain or clouds. These relationships do not yet get us anywhere until there is more information available on the probability of rain at the ground station location. The location is assumed to be near Washington, D.C., and for this reason, the plot in Figure 4-71* of rain rate versus probability of that rain rate occurring applies to the GS. Now the previous relationships can be used to find the reliability of maintaining the link as a function of the margin chosen. A plot of this function, as a function of receiver noise temperature, is shown in Figure 4-72. The curve has an obvious knee with a steep slope below 10 dB, and very little slope above 20 dB of rain margin. To take advantage of as much reliability as possible without a large increment in power, a margin of 17.5 dB has been chosen.

In the above computation, a cooled and uncooled parametric amplifier was compared for the GS front end as shown in Figure 4-72. The reliability for a more sensitive and expensive cooled parametric amplifier ($T_r = 50$ K) is less than an uncooled ($T_r = 200$ K) amplifier. This is because a change in CNR was found rather than absolute CNR levels. The change in system temperature is greater for the cooled amplifier since the contribution of the receiver is less and, therefore, the differential CNR for heavy rain temperature-to-no rain temperature is larger. This is one reason in favor of using an uncooled param receiver. Other reasons include the greater cost and maintenance needed for the cooling system. To make the selection final, it is necessary to trade off the antenna size and transmitter power.

In order to compute the terminal parameters, it is necessary to determine the CNR in a tandem link. In the forward link, CNR is dependent on the channel being discussed. The MDR space-to-space link requires the highest CNR and, therefore, is used as a guide in designing the system. For Δ PSK and P_e of 10^{-5} , a SNR of 9.9 dB is required at the output of the MDR user demodulator. For a tandem link with an allowable degradation of 0.25 dB through the TDRS relay transponder, one of the two links has a CNR of 10.15 dB. The CNR of the remaining link can be determined from

$$CNR_2 = \frac{CNR_f (CNR_1 + 1)}{CNR_1 - CNR_f}$$

and comes out to be 3 dB. With the 10.15 dB CNR on the space-to-user link to conserve power in the satellite, the ground-to-space link must have a CNR of 3 dB.

The antenna on the ground is a 60-foot dish with an efficiency of 75 percent providing a gain of 67.9 dB. If a mixer front end is used in the satellite, a noise temperature of 33.6 dB is obtained. If a paramp is used in the satellite front end, the system temperature drops to 27 dB. However, the weight and power consumption of the receiver increases significantly when the paramp is used so that it is desirable to find enough gain elsewhere to allow a mixer to be used.

* The Climatic Handbook for Washington, D. C. Weather Bureau Technical Paper No. 8, Dept. Comm., January 1949.

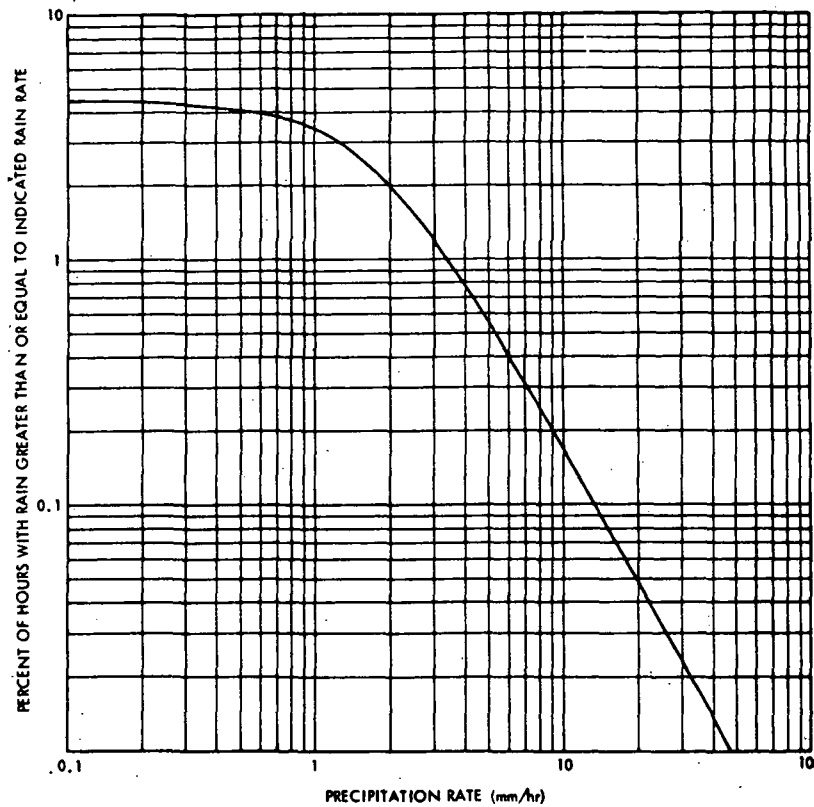


Figure 4-71. Probability Distribution of Rainfall Rates, Washington, D.C.

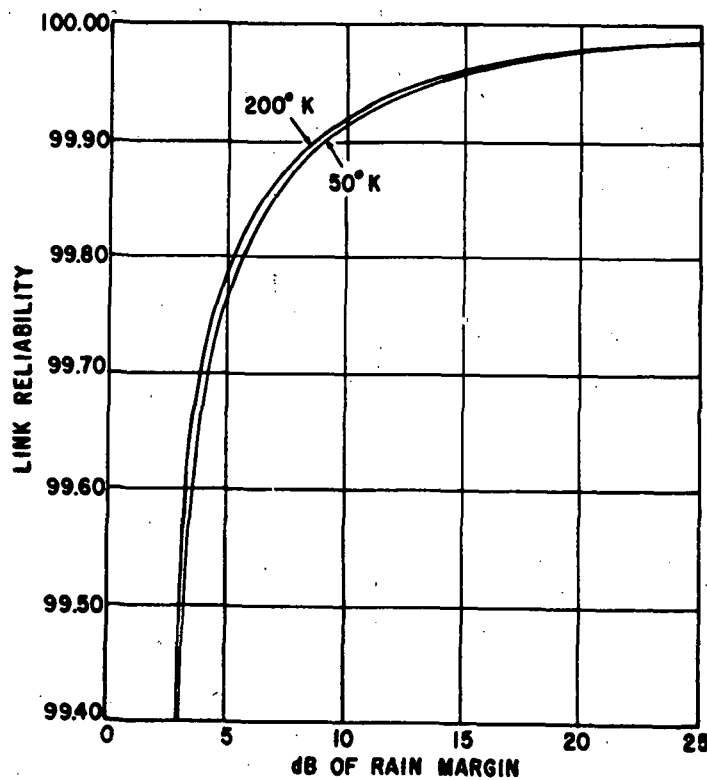


Figure 4-72. Link Reliability versus Rain Margin for Cooled and Uncooled Receivers

Table 4-19 is the transmitter power required for the various combinations of antenna and receiver at the spaceborne and ground based terminals. The power required of the satellite transmitter varies from 1.7 watts to more than 6 watts. The 3.5 dB advantage of the 60-foot ground antenna has little effect on the power system requirements of the satellite, but it does save 1000 watts in the ground transmitter, and at the same time enables the receiver in the satellite to use a mixer front end. This saves more weight and power in the satellite than is saved in the transmitter section. Earlier discussion has shown the uncooled paramp has a slight advantage in reliability. Table 4-19 shows that one more watt of power is needed in the satellite transmitter power which is more than made-up for by using the mixer in the satellite. Therefore, an uncooled paramp can be used at the ground station.

Table 4-19. Transmitter Power in dBw Versus Ground Antenna Diameter and Type of Receiver

Transmitter	Receiver	Power in dBw	
		Ground Antenna Diameter	
		40' (12.2m)	60' (18.3m)
Satellite	Paramp cooled	5.7	2.2
	Paramp uncooled	7.9	4.4
Ground	Mixer	32.4	29.1
	Paramp uncooled	25.8	22.3

Table 4-20 summarizes the TDRS/GS link characteristics based upon the above trade studies for the worst case channel for both the forward and return link.

The tradeoffs performed to develop the TDRS/GS link design are summarized in block diagram form in Figure 4-73. The basic function of the TDRS/GS link is to provide the means for exchanging data between the GS and the TDRS. Figure 4-73 illustrates that the LDR, MDR, telemetry and order wire received data is initially multiplexed for transmission to the GS.

The selected technique for multiplexing the data is FDM/FM. FDM/FM was compared with FDM, PM, and PCM, and it became apparent that the optimum method of implementing the transmitter section was to trade power for bandwidth by utilizing frequency modulation of the composite signal. Trading power for bandwidth also enables the transmitter design to be all solid state rather than TWTA.

Table 4-20. TDRS/GS Link Characteristics

Parameter	Forward Link**	Return Link*
CNR (carrier-to-noise ratio) required	3.0 dB	0 dB
P_T (transmitter power)	13.9 dBw	4.3 dBw
G_T (TDRS antenna gain)	39.6 dB	40.3 dB
G_R (GS antenna gain)	67.0 dB	67.9 dB
α_S (free space losses)	207.2 dB	208.1 dB
α_{ATM} (atmospheric attenuation)	-0.4 dB	0.4 dB
α_2 (miscellaneous losses)	-7.4 dB	-2.1
K (Boltzmanns constant)	-228.6	-228.6
T (system temperature)	33.6 dB	25.2 dB
B (RF bandwidth)	80.0 dB	87.8 dB
M (rain margin)	17.5 dB	17.5 dB

NOTES: *Worst-case--MDR TV Channel
**Worst case--MDR (shuttle--data + 2 voice)

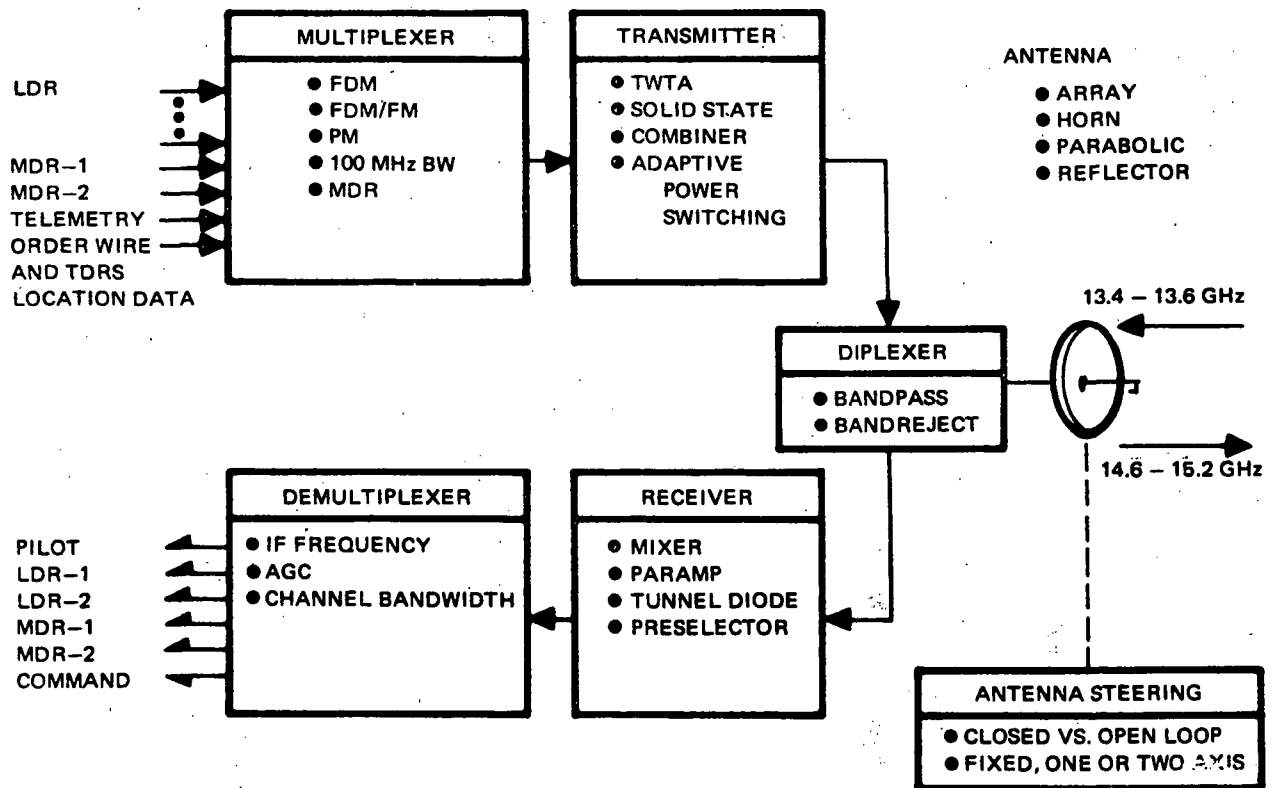


Figure 4-73. TDRS/GS Link Transceiver Tradeoff Considerations



The maximum transmitter output power is based upon operating in a rain rate of 25 mm/hr which requires a 17.5 dB margin for 99.97 percent availability. Since the 25 mm/hr rain rate is a rare occurrence, adaptive power control was included in the design. Therefore, in a heavy rain 10 dB of additional Ku-band power is switched in by controlling the bias on the solid state amplifier. However, the average satellite power requirement is substantially reduced and can be applied to other more critical links.

The output of the transmitter which has a bandwidth of 200 MHz for two 10 MHz MDR's and 600 MHz for a television transmission is coupled through a diplexer as shown in Figure 4-73, to a 3' (0.9m) parabolic reflector. The diplexer design is a bandpass filter in the receiver leg (13.4 to 13.64 GHz) and band reject filter in the transmit leg (14.6 to 15.2 GHz) to minimize losses. The antenna trades compared an array and horn implementation with the parabolic reflector.

For the receiver front end, a mixer, parametric amplifier, and tunnel diode amplifier were compared and a mixer was selected. The choice was based upon putting the transmit power burden on the ground station to minimize the TDRS hardware and power requirements.

The receiver output then drives a demultiplexer where the six data channels are separated to drive the LDR, MDR transceivers, lock the frequency source to the pilot, and inject command signals into the TDRS subsystem. Automatic gain control was selected on each individual demultiplexer output to compensate for changes in signal level due to rain or operating mode.

4.5.2 TDRS/GS Link Antenna

4.5.2.1 Mechanization Trades for TDRS/GS Antenna

A parametric tradeoff of candidate antenna types for use on the space-to-earth link was made, using minimum weight as a selection criteria. The results are compared in Figure 4-74 for the pyramidal horn, planar array, and parabolic dish at the link operating frequency in the Ku-band. Table 4-21 summarizes the pertinent comments of each design.

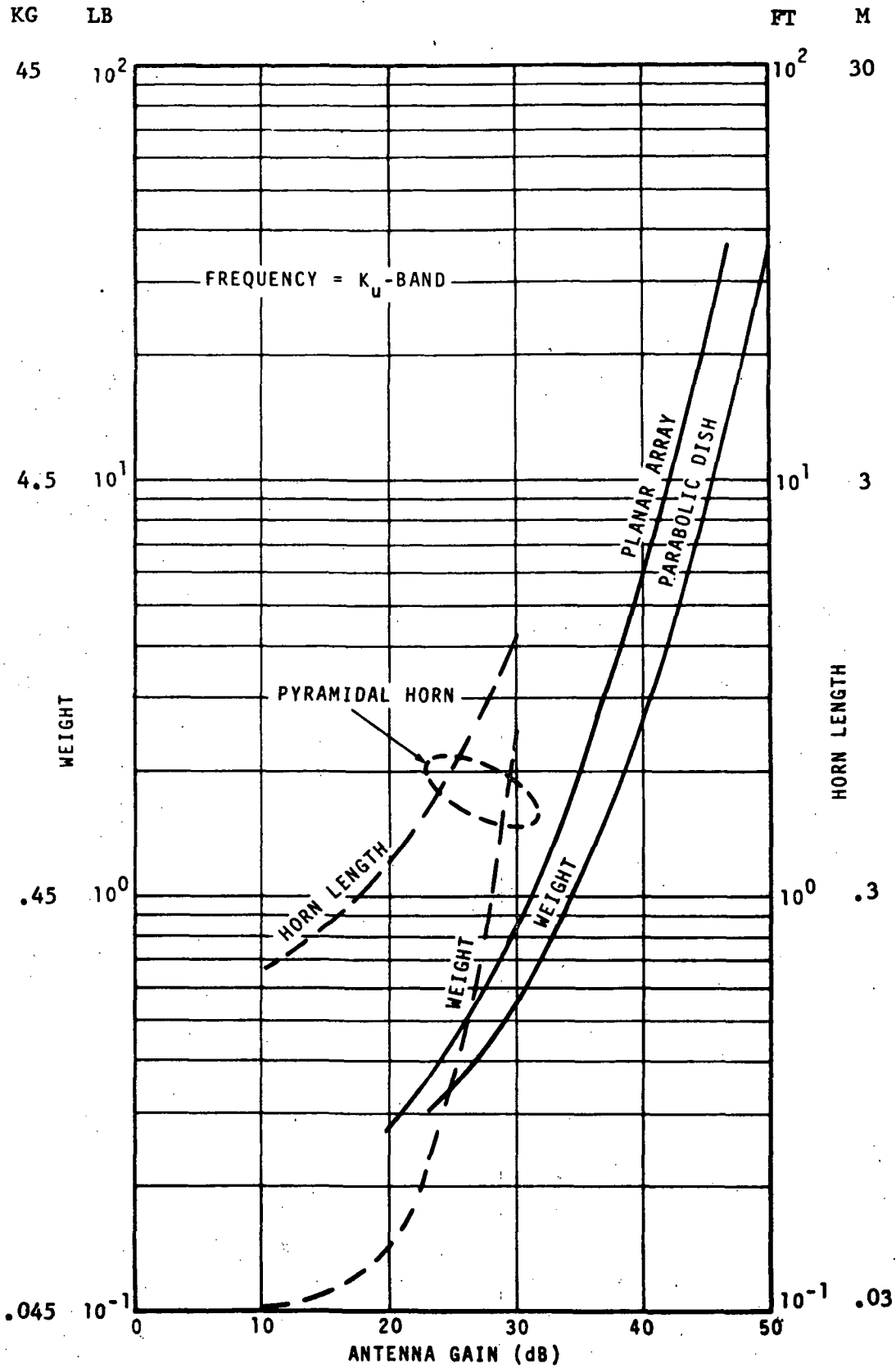


Figure 4-74. Comparison of Antenna Gain vs Weight

Table 4-21. Comments on Candidate Ground Link Antenna Designs

Approaches	Comments
Pyramidal horn	For gains greater than 25 dB this approach has a weight disadvantage associated with the required horn length when compared to a parabolic dish approach.
Planar array	For gains greater than 20 dB the planar array has a weight disadvantage when compared with the parabolic dish.
Parabolic dish	Most favorable on a weight basis for gain ranges of interest. Design is focal point turnstile junction feed with a aluminum honeycomb solid panel.

Link calculations have shown that a 3' (0.9 m) aperture providing nominally 40 dBi gain is required for this link. For this gain, the results of Figure 4-74 and Table 4-21 show that a 3' (0.9 m) parabolic dish is the optimum antenna type to use. Furthermore, since this antenna provides a HPBW of approximately 1.5° (26.2 mr), no closed loop tracking is required to maintain the GS within its 1 dB point. However, the antenna will be mounted on a one-axis gimbal to provide the flexibility to use a common antenna design for both operational TDRS satellite configurations and the spare.

4.5.2.2 Detailed Design - TDRS/GS Antenna

The Ku-band TDRS/GS link uses a 3' (0.9 m) diameter antenna with open loop, one axis tracking. This downlink antenna utilizes an aluminum honeycomb core reflector design with solid panels and a turnstile junction apex Ku-band feed. A gimbal system similar to that for the 6.5' (2 m) antennas is used. An overall efficiency of 52 percent is projected with total weight and peak power requirements of 11.5 lb (5.2 kg) and 9.5 watts, respectively. The detail design of the reflector and positioning is presented in section 5.3.3.

Ku-Band Feed/Microwave Design. Operation in Ku-band with reception in the 13.4 to 13.64 GHz band and transmission in the 14.6 to 15.2 GHz band is accomplished with a circularly polarized turnstile junction feeding the 3 ft (.9m) diameter reflector. A reflector f/D ratio of 0.375 is recommended to provide optimized gain for the turnstile junction feed primary pattern beamwidth.

Mechanically, the feed is supported by WR-75 waveguide and two additional spar support members, oriented 120° (2.1 rad) apart, and attached to the periphery of the reflector, one waveguide rotary joint is used to accommodate the one axis tracking motion of the antenna. A non-contacting choke joint is used at the interface between the stationary and rotating sections of the joint to provide RF continuity without physical contact and long life.



The projected electrical performance of the antenna subsystem is shown below. The projections are based on previously measured data on similar antenna systems.

Operating frequency:

Transmit band	14.6 to 15.2 GHz
Receive band	13.4 to 13.64 GHz
Input VSWR	1.4:1 maximum
Polarization	Right-hand circular
Axial ratio	2 dB maximum
Aperture efficiency	65 percent

Gain at interface:

Transmit band	40.3 dB
Receive band	39.6 dB
Total efficiency	52 percent

Gain at the interface point is developed in detail below by considering the aperture gain and reducing it by the component losses to the interface point for both the transmit and receive bands.

Component	Receive Gain	Transmit Gain
Antenna aperture	40.5 dB	41.2 dB
Turnstile feed	0.10 dB	0.10 dB
Mismatch loss	0.13 dB	0.13 dB
Two rotary joints	0.50 dB	0.50 dB
4 ft (1.2 m) waveguide	0.16 dB	0.16 dB
Interface gain	39.6 dB	40.3 dB

The salient features of this system are shown in Table 4-22.



Table 4-22. Weight Budget and Power Summary for Ku-Band System

Weight Budget		
<u>Item</u>	<u>Weight-Pounds (lb) (Kg)</u>	
Feed, waveguide, rotary joint	3.8	(1.73)
Reflector	2.80	(1.27)
Gimbal system	3.25	(1.48)
Electronics	5.0	(2.27)
Total	14.85	(6.75)

Power Budget Peak	
<u>Item</u>	<u>Power Watts</u>
Motor drive (5 watts/axis)	5.0
Motor clamping (3 watts/axis)	3.0
Electronics	1.5
Total Peak Power	9.5

Power Average is negligible since the antenna is only moved once on its initial arrival on station.

4.5.3 TDRS/GS Transceiver

4.5.3.1 Mechanization Trades for TDRS/GS Transceiver

The mechanization tradeoffs to be performed in the TDRS/GS transceiver are identified in Figure 4-73. In the receiver area, the basic trades were:

1. Low noise amplifier device
2. Type of receiver

No RF amplifier is used in this receiver. Ten dB noise figure can be obtained using a mixer front end in direct conversion. This receiver tolerates the additional loss because the signal is received from the ground station. Additional ERP at the ground station easily makes up for the mixer contribution to the receiver noise figure.

In the types of receiver, single versus double conversion approaches were evaluated. Double conversion was chosen for this receiver with the first IF at 500 MHz. At this frequency ultra low noise amplifiers are available



yet the IF is high enough that the RF image in Ku-band is 1000 MHz away. Wide image spacing means that no RF filtering is required beyond that obtained in the diplexer. To minimize the number of VCO's the second IF has multiple IF frequencies permitting a single L.O. frequency shared by the six second IF mixers. This trade eliminates five L.O. frequencies or ten VCO/PLL's with full block redundancy.

The GS/TDRS receiver uses AGC in the last IF amplifier. AGC here eliminates variation in signal power fed to the forward link (LDR and MDR) transmitters due to variations in the GS/TDRS link. Reduction of power variations at the user spacecraft minimizes the impact of the TDRS system interface with the user spacecraft. The GS/TDRS receiver is an integrated design with the exception of the VCO/PLL's for Ku-band and UHF. This type of construction is essential for minimum size and weight. A summary of the TDRS/GS receiver mechanization trades is presented in Table 4-23.

Table 4-23. TDRS/GS Receiver Mechanization Trades Summary

Trade Possibilities	Decision	Primary Reason
Single conversion Double conversion	Double conversion	Reduces number of L.O.'s and simplifies front end filtering
Paramp front end Mixer front end	Mixer front end	Optimum noise figure not essentially in this receiver
Multiple L.O.'s/ fixed IF's Multiple IF's/ single L.O.	Multiple IF's Single L.O.	Less size and weight Better reliability
AGC (yes/no)	Yes	Minimizes signal variations at user spacecraft
Redundancy	(100%) two-segmented parallel receivers	Better reliability
First IF frequency VHF/S-band	VHF (500 MHz)	(Optimum) lowest possible without producing filtering problems

In the TDRS/GS link transmitter mechanization tradeoffs, the system design for the return segment of the ground link is based upon the transmission of the data shown in Table 4-24. The transmit power requirements of the TDRS/GS, in addition to the link parameters, are a function of the degradation which is permitted in the signal as it passes through the TDRS. The amount of CNR degradation is a function of the received CNR at the TDRS and the CNR received at the GS. Figure 4-75 illustrates the CNR at each point in the overall return link based upon ending up with the final CNR listed in Table 4-24 for each function. Considering the LDR channels, the requirements for this link are based upon providing a CNR = 9.9 dB at the GS. To determine the CNR_{GS} which must be generated on the TDRS/GS link so that the LDR signal degradation is limited to a maximum of 1 dB and to calculate the degradation caused by the tandem link, the expression applied is:

$$CNR_F = \frac{CNR_{TDRS} \cdot CNR_{GS}}{CNR_{TDRS} + CNR_{GS} + 1}$$

where,

CNR_F = final carrier-to-noise ratio

CNR_{GS} = CNR generated on TDRS/GS channel

CNR_{TDRS} = CNR received from the user in the TDRS receiver bandwidth

The degradation in carrier-to-noise is $\Delta CNR = CNR_{TDRS} - CNR_F$. These parameters are plotted in Figure 4-76 and it is with this relationship that the CNR_{GS} can be established for each of the various channels.

Table 4-24. Ground Return Link Requirements

Function	Number of Data Channels	Channel Bandwidth	Maximum Bit Rate	Final CNR-dB
LDR	8	2 MHz	10 kbps data 1 Mbps PN code	9.9 dB
Telemetry	1	1 MHz	31 kbps data 500 kbps PN code	9.9 dB
Order wire and location system	1	1 MHz	100 bps data 500 kbps PN code for all signals	9.94 dB
MDR-2	1	10 MHz	1 Mbps	9.9 dB
MDR-1	1	10 MHz	1 Mbps	9.9 dB
	1	100 MHz	1 Mbps or TV	

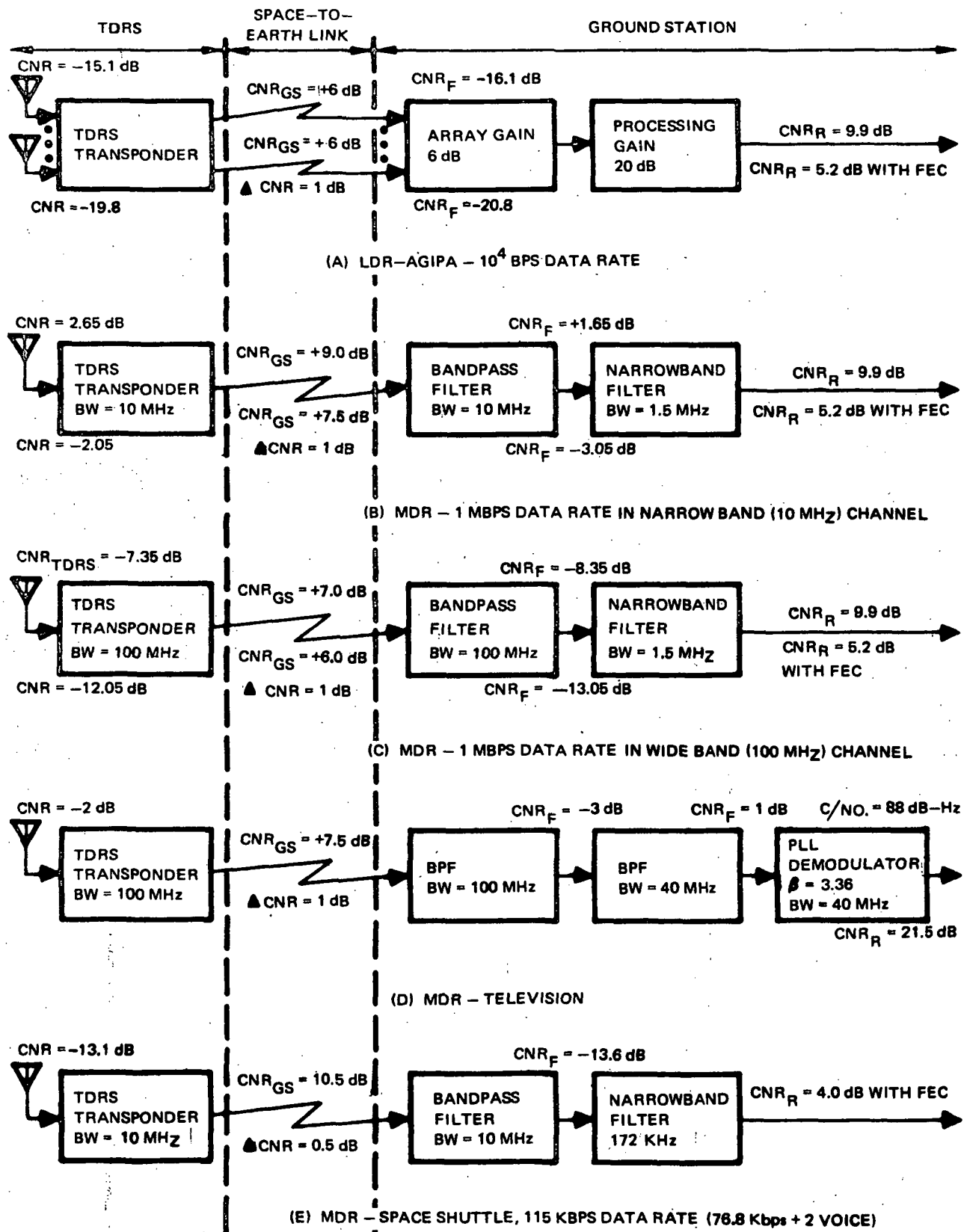
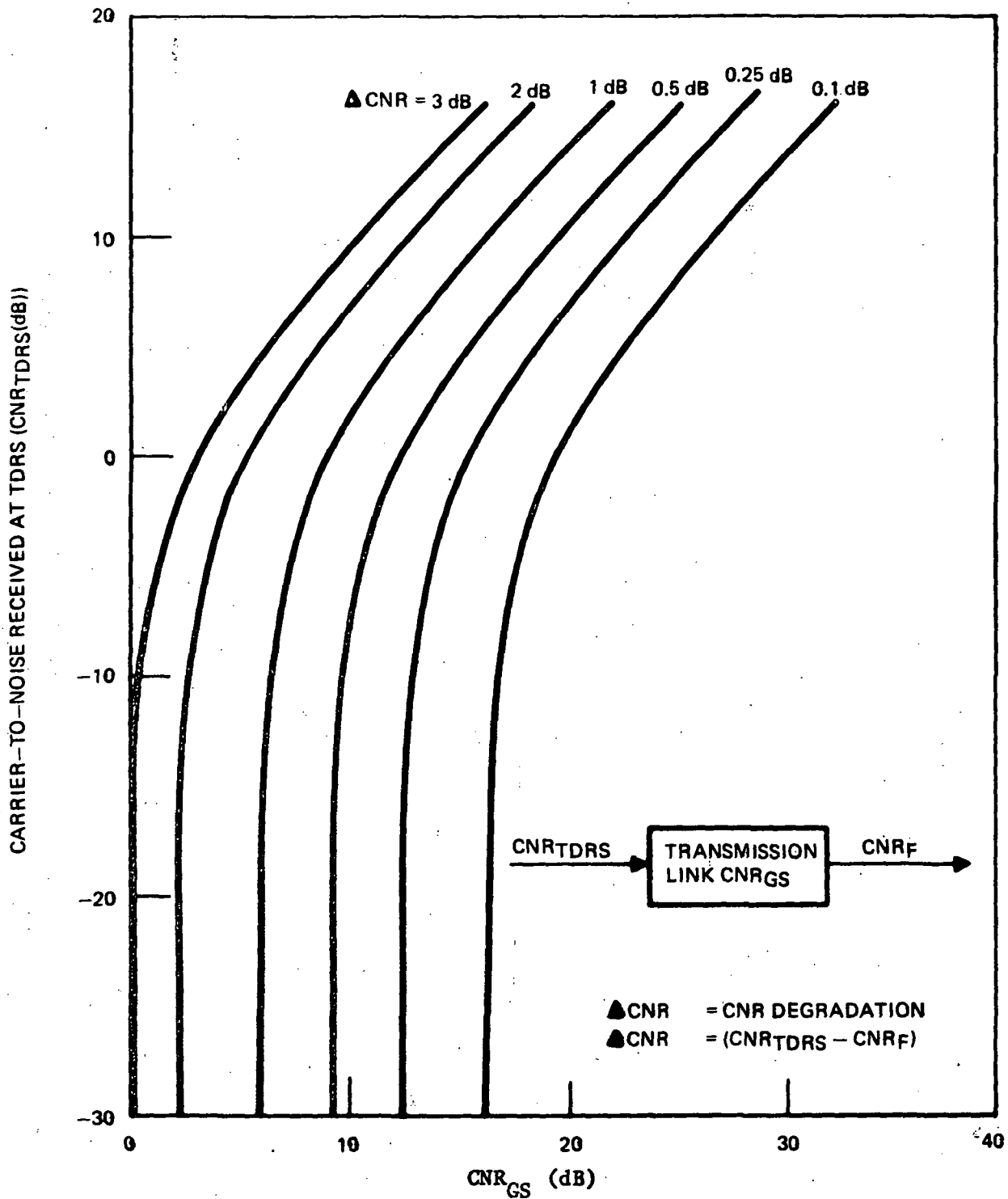


Figure 4-75. Tandem Link Calculation TDRS/GS Return Link



CARRIER-TO-NOISE RECEIVED AT GROUND STATION

Figure 4-76. CNR Requirement in Tandem Link as a Function of CNR Degradation through TDRS



Referring again to Figure 4-75A for a spread spectrum processing gain of 20 dB, assuming a data rate of 10 kbps and chip rate of 1 Mbps, a $CNR = -10.1$ dB is required in a 1.5 MHz bandwidth. For the LDR, combining the four AGIPA array elements at the ground station yields an additional 6 dB of processing gain. Note that no allowance is made for any additional AGIPA processing improvements of RFI or polarization diversity; therefore, this represents a minimum case. Each of the eight LDR channels received on the ground must have a minimum $CNR_F = -16.1$ dB for the LDR to remain above the 9.9 dB threshold level. To permit a maximum degradation in CNR of 1 dB, from Figure 4-76 we enter the curve with a $CNR_{TDRS} = -15.1$ dB and we obtain a $CNR_{GS} = 6.0$ dB (with and without forward error control (FEC) of 4.7 dB). In this manner the CNR_{GS} was determined for each functional channel as follows:

1. The MDR operating at 1 Mbps requires $CNR_{GS} = 9.0$ dB in 10 MHz bandwidth, or 7.5 dB with FEC.
2. The MDR operating at 1 Mbps requires $CNR_{GS} = 7.0$ dB in 100 MHz bandwidth, or 6.0 dB with FEC.
3. The MDR repeating a 40 MHz bandwidth television signal requires 7.5 dB in a 100 MHz bandwidth.
4. The MDR repeating 115 kbps shuttle data requires $CNR_{GS} = 10.5$ dB in a 10 MHz bandwidth. The shuttle case is calculated for a degradation of $\Delta CNR = 0.5$ dB rather than 1 dB for the remaining links, and includes FEC.

Therefore, in establishing the link requirements for each of the user configurations Figure 4-75 shows that operating with CNR_{GS} of 6 dB for the eight LDR channels and 10 dB for the MDR channels regardless of whether the MDR is in the wideband (100 MHz), narrowband (10 MHz), or television mode, is an acceptable operating point.

The TDRS/GS transmitter tradeoff was performed with the channel CNR requirements as stated. The following link parameters were used to calculate the power required for several configurations based upon the range equation:

$$P_T = K + B + CNR + F + \alpha_T - \frac{(G)}{(T)_{GS}} - G_T$$

- where:
- P_T = required transmitter power, dBm
 - K = Boltzmann's constant, -138.6 dBm/MHz
 - B = RF noise bandwidth, dB
 - CNR = required carrier-to-noise ratio, dB
 - F = Fading + rain margin, 17.5 dB



α_T = Space attenuation + system losses, 212.5 dB consisting of:

Free space attenuation, 208.3 dB
Polarization loss, 0.5 dB
Antenna pointing loss, 0.5 dB
Combining and line losses

$\frac{(G)}{(T)_{GS}}$ = Ground station antenna gain/system noise temperature ratio,
40.3 dB*

G_T = Spacecraft 3' (.9m) diameter transmitting antenna gain, 40.3 dB

Substituting the above values into the range equation, we obtain:

$$P_T = 7.6 + B + \text{CNR} + \text{Losses (dBm)}$$

This simplified equation permits a rapid evaluation of the impact of a multiplexing scheme on the transmitter power requirements. All that is needed is the RF bandwidth and the carrier-to-noise ratio in that bandwidth.

Figure 4-77 contains a simplified block diagram of several configurations capable of performing the required functions. Each system has been detailed and analyzed. Evaluations have been made of the power consumed, actual weight of the components, and equivalent weight of the units (latter includes the weight of the power source components--solar paddles, regulators, charging circuits, etc.). Table 4-25 is a summary of these results. The following is a brief description of each configuration.

- A. All input data are combined in a multiplexer whose output is then converted to PCM format. The PCM signal is used to phase modulate the Ku-band power oscillator injection locked to a reference source.
- B. As above, all data are combined in a multiplexer. Its output frequency modulates a low level Ku-band oscillator whose output is amplified in a solid state power amplifier.
- C. Identical to (B) except that a TWTA is used as the final amplifier
- D. Similar to (B) except that a power oscillator is a high power unit. An AFC loop compensates for oscillator frequency drift.
- E. In this system the multiplexer output is used to phase modulate a low level UHF oscillator. A power amplifier increases the power and drives a X 40 frequency multiplier whose output is a wideband phase modulated signal at 14,900 MHz. The low level phase modulation is accomplished at low index to obtain best linearity. The index is also increased in the frequency multiplier.

*For the mechanization tradeoffs, a 40 ft (12.2m) antenna was assumed for the ground station although a 60' dish was finally decided on.

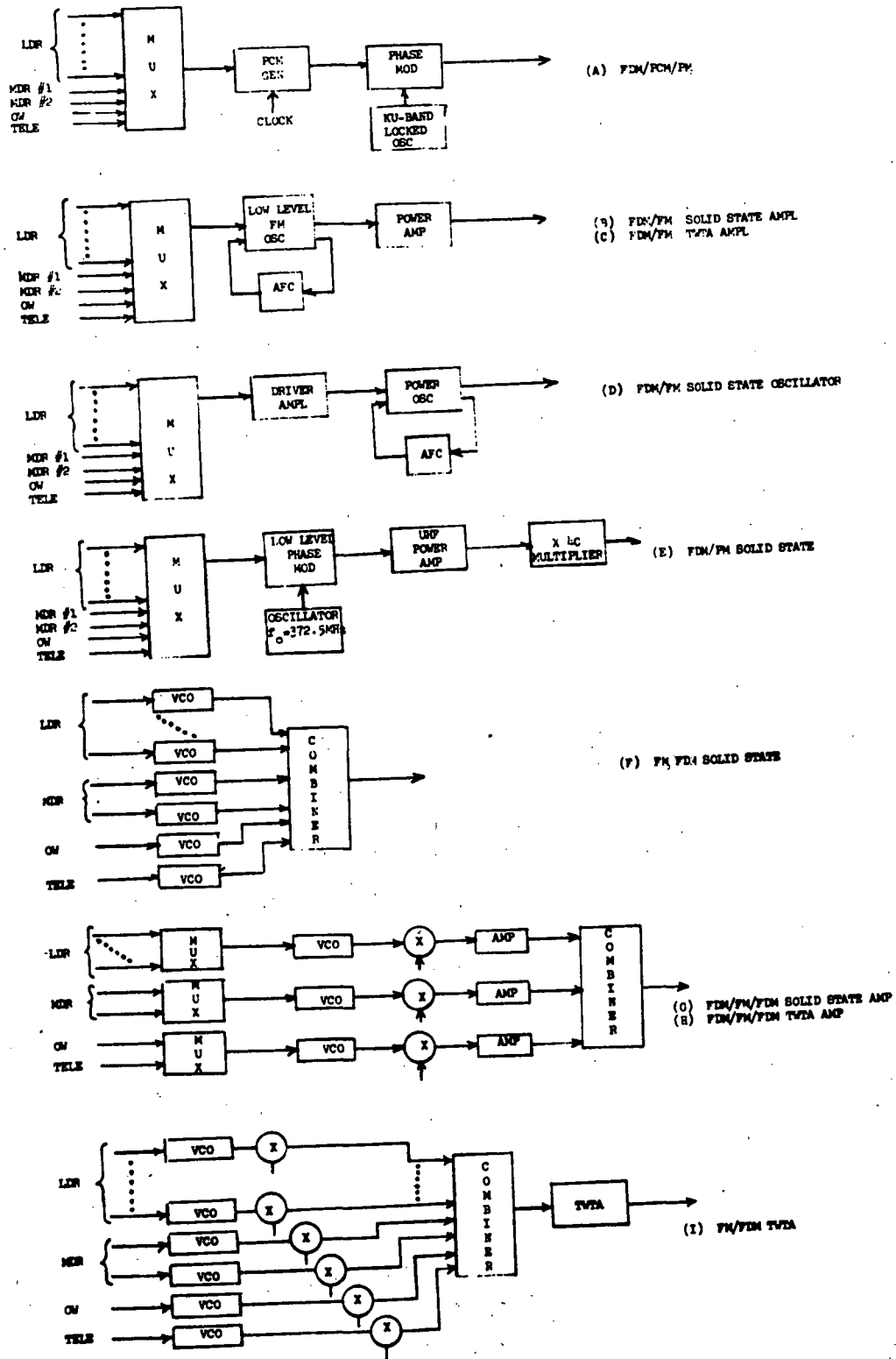


Figure 4-77. Candidate TDRS/GS Multiplexing Configurations

Table 4-25. Transmitter System Summary

Configuration	Output Device	Relative Actual Weight		Relative Equiv. Weight ¹		dc Power Required (Relative)
		lb	kg	lb	kg	
(A) FDM/PCM/PM	Solid state	58.4	26.5	65.4	29.7	279.0
* (B) FDM/FM	Solid state	1.0	0.45	1.0	0.45	4.05
(C) FDM/FM	TWTA	2.9	1.32	1.2	0.54	1.0
(D) FDM/FM	Solid state osc.	1.0	0.45	1.0	0.45	4.05
(E) FDM/PM	Solid state amp.	1.18	0.54	2.12	0.96	10.7
(F) FM/FDM	Solid state osc.	4.12	1.87	1.97	0.89	3.27
(G) FDM/FM/FDM	Solid state amp.	2.89	1.31	1.94	0.88	5.75
(H) FDM/FM/FDM	TWTA	4.75	2.16	1.88	0.85	1.15
(I) FM/FDM	TWTA	4.10	1.86	1.65	0.75	1.17
* Baseline						
NOTE: 1. Equivalent weight = actual hardware weight + weight of power source (assumed to be 0.35 pound (0.16 kg) /watt or 0.16 kg/w).						

4-136

SD 72-SA-0133



- F. In this scheme each signal separately frequency modulates a high level VCO. The frequency of each VCO is different so that the combined spectrum has contiguous FM spectra.
- G. Each functional signal is multiplexed separately, and used to frequency modulate an S-band VCO whose output is up-converted to Ku-band. An amplifier increases the power to the required level and all signals are combined and fed to the antenna. The amplifiers used are avalanche diode solid state units.
- H. Identical to (G) except TWTA amplifiers are employed.
- I. This is similar to (H) except that all signals are combined at low level and only one TWTA is used.

The system selected for detailed investigation is the solid state FDM/FM configuration (Figure 4-77 (B)). This unit weighs less than the others in both actual and equivalent weights. It uses somewhat more power than the TWTA version but weighs less even when the weight of the power source is included. An overall conversion efficiency of 6 percent has been used for the solid state power amplifier. This is a conservative estimate of efficiency that is subject to technological improvements. Such improvements are quite possible as reports are now being made of units with 20 percent to 25 percent efficiency. This would reduce not only the power consumption but also the equivalent weight.

4.5.3.2 Detailed Design of TDRS/GS Link Transceiver

The function of the TDRS/GS receiver is to accept a 240 MHz spectrum at Ku-band and convert it to the appropriate baseband before modulating LDR and MDR forward link transmitters as well as receiving the pilot and command signals. Due to the necessarily close spacing of the individual signals (see Figure 4-78), double conversion is used to separate the IF frequencies and to circumvent a difficult RF filtering problem.

The TDRS/GS receiver (Figure 4-79) is a typical double conversion configuration with multiple IF's. Each element of the receiver block diagram is discussed.

The antenna signal is first fed to the diplexer. The filtering isolation of the diplexer is sufficient to prevent interfering transmitter power from entering the receiver front end within the passband. In addition to this function it will provide some degree of RF preselection to avoid passing wide band noise and RFI from the antenna to the receiver.

From the diplexer the signal passes to the first mixer. The incoming Ku-band spectrum will be down converted to a 500 MHz IF center frequency requiring a 13,020 GHz L.O. Double balanced mixers are used to accomplish this conversion to maintain a low spurious response level. L.O. drive for this mixer is +10 dBm which is necessary to realize low conversion loss. Conversion loss here must be kept low in the absence of RF amplification. After mixing, the IF spectrum is filtered in the first IF bandpass filter. The first IF spectrum is centered at 500 MHz and extends from 380 MHz to 620 MHz.

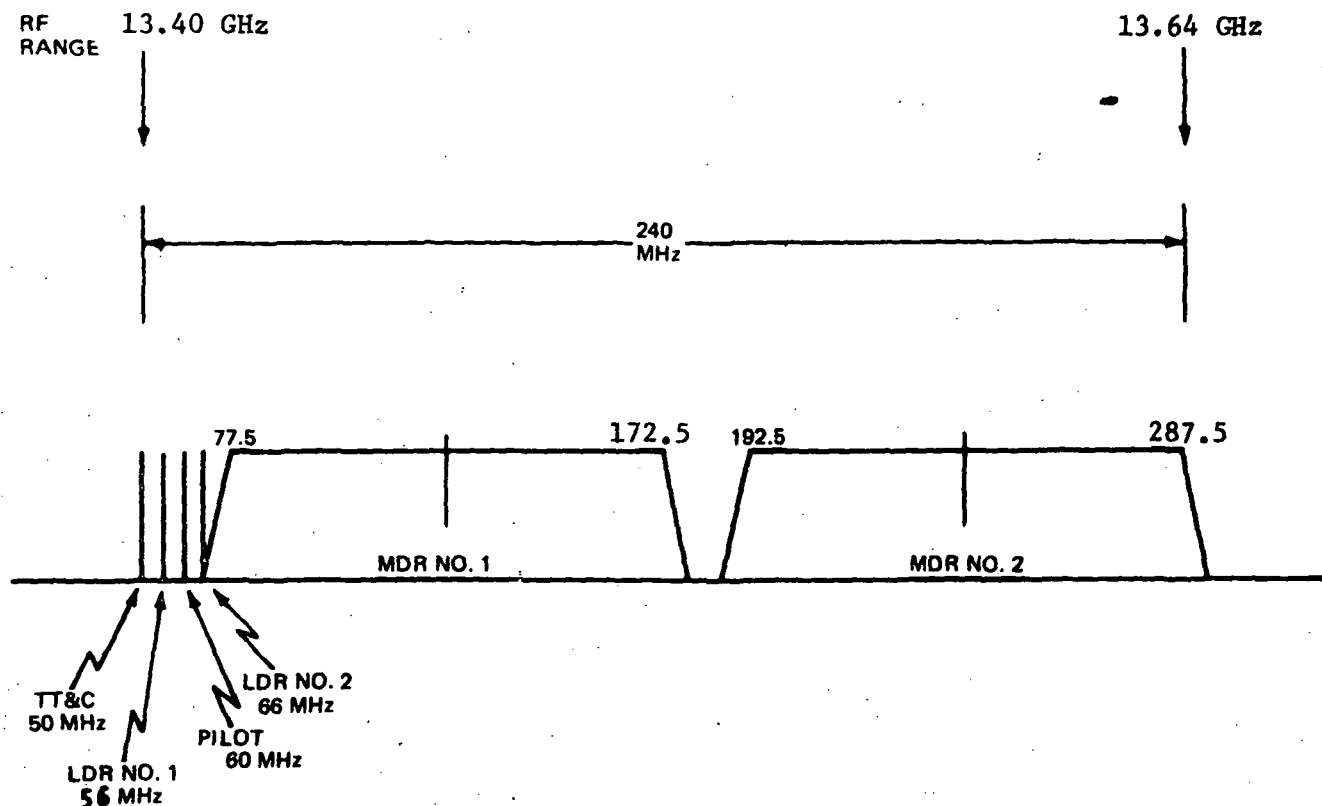


Figure 4-78. Second IF Frequency Spectrum GS/TDRS Receiver

The IF filter is a six-pole lumped constant design with particular emphasis on low insertion loss. This loss, together with the mixer loss and IF preamp noise figure determines receiver noise and subsequently the ground station power requirements to provide an adequate S/N ratio. Overall receiver noise figure, using this method, is 10 dB. The first IF amplifier uses ultra low noise devices such as 2N5650's. The 500 MHz IF amplifier increases the signal to -59 dBm. This amplifier, providing a total of 40 dB gain, is sufficient to eliminate any effect of second stage noise figure. A double balanced mixer is used to down convert the 500 MHz spectrum to the baseband frequencies. The mixer operates with a local oscillator at 670 MHz which in turn produces the desired spectrum of 50 MHz to 290 MHz (see Figure 4-78).

The 50 to 290 MHz second IF is split six ways in a power divider. Each output is fed to separate IF bandpass filter which selects the appropriate signal.

Center Frequency	Function	Bandwidth
1. 50 MHz	TT&C	<1 MHz
2. 56 MHz	LDR No. 1	<1 MHz
3. 60 MHz	Pilot	<1 MHz
4. 66 MHz	LDR No. 2	<1 MHz
5. 120 MHz	MDR No. 1	95 MHz
6. 240 MHz	MDR No. 2	95 MHz

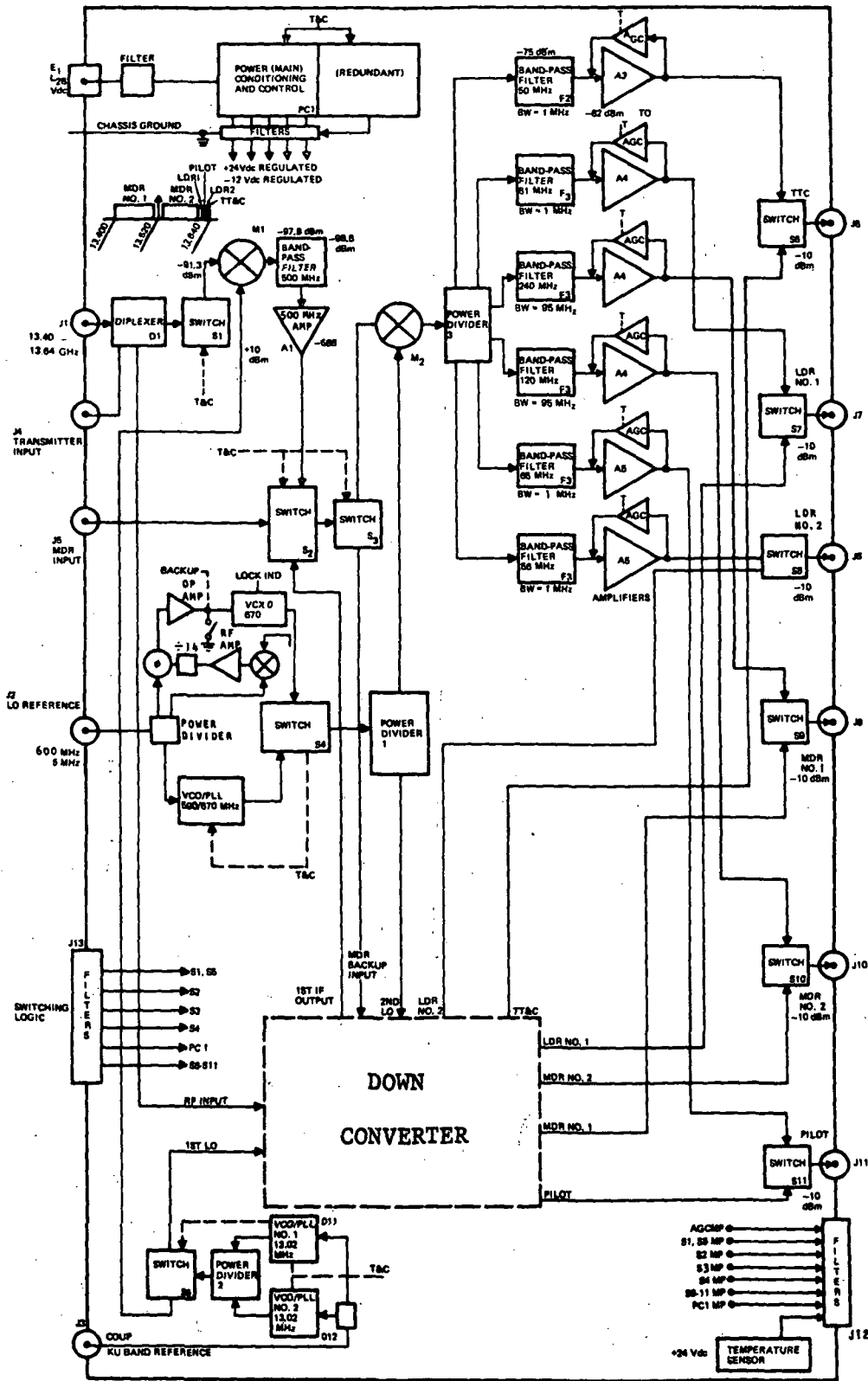


Figure 4-79. GS/TDRS Baseline Receiver

Each IF filter is a six-pole lumped constant design with sufficient skirt rejection to eliminate spurious responses and interference from adjacent spectrums. By keeping the IF power levels low (<-60 dBm) the inband harmonics of the low frequency IF signals do not cause interference in the two MDR spectrums. After the individual IF's are separated by filtering, the signals are amplified to approximately -10 dBm by tuned AGC amplifiers. The amplifiers maintain a constant output power level to the transmitters.

Redundancy in this receiver is obtained by placing RF switches at both input (following the diplexer) and output. In addition to this redundancy, higher reliability is obtained by cross strapping the input to the second mixer to enable operation of either receiver front end with either second IF section. Further backup was obtained since this switching permits using an MDR receiver front end as a replacement for the TDRS/GS link receiver front end.

The packaging concept used to determine size and weight is shown in Figure 4-80 and essentially is divided into a front end and IF section, each duplicated to contain the redundant half.

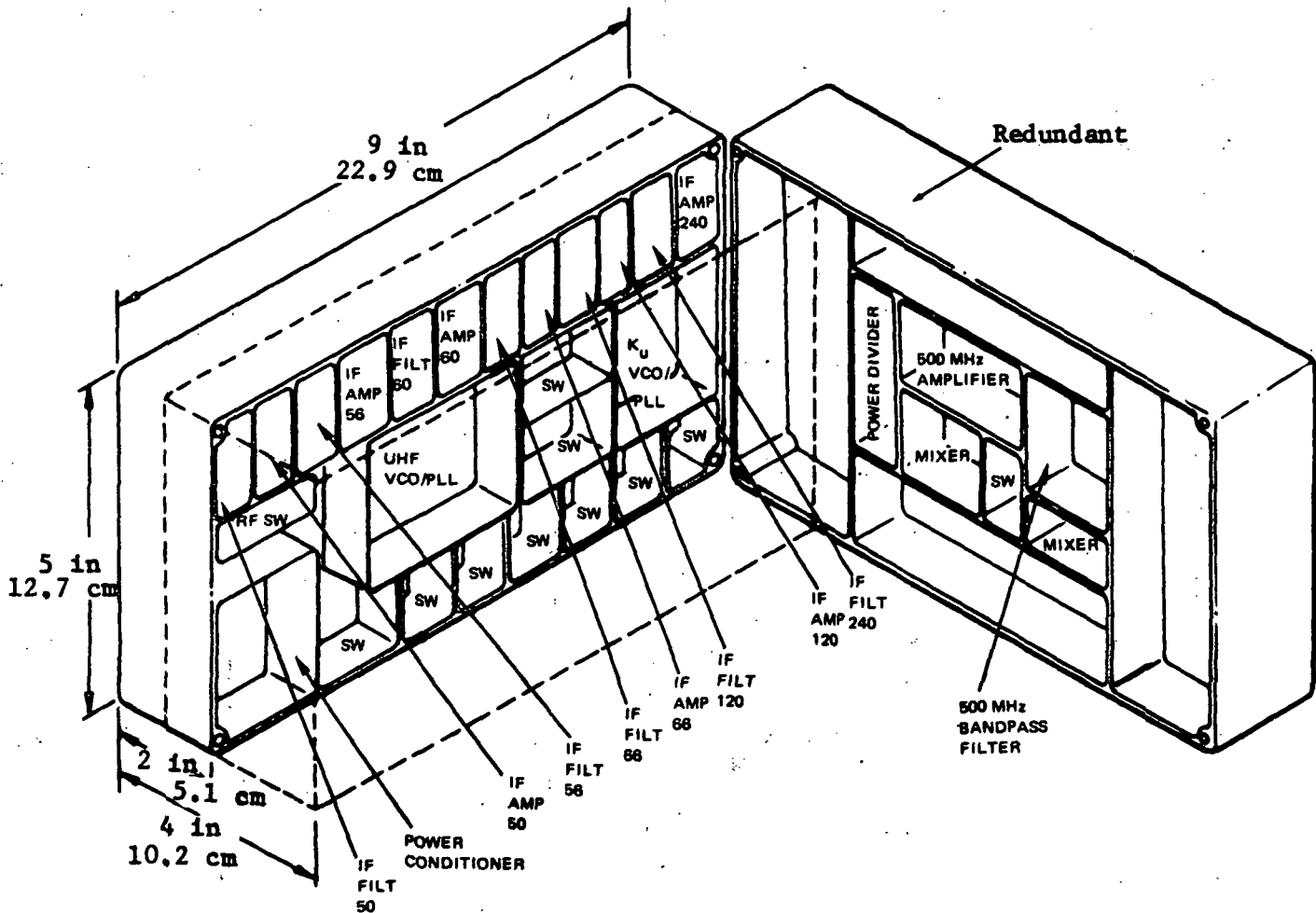


Figure 4-80. TDRS/GS Receiver



Figure 4-81 is a detailed block diagram of the TDRS/GS transmitter. The input signals from five receivers (MDR No. 1, LDR, Order Wire, TT&C, and MDR No. 2) are combined to form an FDM (frequency division multiplex) signal. This signal is used to frequency modulate a Ku-band VCO (voltage controlled oscillator). The output of this low level VCO (FDM/FM) is amplified in a Ku-band amplifier and then directed via a diplexer to the TDRS/GS antenna. The input signals are all at 0 dBm level and have been down-converted to adjacent nonoverlapping frequency bands. These signals are combined in the video module, which also includes preemphasis and equalization to modulate the VCO. The FDM signal occupies a band from 1 to 155 MHz or from 1 to 47.5 MHz depending upon the bandwidth and mode of operation of the MDR No. 1 user. The index of modulation used for the VCO is approximately unity, resulting in an RF bandwidth of 600 MHz or 200 MHz. An AFC loop stabilizes the center frequency of the VCO to 14,900 MHz. A broadband solid state amplifier increases the milliwatt VCO output level to a maximum of 2.75 watts. Lower output levels can be used to conserve prime power when lower rain or fade margins are tolerable or when operating in the narrower band mode (200 MHz).

Figure 4-82 depicts the baseband frequency arrangement. Also shown in Figure 4-82 is the required S/N for each channel of the output of suitable filters following the ground station detector (phase lock detector). The S/N ratio per channel is directly related to the frequency deviation attributable to that channel. Channel deviations were calculated using the relationship:¹

$$\frac{(S)}{(N)_o} = \frac{(C)}{(N)_1} \frac{(B_{RF})}{(B_c)} \frac{(F_m)^2}{(f_n)}$$

where:

- $\frac{(C)}{(N)_1}$ = carrier-to-noise ratio in B, RF bandwidth
- B_c = channel bandwidth
- B_{RF} = RF (or IF) bandwidth
- f_n = channel center frequency
- $\frac{(S)}{(N)_o}$ = channel signal-to-noise output
- F_m = maximum frequency deviation

The bandwidth B is 200 MHz using MDR-1A and 600 MHz with the MDR-1B mode. The threshold (C) was selected as 0 dB for the resulting modulation index of 0.94 which is 2 dB above threshold.²

1. Panter, "Modulation, Noise and Spectral Analysis", McGraw-Hill, page 442.
2. Camp, "A Comparison of the Threshold Extension Capabilities of FM, FB, and Phase-Lock-Loop Demodulators Employed in FDM-FM Communications Systems", PGCT, June 1970.

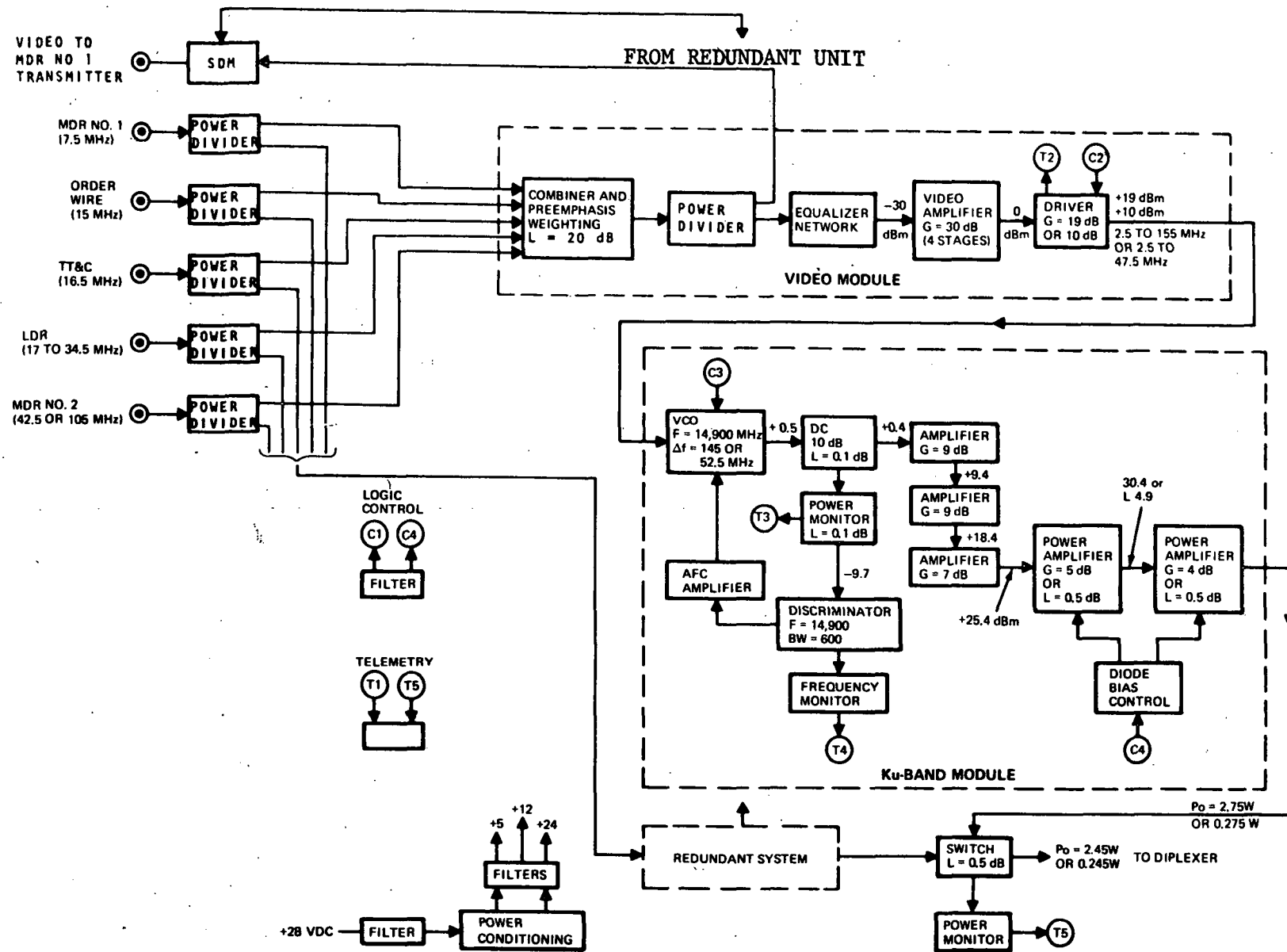
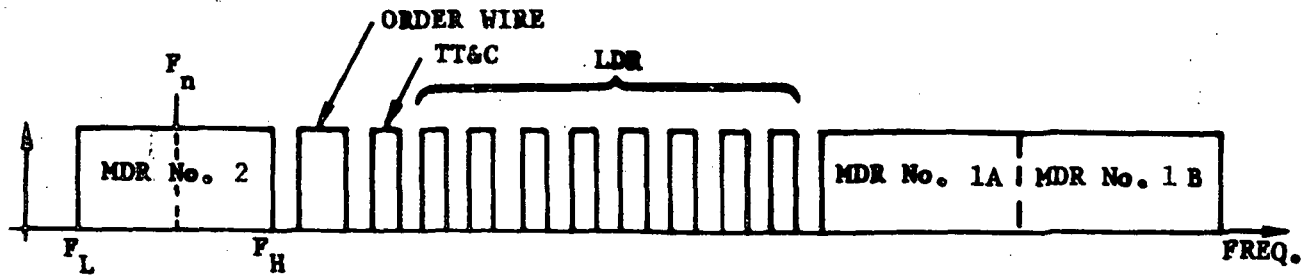


Figure 4-81. TDRS/GS Transmitter

4-142

SD 72-SA-0133



Function	Channel Bandwidth	Required S/N	F_L	F_H	F_n
MDR No. 2	10 MHz	9 dB	1 MHz	11 MHz	6 MHz
Order Wire	1	10	13.0	14.0	13.5
TT&C	1	10	14.5	15.5	15.0
LDR No. 1	2	6	16.0	18.0	17.0
LDR No. 2	2	6	18.5	20.5	19.5
LDR No. 3	2	6	21.0	23.0	22.0
LDR No. 4	2	6	23.5	25.5	24.5
LDR No. 5	2	6	26.0	28.0	27.0
LDR No. 6	2	6	28.5	30.5	29.5
LDR No. 7	2	6	31.0	33.0	32.0
LDR No. 8	2	6	33.5	35.5	34.5
MDR No. 1A	10	10	37.5	47.5	42.5
MDR No. 1B	100	10	55.0	155.0	105.0

Figure 4-82. TDRS/GS Transmitter Baseband Frequency Assignment



It is necessary to determine the parameters of the FM system to limit the bandwidth to 600 MHz, given the baseband frequency configuration and a phase lock demodulator in the GS for threshold extension. To do this, the above equation is rearranged to compute the deviation required per channel to achieve the desired signal-to-noise ratio in that channel:

$$F_m = f_n \sqrt{\frac{(S/N)_o}{(C/N)_i} \times \frac{B_c}{B_{RF}}}$$

A 600 MHz bandwidth is assumed, operation at 0 dB $(C/N)_i$ is used, and the F_m is calculated. Table 4-26 presents these calculations. To verify the BW, Carson's rule for bandwidth computation is used;

$$B_{RF} = 2(F_p + F_H)$$

where:

- B_{RF} = RF (or IF) bandwidth
- F_p = Peak frequency deviation for the composite FDM signal
- F_H = Maximum frequency component in the FDM signal

The peak deviation for the composite signal (F_p) is the RMS combination of the MDR No. 1, order wire, telemetry, LDR, and MDR No. 2 signals. The LDR signals are first combined by adding all the F_{pm} and using the result in the RMS addition. This is done to account for the fact that the LDR signals are not independent and are, in fact, correlated. Thus, they add first on a peak basis, then on a power basis with the other signals. The result of this combination is 137.7 MHz. The highest baseband frequency is 155 MHz. Therefore, Carson's rule results in an IF bandwidth of 585.4 MHz, sufficiently close to the assumed 600 MHz. The final parameters are as follows:

$$F_p = 137.7 \text{ MHz}$$

$$F_H = 155 \text{ MHz}$$

$$\text{Peak index} = 0.9$$

$$\frac{(C)}{(N)_i} = 0 \text{ dB}$$

The combiner shown in Figure 4-81 functions both to combine all signals to a single line and to adjust their relative amplitudes to satisfy the S/N requirement. This adjustment of the relative amplitudes of each signal is equivalent to a step-type preemphasis to obtain the required S/N for each channel. The combining loss of about 20 dB is made up in the following video

Table 4-26. FDM/FM Characteristics

Function	B_n	$\frac{(S)}{(N)}_n$ db	$f_{low}^{(1)}$	$f_{high}^{(2)}$	f_n	F_p
MDR No. 2	10	10	1.0	11.0	6.0	2.183
Order wire	1	10	13.0	14.0	13.5	1.74
Telemetry	1	10	14.4	15.4	14.9	1.92
LDR No. 1	2	6	16.0	18.0	17.0	1.958
No. 2	2	6	18.5	20.5	19.5	2.25
No. 3	2	6	21.0	23.0	22.0	2.53
No. 4	2	6	23.5	25.5	24.5	2.82
No. 5	2	6	26.0	28.0	27.0	3.11
No. 6	2	6	28.5	30.5	29.5	3.4
No. 7	2	6	31.0	33.0	32.0	3.69
No. 8	2	6	33.5	35.5	34.5	3.97
MDR No. 1	100	10	55.0	155.0	105.0	135.6

NOTES: (1) f_{low} = lower frequency limit (2) f_{high} = higher frequency limit

amplifier whose gain is 20 dB and bandwidth extends from 1 to 155 MHz. This signal is further amplified and shaped in the driver that modulates the VCO. Signal shaping is required to obtain linear modulation of the VCO.

The VCO uses a Gunn effect diode whose frequency is controlled by a varactor coupled to the oscillator. The Gunn diode approach is used to achieve low noise. The penalty of low efficiency is not important here because only about 1 milliwatt of RF power is required. With one percent efficiency the dc power is only 0.1 watt. The varactor diode is closely coupled to the Gunn diode to obtain wide deviation capability (150 MHz peak deviation). The modulation sensitivity of 20 MHz per volt specifies 7.5 volts of modulation signal to obtain 150 MHz peak deviation. The driver output easily provides this level into the varactor capacitance of 2 to 3 picofarads. An AFC loop is provided to stabilize the center frequency of VCO to 14.9 GHz. This is accomplished by a 10 dB directional coupler feeding a discriminator at 14.9 GHz. The discriminator output is used to adjust the varactor bias to correct oscillator drift. The entire VCO-discriminator subassembly is constructed on strip line.

Following the VCO is an amplifier assembly consisting of five stages of amplification. The first three are virtually identical and are, in fact, constructed on a single substrate. Each stage comprises an avalanche diode amplifier circulator coupled to the input-output lines. The strip-line configuration lead to a compact configuration with 50 ohm input and output lines



coupling to a low-loss circulator. The low level stages achieve 9 dB gain whereas the gain gradually reduces as the power increases. The first three stages provide 25 dB of gain with an output level of 0.35 watts. The final amplifier stages are similar in configuration except for a remote control of the bias source to permit turning each stage on or off. In the off condition, there is still transmission through the circulator with a loss of 0.5 dB. In the on state the gain is 4 to 5 dB. Thus, the transmitter can be operated with 3, 4, or 5 active stages (remotely selected) and corresponding output levels between 0.275 and 2.75 watts. The power drain is likewise reduced. An alternate method of gain reduction is to employ a latching ferrite circulator. The ferrite material has a square magnetic characteristic with hysteresis. By pulsing the magnetic field (to conserve power) the sense of the magnetic field is reversed as is the circulator polarity. By this means, the input energy is directed to the output without encountering the diode. The output of the final amplifier is fed to a subminiature coaxial latching relay. The other relay input comes from a redundant amplifier selected in the event of failure in the primary amplifier. Reference to Figure 4-81 also shows a redundant video module. This module also serves as a backup unit and is fed from a hybrid assembly.

Power conditioning, command input, and telemetry output signals complete the TDRS/GS transmitter. The command input signals are needed to activate switches to the desired positions, energizing the correct modules, and controlling the power output and peak deviation of the VCO. The telemetry signals represent confirmation of commands and monitoring of internal functions such as VCO output and frequency, transmitter power, and baseplate temperature.

Figure 4-83 shows the packaging concept. The primary and backup units are identical and are configured to make maximum use of volume. The overall package is contained in a volume of 182 in^3 ($2,982 \text{ cm}^3$) and weighs less than 6 lb (2.7 kg) including the redundant modules. Power consumption in the normal mode is 11.0 watts. During rain conditions, the RF power is increased and dc power correspondingly increases to 49 watts.

4.5.4 Performance Specification for the TDRS/GS Link Transponder

4.5.4.1 Scope

This specification establishes the design requirements for the TDRS/GS link transponder located on the TDRS satellite. This equipment provides the space-to-earth interface between the TDRS relay satellite and the TDRS ground station.

4.5.4.2 Components

The major components of the TDRS/GS link transponder are:

1. Antenna
2. Receiver
3. Transmitter

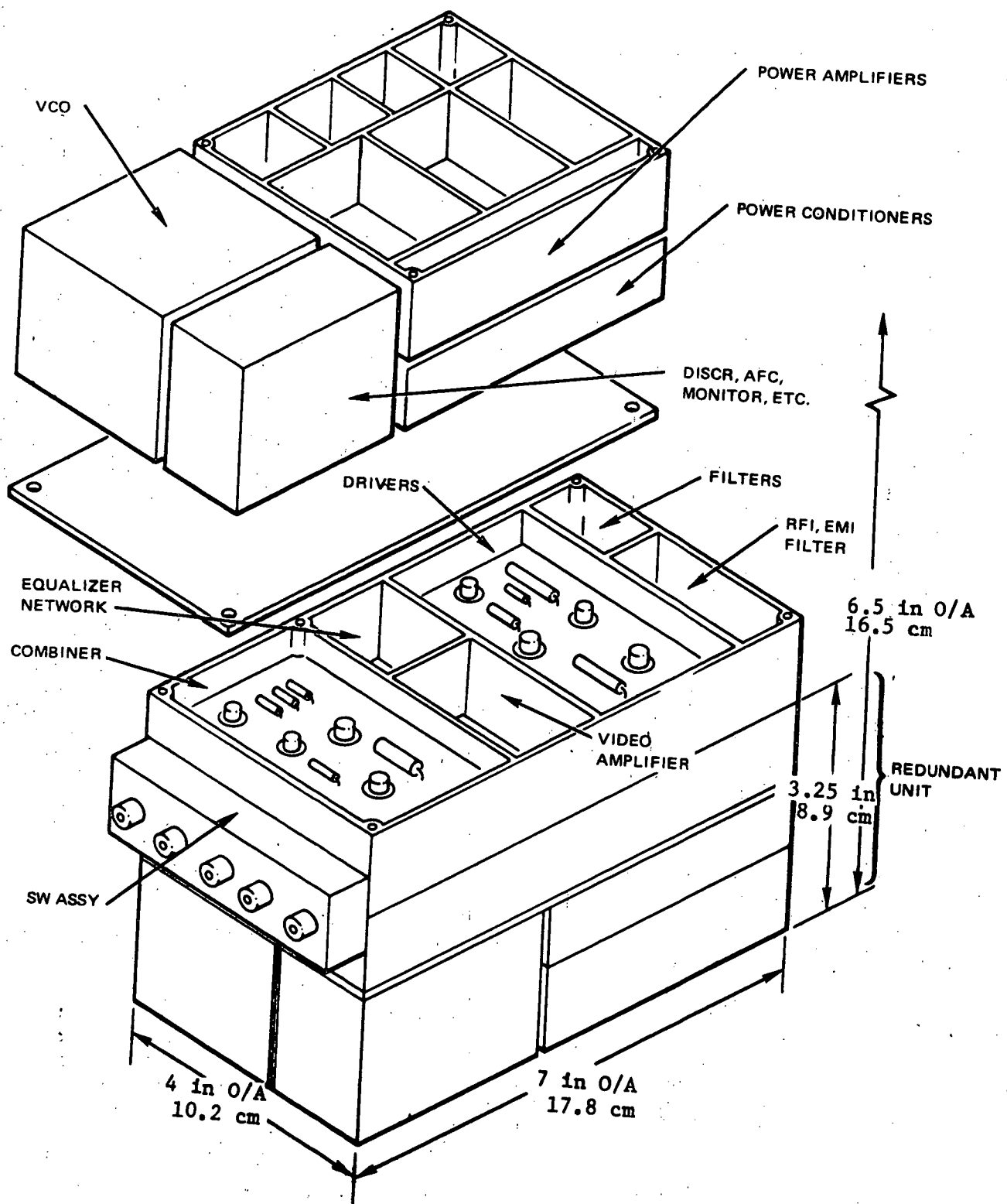


Figure 4-83. TDRS/GS Transmitter Primary and Redundant Units



4.5.4.3 Design Requirements

System Performance Specifications - TDRS/GS Link Antenna

Frequency range:	
Receive	13.4 to 13.64 GHz
Transmit	14.6 to 15.2 GHz
Transmit avg power:	<5 watts
Polarization:	Circular
Axial ratio:	1.5 dB maximum
Input VSWR:	<1.4:1
Side lobe level:	17 dB maximum
Gain, dBi (midband)	40.0
Total antenna efficiency:	>52 percent
Half power beamwidth, degrees or MR	1.6 (28.7 MR)
Aperture size:	3 foot (0.918 m) diameter
Positioning mode:	Open loop
Positioning accuracy:	3 σ of 0.75 degree (13.1 mr)
Gimbal step size:	0.03 degree (0.53 mr)/step
Slew rate:	
Nominal	1.0 degree (17.5 mr)/second
Maximum	\approx 5.7 degrees (0.1 rad)/second
Scan angle:	2 (axis) \pm 8.0 $^{\circ}$ (0.14 rad) off boresight
Total weight, includes	14.85 (6.75 Kg)
Feed, waveguide	
Rotary joints	
Reflector	
Gimbal system	
Electronics	
Power peak (watts), includes	9.5
Motor drive (5 watts)	
Motor clamping (3 watts)	
Electronics	
Total power average (watts),	Negligible since the antenna is
Motor power slew	moved only once on its initial
Motor power track	arrival on station
Electronics	



TDRS/GS Link Receiver

Frequency range: 13,400 to 13,640 MHz

Noise figure: 9.1 dB

IF frequency: 500 MHz

IF bandwidth: 240 MHz

Spurious level: >50 dB down

Baseband frequencies:

TT&C	-	50 MHz
LDR No. 1	-	54 MHz
Pilot	-	60 MHz
LDR No. 2	-	66 MHz
MDR No. 1	-	120 MHz
MDR No. 2	-	240 MHz

Temperature: 0 to 50 C

AGC range: 25 dB

TDRS/GS Link Transmitter

Input Signals

- | | |
|--------------------|--|
| 1. MDR No. 2: | $f_o = 6 \text{ MHz}, BW = 10 \text{ MHz}, P_i = 0 \text{ dBm}$ |
| 2. Order wire: | $f_o = 13.5 \text{ MHz}, BW = 1 \text{ MHz}, P_i = 0 \text{ dBm}$ |
| 3. TT&C: | $f_o = 15 \text{ MHz}, BW = 1 \text{ MHz}, P_i = 0 \text{ dBm}$ |
| 4. LDR: | 8 channels between 16 and 35.5 MHz,
$P_i = 0 \text{ dBm}$ |
| 5A. MDR No. 1A: | $f_o = 42.5 \text{ MHz}, BW = 10 \text{ MHz}, P_i = 0 \text{ dBm}$ |
| or 5B. MDR No. 1B: | $f_o = 105 \text{ MHz}, BW = 100 \text{ MHz}, P_i = 0 \text{ dBm}$ |

Baseband combining: FDM with preemphasis and phase equalization

Modulation: FM with index of modulation of unity
Peak deviation 145 MHz or 52.5 MHz
RF bandwidth: 600 MHz or 200 MHz

Center frequency: 14,900 MHz

Power output: 0.275 to 2.75 watts

Redundancy: 100 percent



Volume: 182 cubic inches (2990 cm³)
Weight: 6 pounds (2.72 kg) maximum
dc input: 28 volts

4.5.5 Size, Weight, and Power Summary of TDRS/GS Link Transponder

The size, weight, and power requirements are summarized below for the recommended TDRS/GS transponder Part I baseline configuration.

Component	Size in. (cm)	Weight lb	Power, watts	
			Peak	Average
Antenna	3-foot (0.91 m) dia.	14.85 (6.75)	9.5 ¹	--
Receiver	9 x 5 x 4 in. (22.8 x 12.7 x 10.1) cm	4.7 (2.1)	5.25	5.25
Transmitter	4 x 7 x 6.5 in. (10.2 x 17.8 x 16.5) cm	6.00 (2.7)	49.0 ²	11.0

- NOTES: 1. Antenna pointing required only once upon arrival on station
2. During rain at ground station, a 10 dB amplifier is inserted



4.6 FREQUENCY SOURCE

4.6.1 System Analysis and Tradeoffs

The various receivers and transmitters in the TDRS spacecraft require a total of 37 individual L.O. frequencies. If each L.O. were to be individually synthesized from the coherent pilot, the distribution problem would be enormous, to say nothing of an extremely complicated frequency source. When this many frequencies are involved, good design recommends use of a voltage tuned oscillator/phase lock loop combination at each output to clean up the output spectrum by reducing noise and spurious responses. Once this configuration is determined, additional techniques can be employed that will greatly reduce the number of reference signals needed to operate the phase lock loops. By using variable and/or fixed logic dividers in each phase lock loop, the same reference signal can be used to generate many different frequencies merely by changing the "divide by" number. Using this technique, the frequency source can be substantially smaller than other approaches and at the same time yield other benefits such as:

1. L.O. power is generated where it is used, eliminating cable losses
2. Low level signals are distributed reducing RFI problems
3. Fewer L.O. cables
4. Better reliability
5. Lower power consumption

Many synthesizer designs make abundant use of long multiplier chains and mixing as a means of generating high frequency signals from low frequency references. This method is inefficient and has the potential of producing serious spurious responses unless special precautions are taken. The TDRS frequency source will use phase locked oscillators extensively. This technique produces spur free outputs, eases filtering requirements, and saves power and weight.

An additional VTO/phase lock loop combination will be used at each L.O. destination rather than route high level L.O.'s around the spacecraft. Only low level reference signals will be distributed to the modules. Distribution of the low level references reduces the danger of RFI problems and minimizes the number of L.O. cables (see Figure 4-84). L.O. power is conserved by generating the L.O. where it will be used, thereby eliminating cable losses. As in the reference loops, the output phase locked loop cleans up the reference. All spurious responses and noise on the reference signals that fall outside the loop bandwidth are greatly reduced.

The frequency source is largely an integrated design up to and including the UHF portions. The S-band and Ku-band areas are discrete components. By integrating the low frequency areas a substantial savings is achieved in size and weight.

The frequency source is divided into two fundamental areas each of which is independently redundant. By separating the low frequency section and the high frequency section and providing appropriate switching, greater reliability is obtained without significantly adding to the hardware.

4-152

SD 72-SA-0133

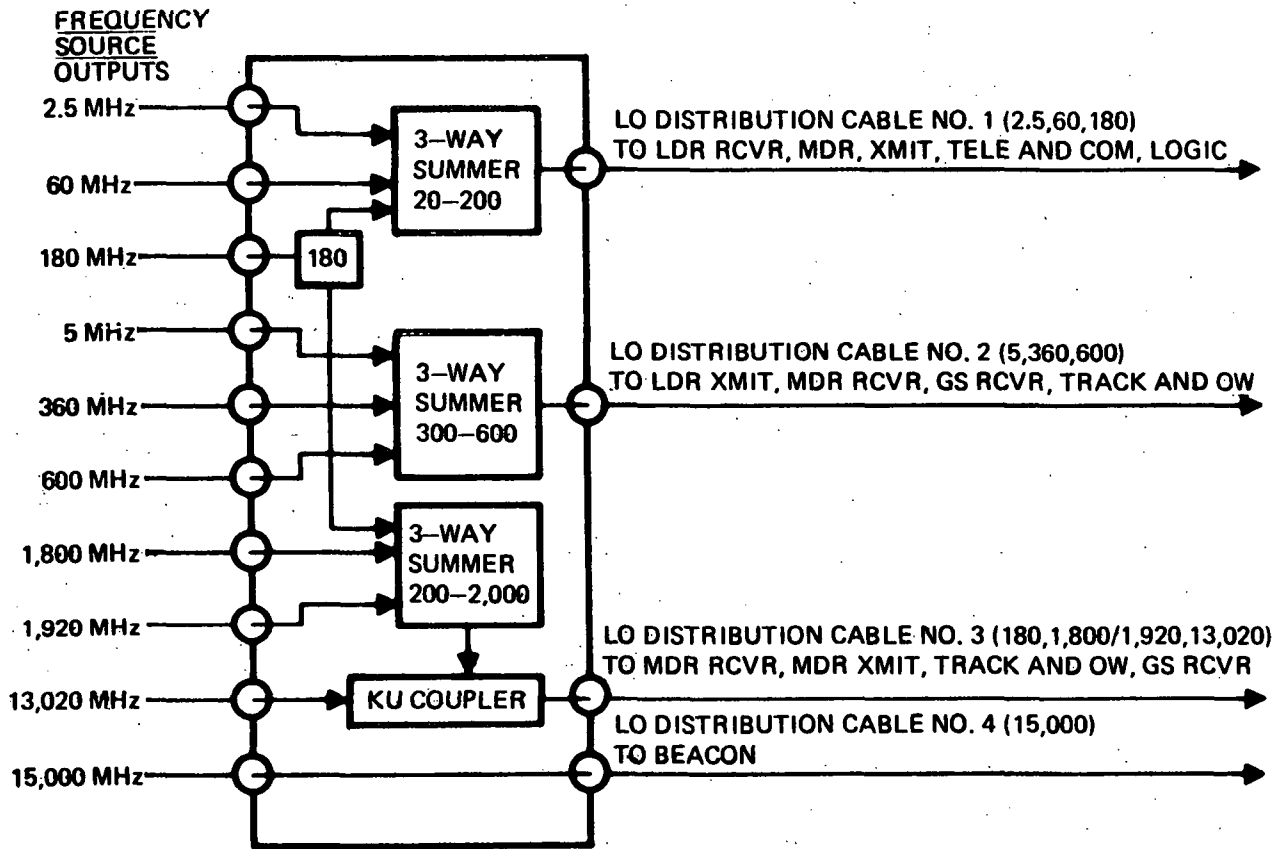


Figure 4-84. LO Power Distribution Network



The frequency source tradeoffs that have been examined in this study are summarized in Table 4-27. It is these tradeoffs that led to the following detail design.

Table 4-27. Frequency Source Tradeoffs

Candidates	Selection	Reason
Multipliers vs. phase locked oscillators	Phase locked oscillators	Cleaner outputs Easier filtering Cleaner L.O.s
Phase lock loop at each location	Yes	Cleaner output saves power
Distribute references only	Yes	Helps reduce RFI Fewer cables
Redundancy	Yes (100%) segmented	More reliable operation
Integrated design	Yes, up to UHF (S & Ku-band not integrated)	Smaller size where feasible

4.6.2 Detailed Description of the Frequency Source

The major components of the frequency source are identified in the overall functional block diagram in Figure 4-85. These components are the phase locked reference loop, frequency generator, and clean-up loops which are described in detail in the subsequent sections.

4.6.2.1 Phase Lock Reference Loop

A reference loop as shown in Figure 4-86 is used to generate the higher reference frequencies without suffering the penalties incurred by long multiplier chains. Where multipliers tend to aggravate noise and spur problems, the phase lock loop technique produces a relatively clean spur free output. The reference loops will use crystal controlled transistor oscillators with a loosely coupled varactor which will tune the output over a narrow range suitable for phase locking.

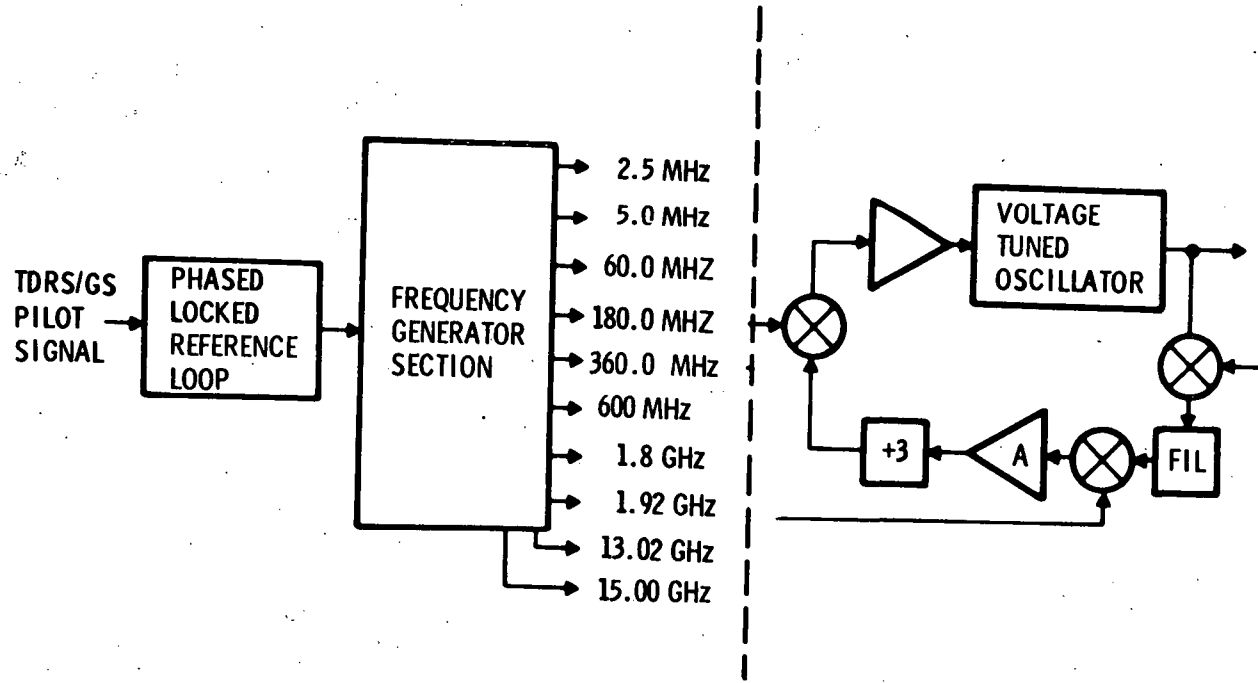


Figure 4-85. Frequency Source Design Approach

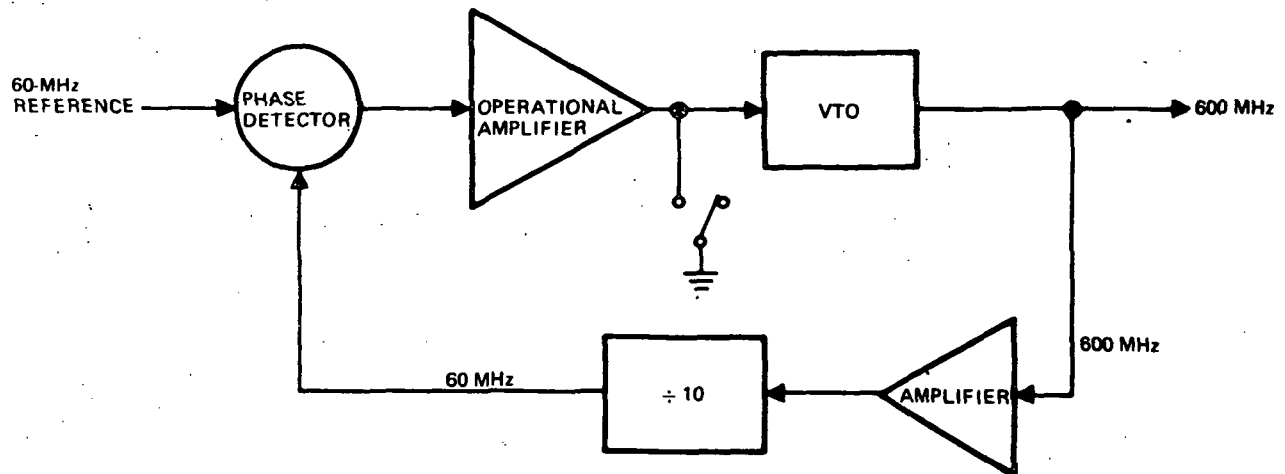


Figure 4-86. Typical Reference Loop

Loop operation is based on a free running VTO at the nominal frequency (600 MHz). A portion of its output is coupled off, amplified, and divided down to 60 MHz using high speed logic. This 60 MHz signal is fed to a phase detector and compared to the coherent 60 MHz reference from the pilot. The phase detector output is the error signal which in turn is amplified and fed to the VTO varactor phase locking the output signal to the pilot.

The loop bandwidth for the reference VCXOS is ± 1 KHz. This bandwidth is not sufficient to capture and phase lock, considering inherent oscillator instability and noise. However, the VCXOS also employ a quasi-discriminator circuit to augment the pull-in range of the oscillator so that the doppler shift associated with the pilot and oscillator noise will not cause the TDRS VTO to break lock. Once lock is achieved, the phase lock range will be sufficient to maintain the locked condition over ± 50 KHz range. Initial lock will be achieved by sweeping the pilot over a narrow range to guarantee acquisition.

4.6.2.2 Frequency Generation

Analysis of the required L.O. frequencies, distributing references only, indicates that from only 10 frequencies the 37 required L.O. frequencies can be synthesized (see Figure 4.88). These 10 frequencies are:

- 2.5 MHz
- 5.0 MHz
- 60.0 MHz
- 180.0 MHz
- 360.0 MHz
- 600 MHz
- 1,800 MHz
- 1,920 MHz
- 13,020 MHz
- 15,000 MHz

These frequencies are formed by phase locking a 60 MHz oscillator with the 60 MHz pilot. The 60 MHz output is then; (1) divided into 5 MHz and 25 MHz forming the low frequency references, and (2) used as a reference for the higher frequency reference loops at 360 MHz and 600 MHz. The 180 MHz reference is derived by dividing the 360 MHz output by two and the 1800 MHz is then produced



by multiplying 600 MHz by three. The 1920 MHz is synthesized using 1800 and 60 as references for a phase lock loop with a "divide-by-two" circuit in the loop. 13,020 MHz is generated by mixing 1920 MHz and 60 MHz to produce 1860 MHz which is then varactor multiplied by seven. The 15,000 MHz is produced from 600 MHz by two times five varactor multipliers. Filtering is provided at appropriate points in the three multiplier circuits to keep the spurious responses, usually associated with multipliers, from becoming a problem. The three stepping L.O.s are basically the same as the others with the addition of programmable variable dividers in the phase lock loop.

4.6.2.3 Clean-up Loops

The appropriate references are delivered to each receiver or transmitter where it will be used to coherently lock its reference VCO. The low frequency oscillators will be voltage-tuned crystal oscillators while the S-band and Ku-band L.O.s will use cavity-tuned Gunn oscillators. Each oscillator will have its own phase lock loop to which two reference signals will be delivered. Figure 4-87 shows a typical clean-up loop for the 345 MHz LDR transmitter L.O. The 345 MHz signal is mixed with the 360 MHz reference, producing 15 MHz.

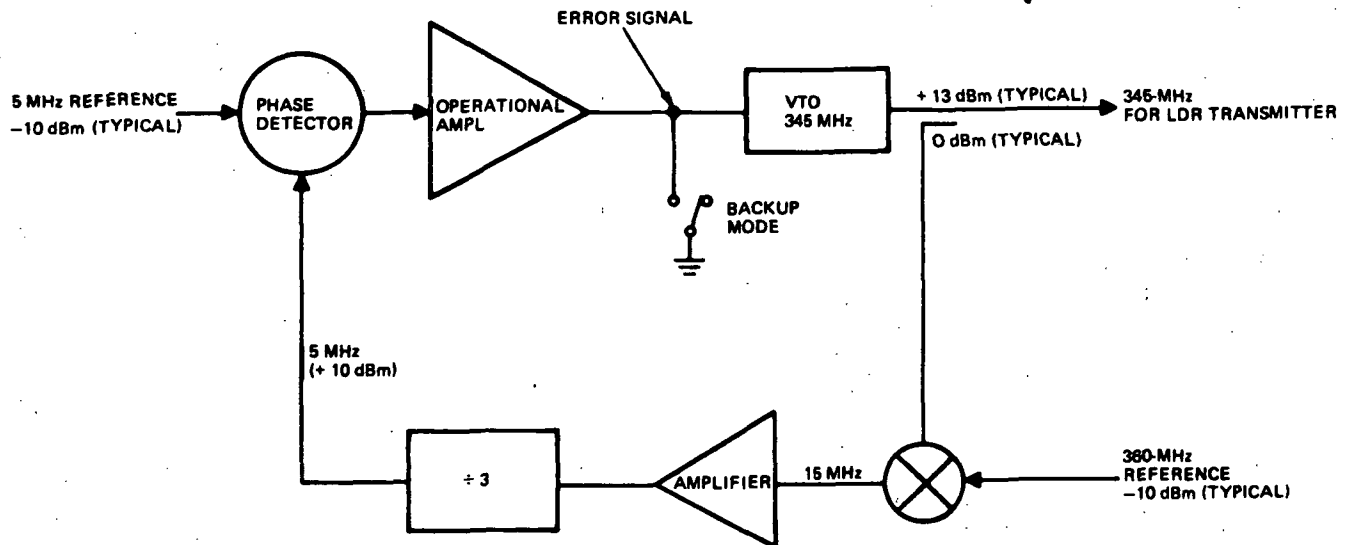


Figure 4-87. Typical Cleanup Loop

15 MHz is then divided by three to 5 MHz and fed to the phase detector where it is compared to the 5 MHz reference. The phase detector output is the 345 MHz VTO error signal which is amplified and fed to the varactor phase locking the oscillator. The phase lock loop has inherent advantages that are used to advantage in the frequency source; viz:

1. Coherent outputs
2. Reduction of spurs and noise on the reference outside the loop bandwidth
3. Higher efficiency



4.6.2.4 Back-up Mode

The frequency source is 100 percent coherent including the Ku-band beacon which normally is used by the Ku-band MDR user for acquisition and tracking the TDRS satellite. Without the pilot the 60 MHz crystal oscillator will free run; however, this highly stable source can now be used as a substitute reference for the UHF phase lock loops and consequently the 15,000 MHz reference as seen in Figure 4-88. The TDRS satellite now becomes the reference source, and the ground station can use the Ku-band beacon as a pilot to re-establish coherency. Since every L.O. on the TDRS including the beacon is derived from the free running 60 MHz oscillator, both TDRS telecommunication systems as well as the ground based systems are now completely coherent. Even with coherency, it is necessary for the on-board source of 60 MHz to be highly stable. In the back-up mode the varactor circuit will uncouple from the oscillator by means of a diode switch and the only frequency control will be the crystal. In this back-up mode temperature stabilization will be employed to restrict the maximum temperature excursions that might be encountered. Under these conditions the back-up stability will be 1 part in 10^8 short term and 1 part in 10^5 over a two-year period.

4.6.2.5 Redundancy

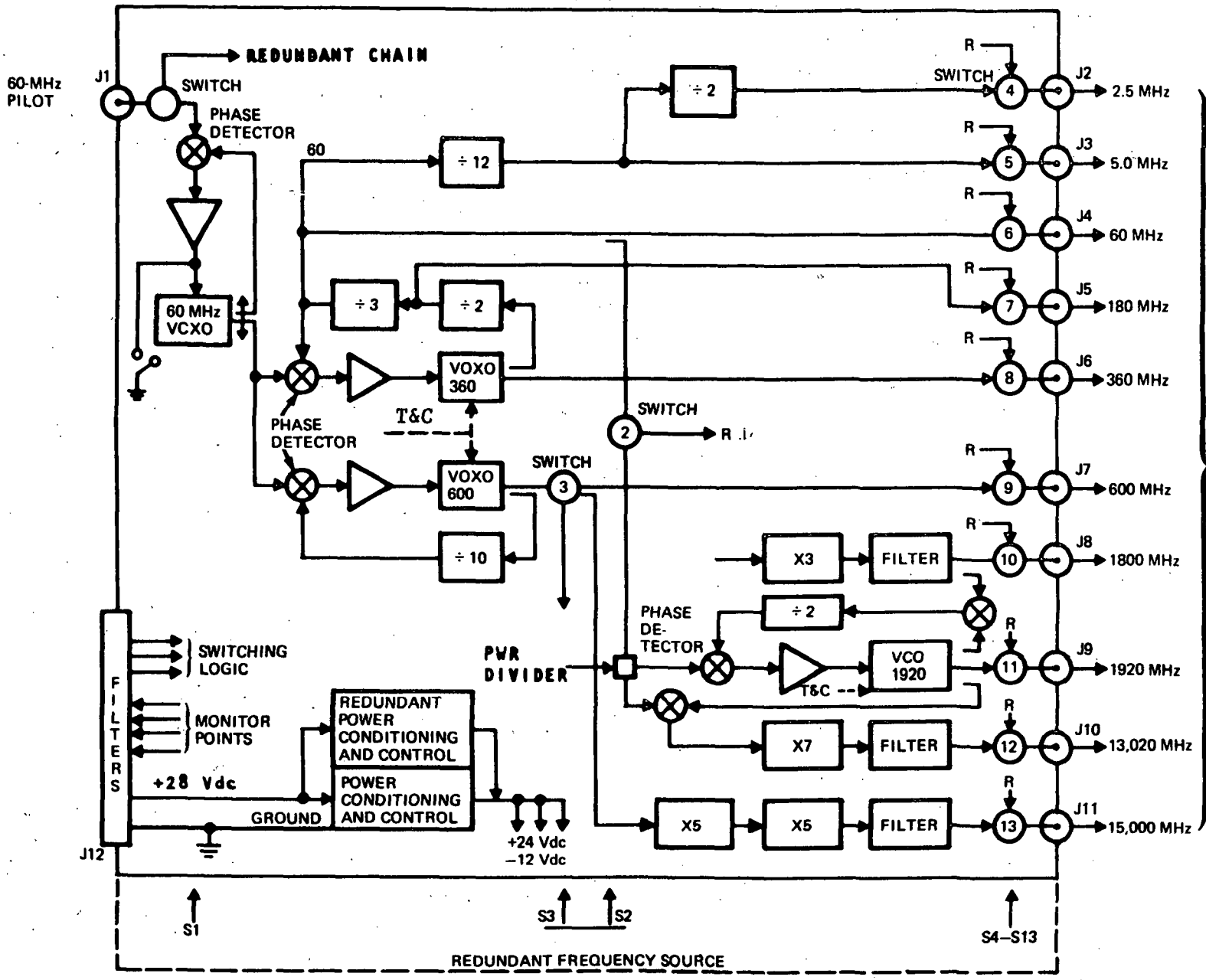
In addition to having two methods of establishing coherent operation, the frequency source will provide 100 percent redundant operation. By using the appropriate commands either the low frequency portion or the high frequency portion of the frequency source can be switched to main or redundant operation, as seen in Figure 4-89. In making these major areas independently redundant a higher probability of success can be enjoyed than in having two parallel frequency source units. Each output VCO/PLL located in the individual receiver or transmitter will consist of two identical units side by side. The reference signals will be continuously fed to both loops with the primary power delivered only to the unit in operation. This method keeps switching to a minimum and reduces complexity.

4.6.2.6 Frequency Source Layout

A physical layout of the recommended frequency source is shown in Figure 4-90. The layout shows the integrated design and the careful use of cavity type enclosures to minimize RR interferences between subassemblies.

4-158

SD 72-SA-0133



REFERENCE OUTPUTS
0 dBm

R - REDUNDANT

Figure 4-88. Frequency Source Block Diagram



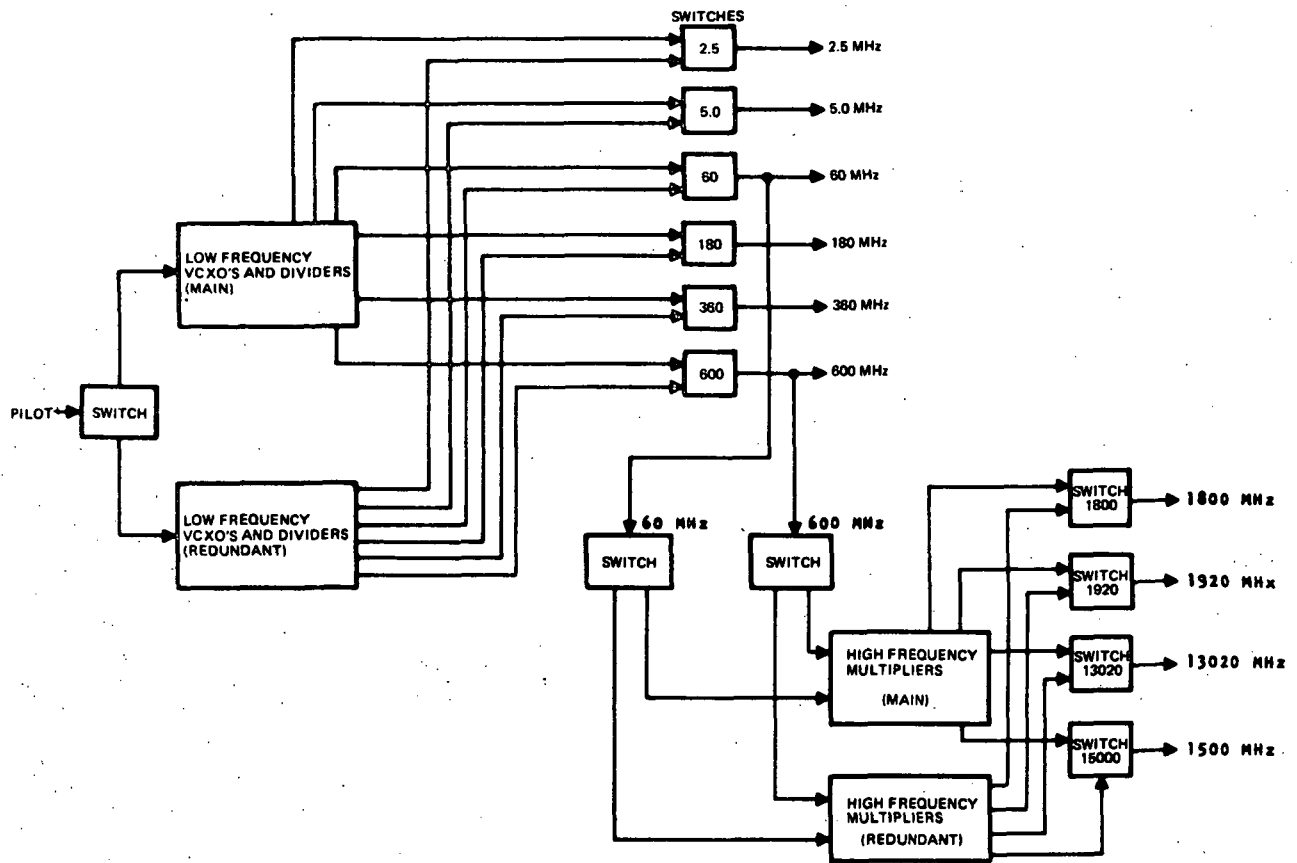


Figure 4-89. Frequency Source Redundancy Model

4.6.3 Performance Specification for the TDRS Frequency Source

4.6.3.1 Scope

This specification establishes the design requirements for the frequency source used to establish all coherent reference signals on the spaceborne TDRS telecommunication system.

4.6.3.2 Components

The major components of the frequency source are:

1. Phase lock loop
2. Frequency generator
3. Clean-up loop

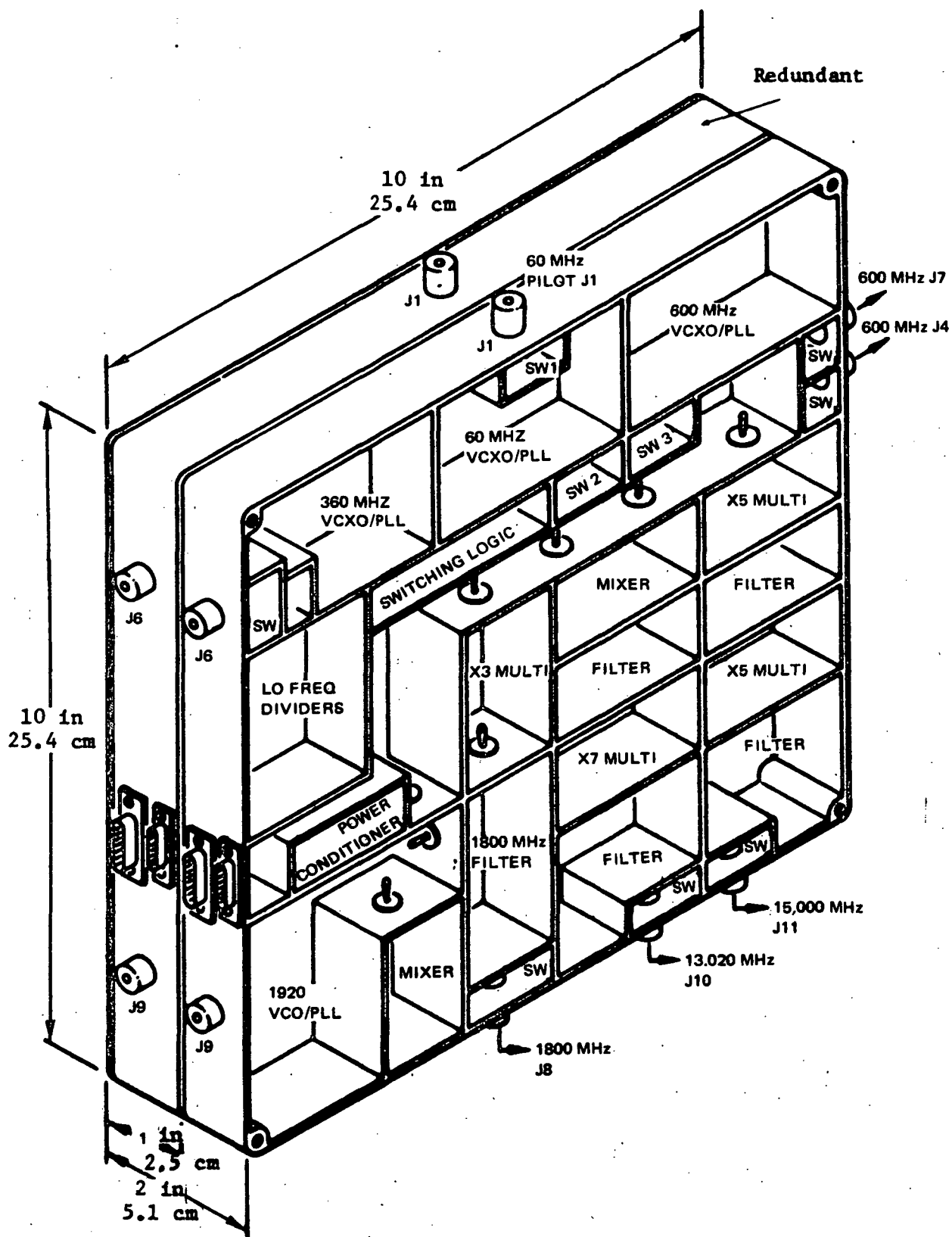


Figure 4-90. Frequency Source Layout



4.6.3.3 Design Requirements for TDRS Frequency Source

- Frequency accuracy - $1/10^5$ two years all signals coherent,
(Back-up mode)*
- Power level - Sufficient to drive balanced mixers + 10 dBm
- Spurs - harmonic - -25 dB down
nonharmonic - -60 dB down, no spur in I.F. range
- Close in - noise - -50 dB + 1 KHz, 1 Hz BW, SSB
-80 dB + 100 KHz, 1 Hz BW, SSB
- Phase shift - Total chain 9 degrees (0.157 rad)
- Short-term stability - 1 part in 10^8 per day (back-up mode)*

4.6.4 Size, Weight, and Power Summary for TDRS Frequency Sources

The size, weight, and power requirements are summarized below for the recommended spaceborne TDRS Frequency Source.

	<u>Size</u>	<u>Weight</u>		<u>Power, Watts</u>	
		<u>(lb)</u>	<u>(kg)</u>	<u>Peak</u>	<u>Avg.</u>
Frequency source	10 x 10 x 2 in. (25.4 x 25.4 x 5.1 cm)	5.6	(2.5)	4.78	4.78

*In normal operation the reference oscillators are phase locked to the ground station pilot.



4.7 TRACKING, TELEMETRY, AND COMMAND SYSTEM

The tracking, telemetry, and command system (TT&C) functions on the TDRS to provide a means for monitoring the performance of the satellite subsystems and changing or initiating operational sequences by insertion of appropriate command signals. The TT&C system provides these functions during the launch, transfer orbit, and on-station phases of the TDRS mission. To provide the TT&C function during the various mission phases, two basic operational modes have been incorporated. These include:

1. VHF for launch and orbit insertion
2. Ku-band TDRS/GS link for on-station mode (VHF backup)

For VHF operation, the TT&C transceiver receives commands and ranging in the 148 to 150 MHz band and transmits telemetry data and ranging at 136 to 138 MHz. On station, the TDRS/GS link provides a receive/transmit channel for TT&C in any one of its primary or backup modes. Therefore, the TT&C function can be provided at either Ku-band or at S-band via the backup MDR mode.

The TT&C system is shown in the simplified block diagram of Figure 4-91. Signals are received during launch or orbit insertion via the VHF antenna system. Commands are PSK along the PN ranging code and the demodulator extracts the received commands and code from the RF carrier. The PN coded IF signal is repeated to the GS at 136 - 138 MHz for tracking purposes after the proper command has switched the ranging signal into the modulator. The modulator output is amplified by the solid state VHF transmitter.

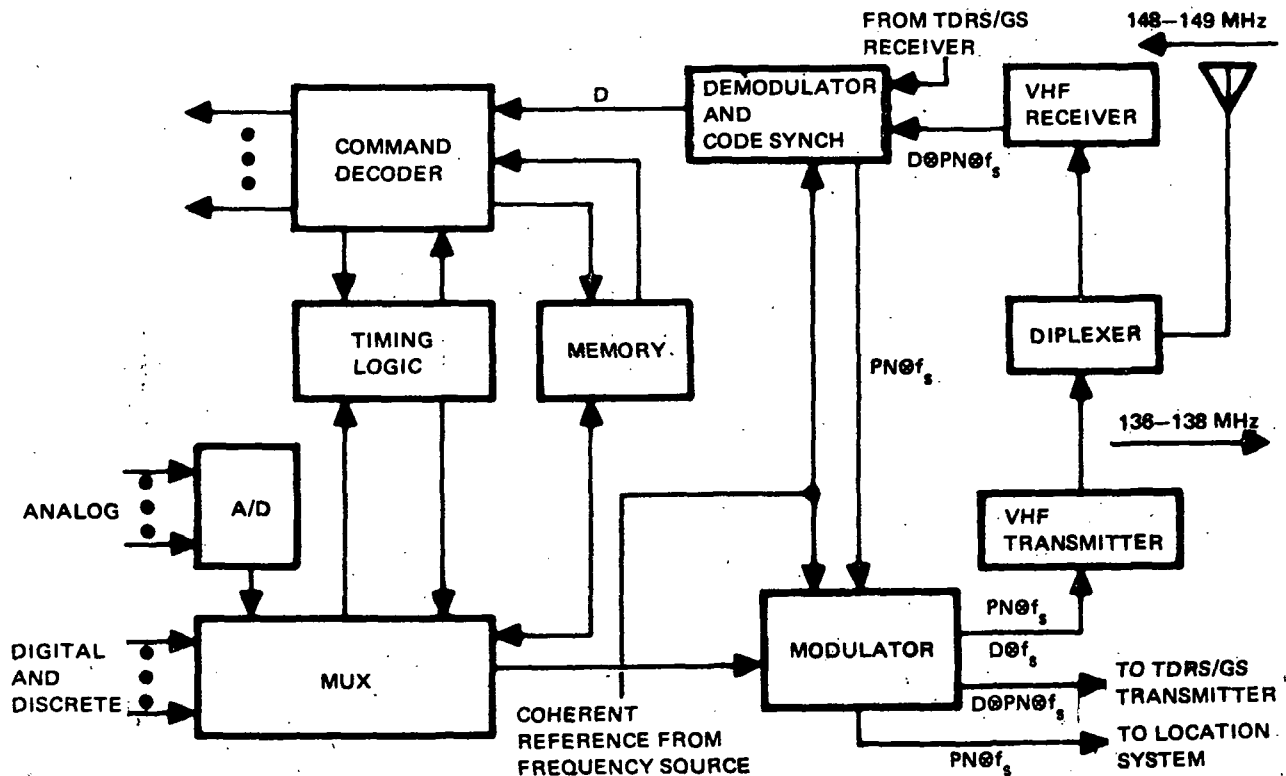


Figure 4-91. TT&C Block Diagram



The modulator also accepts inputs from the multiplexer which places the analog, digital, and discrete outputs from the TDRS into the proper serial digital format. Clock rate, formatting and measurement selection is controlled via the programmed read only memory (PROM) where the operating modes can be selected upon command. This configuration provides a variable bit transmission rate from 1024 bps for normal housekeeping up to the 16 kbps required during the spin mode.

Formatting and device selection is controlled via the memory where the operating modes can be selected upon command.

For on-station operation, inputs to the modulator and demodulator are provided by the TDRS/GS transceiver. During the on-station mode coherent ranging is performed by using a reference frequency from the frequency source. The PN code is extracted and remodulates a carrier to drive the S-band location system as shown in Figure 4-91.

4.7.1 Mechanization Trades

During the design of the TT&C, trades were performed to optimize the weight and power and to keep the bandwidth within the GSFC standard. Trades were performed on the type of memory to be used, how many remote data collection points would be needed and how much integration of the electronics was required. These tradeoffs and recommendations are summarized in Table 4-28.

4.7.2 Detailed Description of TT&C Transponder

4.7.2.1 Antennas

The TT&C antennas are employed to transmit and receive data in the 136 to 150 MHz range. Two sets of antennas are employed, one set functions after the spacecraft has separated from the third stage (transfer orbit) and the other set is used when the spacecraft is on-station and earth oriented. The first set provides linearly polarized omnidirectional coverage in the azimuth plane. The on-station antenna set provides linearly polarized coverage of the earth.

The inflight transfer array consists of four canted monopole antennas fed with equal amplitude and equal phase. These antenna elements are equally spaced on 1.6 meter diameter ring at the aft end of the spacecraft. The 1.6 meter diameter circle translates to a circumference of 2.53 wavelengths at 150 MHz and 2.3 at 137 MHz. Figure 4-92 shows the antenna coverage fluctuation in dB that will be experienced in the azimuth plane as a function of the number of elements and the array spacing (circumference in wavelengths). Four elements (each element having an assumed omnidirectional radiation pattern) with an array circumference between $> 2.25 \lambda$ will produce fluctuations of the order of 1 dB.

Dependent upon the final geometry of the spacecraft, the above noted 1.6 meter diameter array placement might not be possible and placement of canted quarterwave elements at other positions may be dictated. At other positions (larger array diameters) the canted monopole radiation pattern will not approach omnidirectional coverage in the azimuth plane but will present more of a cardioidal type ($F(e) = JS + \cos(e)$) pattern, Figure 4-92.

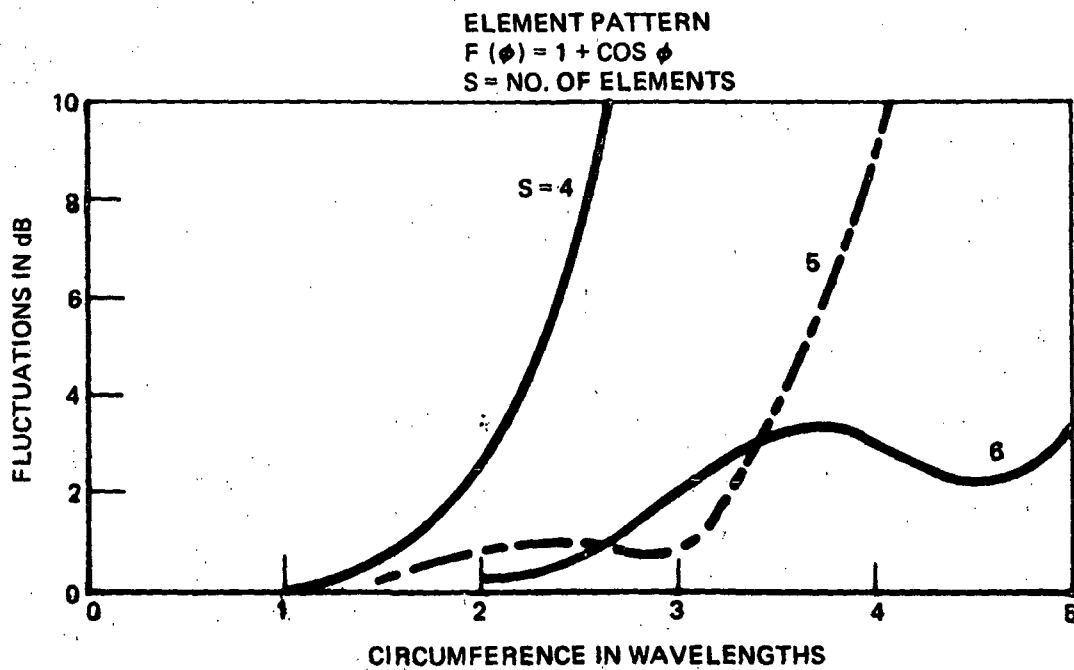
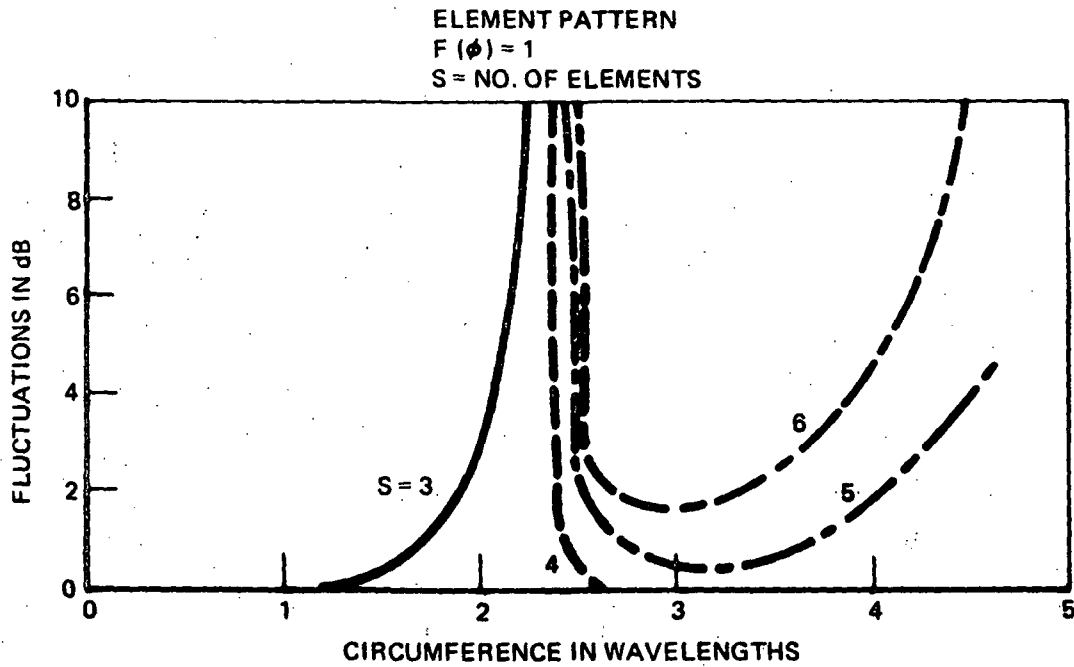


Figure 4-92. Element Patterns



4.7.2.2 TT&C Transponder

The TT&C transponder performs four functions:

1. Provides a telemetry link during launch
2. Acts as a ranging transponder during launch
3. Provides a telemetry backup link on station
4. Acts as backup ranging transponder on station

The normal mode of operation is to provide a telemetry link. When a 4 kHz tone is received the transponder enters the ranging transponder mode by modulating the transmitter signal at 136.11 MHz with the received signal at 148.26 MHz.

The receiver must be able to operate on signals as low as -115 dBm. This performance requires use of low noise techniques to minimize degradation. After establishing a low noise figure the signal is double converted down to a baseband of 807.5 KHz. At this point the baseband spectrum is used to modulate a 22.685 MHz signal which is multiplied six times to 136.11 MHz. The modulated 136.11 MHz signal receives a total of 35 dB gain in a transistorized driver/power amplifier before being fed to the diplexer and antenna.

Referring to the block diagram (Figure 4-93), the incoming R.F. signal at 148.26 MHz is first passed through the diplexer. This device provides isolation between the transmitter output and the receiver low level input stages avoiding saturation. In addition, it provides R.F. preselection so that wideband noise and RFI are not introduced into the RF preamplifier.

The RF preamplifier will be a three-stage transistor amplifier having a narrowband device noise figure of 1 dB. Ultra low noise figure here assures maximum performance under any conditions. The 149 MHz RF preamplifier gain of 40 dB further eliminates any second stage noise contributions as well as reducing the post mixer gain requirements. The first mixer down converts the 148.28 MHz signal to 12.15 MHz using a +10 dBm L.O. at 136.11 MHz. This mixer is double balanced to reduce spurious responses and provide maximum rejection to L.O. re-radiation. Since this L.O. is at the transmit frequency, the mixer conversion loss is approximately 8 dB. Following the mixer, the 12.15 MHz I.F. signal is filtered in a linear phase filter having 60 KHz BW at 12.15 MHz. Filter loss at this point is not a determining factor in receiver noise figure. After the I.F. filter, the signal is amplified and the output level is controlled by automatic gain control (AGC). In this AGC amplifier most of the receiver gain of 70 dB is achieved. Typical input signal levels of -115 dBm will be amplified to -14 dBm with higher levels receiving less gain due to the AGC action. The amplifier is designed with a 1 dB compression point of 0 dBm to avoid becoming non-linear on noise peaks and for launch pad signal levels for test and lock-on purposes. The amplifier signal output is split with one output being directly demodulated for the telemetry command channel and the other being down converted to 807.5 KHz for modulating the transmitter. This second mixer operates at a signal input level of 3 dBm at 12 MHz and is mixed with a +10 dBm L.O. at 11.4 MHz producing an 807.5 KHz second I.F. During ranging, the baseband is phase modulated with the 22.685 MHz oscillator signal and is multiplied six times to 136.11 MHz. Then 35 dB of gain is provided by the transistorized driver/power amplifier so that a two-watt signal is transmitted back to the GS.

4-167
SD 72-SA-0133

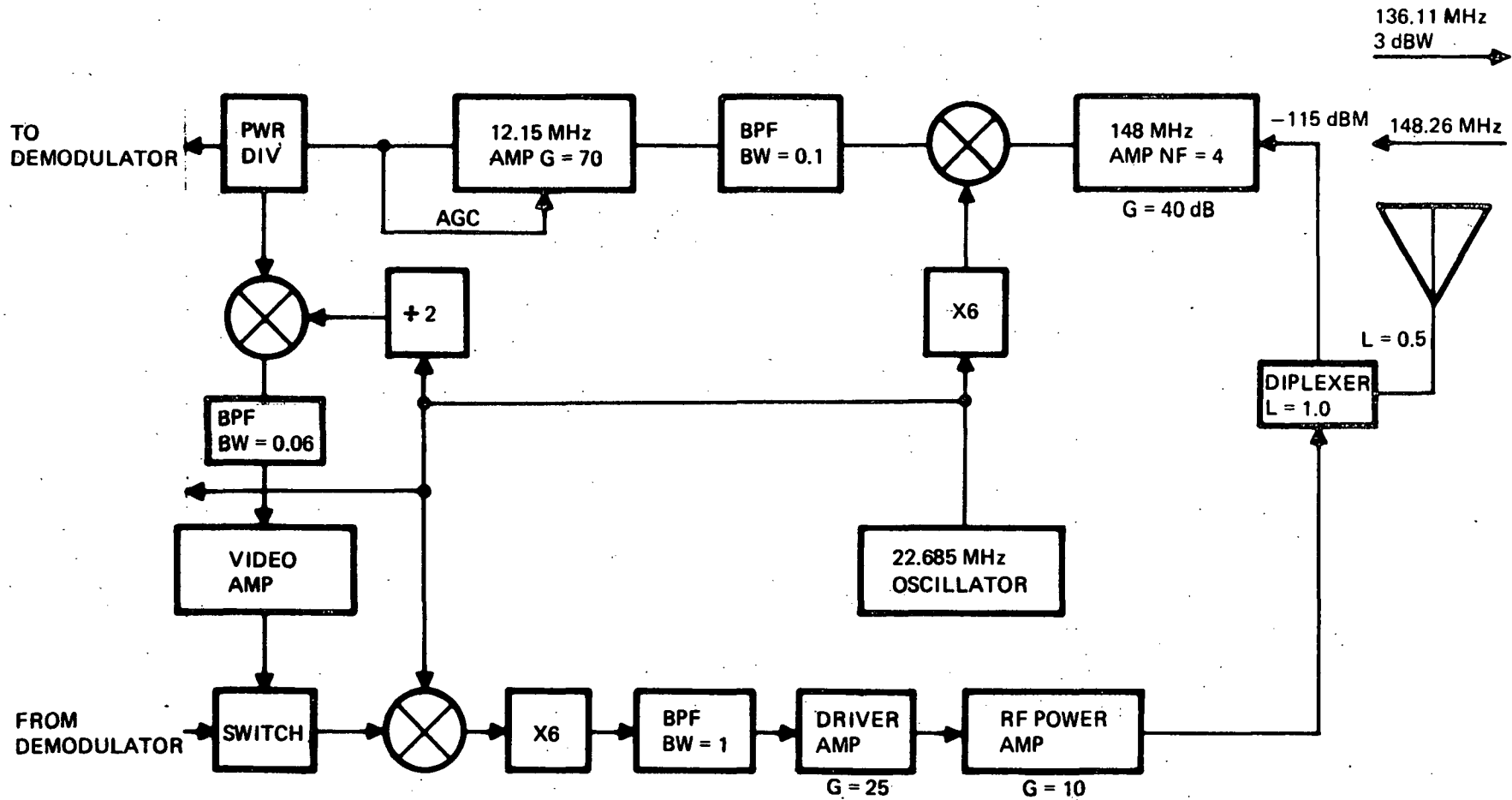


Figure 4-93. TT&C Transponder Block Diagram



4.7.2.3 Detailed Description of TT&C Modem

Modulation and demodulation of data in the TT&C subsystem is performed in the modem unit shown in Figure 4-94. The telemetry data and commands are transferred between the TDRS and GS by the TDRS/GS link or the VHF transponder link. The modulation used in each case is different and the modem must be capable of handling either type. The link selection is made in the modem.

The signal arriving from the VHF transponder is a delta PSK modulated 12.15 MHz carrier while the signal arriving from the TDRS/GS receiver is APSK plus a unique PN code modulating a 50 MHz carrier. During VHF operation, the signal goes directly to the COSTAS loop demodulator and is converted to NRZ data. During TDRS/GS receiver operation, the 12.15 MHz VCXO output is mixed with 50 MHz from the TDRS frequency source to produce 37.85 MHz. This signal is mixed with the synchronized PN code and the result is mixed with the 50 MHz input to produce the same IF frequency as in the VHF transponder mode.

Modulation for the VHF transmitter consists of delta modulated data. When the telemetry data is transmitted to the GS by the TDRS/GS transmitter, it is combined with the PN code which phase modulates the 15 MHz signal.

The signal output which drives the S-band location transmitter consists only of the PN code phase modulated onto the 15 MHz carrier.

4.7.2.4 Detailed Description of TT&C Processor

The telemetry and command processor is shown in block form in Figure 4-95. A command and its complement are received in one transmitted word. These are compared and stored in registers while a copy is sent back to the GS. Upon verification, the GS sends an execute command. The command then addresses the coded matrix memory and is sent to the proper part of the decoder and, if necessary, the D/A converter is time shared between the 17 analog channels to conserve power. The analog levels are stored in 17 capacitors with buffered outputs. When commands are not being received, power is conserved by removing power from the command section except for the analog refreshing circuit.

The telemetry data comes from four sources. The 110 analog signals are all sampled by a common programmable amplifier. An address from the formatter selects a code word from a read only memory which controls the offset voltage and gain of the amplifier. The output voltage goes to the D/A converter along with the 29 high level analog signals on a time-shared basis. The output of D/A is combined with the bilevel, sun sensor, and the command verification inputs to the multiplexer. The multiplexer output goes to the modulator.

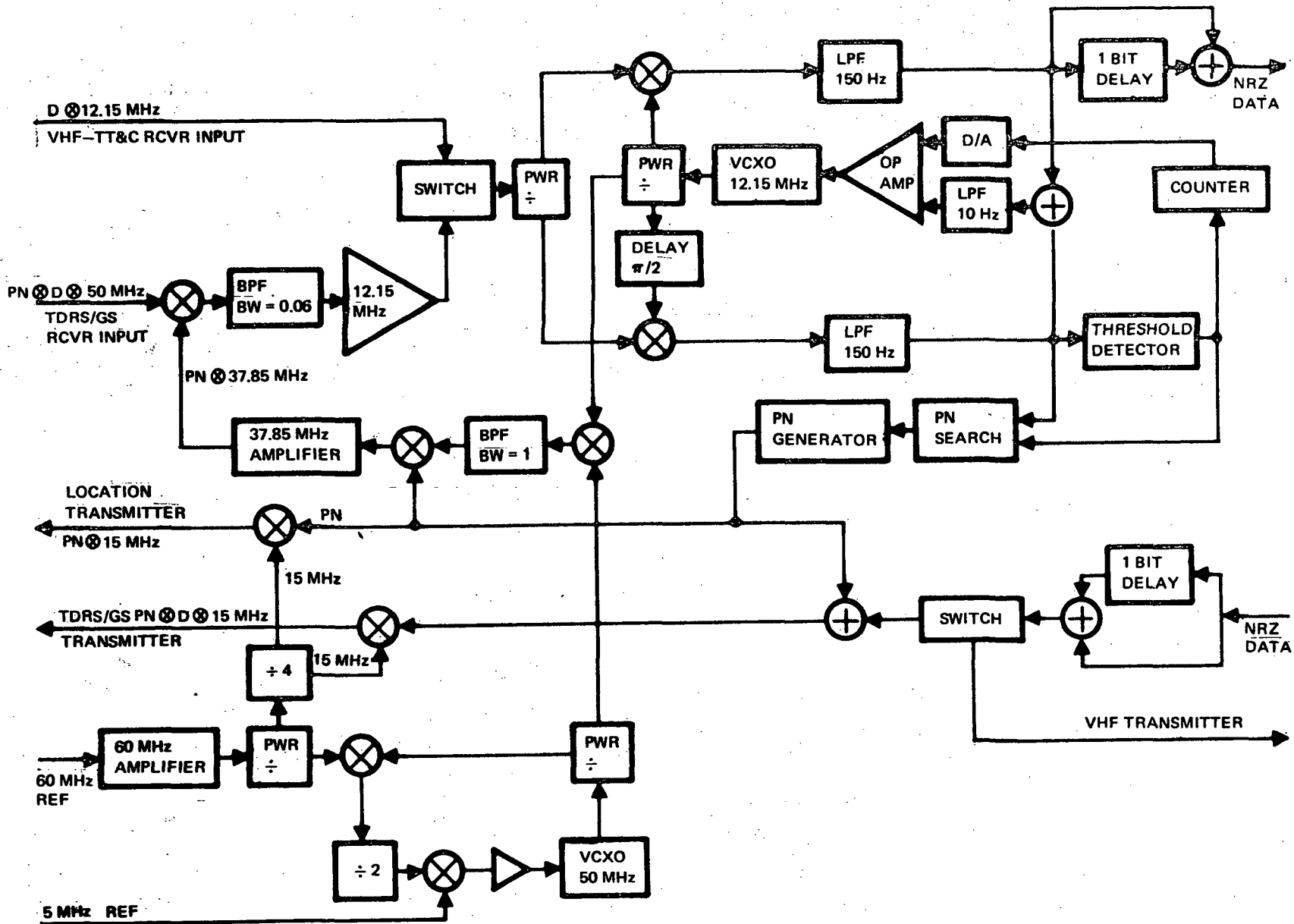


Figure 4-94. TT&C Modem

4-169

SD 72-SA-0133



Space Division
North American Rockwell

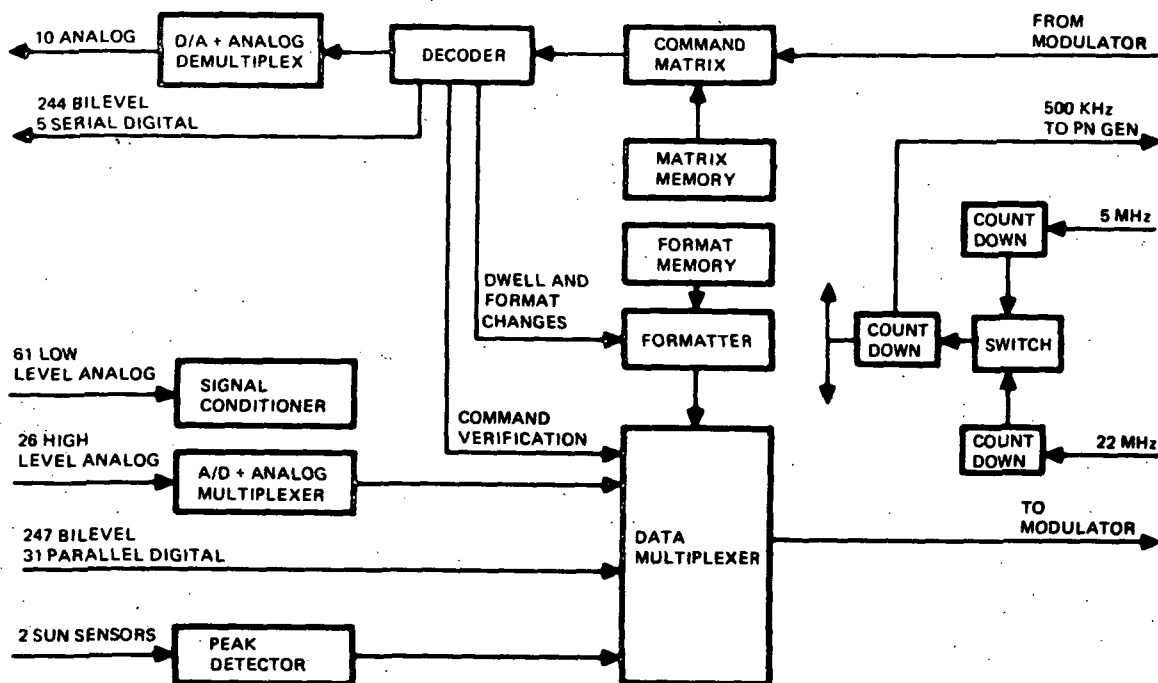


Figure 4-95. TT&C Processor Block Diagram

The two sun sensors each require 50-microsecond resolution of 12-bit data. This is achieved in minimum bandwidth by digitally detecting the peak output and supplying a time tag to identify the time of occurrence. The peak and time tag are then fed serially to the multiplexer. Spinning horizon sensors are simpler to process since only one bit changes. This bit plus the time tag are sent to the multiplexer.

The clock signal for the processor is derived from two sources. Normally, the clock is counted down from the 2.5 MHz line from the main frequency source. Should the main source fail, the clock source becomes the master oscillator for the VHF transponder. After either source has been reduced to a common frequency, the selected source is counted down to the required frequency.

4.7.3 Performance Specification for the TDRS Tracking, Telemetry and Command Subsystem

4.7.3.1 Scope

This specification establishes the design performance requirements for the spaceborne TDRS tracking, telemetry, and command subsystem.



4.7.3.2 Components

The major components of the TT&C are:

1. Antenna in-transit
2. Antenna on-station
3. VHF Transceiver
4. Processor

4.7.3.3 Design Requirements for TDRS TT&C Subsystem

TT&C Antennas

Frequency range

Receive

148 to 150 MHz

Transmit

136 to 138 MHz

Transmit average power

2.0 watt

Polarization (predominant)

Linear

Coverage requirement

1. Omnidirectional in azimuth plane of spacecraft
2. Earth coverage when on station

Gain (peak)

0 dbi linear

VSWR

1.25:1

Element length

20.0 inches (51 cm)

Element weight

0.1 pound (45 gm)

Transfer orbit array

4 canted monopoles spaced on a 63 inch (1.6 m) diameter at aft end of spacecraft

On station array

4 canted monopoles (around periphery of 3' (0.91 m) TDRS/GS antenna) hooked up as 2 dipole pairs

Switching

Between "transfer orbit" and "on station" arrays

Between "on station" dipoles for redundancy

TT&C processor



Size 6.2 x 4.5 x 5.4"
(15.7 x 11.4 x 13.7 cm)

Weight 9.6 lb (4.4 kg)

Reliability 0.965 for 5 years

Bit rate (commands) 128 bps

Bit rate (data) 16 bps max

Power 14.5 watts

VHF Transceiver

Noise figure 2.5 dB

Output power 2 watts

Transmit frequency 136.11 MHz

Receive frequency 148.62 MHz

Weight 4 pounds (1.8 kg)

Reliability MTBF = 400,000 hours

4.7.4 Size, Weight, and Power Summary for TT&C

One of the design parameters controlling the configuration of the TT&C processor is the quantity of connector pins required for the unit (approximately 689). To accommodate this pin count and to minimize internal wire length, seven signal, one power, and four coax connectors are located on the top face of the unit.

Component	Size in. (cm)	Weight lbs (kg)	Power (watts)	
			Intransit	On station
Processor	6.2 x 4.5 x 5.4 in (15.7x11.4x13.7 cm)	9.6 (4.37)	10.0	10.0
Transceiver	5.5 x 5.5 x 2.63 in (14x14x6.7 cm)	4.0 (1.81)	4.5	0.5 (receive only)
Antenna		3.0 (1.36)		
Total		16.6 (7.55)	14.5	10.5

4.8 TDRS TRACKING/ORDER WIRE TRANSPONDER

4.8.1 System Analysis and Trades

The functions provided by the S-band location system are shown in Figure 4-96. To locate the position of the TDRS by trilateration, the PN₁ code is transmitted to the TDRS/GS receiver by combining the code with the common data at 500 kbps. PN₁ is extracted from the command data and transmitted to the two remote ground transponders at 2066 MHz. The ground transceivers receive and retransmit codes PN₂ and PN₃ at 2249 MHz using coherent processing, where they are received at the TDRS by an earth coverage S-band antenna. The sum of the two remote signals are both retransmitted to the GS via the TDRS/GS link.

For S-band users with high gain antennas, the PN₁ modulated signal which is transmitted from the S-band location transmitter acts as a beacon which locates the TDRS for the MDR user. Once the user is pointing in the correct direction and acquires the beacon, a request for MDR service may be transmitted via the order wire. This request is handled simultaneously with any other requests through the order wire system to establish the order of priority (by ground controllers) for the TDRS MDR service. The requests are sorted at the GS and the MDR antenna pointing commands enable service to the selected users.

The location receiver must be sensitive enough to receive the location signals from the ground stations and the order wire signals from users with omni antennas. Of these two, the order wire signals are the most critical since the satellites are limited in output power to 16 dBw. The point of greatest loss between TDRS and a user is when the user is in a 2700nm (5000 km) orbit and is at an aspect angle of 110° (1.92 rad) where the range is 24,105 (44,642 km) and the TDRS antenna gain is 12 dB. For an error rate of 10⁻⁵, ΔPSK transmission requires a CNR of 9.9 dB. With 0.5 dB degradation in TDRS relay transponder, the final CNR is 10.4 dB. The TDRS receiving loss between the antenna and the first amplifier is 1.1 dB. The information bit rate is 100 bps and the bandwidth is 150 Hz. These numbers are summarized in Table 4-29.

Table 4-29. Location Receiver Parameters

CNR	10.4 dB
P _T	16.0 dBw
G _T	3.0 dB
G _R	12.0 dB
α _{space}	192.4 dB
α _{loss}	4.0 dB

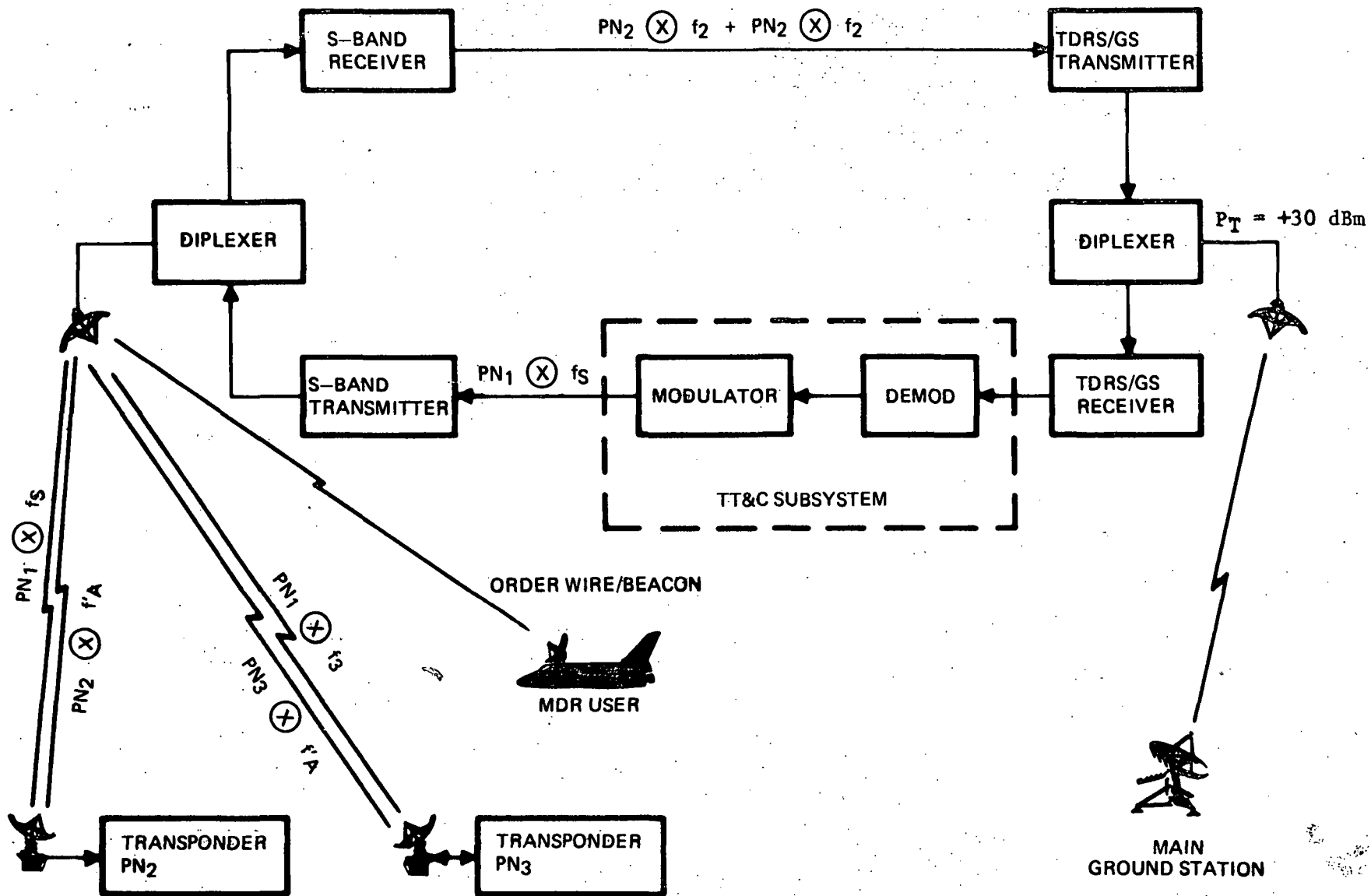


Figure 4-96. Location System Block Diagram



These parameters result in a system temperature of 31.0 dB. If we use 5 dB of this as a margin, the system temperature becomes 27.5 dB or 561°K. With an antenna temperature of 34.8 K (15 dB gain at 22,748 nm (42,129 km), the receiver must have a system noise figure of 4.6 dB. This can be achieved with a transistorized preamp having a 3.5 dB noise figure and a gain of at least 20 dB.

4.8.2 Detailed Description of TDRS Tracking/Order Wire

4.8.2.1 TDRS S-Band Beacon Antenna

The requirements of providing a 31° (0.54 rad.) FOV (half power beamwidth) operating in the S-band frequency range of 2.066 GHz transmit and 2.249 GHz received are satisfied with the use of a bifilar helix. This element is a simple and efficient design providing circular polarization on axis when operating in the axial mode. The HP BW as a function of helix parameters is shown in Figure 4-97. To cover the entire FOV a HP BW of 31 (0.54 rad.) is required. This requires an axial length (nλ) of approximately 1.9 wave lengths for a helical turn (n) circumference (Cλ) of 1.2 wave lengths. For a nominal operating frequency of 2.1 GHz, the helix element is approximately 9.1 in. (23.2 cm) long with a helix diameter of two in. (5.1 cm). A ground plane of approximately 10 in. (25.4 cm) diameter is required. The element gain (G_{e1}) can be computed from the following expression.

$$G_{e1} = 28,000 / (\theta_{3 \text{ dB}})^2$$

which indicates that an element gain of 15 dBi is achievable.

Figure 4-98 shows the proposed construction of the antenna. The unit consists of the bifilar windings of a thin wall fiberglass tube which is attached to a base unit containing an integral stripline power divider and the required phasing network. The estimated weight of the antenna including ground plane and mounting ring is .25 lb (.1 kg). The incorporated feed for the bifilar helix is a 3 dB, 180° (π rad.) hybrid similar in design to Anaren Model 30056. The power handling requirements of one watt present no problems. Selection of the bifilar helix over a single element provides both improved axial ratio and increased gain.

4.8.2.2 TDRS Tracking/Order Wire Transceiver

The S-band location and order wire receiver is a double conversion configuration as shown in Figure 4-98. The receiver operates at 2249 MHz, receiving signals from the remote ground stations. Signals from the antenna are passed through the diplexer to isolate the transmitter frequency from the receiver input by more than 70 dB. In addition to this isolation the diplexer provides RF preselection which eliminates out-of-band spurious and noise. The RF signal is then fed to the RF preamp (A1). This amplifier is a low-noise device (3.5 dB N.F.) that produces 20 dB of gain. The RF preamp reduces the high noise figure that would normally be produced by the first mixer (M1) and first IF bandpass filter (F1). Without the RF preamp a typical receiver noise figure would be about 13.5 dB

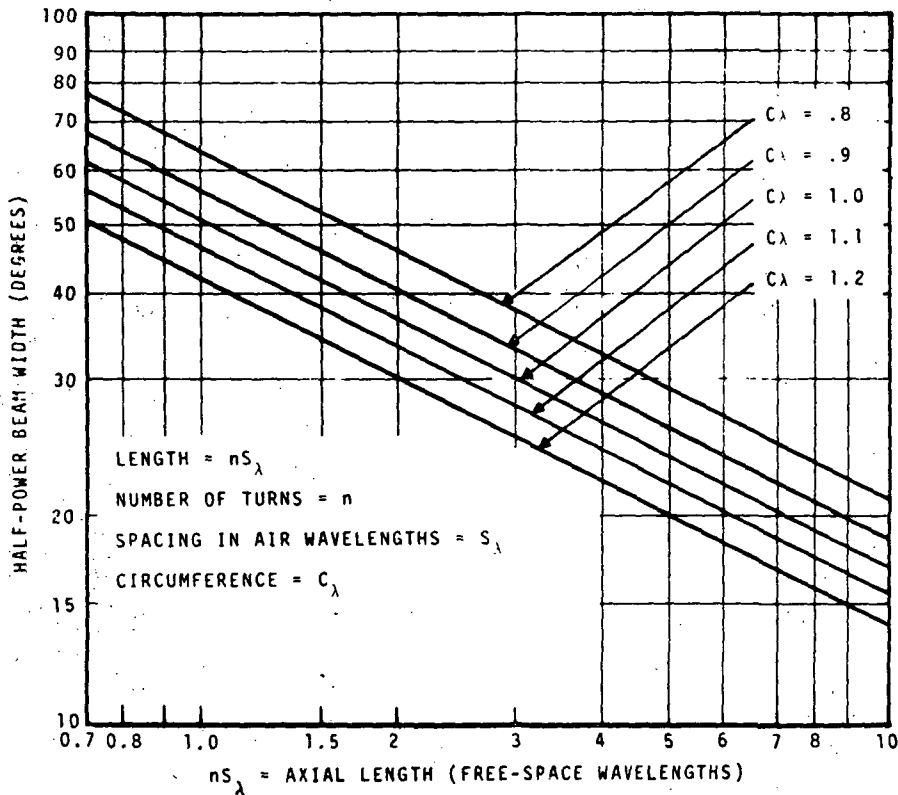


Figure 4-97. Axial Mode Helical Antenna Beamwidth versus Length

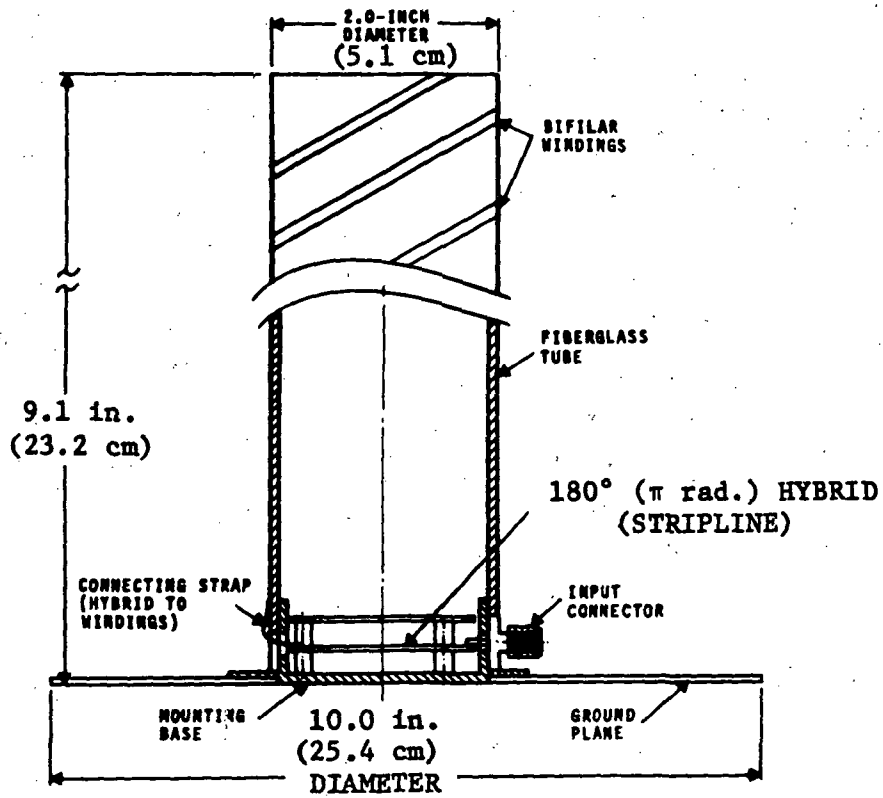


Figure 4-98. Proposed Construction of S-Band Beacon Antenna



After amplification the signal is down converted to a 329 MHz IF by a double balanced mixer (M1). By mixing 2249 MHz with a 1920 MHz L.O., the desired frequency is generated. The IF signal is then filtered in a lumped constant filter, F1, having a 3 dB insertion loss. This filter provides sufficient selectivity that spurious responses are maintained within acceptable limits.

The IF amplifier (A2) is a MIC amplifier producing 24 dB of gain. The noise figure of this device, although not critical is moderately low (3 to 4 dB). The 24 dB of gain is necessary to overcome the distributed losses in M2 and F2 such that these components do not introduce additional system noise.

The 329 MHz IF is mixed with a 342.5 MHz second L.O. producing a 13.5 MHz second IF. This double balanced mixer, in turn, feeds the second IF bandpass filter which has a 3-dB insertion loss and further improves the selectivity, while maintaining phase linearity in the channel.

The AGC amplifier and post amplifier following this last filter provides most of the receiver gain. The AGC amplifier produces up to 60 dB of gain depending upon the drive level. This device maintains a constant output at -21 dBm. The post amplifier gain is fixed (21 dB) to maintain the overall receiver output at 0 dBm. The receiver is 100 percent redundant.

The transmitter generates an output power of one watt into the antenna at a frequency of 2066.5 MHz. The signal transmitted is received from the TT&C modulator at 15 MHz and converted to 365.1 MHz in the first IF. The transmitter is an all solid state design generating 33 dBm at the output of A7. Losses reduce this level to 30 dBm at the antenna

4.8.3 Performance Specification for TDRS Tracking/Order Wire Transponder

4.8.3.1 Scope

This specification establishes the design performance requirements for the tracking/order wire transponder located on the TDRS satellite. This transponder provides three functions:

1. TDRS satellite location and tracking reference for an overall trilateration ranging system
2. Order wire receiver to establish order of priority for MDR users
3. Beacon for acquisition and tracking by high gain S-band MDR users

4.8.3.2 Components

The major components of the TDRS tracking/order wire transponder are:

1. Antenna
2. Transceiver



4.8.3.3 Design Requirements

TDRS S-Band Beacon Antenna

Frequency range:

Receive	2.200 to 2.290 GHz
Transmit	2.025 to 2.2110 GHz

Transmit average power: ≤ 1.0 watt

Polarization: Circular

Axial ratio: ≤ 0.5 dB

Input VSWR: $\leq 1.25:1$

Gain: ≥ 15.0 dBi

Half power beamwidth
(for any linear pol.) ≥ 31 degrees

Side lobe level (as a function
of rotating linear) ≥ 12 dB

Size:

Height	9.1 inches (23.2 cm)
Winding diameter	2.0 inches (5.1 cm)
Ground plane diameter	10 inches (25.4 cm)

Weight: 0.3 pounds (25.4 cm)

Tracking and Order Wire Transceiver

RF range: 2249 ± 0.5 MHz

Phase linearity: $\pm 5^\circ$ over 1 MHz bandwidth

System noise figure: 4.6 dB

First IF frequency: 329 MHz

Second IF frequency: 13.5 MHz

AGC range: 20 dB

3 dB bandwidth: 1 MHz

Spurious levels: > 50 dB down

Temperature range: 0 to 50 C



Transmitter

Power output:	1 watt
Center frequency:	2066.5 MHz
3 dB bandwidth:	1 MHz
Phase linearity:	+5° over 1 MHz bandwidth

4.8.4 Size, Weight, and Power Summary for the TDRS Tracking/Order Wire Transponder

The size, weight, and power requirements are summarized below for the recommended TDRS tracking/order wire transponder.

Component	Size (in.) (cm)	Weight (lb) (kg)	Power, watts
Antenna	9.1 x 10 (23.2 x 25.4)	0.3 (114gm)	
Transceiver	8 x 4 x 0.5 (20.3 x 10.2 x 1.3)	5.4 (2.5)	7.9

4.9 Ku-BAND BEACON

4.9.1 System Description

The Ku-band beacon provides a means for an MDR user to acquire the TDRS with a high-gain antenna. The power required from the beacon is presented in Table 4-30, where it is shown that a transmitted power of 1 watt is sufficient to provide a C/N_o of 37.7 dB-Hz at the user receiver. If we allow a design margin of 5 dB, this leaves $C/N_o = 32.7$ dB-Hz which is more than adequate to send beacon data.

Table 4-30. Ku-Band Beacon Power Budget

Transmit power	1.0 dB
TDRS antenna gain at 31 degrees FOV	12 dB
Path loss	208.1 dB
Other losses	1.0 dB
Receive antenna gain	30 dB
Received power	-166.1 dBw
P_n ($T_s = 300$ K)	-203.8 dBw
C/N_o	37.7 dB-Hz

The beacon consists of a cavity-tuned oscillator whose output is coupled to a phase detector so that the beacon can be locked to a coherent source from the frequency source unit. Since this beacon is coherently locked to the frequency source and consequently to the entire on-board telecommunication system, it can be used as a pilot signal by the ground system to coherently lock-on to in the event that the spaceborne telecommunication system cannot lock-on to the pilot signal from the ground station. In this mode, the spaceborne frequency source becomes the overall frequency reference, and provides an additional functional redundant mode to maintain an overall frequency coherency. A block diagram is shown in Figure 4-99. The power output is 1.4 watts. A simple conical horn providing peak gain of 15 dBi is used for this link.

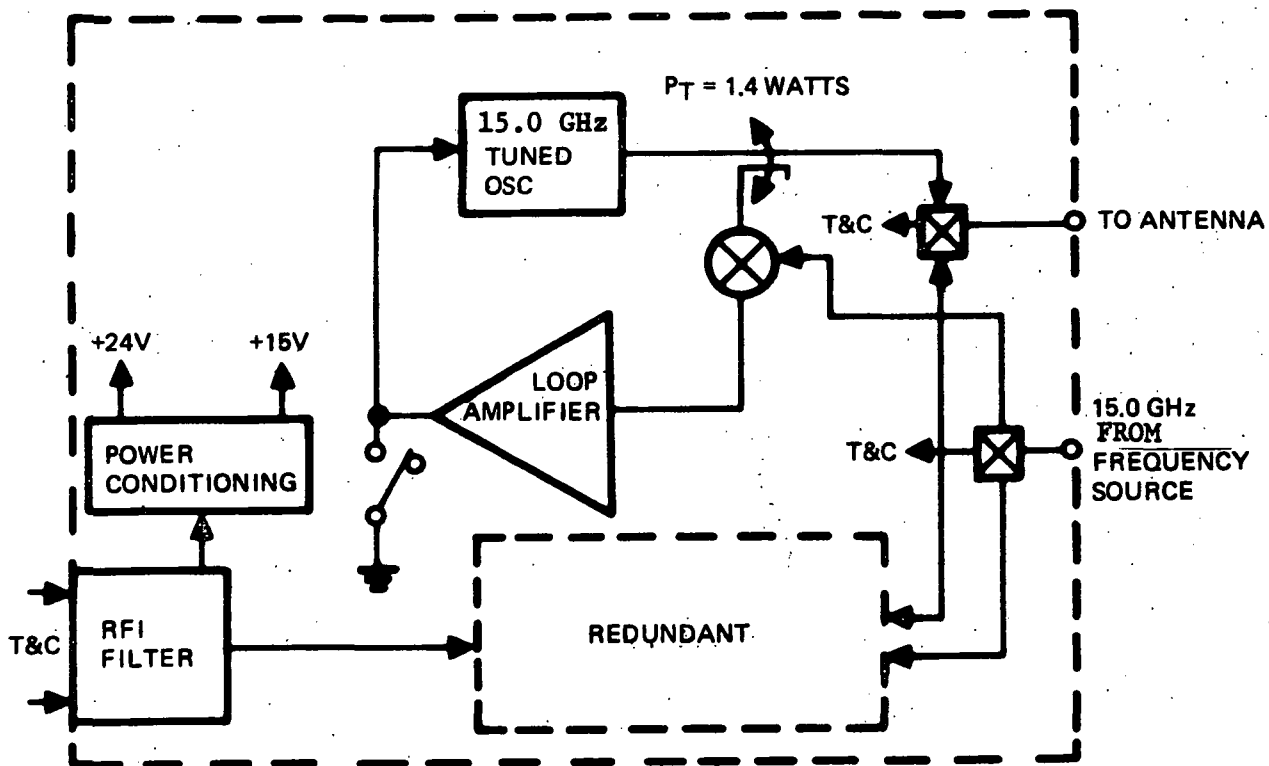


Figure 4-99. Ku-Band Beacon



4.9.2 Performance Specification of the Ku-Band Beacon

4.9.2.1 Scope

This specification establishes the requirements for the Ku-band beacon that is used by the MDR Ku-band users with high gain antenna to acquire and track the TDRS satellite.

4.9.2.2 Design Requirements

Antenna gain (dBi) - peak	15.0
- 31° (0.54 rad) FOV	12.0
Transmit power, watts	1.4
Frequency, GHz	15.0*

NOTE: *Coherently locked to frequency source

4.9.3 Size, Weight, and Power Summary of the Ku-Band Beacon

Component	Size (in.)	Weight		Power, watts
		(lb)	(kg)	
Antenna		0.3	0.14	
Beacon	3 x 3 x 4	3.6	1.6	8.3